PROTRACTED MAGMATISM WITHIN THE NORTH CARIBOU TERRANE, SUPERIOR PROVINCE: PETROLOGY, GEOCHRONOLOGY, AND GEOCHEMISTRY OF MESO- TO NEOARCHEAN TTG SUITES

by

AMANDA VAN LANKVELT

BA, Lawrence University—Appleton, WI, 2010

A THESIS SUBMITTED IN PARTIAL FULFILMENT OF THE REQUIREMENTS FOR THE DEGREE OF

MASTER OF SCIENCE

in

THE FACULTY OF GRADUATE AND POSTDOCTORAL STUDIES

Department of Earth Sciences

We accept this thesis as conforming to the required standard

University of Ottawa

April 2013

Protracted magmatism within the North Caribou Terrane, Superior Province: petrology, geochronology, and geochemistry of Meso- to Neoarchean TTG suites

A. Van Lankvelt
University of Ottawa

ABSTRACT

The North Caribou Terrane forms the core of Superior Province and records a protracted history of crustal growth and modification. At the centre of the North Caribou Terrane, lies the North Caribou greenstone belt, which is surrounded by granitoids of diverse compositions and ages. This study reports whole-rock geochemistry, zircon and titanite geochronology, and hornblende geobarometry on these plutonic rocks. Although zircons as old as 3132 ± 7 Ma were found, the main magmatic pulse occurred between 2880 and 2830 Ma, and geobarometry indicates tectonic thickening during this period. This was followed by widespread hydrothermal alteration and limited magmatism from 2760 to 2680 Ma, and shallow, brittle-ductile intrusions at *circa* 2630 Ma. From 2730 to 2630 Ma, intrusions were emplaced at increasingly shallow crustal levels. All of the rocks, except for the youngest pegmatitic intrusions, show similar patterns in major and trace elements, with a general trend toward more evolved compositions through time. These patterns indicate that the granitoids record mostly reworking of early intrusions, which is also consistent with patterns observed in the geochronology.

Magmatisme prolongée dans le terrane Caribou Nord, la Province du Supérieur: la pétrologie, la géochronologie et la géochimie des suites TTG du Méso- au Néoarchéen

A. Van Lankvelt
Université d'Ottawa

RÉSUMÉ

Le terrane Caribou Nord constitue le cœur de la Province du Supérieur et enregistre une histoire prolongée de croissance et modification de la croûte terrestre. Au centre du terrane réside la ceinture de roches vertes Caribou Nord, laquelle est entourée de granitoïdes de divers âges et compositions. Cette étude documente la géochimie de ces roches, la géochronologie sur zircons et titanites ainsi que la géobarométrie à partir de hornblende de ces roches plutoniques. Bien que des zircons aussi vieux que 3132 ± 7 Ma furent trouvés, la principale pulsion magmatique eut lieu entre 2880 et 2830 Ma, accompagnée d'un épaississement tectonique tel que l'indique la géobarométrie. Une altération hydrothermale répandue et un magmatisme limité de 2760 Ma à 2680 Ma s'ensuivirent, ainsi que des intrusions cassantes-ductiles peu profondes *circa* 2630 Ma. De 2730 à 2630 Ma, les intrusions furent mises en place à des niveaux peu profonds de la croûte terrestre. Toutes les roches, à l'exception des plus jeunes intrusions pegmatitiques, montrent des similarités dans leurs éléments traces et majeurs, avec une tendance générale vers des compositions plus évoluées avec le temps. Ceci indique que les granitoïdes enregistrent principalement les modifications subies par les jeunes intrusions, ce qui est d'ailleurs corroboré par les données géochronologiques.

[Traduit par Élise Cossette]

Table of Contents

LIST OF FIGURES

LIST OF TABLES AND APPENDICES

ACKNOWLEDGEMENTS

Helen Keller said, “Alone we can do so little; together we can do so much,” and there is very little I could have done without the help of many others. Accordingly, here are a few people who deserve my thanks.

First, financial support and project funding was supplied jointly through an NSERC CRD and Goldcorp’s Musselwhite mine. Additional funding was provided by an Ontario Graduate Scholarship.

For their patience and willingness to share their expertise, I am indebted to the many lab managers who helped with data collection. This includes Glen Poirier of the Canadian Museum of Nature and Peter Jones for their assistance with the microprobe analyses at the University of Ottawa and Carleton University respectively. Pam King and Tara Kell preformed the XRF analyses at Memorial University and the University of Ottawa. And at the University of New Brunswick LA-ICP-MS lab, for their many hours of assistance and prompt answers to e-mail questions, I’d like to thank Yan Luo and Chris McFarlane.

In addition to project funding, the geologists at Musselwhite Mine provided significant support for fieldwork. Senior exploration geologist John Biczok coordinated much of the field logistics, including helicopter access. Dan Grabiec, a summer student at Musselwhite, was an excellent field assistant during helicopter sampling. And Mary Ellen Thomas did a fantastic job coordinating our food supplies. All of the personnel at Musselwhite helped accommodate our needs while on-site.

There have been a core group of North Caribou people at the University of Ottawa who have helped and supported me. This includes Colter Kelly and Élise Cossette who were amazing, cheerful field assistants. Tash Kalbfleisch and Jason Duff have been incredibly helpful, sharing their field and technical experience as well as their upbeat personalities and positive attitudes. My advisor Keiko Hattori has helpfully challenged me to think and explain myself more precisely, and my advisor David Schneider has been extremely patient and supportive.

I would also like to thank my undergraduate advisor, Marcia Bjornerud, for sharing her passion of rocks, and the petrology group at the University of Massachusetts, especially Sheila Seaman, Mike Williams, Laurie Brown, Tony Morse, and Sean Regan, for their patience and support during my transition between uOttawa and UMass.

Finally, I would like to thank all of the people, several of whom are listed above, who have supported and nurtured my growth as a scientist and a member of society. Thank you.

1. INTRODUCTION

Archean cratons are fundamental constituents of modern continents with stable lithospheric roots that control modern tectonic processes. Cratons contain substantial mineral resources (cf. Percival, 2007) and have controlled the geometry and dynamics of continental tectonics since the Proterozoic, whether by remaining buoyant during continent-continent collisions or by forming rigid blocks onto which younger crust were accreted. Despite the importance of the Archean cratons, cratonization is still a poorly understood process. However, global studies of Archean terranes have highlighted the important role that accretion and the accompanying magmatism play in the cratonization process (cf. Pollack, 1986).

The Superior Province, the largest of the Archean cratons, is easily accessible and rich in economic mineral deposits and is, therefore, thoroughly studied. The wealth of data about the Superior Province offers a unique opportunity to study the rates and types of processes involved in crustal growth and accretion. At the core of the Western Superior Province lies the North Caribou Terrane, which is a structurally complex tectonic block consisting of several domains (Stott *et al.*, 2010). Other terranes of the Western Superior Province accreted to the North Caribou Terrane throughout the Neoarchean, which makes it an ideal location to study the growth and development of the craton. The most abundant rocks in the North Caribou Terrane are granitoids that contain abundant accessory zircon and titanite, which can reveal the timing of important tectonic and magmatic histories. The rocks in the North Caribou Terrane record a pre-assembly history, as well as offering insight into the final assembly of the Western Superior Province.

This study examines the granitoid intrusive rocks surrounding the North Caribou greenstone belt at the centre of the North Caribou Terrane. I combine new, high-spatial-resolution geochronology on zircon and titanite with mineral and whole-rock geochemistry and thermobarometry to elucidate the magmatic and hydrothermal/ metamorphic processes associated with the assembly of the Superior craton. These data suggest a protracted history of reworking and remobilization of crustal rocks starting by 3.0 Ga and continuing into the Neoarchean. Additionally, timing of most of the major regional accretionary events is recorded in the plutonic rocks of the North Caribou Terrane.

2. REGIONAL GEOLOGY

2.1 Western Superior Province

The Western Superior Province is an Archean craton consisting of east-west-trending greenstone, metasedimentary, and gneissic tonalite-trondhjemite-granodiorite (TTG) terranes, which have been variably intruded by younger granitoids (e.g., Percival *et al.*, 2007). In the north-central part of the Western Superior Province, in an area dominated by TTG suites, lies the North Caribou greenstone belt (NCGB), which is the focus of this study (**Fig. 1**). The area surrounding the NCGB has been subjected to various interpretations attempting to subdivide the Western Superior Province into coherent terranes. The NCGB was originally part of the Cat Lake subprovince of Stockwell (1982) and it was re-assigned to the Sachigo Volcanic Belt originally by Douglas (1973), which was re-defined and re-named the Sachigo Subprovince by Card and Ciesielski (1986). Thurston *et al.* (1991) further subdivided the Sachigo Subprovince into a series of terranes, and the NCGB was placed in the North Caribou Terrane, near the contact with the Muskrat Dam Terrane, which borders the NCGB to the northwest. These divisions were further revised by Easton (2000), who includes the northern edge and western half of the NCGB in the Wachusk metamorphic domain. Recent geophysical studies have led to substantial revisions of domains within the Superior Province (cf. Percival *et al.*, 2006*b*; Percival, 2007; Stott *et al.*, 2010). The most recent of these revisions places the NCGB in the centre of the North Caribou Terrane, at the northern boundary of the North Caribou Core with the Island Lake Domain (Stott *et al.*, 2010). According to these revised terrane boundaries, the granitoids that border the northern margin of the North Caribou Lake greenstone belt belong to the Island Lake Domain (ILD), whereas the greenstone belt itself and granitoids to the south are part of the North Caribou Core. The North Caribou Terrane forms the core of the Superior Province, with evidence from geophysical surveys that other terranes were accreted to its present-day northern and southern margins (Percival *et al.*, 2006*a; b*; Lin *et al.*, 2006).

2.2 The Island Lake Domain

The Island Lake Domain (ILD) was originally distinguished from the North Caribou Core (NCC) by Thurston *et al.* (1991) for containing slightly younger greenstone belts, lacking quartz-rich epicratonic platform sequences, and possessing slightly lower magnetic

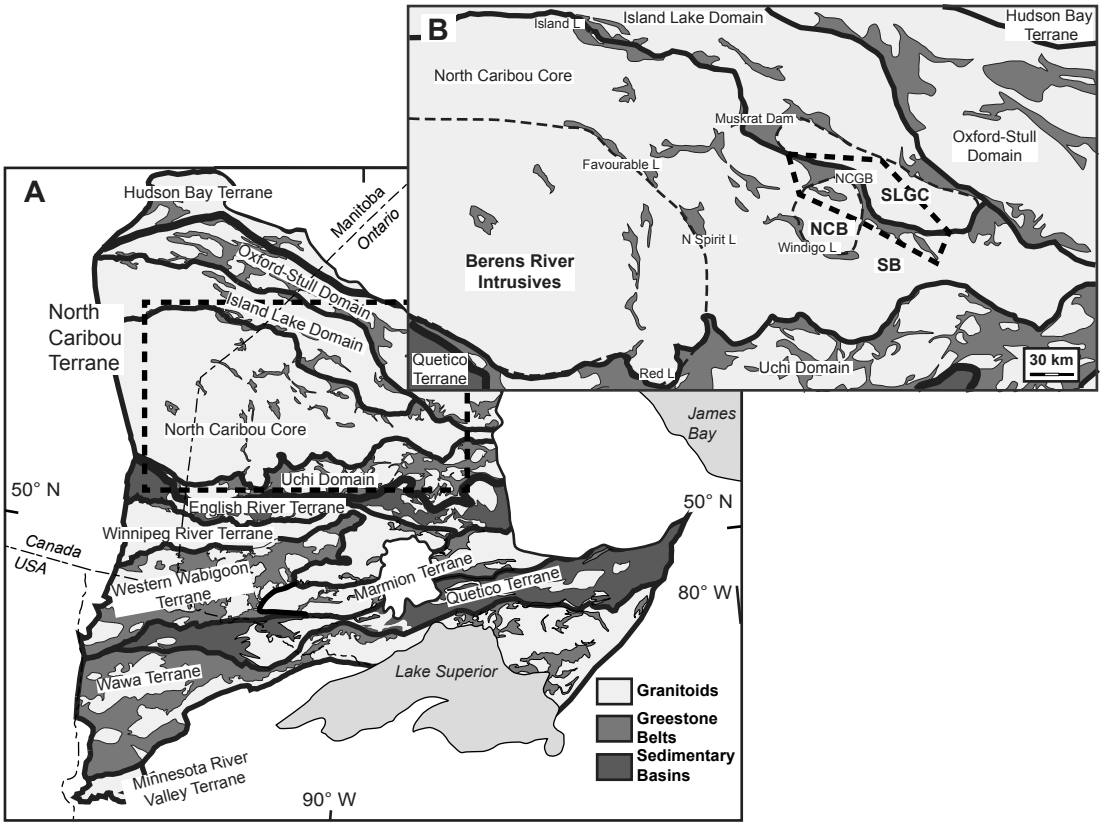

Figure 1: A. Simplified geologic map of the Western Superior Province. Domain boundaries after Stott et al. 2010. B. Simplified geologic map of the greenstone belts of the North Caribou Terrane and intrusive units surrounding the North Caribou greenstone belt. Dashed outline represents location of Figure 2. SLGC: Schade Lake gneissic complex, NCB: North Caribou Lake batholith, SB: Southern batholith. Both maps after Thurston et al. (1991), Stott et al. (2010), and Wyman et al. (2011).

anomalies within the granitic units. However, quartz arenites have been mapped in several belts within the ILD (Donaldson & de Kemp, 1998), suggesting that this criterion may not accurately characterize the ILD. Volcanic sequences in the Island Lake greenstone belt are slightly younger than those in many of the belts in the NCC, with volcanic sequences dated at 2.90 to 2.74 Ga (Corfu & Lin, 2000; Parks *et al.*, 2006), but there is a paucity of geochronologic data from the ILD outside of the Island Lake greenstone belt. Those ages that do exist for other greenstone belts in the ILD are around 2.86 Ga (Stone, 2005), which is similar to some of the younger ages prevalent in the NCC (e.g. Biczok *et al*., 2012). Despite the younger crystallization ages from the greenstone belts in the ILD, Nd and Hf model ages from these rocks are quite old, with most of the early intrusive rocks yielding model ages older than 2.9 Ga (Stevenson & Turek, 1992; Davis *et al.*, 2005). This has led several authors to suggest that the ILD is an original part of the North Caribou Terrane, rather than an accreted terrane (Davis *et al.*, 2005; Parks *et al.*, 2006). The most recent terrane divisions acknowledge the likely common underlying basement or perhaps significant NCC influence on magmas in the ILD, while highlighting the younger volcanic and sedimentary sequences that are absent from the NCC (Stott *et al.*, 2010). In addition to the 2.90-2.85 Ga volcanics and sediments in greenstone belts of the ILD, there is a significant Neoarchean component to these belts—both in crystallization and Nd model ages—with ages between 2.78 and 2.70 Ga (Stevenson & Turek, 1992; Corfu & Lin, 2000; Parks *et al.*, 2006), and this younger component has supported the current division of the ILD from the NCC (Stott *et al.*, 2010). Younger activity in the ILD is evident by post-depositional deformation and Au-mineralization in the Island Lake greenstone belt, which has been dated between 2.69 and 2.66 Ga (Lin & Corfu, 2002).

2.3 The North Caribou Core

Whereas the ILD has supracrustal depositional ages from 2.90 to 2.70 Ga (Stevenson & Turek, 1992; Corfu & Lin, 2000; Parks *et al.*, 2006), supracrustal assemblages of the NCC tend to be between 3.0 and 2.9 Ga (Percival *et al.*, 2006*b*, and references therein), with minor 2.73 Ga supracrustal rocks of the North Spirit Lake and Favourable Lake greenstone belts (Thurston *et al.*, 1991; Stevenson, 1995). Additionally, Nd and Hf isotopic data are similar between supracrustal rocks of the ILD and the NCC, yielding model ages of 2.9-3.0 Ga (Stevenson & Turek, 1992; Stevenson, 1995; Davis *et al.*, 2005; Biczok *et al.*, 2012). Quartz

arenites are fairly common in the greenstone belts within this domain, and accompany nearly every belt (Donaldson & de Kemp, 1998). However, the NCC is dominated by the intrusive rocks of the Berens River magmatic complex, which forms the southwestern side of the domain and extends at least as far east as the North Spirit Lake greenstone belt to the north and the Lang Lake greenstone belt to the south, encompassing an area of ~35,000 km^2 (**Fig. 1b**; Corfu & Stone, 1998*a*). Zircon geochronology indicates a 3.0 to 2.8 Ga tonalitic basement underlying the Berens River Intrusions, which record continuous magmatism from 2.75 to 2.69 Ga (Corfu & Stone, 1998*a*). Structure, geochemistry and thermobarometry within the Berens River Intrusions indicate a east-west extensional regime between 2.75 and 2.72 Ga, which evolved into a north-south compressional regime that was coeval with the Uchi orogeny (Corfu & Stone, 1998*b*), followed by a decrease of pressure likely related to unroofing. The earliest intrusions show interaction with mafic magmas, likely the result of basaltic underplating, and some later intrusions may have been partial melts of this basalt. However, magmas associated with compression show an arc affinity, with increasing continental contamination through time (Corfu & Stone, 1998*a*; Stone, 2000). The most recent Nd-isotopic data generally supports these previous interpretations, and the authors suggest that the data are consistent with north-directed subduction under the North Caribou Core during the accretion of the English River Terrane from 2.75-2.71 Ga (Percival *et al.*, 2006*b*; Stevenson *et al.*, 2009).

2.4 North Caribou greenstone belt

The North Caribou greenstone belt is "z"-shaped in map view and is composed of sequences of metavolcanic and metasedimentary rocks, which have variably been divided into eastern and western branches (**Fig. 2**). Both branches are generally similar, with volcanic rocks on the margins of the belt flanking sedimentary sequences in the centre. In the western branch, the northern and southern volcanic sequences are referred to as the North Rim (NRV) and South Rim Volcanic Assemblage (SRV), respectively, whereas the metasediments form the Eyapamikama Lake Metasedimentary Assemblage (ELS). The far western side of the NCGB is formed by a package of metavolcanics and metasediments of the Agutua Arm and Keeyask Lake Assemblages (Bartlett *et al.*, 1985; Breaks *et al.*, 2001). These rocks represent the oldest material in the belt, as the lower units are intruded by the 2990 ± 1.8 Ma Weagamow batholith (Donaldson & de Kemp, 1998), and the upper

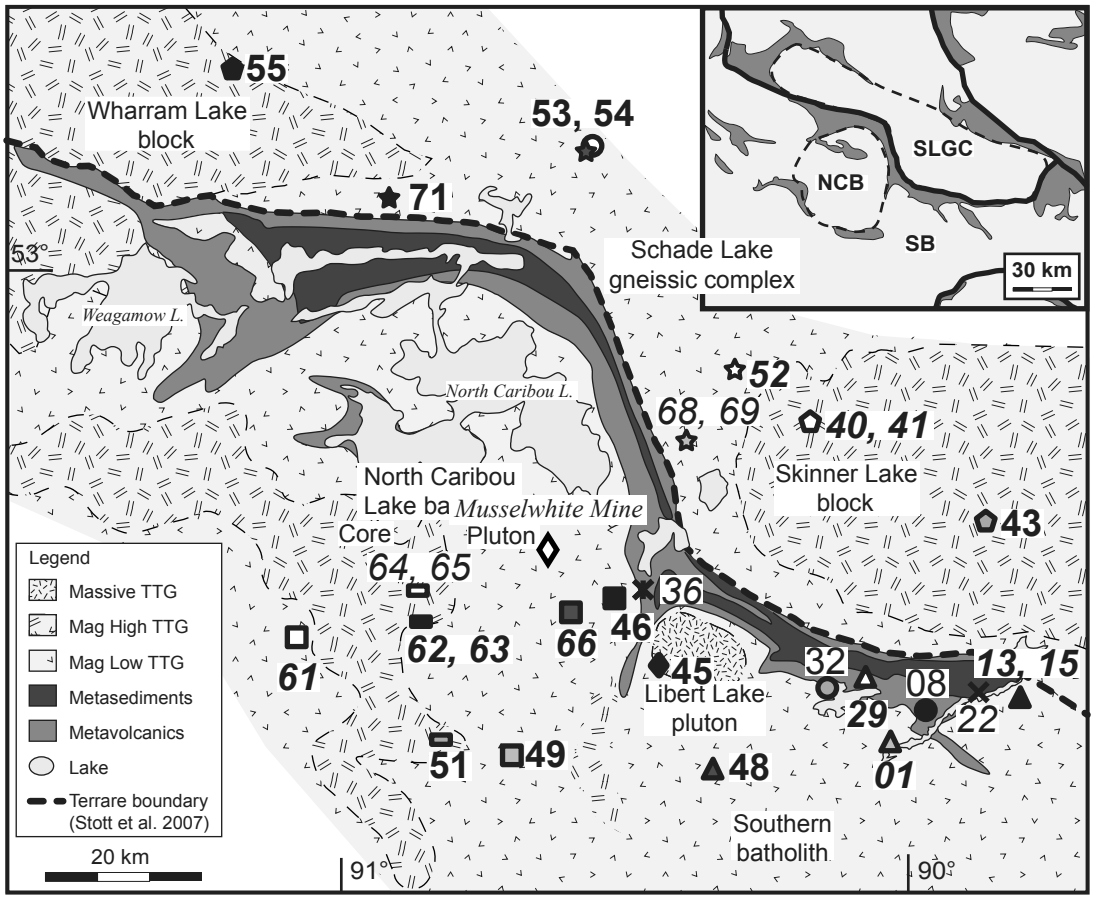

Figure 2: Simplified geologic map of the North Caribou greenstone belt showing location of samples used in this study. Bold labels are samples used for geochronology; italicized labels indicate thermobarometry samples; pegmatites with garnet are neither bold nor italicized. The TTGs are divided based on magnetic signature (Mag high; Mag low). Modified after Wyman et al. (2011), and Ontario Geological Survey (2011).

sequences and have been dated to 2981 ± 1.8 Ma (Biczok *et al.*, 2012). U-Pb ages from the SRV are similar to those from the Keeyask Lake rocks, with one sample from the centre of the belt yielding an age of 2981.9 ± 0.8 Ma, whereas the ages from the NRV are younger, likely < 2870 ± 2 Ga (Davis & Stott, 2001). Rocks of the SRV are tholeiites with occasional intercalated intermediate to felsic flows and tuffs, whereas the NRV, which is also predominately tholeiitic, has scarce felsic units. Textures in both units are massive to pillowed (Breaks *et al.*, 2001). The maximum depositional age of the ELS is similar to the proposed age of the NRV (J. Duff, *personal communication,* 2012).

The sedimentary and volcanic packages in the eastern arm of the NCGB are far more disrupted than their counterparts in the west. The volcanic units in the far eastern part of the NCGB are referred to as the Forester-Neawagank Metavolcanics (FNV), whereas those near the centre of the belt compose the Opapimiskan-Markop Metavolcanic Suite (OMV). The clastic metasediments in this part of the belt are the Zeemel-Pipestone-Heaton Metasediments (Breaks *et al.*, 1987*a*). The only ages from the eastern part of the NCGB are a maximum depositional age of the Heaton metasediments dated by both Davis & Stott (2001) to 2853 ± 1 Ma and Duff (*personal communication,* 2012) to ca. 2720 Ma. The FNV and OMV are primarily mafic to ultramafic massive to pillowed flows, with an abundance of komatiites and very few felsic to intermediate flows (Breaks *et al.*, 2001). Rocks of the OMV underlie and are interfingered with SRV, and Hollings and Kerrich (1999) have interpreted trace elements from these series as a progression from TTG-contaminated magmas with a mantle plume signature to uncontaminated mantle plume melts. Rocks of the FNV have not yet been fully characterized.

At the centre of the NCGB, where the western and eastern branch meet, lies the Musselwhite deposit, a structurally controlled, banded-iron-formation hosted, orogenic gold deposit, with mineralization concentrated in fold hinges and flexures in the fabric (Biczok *et al.*, 2012). Mineralizing fluids have been thought to emanate from the intrusion of the North Caribou batholith/ pluton (Breaks *et al.*, 1984; Stott & Biczok, 2010) or late pegmatitic dykes (Piroshco *et al.*, 1989). Stable isotopic signatures in biotite and quartz primarily support a magmatic origin for mineralizing fluids (Isaac, 2008), whereas trace elements in garnet support a metamorphic fluid source (Duff *et al.*, 2012). Mineralization has been dated using Sm/Nd in garnet to between 2717 ± 14 and 2664 ± 19 Ma (Biczok *et al.*, 2012).

The general metamorphic grade in the NCGB ranges from chlorite to amphibolite facies. Additionally, there are areas of contact metamorphism, most prominently at the margins of the North Caribou batholith to the southwest of the belt, where basalts are locally metamorphosed to amphibolites. There is also minor contact metamorphism surrounding some pegmatitic dykes within sedimentary sequences (Breaks *et al.*, 2001). Breaks *et al.* (2001) estimated the peak metamorphic conditions of medium-grade staurolite-bearing assemblages to be 400-500 °C at 3 kbar or less, which is consistent with garnet-biotite thermometry preformed at Musselwhite Mine (Hall & Rigg, 1986). Otto (2002), however found a wider range of pressures, from 5.1 to 9.4 kbar from garnet-hornblende-plagioclase-quartz geobarometer of Kohn & Spear (1990) and the quartz-biotite-plagioclase-garnet geobarometer of Hoisch (1990), but the temperatures he calculated from various geothermometers are similar to those previously reported.

In addition to the metamorphic pattern, Breaks *et al.* (2001) recognized three deformation events. The first event disrupted and folded fine laminae in banded-iron formations, while the second event formed the prominent regional-scale folding with associated pervasive near-vertical foliation. D_3 is localized and recognized in a gentle and broad folding of the regional foliation. In addition to or accompanying these deformation events are crustal-scale shear zones, which commonly border the NCGB to the north. There is new evidence from in-situ monazite geochronology that some of the shear zones may have remained active into the Paleoproterozoic (Kalbfleisch *et al.*, 2011; Kalbfleisch, 2012).

2.5 Granitoids of the NCGB

Compared to the rocks within the NCGB, the surrounding intrusive felsic rocks are poorly studied, and most workers divide these rocks into units based primarily on air-borne geophysical surveys (Thurston *et al.*, 1979; Ontario Geological Survey, 1991; Ontario Geological Survey, 2011). Since magmatic fluids may be implicated in the mineralization at Musselwhite (Breaks *et al.*, 1984; Piroshco *et al.*, 1989; Isaac, 2008; Stott & Biczok, 2010; Biczok *et al.*, 2012), there has recently been an increased interest in these rocks, with various authors investigating their geochronology (Biczok *et al.*, 2012), whole-rock geochemistry, and Sm and Nd isotopes (Wyman *et al.*, 2011). These authors have divided these rocks based on a combination of geography, amount and type of deformation, composition, and age.

Below I describe the major batholiths, minor plutons, and pegmatites, and discuss what is known of the rocks in each of these categories.

2.5.1 Major batholiths

For most of the mapping history of the NCGB, most of the intrusive rocks have been lumped together into the "grey gneisses" of Satterly (1941) or the migmatites and plutons of Thurston *et al.* (1979). Two primary divisions are consistently distinguished: the Schade Lake gneissic (or intrusive) complex (SLGC), which lies along the northwestern or entire northern margin of the NCGB, and the North Caribou Lake pluton and/ or batholith (NCB), which intrudes the southwestern segment of the NCGB (Thurston *et al.*, 1979; Breaks & Bartlett, 1991; Stott & Biczok, 2010; Wyman *et al.*, 2011). Two additional batholiths, the Eastern and Southern batholiths, have been referenced less often, with the Southern batholith occupying the area southeast of the NCGB and the Eastern batholith lying northeast of the belt when this area is not included in the SLGC (e.g. Wyman *et al.*, 2011; Biczok *et al.*, 2012). Petrogenesis of these rocks is somewhat ambiguous. Many of the 2.75-2.68 Ga felsic intrusive rocks elsewhere in the Superior Province are interpreted as arc-related (Percival *et al.*, 2006*b*), but the origins of the older rocks are more cryptic. Wyman *et al.* (2011) conclude that the TTGs surrounding the NCGB formed as a result of fractional-crystallization of a TTG-type melt and assimilation of pre-existing crustal rocks, with progressively greater amounts of assimilation through time. Although the geochemical data are consistent with a subduction signature, the tectonic setting is poorly understood.

The Weagamow batholith is a discrete intrusion within the Agutua Arm metavolcanic assemblage on the western side of the NCGB. It is approximately 60 km^2 and is the oldest of the intrusive rocks, with a zircon U-Pb age of 2990 ± 1.8 Ma (de Kemp, 1987). Since the first maps of the North Caribou region, authors have noted that the Weagamow batholith is distinct from the other felsic intrusive rocks in the area, and Satterly (1941) describes it as light- to dark-green and less gneissic than the rocks of the North Caribou batholith. Breaks *et al.* (2001), describe the rocks of the Weagamow batholith as predominately trondhjemitic, with up to 10% biotite, but note that some samples also contain small, interstitial K-feldspar crystals. Texturally, the rocks are massive and medium-grained, containing subhedral plagioclase and irregular "clots" of mafic minerals, especially biotite (Breaks *et al.*, 2001).

The Schade Lake gneissic complex (SLGC) was first distinguished from the granitoids south of the NCGB by Breaks *et al.* (1986; 1991), who note that the contact between the NCGB and the intrusive rocks to the north is marked by a zone of high strain, whereas the southern margin of the NCGB is an intrusive contact. As Breaks & Bartlett (1991) only describe the western part of the NCGB, some subsequent authors reserve the SLGC for the rocks bordering the northwestern arm of the NCGB (Wyman *et al.*, 2011), but no authors have reported an intrusive contact anywhere along the northern margin of the NCGB. Some workers have separated the eastern portion of the Schade Lake gneissic complex (i.e. Wyman *et al.*, 2011) as the Eastern batholith, but since there are no geologic features to delineate the two areas, observations and data from the Eastern batholith are included here in the SLGC. The SLGC is large, with an aerial extent of ~8000 km^2, but all of the available data is from rocks no more than 5 km from the margins of the NCGB. Rocks of the SLGC vary in composition and amount deformation, but most are low K-feldspar granitoids that exhibit gneissic textures and contain scattered amphibolitic enclaves (Breaks *et al.*, 2001). One sample from the western part of the SLGC has been dated using zircon U-Pb at 2856 ± 1.8 Ma (de Kemp, 1987), and one sample east of Musselwhite has been dated using zircon U-Pb at 2857 ± 1.4 Ma (Biczok *et al.*, 2012). Wyman *et al.* (2011) analyzed the whole-rock geochemistry of four samples from the eastern part of the SLGC, which they call the Eastern batholith, and both major and trace element patterns are similar to those in granitoids to the south (Southern and North Caribou Lake batholiths), suggesting that all of the TTG rocks are closely related. Isotopic studies of one of these samples had higher εNd, 3.3 (t = 2860 Ma), than any samples previously analyzed in the North Caribou Core (Wyman *et al.*, 2011), implying that these rocks experienced less crustal contamination and a shorter crustal residence time.

The North Caribou Lake batholith (NCB) extends from the south and southwest margins of the NCGB to the Upper Windigo and Horseshoe Lake greenstone belts, an area of ~4000 km^2, and is the best-studied of the major batholiths surrounding the NCGB. Satterly (1941) mapped the rocks of the NCB extensively, but did not distinguish separate mappable units within it, and Thurston *et al.* (1979) named these rocks the North Caribou pluton. Breaks *et al.* (2001) describe the rocks of the NCB as a TTG complex that is typically massive, with stronger foliation and recrystallization near its northern edge, and they

postulate that ballooning diapiric emplacement of the NCB could have folded the NCGB into its present z-shape. This is disputed by Stott & Biczok (2010) who propose that the edge of the NCB, along the contact with the NCGB, is a discrete, younger intrusion—the North Caribou pluton (NCBp)—that was emplaced as a ballooning pluton that deformed the NCGB. Four ages from zircon U-Pb have been obtained from the NCB, and they range from 2870 ± 2 to 2728 ± 1 Ma, with 75% of those ages falling between 2870 ± 1 and 2864 ± 1.1 Ma (de Kemp, 1987; Thurston *et al.*, 1991; Davis & Stott, 2001; Biczok *et al.*, 2012). Wyman *et al.* (2011) analyzed six samples from the NCB for whole-rock geochemistry and found significant variation within the batholith in both major and trace elements; however, the three samples that they analyzed for Nd and Sm isotopes had very consistent εNd values of -1.2 to -1.6 (t = 2860 Ma) indicating a crustal component in the source magma.

The Southern batholith extends from the NCB to the east, bordering the NCGB to the south and east. Rocks in this area are the most poorly understood of the felsic intrusive rocks surrounding the NCGB, with no extensive mapping performed within them. They are described in maps by Breaks *et al.* (1987*a*; *b*) as variably deformed tonalites. There is one age from U-Pb in zircon from the far western edge of the Southern batholith, which, at 2729 ± 7 Ma, is younger than most of the rocks from SLGC or NCB (Biczok *et al.*, 2012). Wyman *et al.* (2011) analyzed seven samples from this area for whole-rock geochemistry, all from the far western side of the batholith, and they found fairly consistent trends in both major and trace elements, which suggests a genetic relationship among their samples. The four samples that they used for Nd and Sm isotopes all gave low εNd values from -1.0 to -5.9 at 2730 Ma, reflecting a significant crustal component in the melt source.

2.5.2 Minor plutons

Plutons were first distinguished from the major batholiths surrounding the NCGB by the geophysical mapping of Thurston *et al.* (1979). These authors recognized the North Caribou batholith as an intrusive pluton and also included Wastayanipi pluton (the Wunnummin Lake pluton of Easton, 2000), which came to be called the Skinner Lake pluton (Wyman *et al.*, 2011). Most authors distinguish the plutons of the NCGB as younger intrusions that cross-cut the major batholiths, and by this definition, several plutons have been added to the Skinner Lake pluton, including the North Caribou pluton along the margin

of the NCB (Stott & Biczok, 2010) and the Libert Lake pluton, which lies south of Musselwhite (Wyman *et al.*, 2011).

The North Caribou Lake pluton is an area of low magnetic susceptibility that lies between the North Caribou Lake batholith and the NCGB. Stott and Biczok (2010) inferred the existence of this intrusion based on the contact metamorphic halo along the southern and western boundaries of the NCGB, the magnetic anomaly, the young U-Pb age (2728 ± 1 Ma; Biczok *et al.*, 2012) from a sample within this area, the curvature of the NCGB along this contact, the orientation of foliation within the NCGB near this contact, and similarities between these features and similarly young plutons in the Wawa and Western Wabigoon Subprovinces (Schwerdtner *et al.*, 1983).

The Skinner Lake pluton is a poorly defined area of high magnetic susceptibility that is slightly to the northeast of the NCGB. There has been no geochronologic work done in this area, and the three samples that Wyman *et al.* (2011) analyzed show significant variation in whole-rock geochemistry and Nd and Sm isotopic compositions.

The Libert Lake pluton (LLP) is likely a collection of approximately round intrusions just south of Musselwhite. Rocks from the Libert Lake pluton are similar texturally and compositionally to pegmatites, and they have low εNd values of -6.8 to -3.5 at 2690 Ma (Wyman *et al.*, 2011). One sample from the LLP was dated using U-Pb in zircon at 2723.1 ± 0.8 Ma (Biczok *et al.*, 2012).

2.5.3 Pegmatites

There are abundant pegmatitic to aplitic dykes throughout the area that have been noted by all authors (Satterly, 1941, Thurston *et al.*, 1979, Breaks *et al.*, 2001). Breaks *et al.* (2001) concluded that these dykes are a late D_2 event, because some are folded and some cross-cut foliation. There is a broad range of compositions observed in these dykes, and they have been of interest as a possible source of Au-mineralizing fluids and deposits of rare metals, including Li, Rb, Ta, and Sb (Piroshco *et al.*, 1989). A subset of these pegmatites, primarily those that intrude metasedimentary rocks, are S-type granitoids and contain fluorite, tourmaline, muscovite, and/ or garnet (Breaks *et al.*, 2001). Some of these S-type, or in Wyman *et al.* (2011), leucogranitic, pegmatites are found in mineralized zones of the Musselwhite deposit (Piroshco *et al.*, 1989). Two U-Pb ages from monazite, 2715.8 ± 1.6 Ma and 2668.8 ± 1.1 Ma, were obtained from leucogranitic pegmatitic dykes near Musselwhite,

which are similar to the age of the Libert Lake pluton (Biczok *et al.*, 2012). Chemically, the pegmatites are rich in SiO_2 and are characterized by extreme (high or low) concentrations of incompatible trace elements when compared with the other plutonic rocks (Wyman *et al.*, 2011). Throughout the Superior Province, the late pegmatites have been interpreted as partial melts of supracrustal as well as plutonic rocks, and Wyman *et al.* (2011) conclude that the same is true of the pegmatites in the NCGB.

3. METHODS & RESULTS

3.1 Mapping and petrology

In the following sections, I present new petrologic observations, and geochemical and geochronologic data from granitoids surrounding and intruding the NCGB to expand our understanding of the internal anatomy of the intrusions and refine models describing the evolution of the North Caribou Terrane. Mapping and petrologic work identified two distinct groups of felsic plutonic rocks in the region: i) voluminous, massive to gneissic tonalite, trondhjemite, and granodiorite (TTG) batholiths and plutons and ii) massive, pegmatitic to aplitic dykes.

The samples used in this study were collected during the summers of 2010 and 2011, and field sites were principally accessed by helicopter. I collected all of the samples, except samples T-05, T-06, and T-25, which were collected by Netasha Kalbfleisch in the summer of 2010.

3.1.1 TTG suites

The TTG intrusions have a wide variety of compositions, ranging from tonalites to granites (*sensu stricto*). Important accessory minerals include biotite, hornblende, titanite, zircon, apatite, pyrite, magnetite, and epidote. Epidote tends to be spatially associated with centimeter-scale crosscutting quartz veins, which are found in all rock types, but occasionally it occurs as inclusions in biotite. The TTG suites are ubiquitously deformed, and exhibit deformation structures in quartz along with planar alignment of biotite and occasionally, hornblende or titanite. Most TTG rocks also contain some compositional differentiation, if not well-formed gneissic banding. In addition to gneissocity, textures in many outcrops, such as schlieren and blebby leucocratic patches, suggest that these intrusions experienced a complex history of multiple cross-cutting intrusions, magma mixing, melt segregation, deformation, or partial re-melting. There is no obvious pattern to deformation styles, although most of the samples with strong planar fabric are located immediately adjacent to the supracrustal rocks. In addition, the centres of the large intrusive provinces are dominated by gneissic fabrics.

TTG rocks were divided into six separate units based on previous mapping and geophysical characteristics (**Fig. 2**). I use batholith to designate an area of intrusive rock lacking both a consistent geophysical signature and a clear intrusive boundary, whereas

pluton is reserved for an area that is geophysically homogenous and has a clear contact with the surrounding rock. Three general intrusive areas are the Schade Lake gneissic complex (SLGC), which includes all of the intrusive rocks north of the NCGB, the North Caribou batholith (NCB), comprised of the rocks southwest of the NCGB, and the Southern batholith, containing the rocks to the southeast of the NCGB (**Fig. 2a**). All of these areas are geophysically complex and may be composed of distinct domains. The SLGC includes two such areas delineated by high magnetic anomalies: the Skinner Lake and Wharram Lake blocks (SLB and WLB, respectively; **Fig. 3**). The SLB is located roughly near the Skinner Lake pluton as illustrated on Ontario Geological Survey maps (1991, 2011), but it more closely matches the boundaries of the Wastayanipi pluton of Thurston *et al.* (1979). It is northeast of Musselwhite and extends west, approximately paralleling the NCGB, covering a total of ~2000 km^2. The WLB, ~200 km^2, is located north of the western branch of the NCGB, centred between the NCGB and the Muskrat Dam Lake greenstone belt. The NCB is also divided into domains after Stott & Biczok (2010). The low-magnetic-susceptibility ring around the NCB forms the North Caribou Lake batholith pluton (NCBp), whereas the area of high magnetic susceptibility in the centre is the North Caribou Lake batholith core (NCBc). The delineation of the NCBp is slightly different from that of Stott & Biczok (2010) due to new air-borne geophysical surveys conducted by Musselwhite Mine. The final intrusive body is the Libert Lake pluton (LLP), which is an area of ~100 km^2 of low magnetic susceptibility directly south of Musselwhite. The outline of the LLP used here is more similar to that of Biczok *et al.* (2012), than the definition used by other authors (e.g. Wyman *et al.*, 2011).

3.1.2 Pegmatites

These younger intrusive units crosscut all rock types and typically occur as convoluted, brittle-ductile dykes (**Figs. 4a, b**). There are two types of pegmatitic rocks: a suite dominated by K-feldspar, referred to as K-feldspar pegmatites, and a series of S-type intrusions, herein leucogranitic pegmatites. Both types of pegmatites are texturally similar, and vary from coarse pegmatites (crystals ≥ 1cm in diameter) to aplites, and both textures are frequently found in the same intrusion, with pockets of pegmatites usually surrounded by aplitic material (**Fig. 4d)**. Additionally, both suites are also weakly deformed, exhibiting undulose extinction in quartz, but not preferential alignment of minerals. Generally, and somewhat surprising, zircon and titanite are absent from pegmatites, although one K-feldspar

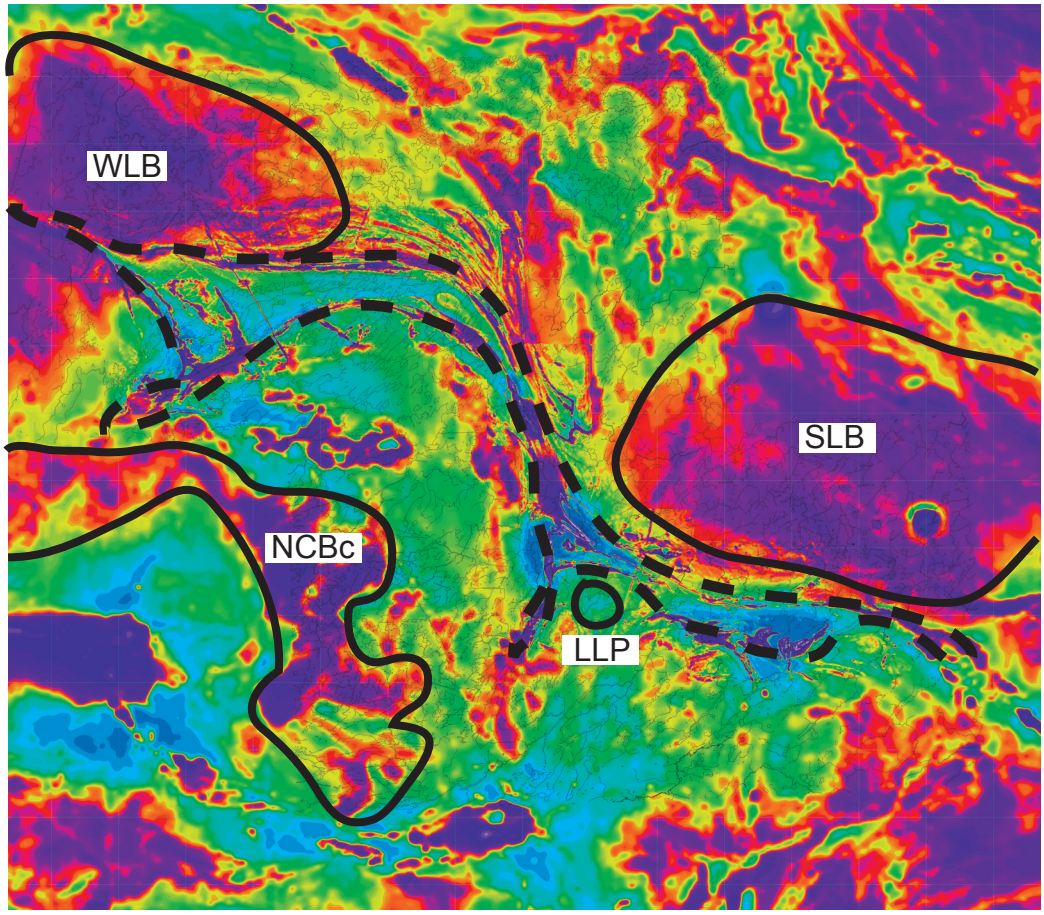

Figure 3: Areomagnetic map of the North Caribou greenstone belt (NCGB). Dashed outline represents location of the NCGB. NCBc: North Caribou Lake batholith core, SLB: Skinner Lake block, WLB: Wharram Lake block, LLP: Libert Lake pluton.

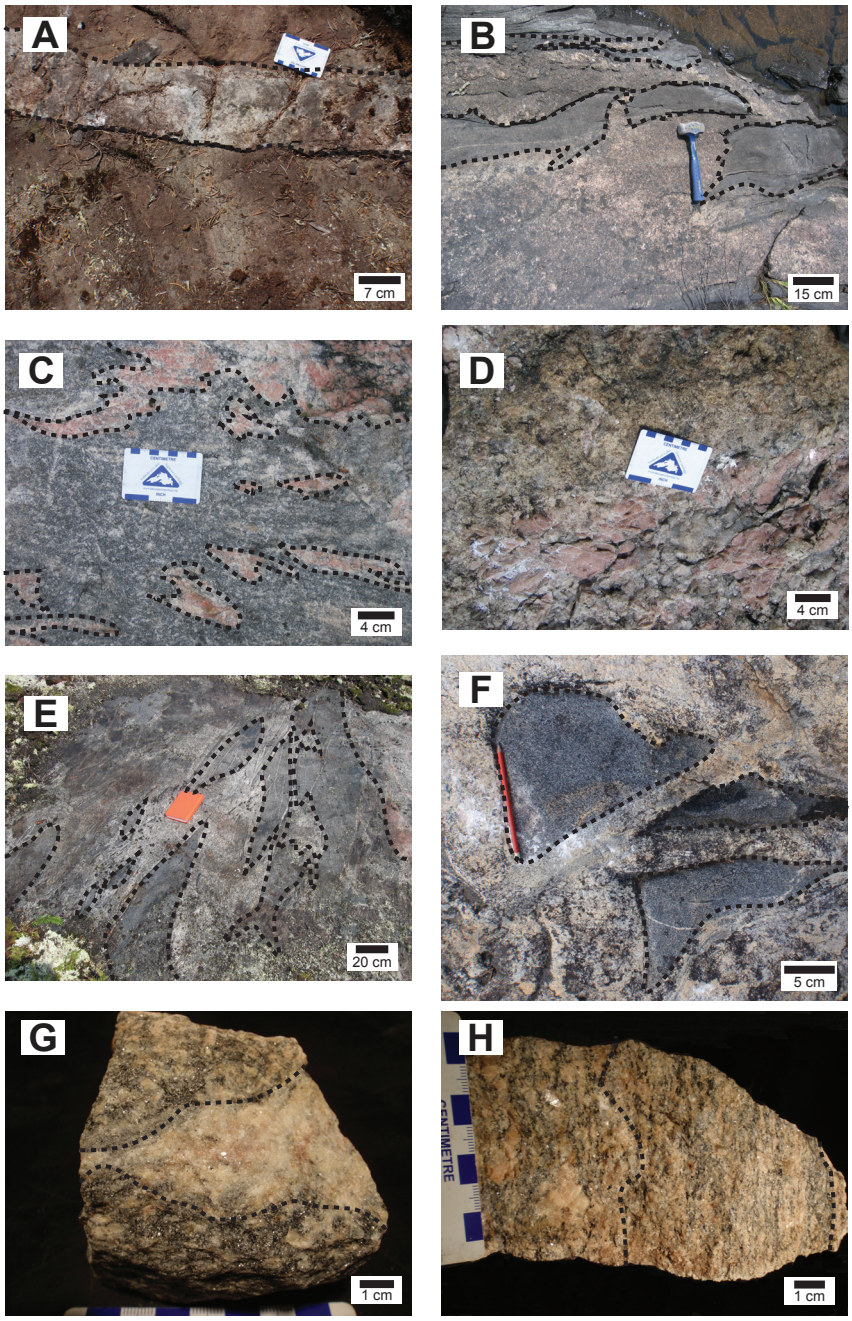

Figure 4: A. Field photo of pegmatitic dyke (sample 72) intruding metawacke. Note the sharp contacts suggesting shallow intrusion. B. Field photo of brittle-ductile pegmatitic intrusion into amphibolite (sample 2). Note the prominent foliation-normal opening direction. C. Field photo of coarse-grained, blebby pegmatitic material in deformed TTG (sample 40). The lack of connection between the pegmatitic pockets suggests an in-situ partial melt. D. Field photo of coarse- and fine-grained pegmatites (sample 37). E. Field photo of schlieren structure in TTG (sample 51). Diffuse contacts make nature (intrusion, disarticulated gneissic bands, melt segregation, etc.) ambiguous. F. Field photo of amphibolite enclaves in TTG (samples 64, 65). Sharp contacts indicate an intrusive contact between TTG and amphibolite. G. Hand sample photo of wormy-textured pegmatite parallel to foliation in TTG. Quartz-epidote vein was to the right (outside of photograph; sample 71). H. Hand sample photograph of coarse-grained, k-spar-rich (left) and fine-grained, k-spar-poor (right) bands in sample 53. Geochronology indicates that mafic bands are xenolithic.

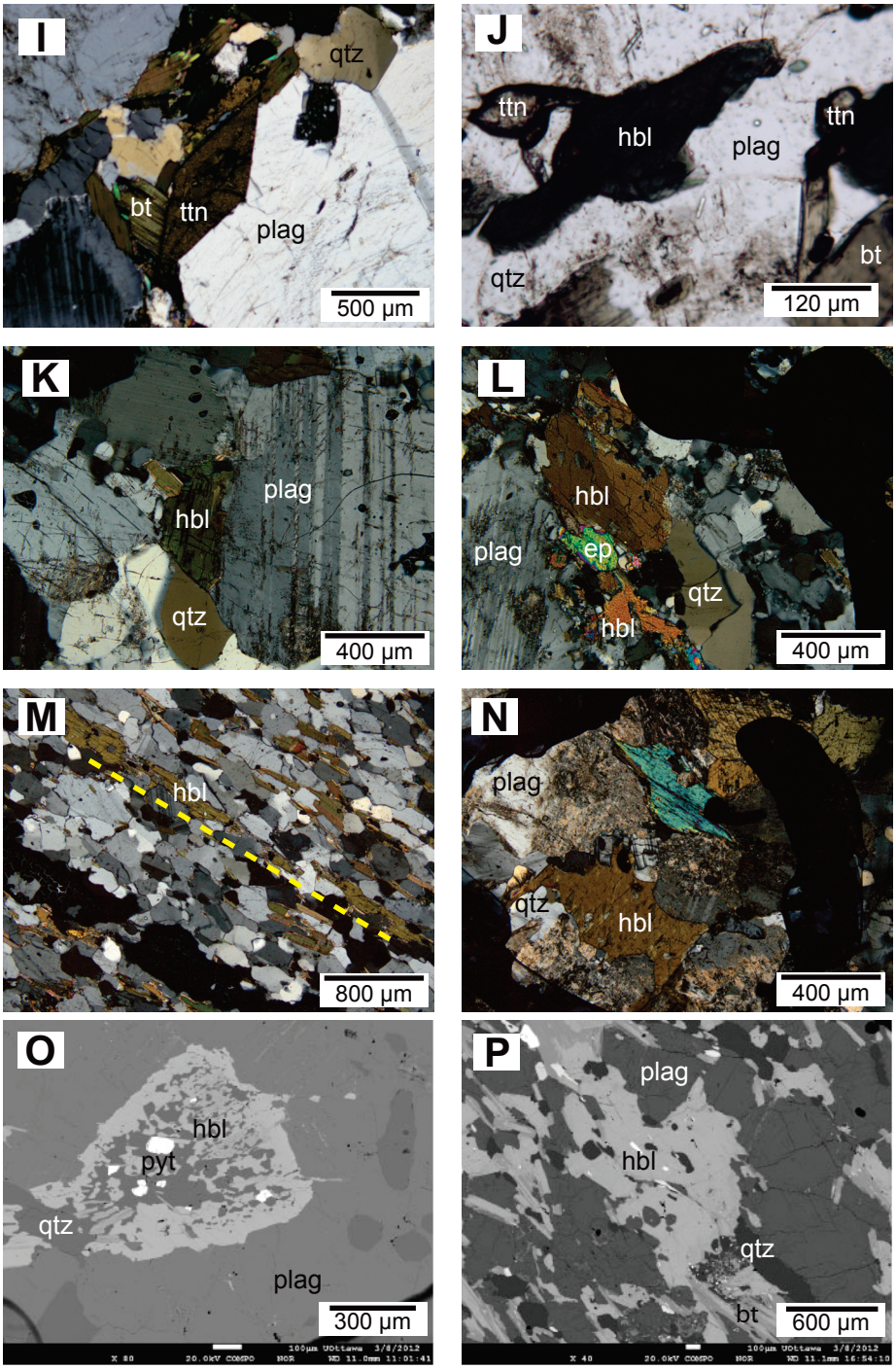

Figure 4 (cont.): I. Crosspolar photomicrograph of igneous titanite with metamorphic overgrowths aligned with foliation (sample 29). J. Plane-polarized photomicrograph of round metamorphic titanite (sample 66). K. Crosspolar photomicrograph of primary igneous hornblende without overgrowths (sample 01). L. Crosspolar photomicrograph of hornblende with hydrothermally altered rims (sample 15). M. Crosspolar photomicrograph of metamorphic hornblende aligned within foliation (sample 36). N. Crosspolar photomicrograph of "contact metamorphism" hornblende (sample 40). O. Backscatter (BSE) photomicrograph of hornblende with magmatic cores and metamorphic rims (sample 64). P. BSE photomicrograph of hornblende with magmatic cores and overgrowths (sample 22).

pegmatite did have abundant, U-rich (> 3000 ppm) zircons. K-feldspar pegmatites are found in all rock types and throughout the entire study area, whereas the leucogranites were only found within the greenstone belt, and they have been observed intruding both supracrustal and intrusive rocks. These two pegmatites are also mineralogically distinct, with K-feldspar pegmatites containing K-feldspar, quartz, plagioclase, and minor oxides and sulphides, primarily magnetite and pyrite. Leucogranites tend to have approximately equal amounts of K-feldspar, plagioclase and quartz, as well as biotite and muscovite, and minor pyrite and magnetite. Leucogranites in the west contain fluorite, whereas those in the east contain garnet.

3.2 Whole-rock geochemistry

Samples for whole rock geochemistry were prepared following standard methods for crushing and homogenization using ~40-100 cm^3 of rock. Major elements were analyzed using x-ray fluorescence (XRF) of pressed pellets at Memorial University of Newfoundland, St. John's, Canada (samples 01-52), and fused disk at the University of Ottawa, Ottawa, Canada (samples 53-75), and results are reported in **Appendix A**. Minor, trace, and some major elements were analyzed using solution inductively coupled plasma mass spectrometry (ICP-MS) at Actlabs, Inc. commercial laboratories in Ancaster, Ontario. For ICP-MS, rock powders were fused into glass beads using a sodium peroxide flux and dissolved in a nitric acid solution. Data from these analyses are reported in **Appendix B**. Whole-rock geochemistry was conducted on 58 samples from felsic intrusions within and around the NCGB. Sample locations from the various intrusive units described above are listed in **Table 1.** Rock types were determined using both QAP discrimination diagram of Streckeisen (1976) with stained hand samples and the normative feldspar An-Ab-Or plot of Barker (1979; **Fig.5**). Normative mineralogy was calculated after the methods of Irvine & Baragar (1971) and Kelsey (1965). All of the tonalites classified from the QAP diagram could also be considered trondhjemites, since they are light-coloured and contain plagioclase with 50-10% An (Streckeisen, 1976).

3.2.1 TTG samples

Forty-one samples from various TTG suites were analyzed. Unsurprisingly, tonalites, trondhjemites, and granodiorites are the dominant rock types, but about 20% of the rocks sampled were granites (*sensu stricto*). There is no obvious spatial relationship between rock

Table 1. Summary of sample locations and geochemistry of granitoids surrounding the NCGB

Sample	Zone	Northing	Easting	QAP	Norm feldspar	A/CNK	Norm Al	Mg/Mg+Fe
Southern batholith (SB)								
21/22	16U	0307985	5815908	tonalite (tdj)	granodiorite	1.07	17	0.33
47	15U	0675894	5808189	tonalite (tdj)	trondhjemite	1.17	16	0.32
1	16U	0296863	5810470	granodiorite	tonalite	0.99	17	0.43
13/14/15	16U	0310834	5816368	granodiorite	ton/gd	0.93	18	0.41
29	15U	0700588	5816951	granodiorite	trondhjemite	0.96	18	0.43
31	15U	0697343	5815952	granodiorite	trondhjemite	1.06	17	0.37
T-06	15U	0689801	5820721	granodiorite	trondhjemite	1.13	15	0.26
T-07	15U	0689801	5820721	granodiorite	trondhjemite	1.07	16	0.24
18	16U	0299825	5811858	granite	granite	1.10	16	0.35
19	16U	0301660	5811876	granite	granite	1.25	15	0.20
44	15U	0679326	5823497	granite	granite	1.16	14	0.21
48	15U	0681996	5807305	granite	granite	1.16	16	0.27
Schade Lake gneissic complex (SLGC)								
52	15U	0683290	5858973	tonalite (tdj)	tonalite	1.00	17	0.35
56	15U	0634556	5874381	tonalite (tdj)	gd/granite	1.07	14	0.21
69	15U	0676773	5846763	tonalite (tdj)	tonalite	1.05	16	0.28
9	16U	0312341	5820351	granodiorite	granodiorite	1.08	18	0.48
11	16U	0312529	5820258	granodiorite	granodiorite	1.10	17	0.47
71D	15U	0638939	5872856	granodiorite	trondhjemite	1.00	16	0.22
53	15U	0663611	5880262	granite	granite	1.10	14	0.21
Wharram Lake block (WLB)								
55	15U	0618918	5890381	granodiorite	trondhjemite	1.05	15	0.29
Skinner Lake block (SLB)								
40	15U	0696956	5846596	tonalite	tonalite	1.05	17	0.33
41	15U	0697277	5846200	tonalite	tonalite	1.05	17	0.33
42D	15U	0696892	5846718	granodiorite	tonalite	1.09	17	0.34
43	16U	0312332	5832188	granite	granite	1.13	16	0.35
North Caribou batholith - pluton (NCBp)								
36	15U	0673225	5826758	tonalite (tdj)	tonalite	1.08	18	0.38
66	15U	0664274	5823980	tonalite (tdj)	tonalite	0.83	21	0.33
58	15U	0624633	5852125	tonalite (tdj)	tonalite	1.03	16	0.22
38	15U	0679809	5825663	granodiorite	trondhjemite	1.11	14	0.21
46	15U	0670528	5826608	granodiorite	granodiorite	1.07	17	0.33
49	15U	0659278	5807236	granodiorite	trondhjemite	1.10	16	0.32
74A	15U	646996	5862814	granodiorite	trondhjemite	1.05	14	0.22
75	15U	0648398	5864400	granodiorite	trondhjemite	1.06	16	0.24

Table 1. (cont)

Sample	Zone	Northing	Easting	QAP	Norm feldspar	A/CNK	Norm Al	Mg/Mg+Fe
North Caribou batholith - core (NCBc)								
59	15U	0621890	5845269	tonalite (tdj)	tonalite	1.07	16	0.24
61	15U	0628579	5822056	tonalite (tdj)	trondhjemite	1.05	14	0.25
62	15U	0643708	5823562	tonalite (tdj)	tonalite	1.07	17	0.26
63	15U	0643708	5823562	tonalite (tdj)	tonalite	0.99	18	0.24
64	15U	0644882	5827930	tonalite (tdj)	tonalite	0.93	22	0.29
65	15U	0644882	5827930	tonalite (tdj)	tonalite	1.05	18	0.23
51	15U	0645355	5807490	granite	trondhjemite	1.07	18	0.34
60	15U	0628579	5822056	granite	gd/granite	1.05	14	0.22
Libert Lake pluton (LLP)								
45	15U	0677508	5818236	granite	granite	1.10	16	0.27
K-feldspar pegmatites								
2	16U	0296863	5810470	granite	granite	1.15	14	0.08
5	16U	0299692	5810283	granite	granite	1.00	14	0.16
10	16U	0312341	5820351	granite	granite	1.14	14	0.06
26	15U	0699957	5815428	granite	granite	1.13	16	0.00
28	15U	0699955	5815378	granite	granite	1.13	16	0.11
37	15U	0673225	5826758	granite	granite	1.12	8	0.06
42L	15U	0696892	5846718	granite	gd/granite	1.15	15	0.20
50	16U	0659278	5807236	granite	granite	1.13	15	0.06
54	15U	0663611	5880262	granite	granite	1.08	13	0.15
67	15U	0664274	5823980	granite	granite	1.06	14	0.19
71P	15U	0638939	5872856	granite	trondhjemite	1.05	15	0.26
74B	15U	646996	5862814	granite	granite	1.04	12	0.16
Leucogranitic pegmatites								
8	16U	0301329	5813410	granite	granite	1.19	17	0.10
32	15U	0696480	5816013	granite	granite	1.14	16	0.08
70	15U	0627908	5868742	granite	granite	1.18	14	0.21
72	15U	0657307	5867652	granite	trondhjemite	1.24	14	0.25
T-25	15U	0694245	5824386	granite	granite	1.04	14	0.21

Notes:

Coordinates are UTM NAD 83

QAP rock types based on stained handsamples and Steckeisen (1976); tonalites all light-coloured

Normative feldspar rock types from Barker (1979)

A/CNK: $Al_2O_3/(CaO+Na_2O+K_2O)$

Norm Al: Al_2O_3 for 70 wt% SiO_2; >15 high-Al TTG (Barker & Arth, 1976)

Tdj: trondhjemite, gd: granodiorite, ton: tonalite

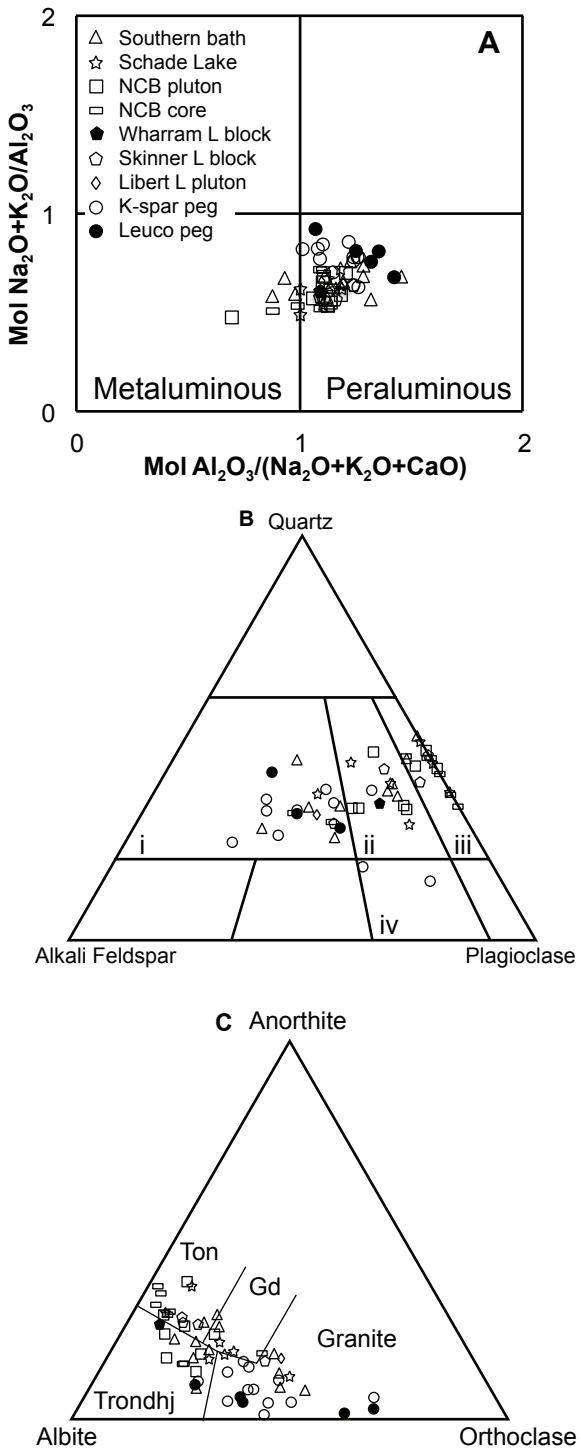

Figure 5: Major element discrimination diagrams of granitoids from this study. A. Shand's index after Maniar & Piccoli (1989). B. QAP diagram after Streckeisen (1979). Modal mineralogy estimated from stained hand samples. Fields: i: granite, ii: granodiorite, iii: tonalite, iv: monzodiorite C. Normative feldspar discrimination diagram after Barker (1979). Ton: tonalite; Gd; granodiorite; Trondhj: trondhjemite. All of these diagrams show relatively narrow, linear compositional variations.

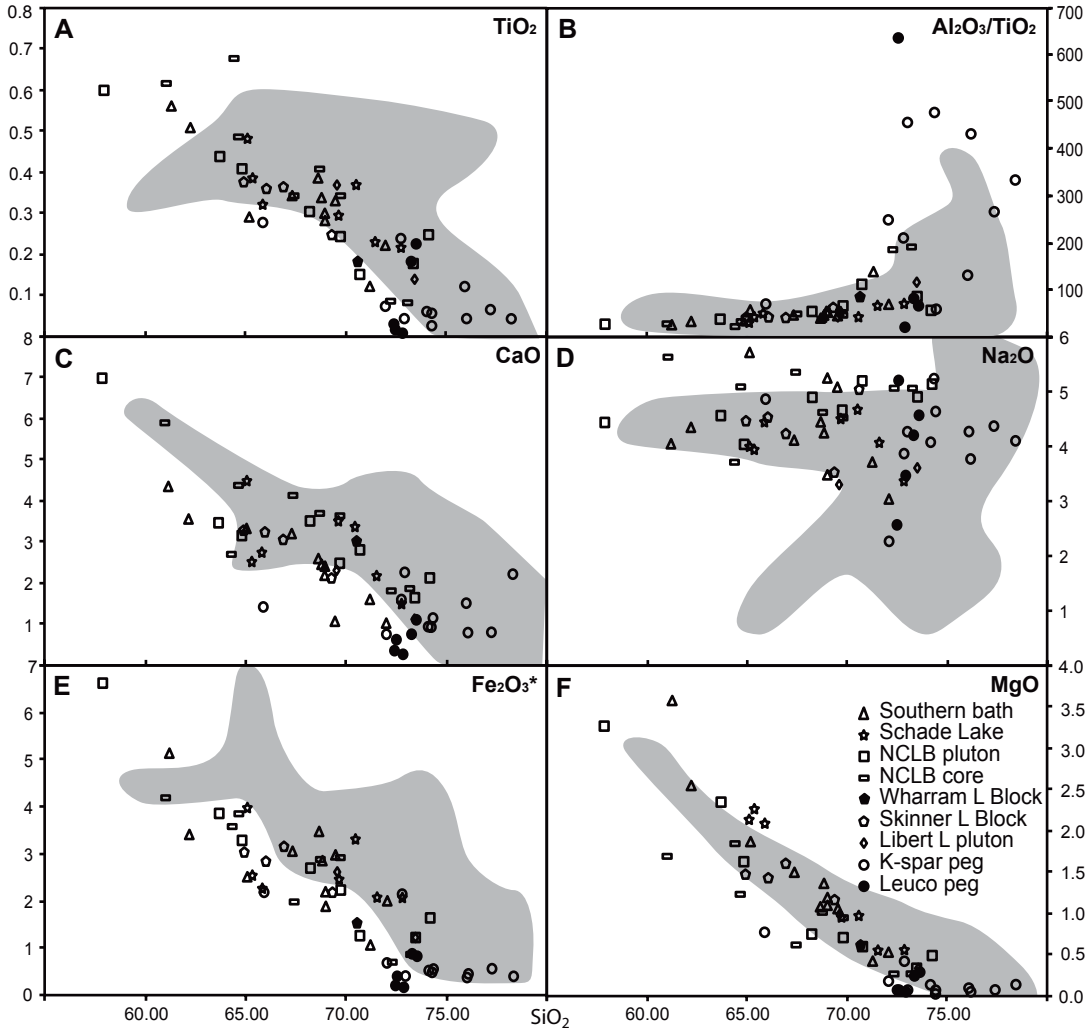

Figure 6: Harker-type diagrams (weight percent major oxides versus SiO_2) of granitoids from this study. Shaded fields indicate TTG samples of the North Caribou Terrane from Wyman et al. (2011). The rocks analyzed in this study generally overlap the compositions reported by Wyman et al. (2011).

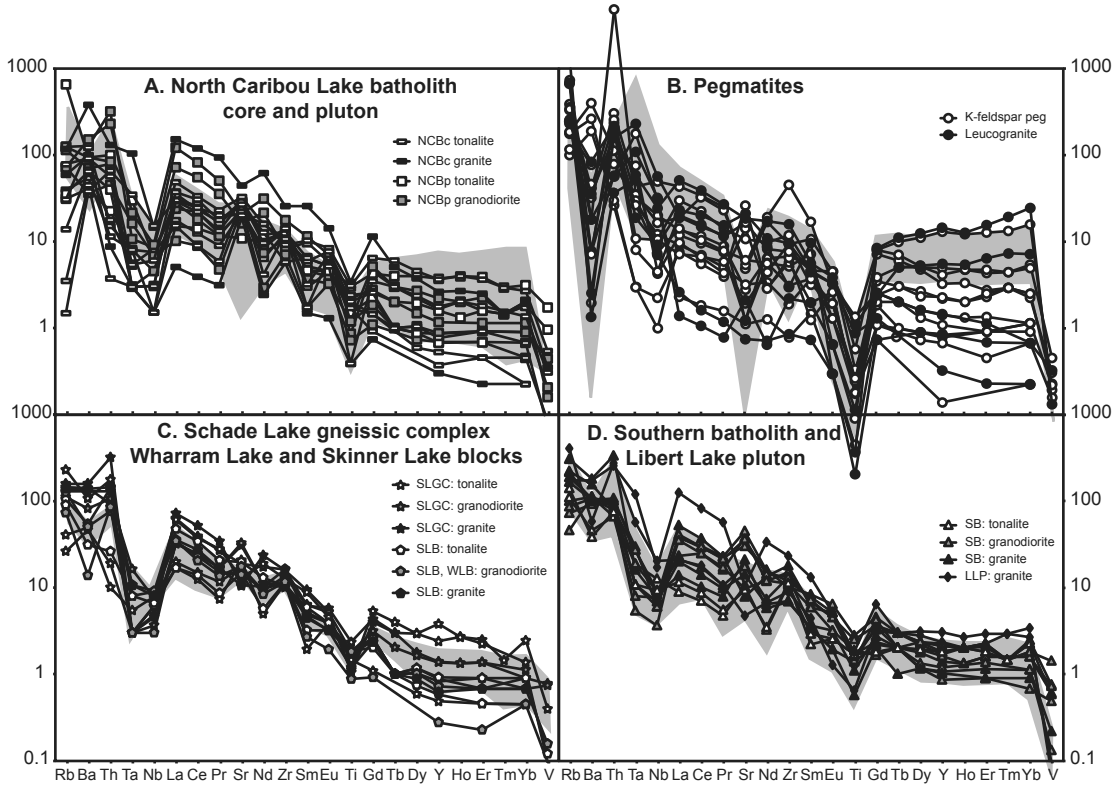

Figure 7: Primitive-mantle-normalized spider diagrams of granitoids from this study. Normalizing values from McDonough & Sun (1995). Shaded areas are ranges reported by Wyman et al. (2011). These plots show similar trace element patterns among all of the TTG samples, but distinctly different patterns in pegmatites.

types or chemistry. In Harker-type major element discrimination diagrams, the samples from all of the TTGs form coherent trends in both major and trace elements as a function of SiO_2 (**Figs. 6 & 7**). Trace element concentrations range over ~2 orders of magnitude, but the consistent patterns exhibit strong negative Ta, Nb, and Ti anomalies, no Eu anomaly, and negative slopes in rare earth elements (REEs), which are steeper in LREEs (La-Gd; La/Gd: 45-4) than in HREEs (Gd-Yb; Gd/Yb: 1-7). Most of the TTG samples are high-Al rocks typical of Archean terranes as described by Barker & Arth (1976) with greater than 15 wt% Al_2O_3 at 70% SiO_2, and most are also weakly peraluminous (cf. Miller, 1985). These rocks have high Mg concentrations, within the range on sanukitoids, which are common in the southern Superior Province (*Percival et al.*, 2006*b*), but have Ni and Cr concentrations far below typical sanukitoid values reported by Shirey & Hanson (1984), so the TTGs in this area are not sanukitoids. Based on mineralogy and composition, the TTGs conform most closely to I-type granitoids (e.g. Frost *et al.*, 2001) and are generally TTGs (*sensu stricto*) as defined by Moyen and Martin (2012). All of the geochemical signatures of these samples are similar to those reported by Wyman *et al.* (2011).

3.2.2 Pegmatites

Seventeen samples of pegmatites were analyzed, 12 from K-feldspar pegmatites and 5 from leucogranitic pegmatites. In major element compositions, both pegmatite suites follow the trends displayed in the major elements, but there is more scatter within the pegmatite data than in the TTG data (**Fig. 6**). Additionally, despite the relative homogeneity of the mineralogy of these rocks, there is a large range (2 orders of magnitude) in trace element distributions, with similar patterns in both pegmatite suites (**Fig. 7b**). Primitive-mantle normalized spider diagrams show very different patterns between TTGs and pegmatites, with strong negative Ba and Ti and positive Th anomalies and a slight positive slope in HREEs in pegmatites. Pegmatites are generally not high-Al rocks, as defined by Barker (1979), but tend to be strongly peraluminous. Geochemically, the pegmatites analyzed in this study are similar to the pegmatites and rocks of the Libert Lake pluton analyzed by Wyman *et al.* (2011).

3.3 Garnet major and trace element geochemistry

To characterize the source of the pegmatites, garnets from two S-type pegmatites intruding the central sedimentary sequence in the eastern arm of the NCGB were analyzed.

Both samples were leucogranitic, containing about 30% quartz, 30% alkali feldspar, and 30% plagioclase, in addition to biotite, muscovite, and garnet.

Major elements in the garnets were analyzed in a rim-to-core transect on the Camera SX-100 electron microprobe at New Mexico Tech, Socorro, USA, with an accelerating voltage of 15 kV and beam current of 20 nA. Trace element concentrations were collected from individual spots on rims and cores using the LA-ICP-MS on the Photo-Machines Analyte 193 μm ArF Excimer laser coupled with an Agilent 7700 quadrupole ICP-MS at the Geologic Survey of Canada, Ottawa, Canada. A beam diameter of 43 or 52 μm was used in static mode with a repetition rate 16 Hz. Each ablation of 60 seconds was preceded by 45 seconds on background counting, and concentrations were calibrated with BCR-2G and GSD-1G synthetic glasses. The time-resolved signals for each analysis were reduced using the GLITTER data reduction software developed by ARC National Key Centre for Geochemical Evolution and Metallogeny of Continents and CSIRO Exploration and Mining. Mean Ca concentrations from microprobe analysis were used as an internal standard. Major and trace element analyses are reported in **Appendices C & D** respectively.

3.3.1 08: Pegmatitic leucogranite intruding metabasalt

Garnets in this sample were rather large, with an average diameter of ~1 cm. They also contained abundant inclusions of quartz, biotite, oxides, and sulphides. To determine the major element characteristics of these garnets, three transects on two garnets were analyzed. All of the transects show equal parts spessartine and almandine, with negligible Ca (< 0.04 atoms per formula unit; apfu) and Mg (< 0.10 apfu), in the cores, which grades into rims that are ~20% spessartine and ~80% almandine. At the rims of the crystals, there is a moderate to sharp increase of spessartine content, with a corresponding drop in almandine content, to near 30% spessartine and 70% almandine (**Fig. 8a**).

For trace elements, two spots were analyzed from the cores and rims of both garnets. Both rims and cores have a pronounced negative Eu anomaly ($Eu/Eu^* < 0.002$), and similar, high concentrations of heavy REEs. Cores, however, show an enrichment of light REEs over rims (**Fig. 9a**).

3.3.2 32: Pegmatitic leucogranite

In this sample, garnets were about 1 mm in diameter, and generally inclusion-free, although some crystals were intergrown with biotite, and a few nucleated on sulphides or

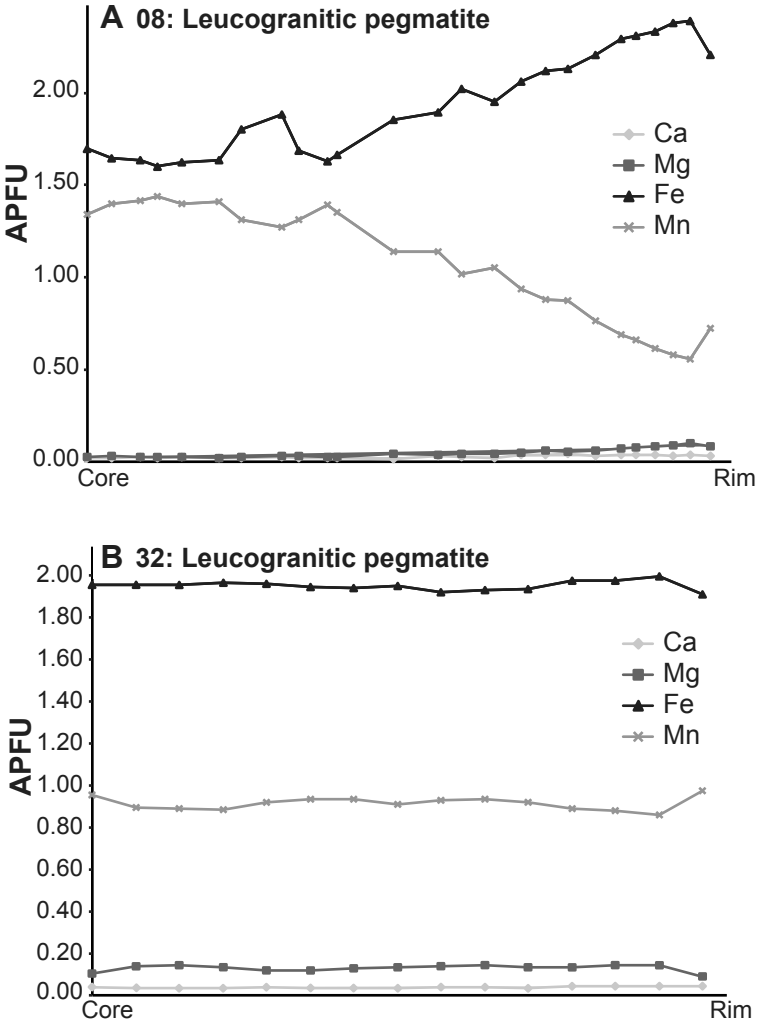

Figure 8: Representative core to rim major element transects of igneous garnets reported in atoms per formula unit (APFU). Both samples show rim effects of Mn enrichment and Fe depletion, but the garnets from sample 8 also show much more pronounced compositional zoning throughout the garnet.

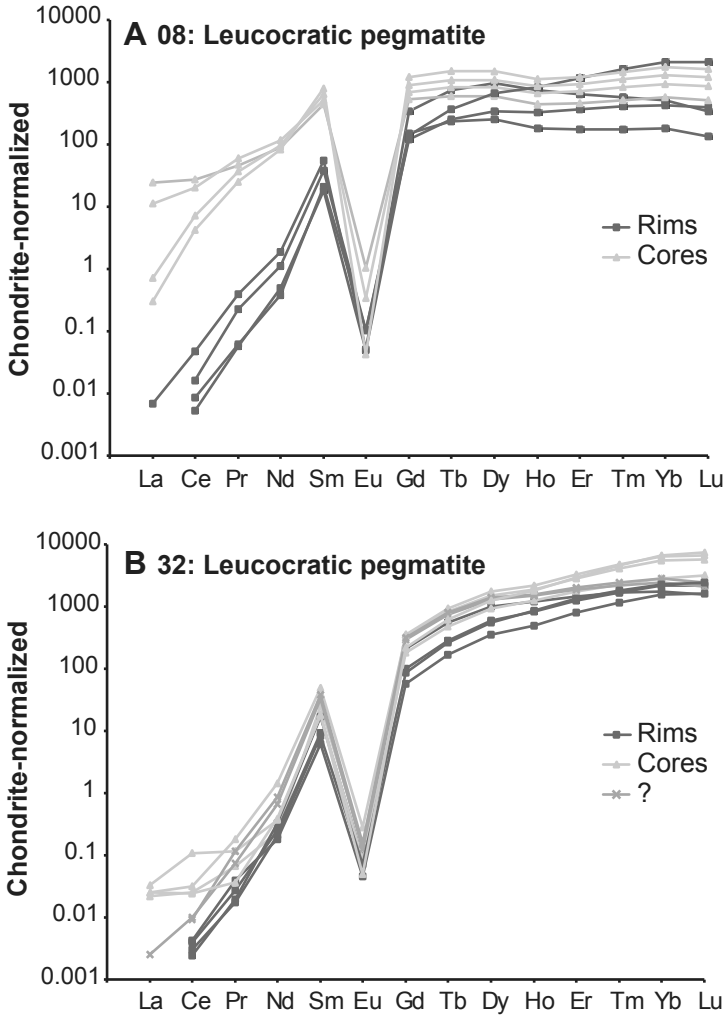

F*igure 9: Chondrite-normalized REE plots for garnet cores and rims. Data collected via LA-ICPMS. Normalizing values from McDonough & Sun (1995). As in major elements, sample 8 shows distinct rim and core compositions, where the zoning in sample 32 is subtler.*

quartz. Major element concentrations were characterized by 6 core-to-rim transects on 6 crystals. Garnets in this sample are much more homogenous, and have a more significant pyrope component (about 5-10% Mg), which follows the same trends as the almandine component, although major element chemistry is still dominated by Fe and Mn. These garnets have cores that are slightly enriched in spessartine compared to rims (30% and 25%, respectively), with an inverse pattern in almandine (~65% in cores to ~60% in rims). Similar to sample 08, at the edge of the crystal, there is a sharp increase in spessartine, and a decrease in both pyrope and almandine (~65% almandine, ~30% spessartine, and ~5% pyrope; **Fig. 8b**).

Ten spots were analyzed for trace elements in this sample: 4 from cores, 4 from rims, and 2 that were a mix of core and rim compositions. Similar to sample 08, there is a prominent negative Eu anomaly ($Eu/Eu^* < 0.003$) in all of the samples, and cores are enriched in LREEs compared to rims. However, in this sample, cores are also slightly enriched in HREEs as well. The spots that represent a mix of cores and rims fall between the two populations. Trace elements are also more strongly fractionated in this sample, with lower concentrations of LREEs and higher concentrations of HREEs than in sample 08 (**Fig. 9b**).

3.4 Zircon and titanite geochronology and trace element geochemistry

Zircons and titanites in an epoxy mount were analyzed for U-Pb geochronology using laser ablation-inductively-coupled plasma mass-spectrometric (LA-ICP-MS) methods at the University of New Brunswick, Fredericton, Canada. Grain mounts were prepared using standard rock crushing and mineral separation techniques, and zircon and titanite were handpicked from heavy mineral separates to represent the full variation of grain size, colour, and morphology in the sample. All grains used in this study were separated from a size fraction of 100-250 μm unless otherwise noted. Prior to LA-ICP-MS analysis, all of the grains were imaged using Bausch and Lomb cathodoluminescence (CL) system and Lamont back-scattered electron (BSE) detector on the Camebax MBX Electron Microprobe at Carleton University, Ottawa, Canada (2011), or the JEOL 6610LV scanning electron microscope housed at the University of Ottawa, Ottawa, Canada (2012). Following LA-ICP-MS analysis, zircons and titanites were similarly imaged using BSE to accurately determine the location of ablation pits. LA-ICP-MS analyses were performed on the Resonetics M-50-

LR 193nm Excimer laser ablation system coupled with an Agilent 7700x quadrupole ICP-MS. In 2011, zircons were analyzed using a 24 μm circular spot with a repetition rate of 4 Hz for 30 seconds proceeded by 30 seconds of background counting. FC 1 zircon (see Paces & Miller, 1993) and NIST 612 glass were external standards used for calibration. Titanite was analyzed with a 33 μm circular spot with a repetition rate of 4 Hz for 30 seconds preceded by 30 seconds of background counting. Khan titanite and NIST 612 glass were used for external standards. In 2012, both zircon and titanite were analyzed with a 33 μm circular spot for 30 seconds preceded by two laser pulses to clean the surface of the sample. A repetition rate of 4.5 Hz for zircon and titanite was used. Standards used with zircon in 2012 were 91500 and Temora zircons, with NIST 610 glass, whereas Khan titanite and NIST 610 glass were used with titanite. ICP-MS raw data was reduced using the Iolite freeware program produced by Melbourne Isotope group at the University of Melbourne. A description of Iolite's U-Th-Pb data reduction scheme is available in Paton *et al.* (2010) and the Iolite Users' Manual (http://iolite.earthsci.unimelb.edu.au/wiki/doku.php?id=manual_page). Iolite allows users to select only a portion of the ICP-MS data to use in calculating the output, and this was used for spots that showed two distinct $^{207}Pb/^{206}Pb$ plateaus, as these patterns were interpreted as resulting from the laser ablating areas with several age domains. Additionally, a smaller integration interval was selected when one part of analysis showed anomalous ^{204}Pb concentrations. This allowed me to use data from spots that might have otherwise been excluded because of ablation through cracks or inclusions. Spots that lacked an inclusion- or crack-free interval, as well as grains with elevated ^{204}Pb concentrations, were excluded from the age calculations. Data from Iolite were further reduced using Isoplot (Ludwig, 2012). Results reported here are all U-Pb upper intercept ages, unless otherwise mentioned, calculated using Isoplot and reported at 2σ error, with a free-fit for lower intercept. For inherited grains, ages were only reported for spots with ≤10% discordance, unless there were two or more spots of the same age, in which case a $^{207}Pb/^{206}Pb$ weighted-average age, or with >3 spots, a upper intercept age, was calculated.

Zircons were also analyzed for trace elements using LA-ICP-MS system at the University of New Brunswick. A 33 μm circular spot was used and other settings were identical to those used for zircon geochronology in 2012. NIST 610 and 612 glasses, along with the 91500 zircon standard were used for calibration. Some of the analyses were

processed using two separate methods while a standard method was being developed, but data from the different methods (except for Pb concentrations) were identical, so both are reported. Data were reduced using the Iolite trace elements data reduction scheme, using Zr as an internal standard for all elements except Pb, which used Si as an internal standard. Data are reported in ppm for the following elements: P, Ti, Hf, Pb, Th, U, and REEs (La, Ce, Pr, Nd, Sm, Eu, Gd, Tb, Dy, Ho, Er, Tm, Yb, Lu).

Twenty-one samples were selected for U-Pb geochronology, based on location, rock type, geochemistry, and outcrop-scale complexity, eleven of which contained titanite as well as zircon. Three pairs of samples from the same outcrops (six samples in total) were selected based on structures in outcrop suggesting complex histories. This was done in an attempt to characterize distinct geochemical or age signatures associated with different compositional or structural characteristics. Of four pegmatite samples with elevated whole-rock Zr concentrations (>100 ppm), only one contained zircon. A summary of geochronologic data is presented in **Table 2** and **Figs. 10** and **11**, and complete analyses are reported in **Appendices E & F**.

For zircons, trace element data are reported in **Appendix G** in ppm for the following elements: P, Ti, Hf, Pb, Th, U, and REEs (La, Ce, Pr, Nd, Sm, Eu, Gd, Tb, Dy, Ho, Er, Tm, Yb, Lu). REEs are displayed in **Fig. 12** on chondrite-normalized spider plots. In general, chondrite-normalized REE plots show flat profiles in LREEs (La-Sm) and MREEs (Eu-Dy), with positive slopes in HREEs (Ho-Lu), and areas from cores and rims of zircons within the same sample tend to have similar REE patterns, even if these domains are different ages.

3.4.1 Southern batholith

01: Leucocratic granodiorite

This sample, from the far southeast margin of the NCGB, is a white, weakly foliated granodiorite, containing approximately 10% alkali-feldspar, 45% plagioclase feldspar (An_{21}), 35% quartz, 5% biotite, 3% hornblende (edenite), 1% epidote, 1% titanite, and trace apatite, pyrite, and magnetite. Millimeter-scale, epidote-bearing quartz-carbonate veins were present in outcrop, and there is also minor epidote in the rock, which occurs as individual grains and as an alteration product of hornblende and titanite. In addition to quartz-carbonate veins, there were also several brittle-ductile pegmatitic dykes and amorphous intrusions, which did not contain zircon.

Table 2. Summary of zircon and titanite geochronlogy and amphibole thermobarometry

	Zr (Ma)	#	Th/U	Zr In (Ma)	Th/U	Ttn (Ma)	#	Ttn In (Ma)	Ti-zr (°C)	T (°C)	P (kbar)	depth (km)
Southern batholith												
01	2860 ± 13	23	0.32	2971 ± 6	0.58	2868 ± 33	5	--	742 ± 50	607 ± 16	5.1 ± 0.2	19 ± 1
13/15	--	--	--	--	--	--	--	--	--	***561 ± 16***	***1.8 ± 0.3***	***7 ± 1***
	--	--	--	--	--	--	--	--	--	***554 ± 12***	***3.6 ± 0.2***	***13 ± 1***
	2727 ± 12	14	0.80	--	--	2766 ± 7	24	2889 ± 16	735 ± 51	611 ± 21	6.2 ± 0.7	23 ± 2
22	--	--	--	--	--	--	--	--	--	***613 ± 14***	***7.9 ± 0.3***	***29 ± 1***
	--	--	--	--	--	--	--	--	--	602 ± 21	5.8 ± 0.7	22 ± 3
29	***2731 ± 13***	***13***	***0.17***	2982 ± 23	0.50	***2764 ± 7***	***5***	--	--	***585 ± 30***	***5.4 ± 0.3***	***20 ± 1***
	2853 ± 10	7	0.42	--	--	2822 ± 32	6	--	767 ± 150	593 ± 31	6.5 ± 0.3	24 ± 1
48	***2710 ± 33***	***3***	***0.08***	--	--	--	--	--	--	--	--	--
	2837 ± 15	17	0.37	--	--	--	--	--	839 ± 45	--	--	--
Schade Lake gneissic complex												
52	2844 ± 15	11	0.46	--	--	--	--	--	--	642 ± 29	7.4 ± 0.3	27 ± 1
	2886 ± 8	23	0.38	--	--	--	--	--	833 ± 69	--	--	--
53	***2642 ± 10***	***30***	***0.20***	2841 ± 29	0.40	--	--	--	--	--	--	--
	2715 ± 18	7	0.45	--	--	--	--	--	774 ± 35	--	--	--
68/69	--	--	--	--	--	--	--	--	--	637 ± 17	7.5 ± 0.3	27 ± 1
71	2702 ± 57	5	0.35	--	--	--	--	--	665 ± 104	--	--	--
	2858 ± 5	34	0.36	--	--	2854 ± 7	34	--	792 ± 50	--	--	--
Skinner Lake block												
40/41	--	--	--	--	--	--	--	--	--	***574 ± 21***	***2.4 ± 0.4***	***9 ± 1***
	2828 ± 9	9	0.28	2932 ± 8	0.21	--	--	--	659 ± 69	--	--	--
	2871 ± 6	19	0.25	2955 ± 10	0.36	--	--	--	708 ± 46	--	--	--
	--	--	--	2996 ± 10	0.37	--	--	--	--	--	--	--
43	***2735 ± 7***	***12***	***0.19***	--	--	--	--	--	--	--	--	--
	2835 ± 13	***5***	***0.19***	--	--	--	--	--	--	--	--	--
	2871 ± 9	6	0.47	--	--	--	--	--	695 ± 73	--	--	--
Wharram Lake block												
55	***2678 ± 18***	***9***	***0.14***	2976 ± 15	0.22	***2689 ± 13***	***15***	--	--	--	--	--
	2928 ± 12	10	0.26	--	--	--	--	--	800 ± 240	--	--	--
North Caribou Lake batholith- pluton												
36	--	--	--	--	--	--	--	--	--	660 ± 12	7.1 ± 0.3	26 ± 1
46	--	--	--	3005 ± 6	0.26	***2742 ± 35***	***6***	--	--	--	--	--
	2867 ± 9	16	0.32	--	--	2869 ± 15	4	--	829 ± 45	--	--	--
49	***2857 ± 9***	***5***	***0.06***	--	--	--	--	--	--	--	--	--
	3002 ± 14	6	0.33	--	--	--	--	--	921 ± 130	--	--	--
	3132 ± 7	12	0.51	--	--	--	--	--	--	--	--	--
66	--	--	--	--	--	***2733 ± 33***	***8***	--	--	***604 ± 16***	***6.3 ± 0.2***	***23 ± 1***
	2829 ± 13	4	0.56	--	--	--	--	--	892 ± 65	--	--	--
North Caribou Lake batholith- core												
51	2693 ± 12	9	1.68	--	--	--	--	--	811 ± 54	--	--	--
	2834 ± 32	4	0.38	--	--	2810 ± 17	18	--	795 ± 230	--	--	--
61	--	--	--	2913 ± 11	0.75	***2786 ± 14***	***11***	--	--	***644 ± 11***	***7.1 ± 0.2***	***26 ± 1***
	2833 ± 13	20	0.54	--	--	--	--	--	784 ± 31	639 ± 12	7.9 ± 0.3	29 ± 1
62/63	--	--	--	--	--	--	--	--	--	***641 ± 17***	***5.9 ± 0.3***	***22 ± 1***
	2854 ± 8	38	0.57	2953 ± 10	0.26	--	--	--	718 ± 28	659 ± 24	6.8 ± 0.4	25 ± 1
	--	--	--	3094 ± 15	0.50	--	--	--	--	--	--	--
64/65	--	--	--	--	--	--	--	--	--	***635 ± 19***	***6.6 ± 0.3***	***24 ± 1***
	--	--	--	--	--	--	--	--	--	631 ± 28	7.7 ± 0.3	28 ± 1
Libert Lake pluton												
45	2700 ± 8	2	0.52	2872 ± 12	0.51	2700 ± 27	11	--	715 ± 62	--	--	--
	2730 ± 8	15	0.40	2945 ± 9	0.17	2830 ± 51	4	--	--	--	--	--
Pegmatite												
54	2619 ± 14	13	0.13	2758 ± 5	0.12	--	--	--	624 ± 46	--	--	--

Notes:
Bold italics are metamorphic or hydrothermal ages or T-P conditions
All errors for ages and Ti-in-zircon thermometry reported as 2σ and P-T conditions from hbl-plag thermobarometry reported as 1σ
Zr: zircon ages; #: number of analyses; Th/U: median Th/U ratios; Zr In: inherted zircon ages; Ttn: titanite ages; Ttn In: inherted titanite ages
Ti-zr: Ti-in-zr temperature (Ferry & Watson, 2007); T: hbl-plag temperature (B; Holland & Blundy, 1991); P: Al-in-hbl pressure (Anderson & Smith, 1995)

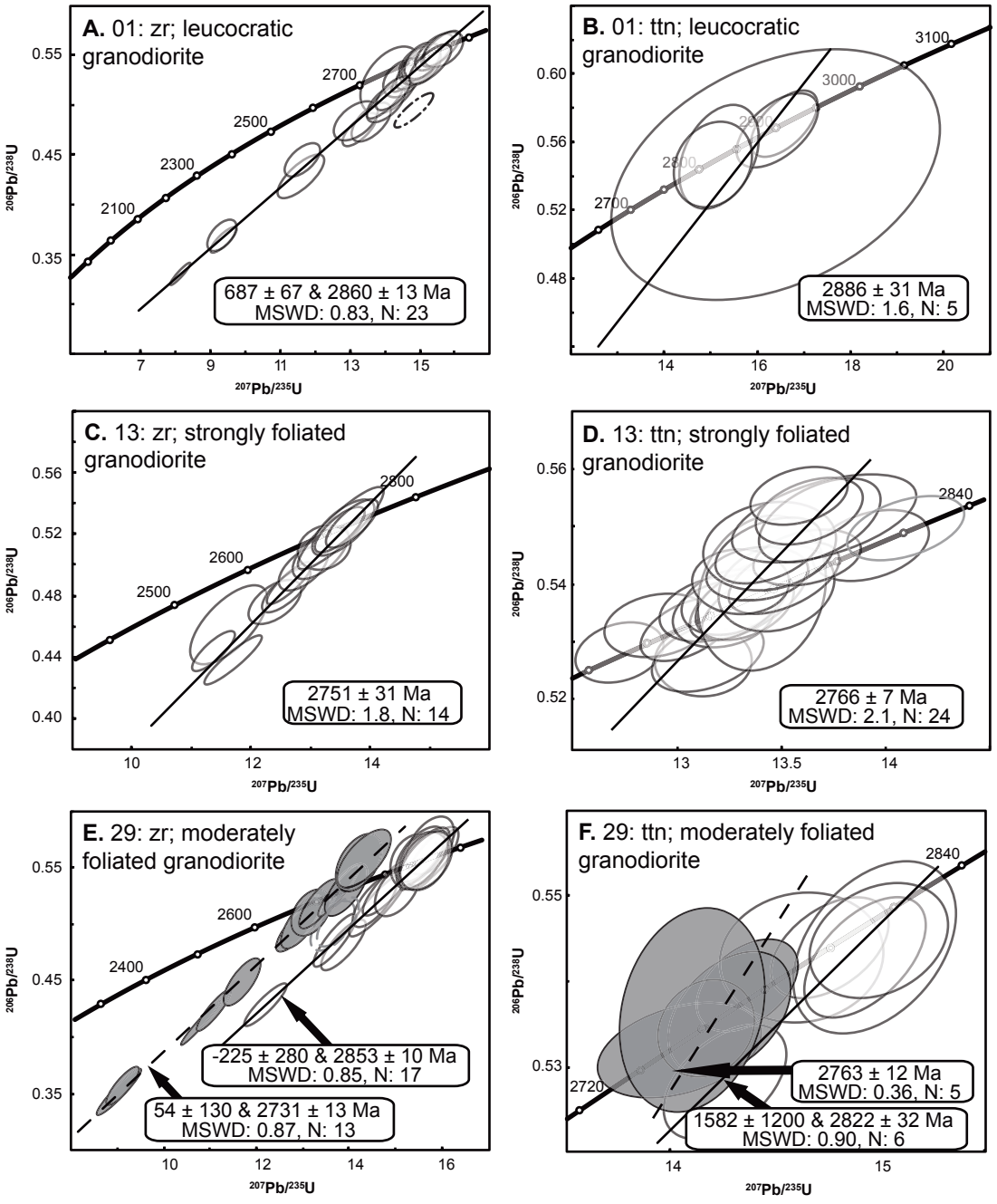
A. 01: zr; leucocratic granodiorite
687 ± 67 & 2860 ± 13 Ma
MSWD: 0.83, N: 23
B. 01: ttn; leucocratic granodiorite
2886 ± 31 Ma
MSWD: 1.6, N: 5
C. 13: zr; strongly foliated granodiorite
2751 ± 31 Ma
MSWD: 1.8, N: 14
D. 13: ttn; strongly foliated granodiorite
2766 ± 7 Ma
MSWD: 2.1, N: 24
E. 29: zr; moderately foliated granodiorite
-225 ± 280 & 2853 ± 10 Ma
MSWD: 0.85, N: 17
54 ± 130 & 2731 ± 13 Ma
MSWD: 0.87, N: 13
F. 29: ttn; moderately foliated granodiorite
2763 ± 12 Ma
MSWD: 0.36, N: 5
1582 ± 1200 & 2822 ± 32 Ma
MSWD: 0.90, N: 6
206Pb/238U
207Pb/235U

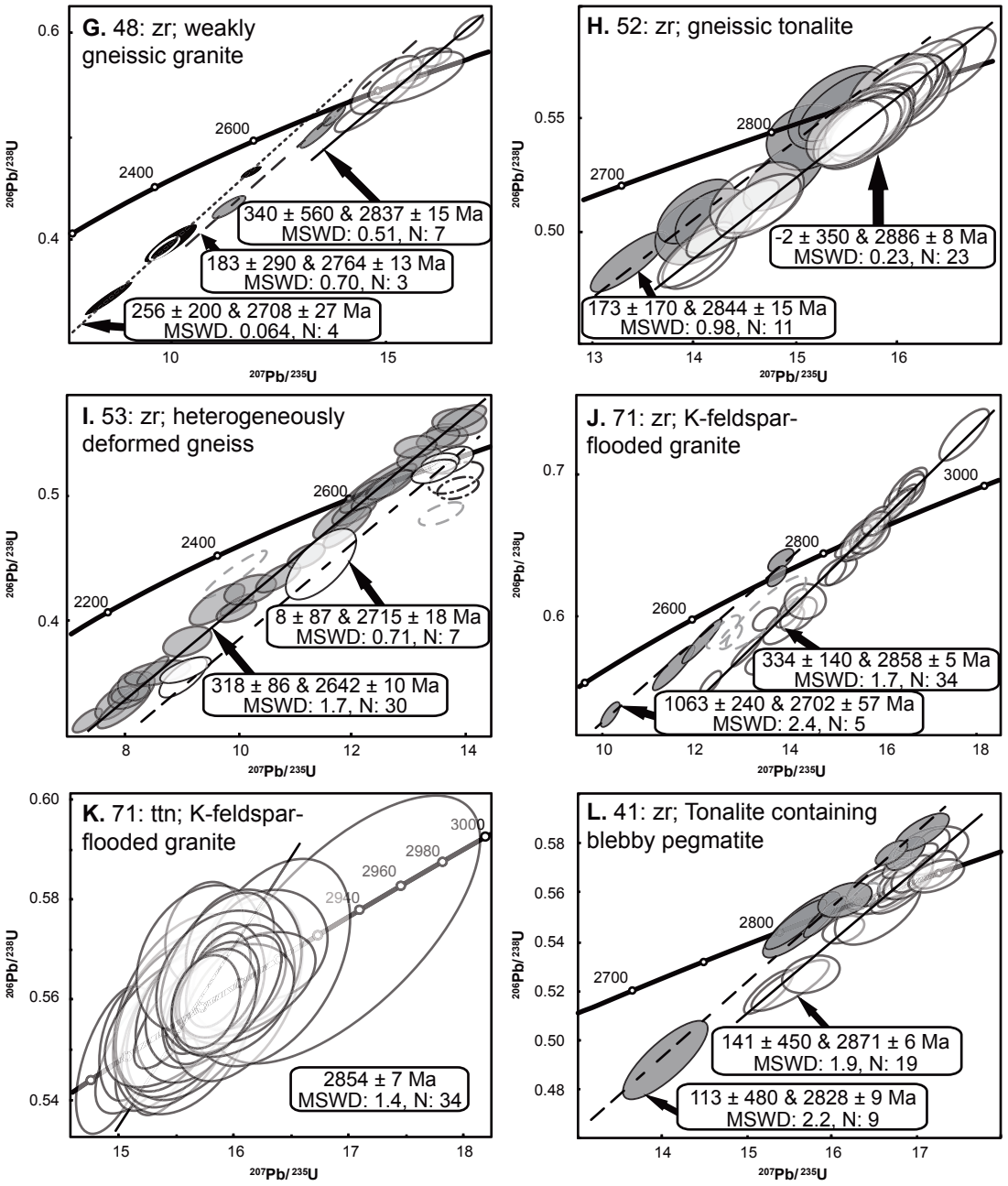
G. 48: zr; weakly gneissic granite
340 ± 560 & 2837 ± 15 Ma
MSWD: 0.51, N: 7
183 ± 290 & 2764 ± 13 Ma
MSWD: 0.70, N: 3
256 ± 200 & 2708 ± 27 Ma
MSWD. 0.064, N: 4
H. 52: zr; gneissic tonalite
-2 ± 350 & 2886 ± 8 Ma
MSWD: 0.23, N: 23
173 ± 170 & 2844 ± 15 Ma
MSWD: 0.98, N: 11
I. 53: zr; heterogeneously deformed gneiss
8 ± 87 & 2715 ± 18 Ma
MSWD: 0.71, N: 7
318 ± 86 & 2642 ± 10 Ma
MSWD: 1.7, N: 30
J. 71: zr; K-feldspar-flooded granite
334 ± 140 & 2858 ± 5 Ma
MSWD: 1.7, N: 34
1063 ± 240 & 2702 ± 57 Ma
MSWD: 2.4, N: 5
K. 71: ttn; K-feldspar-flooded granite
2854 ± 7 Ma
MSWD: 1.4, N: 34
L. 41: zr; Tonalite containing blebby pegmatite
141 ± 450 & 2871 ± 6 Ma
MSWD: 1.9, N: 19
113 ± 480 & 2828 ± 9 Ma
MSWD: 2.2, N: 9
206Pb/238U
207Pb/235U

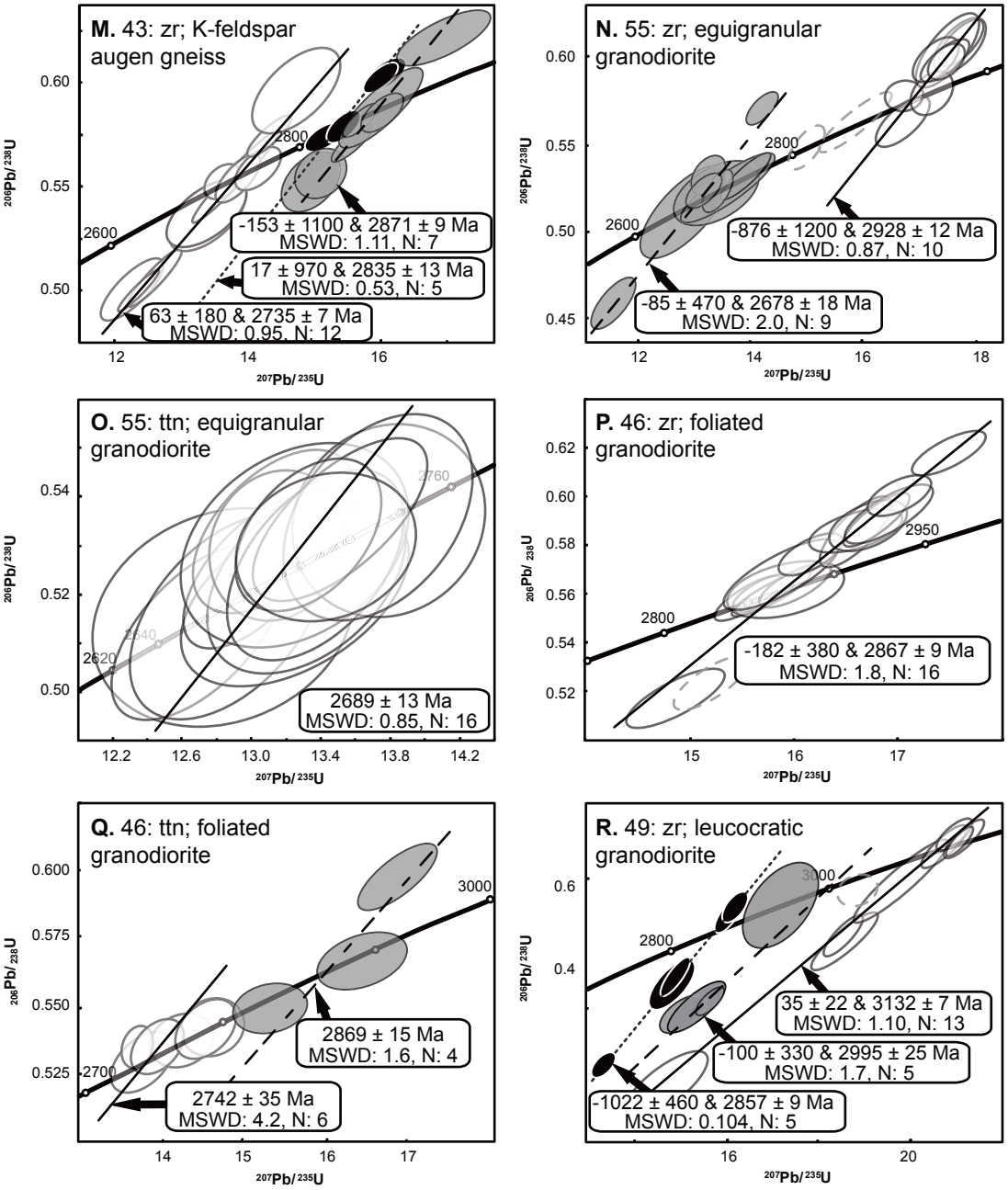
M. 43: zr; K-feldspar augen gneiss
-153 ± 1100 & 2871 ± 9 Ma
MSWD: 1.11, N: 7
17 ± 970 & 2835 ± 13 Ma
MSWD: 0.53, N: 5
63 ± 180 & 2735 ± 7 Ma
MSWD: 0.95, N: 12
N. 55: zr; eguigranular granodiorite
-876 ± 1200 & 2928 ± 12 Ma
MSWD: 0.87, N: 10
-85 ± 470 & 2678 ± 18 Ma
MSWD: 2.0, N: 9
O. 55: ttn; equigranular granodiorite
2689 ± 13 Ma
MSWD: 0.85, N: 16
P. 46: zr; foliated granodiorite
-182 ± 380 & 2867 ± 9 Ma
MSWD: 1.8, N: 16
Q. 46: ttn; foliated granodiorite
2869 ± 15 Ma
MSWD: 1.6, N: 4
2742 ± 35 Ma
MSWD: 4.2, N: 6
R. 49: zr; leucocratic granodiorite
35 ± 22 & 3132 ± 7 Ma
MSWD: 1.10, N: 13
-100 ± 330 & 2995 ± 25 Ma
MSWD: 1.7, N: 5
-1022 ± 460 & 2857 ± 9 Ma
MSWD: 0.104, N: 5
206Pb/238U
207Pb/235U

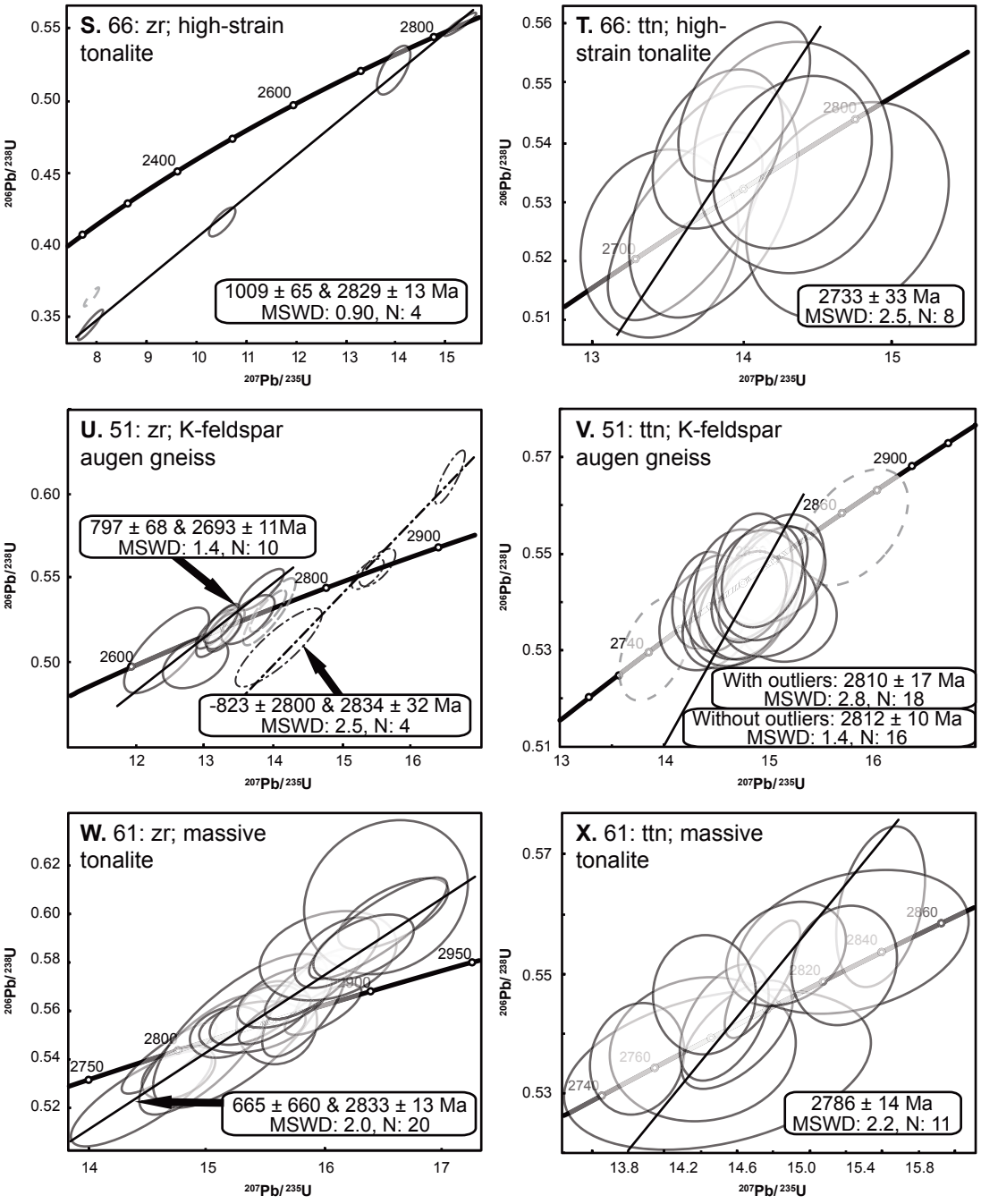
S. 66: zr; high-strain tonalite
1009 ± 65 & 2829 ± 13 Ma
MSWD: 0.90, N: 4
T. 66: ttn; high-strain tonalite
2733 ± 33 Ma
MSWD: 2.5, N: 8
U. 51: zr; K-feldspar augen gneiss
797 ± 68 & 2693 ± 11Ma
MSWD: 1.4, N: 10
-823 ± 2800 & 2834 ± 32 Ma
MSWD: 2.5, N: 4
V. 51: ttn; K-feldspar augen gneiss
With outliers: 2810 ± 17 Ma
MSWD: 2.8, N: 18
Without outliers: 2812 ± 10 Ma
MSWD: 1.4, N: 16
W. 61: zr; massive tonalite
665 ± 660 & 2833 ± 13 Ma
MSWD: 2.0, N: 20
X. 61: ttn; massive tonalite
2786 ± 14 Ma
MSWD: 2.2, N: 11
206Pb/238U
207Pb/235U

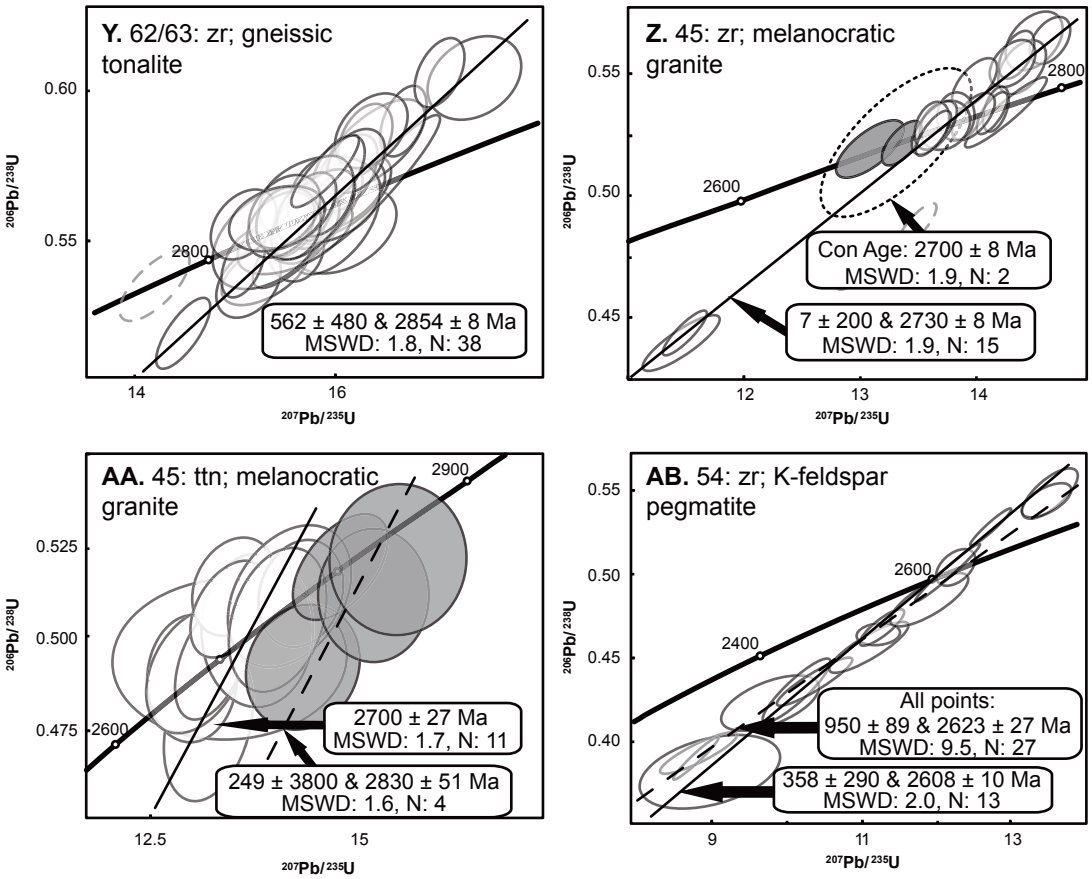

Figure 10: LA-ICPMS U-Pb concordia diagrams of samples dated in this study. Each ellipse is a single spot analyses reported as 2 sigma. White ellipses and solid discord are primary ages; grey ellipses and dashed discord are secondary ages; black ellipses and dotted discord are tertiary ages. Grey dashed ellipses are spot analyses that likely represent a mixed age and are not used in the age calculations, and dot-dashed ellipses are inherited ages. Strongly discordant data and some inherited ages are not shown; see Tables 7 and 8 for isotopic analyses and additional data.

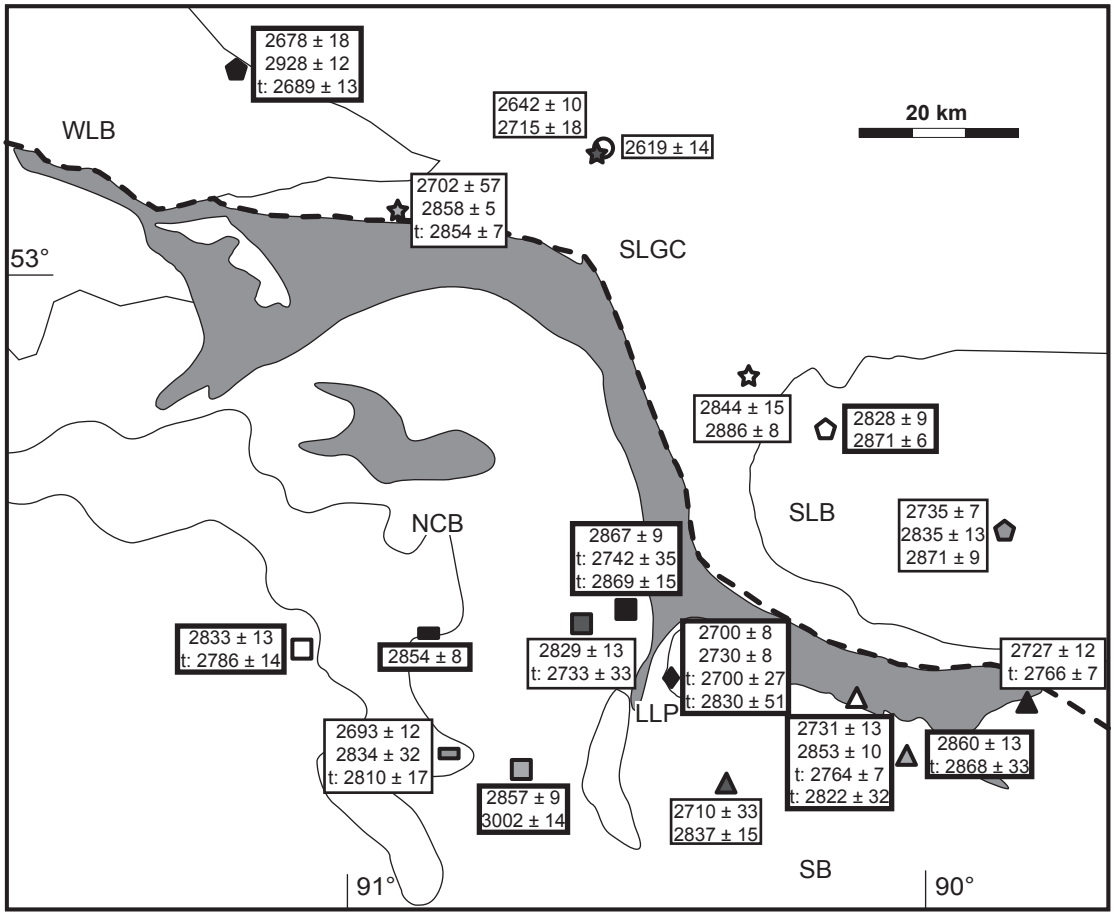

Figure 11: Location map of U-Pb ages (Ma) for zircon and titanite analyzed in this study. Titanite ages distinguished by t, and samples with inherited zircon ages are outlined in bold boxes. NCB: North Caribou batholith; LLP: Libert Lake pluton; SB: Southern batholith; SLB: Skinner Lake block; WLB: Wharram Lake block.

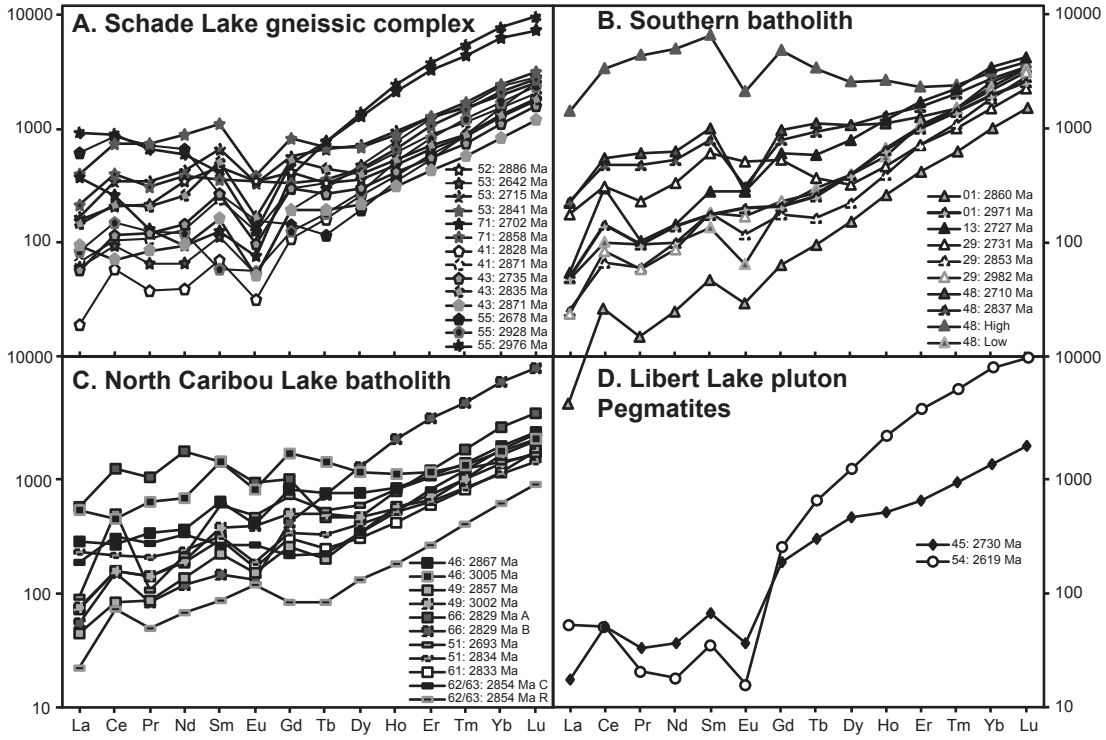

Figure 12: Chondrite-normalized REE plots for zircons dated in this study. Data collected via LA-ICPMS. Normalizing values from McDonough & Sun (1995). Note that zircons with hydrothermal rims (29, 48, 53, 43, 55, 49) have similar trace element patterns in rims and cores, but varying concentrations of LREE's.

Zircons generally have aspect ratios 1:2 regardless of size, which ranges from ~150 μm to ~350 μm along the long axis. Many contain xenocrystic cores, and very thin rims (5 μm), which were too thin to analyze with the lateral dimensions of the laser spot. Zircons were relatively inclusion-rich, and most were oscillatory-zoned, in both the cores and rims, although two of the analyzed grains exhibited sector zoning as well. About a third of the zircons also contained resorption shadows, which generally occurred around cores, sector-zoned areas, or areas with disrupted oscillatory zoning. For U-Pb geochronology, 25 spots on 12 grains were analyzed. Despite the complex textures, only two age populations emerged: 23 single spot analyses formed a discordia line with an upper intercept of 2860 ± 13 Ma and a lower intercept of 687 ± 67 Ma (MSWD: 0.83), whereas two spots from inherited cores had a weighted average $^{207}Pb/^{206}Pb$ age of 2971 ± 6 Ma (MSWD: 0.03; **Fig. 10a**).

Titanite grains from this sample are generally fairly homogeneous in BSE, but like the zircons, are inclusion rich, and many have a thin rim up to 50 μm thick, but generally ~10 μm thick (**Fig. 13i**). Titanites tend to be somewhat larger than zircon, roughly 500 μm in diameter, but grains used for geochronology are ~250 μm across their narrowest point. For geochronology, 15 spots on 13 grains were analyzed. Ten spots were on titanite grains possessing either elevated ^{204}Pb or with U concentrations too low for accurate analysis. The 5 remaining spots formed a cluster on concordia at 2868 ± 33 Ma (MSWD: 2.2; **Fig. 10b**).

For trace element concentrations in zircon, 5 spots were analyzed. Four of these points are from zircons in the 2860 Ma population, and one is from a xenocrystic core. Chemically, the populations are identical, except the Th/U ratio is lower and the Eu anomaly is positive in the xenocrystic core. Chondrite-normalized plots show a slight positive Ce and a slight negative Eu anomaly, and unlike most other samples, there is a steep positive slope in the LREEs as well as the HREEs. The REE trend in the xenocrystic core is nearly identical to the 2860 Ma population, but it lacks the Eu anomaly and has higher concentrations of LREEs (**Fig. 12**).

13: Strongly foliated granodiorite

This sample is from the eastern edge of the NCGB, near the northern boundary of the Southern batholith, in an area of a small low magnetic anomaly. It is dark grey and strongly foliated with biotite defining the fabric, which wraps around blocky plagioclase crystals up to 5 mm in diameter. Alkali feldspars are generally found in pressure shadows around the

plagioclase. In outcrop, there are prominent, resistant "ribs" that are ~5 cm wide and protrude up to 5 cm above the rest of the rock and are associated with mm-scale quartz-carbonate-epidote veins. Compositionally, this rocks is a granodiorite, containing 10% alkali feldspar, 40% plagioclase (An_{22}), 30% quartz, 20% biotite, and 5% hornblende (magnesiohornblende to ferro-edenite), with trace hematite, epidote, titanite, and minor chlorite replacing biotite and hornblende associated with quartz-carbonate veins. Although biotite forms the main foliation in this rock, titanite, hornblende, and deformed quartz are also strongly aligned in the foliation plane.

There were only 7 zircons recovered from this sample, and unbroken grains exhibit aspect ratios ≥1:4, making them more acicular than those in most other samples (but see sample 66). They range in size from ~150 μm to >400 μm along their long axes. Most grains also contain biotite inclusions parallel to the long axis, and frequently have corroded, disturbed, metamict cores surrounded by oscillatory-zoned rims, although sector zoning is observed in one grain. For geochronology, 15 spots on 7 grains yielded a upper intercept age of 2727 ± 12 Ma, with a lower intercept fixed at 0 (MSWD: 1.8). One spot was excluded because the ablation pit was on a crack (**Fig. 10c**).

Titanite crystals in this rock are characterized by patchy zoning in BSE, which is not correlated with age or grain morphology. In thin section, titanite is nearly perfectly euhedral and 0.5-1 mm long, although all of the analyzed grains (~150-450 μm along the long axis) were broken. Twenty seven spots on 13 grains were analyzed, with 24 spots clustering tightly around concordia, and yielding a upper intercept age of 2766 ± 7 Ma, with a lower intercept fixed at 0 (MSWD: 2.1). There was one spot with a concordant $^{207}Pb/^{206}Pb$ age of 2889 ± 16 Ma, and 2 spots were not included due to high ^{204}Pb (**Fig. 10d**).

In zircons, 5 spots were analyzed for trace element concentrations. All of the spots are from the 2727 Ma population, although one is metamict. These zircons are characterized by high Ce and Th/U, and the metamict grain has a positive Eu anomaly. Chondrite-normalized plots show a slight positive Ce anomaly ($Ce/Ce^* = 6.5$), and unlike most other samples, there is a consistent positive slope throughout the entire REE profile (**Fig. 12**).

29: Moderately foliated granodiorite

This sample comes from the centre of the northern margin of the Southern batholith. It is pinkish-grey and moderately foliated, with foliation defined by biotite and titanite (**Fig.**

4i). It is a granodiorite, with a composition of 10% alkali feldspar, 45% plagioclase (An_{16}), 30% quartz, 10% biotite, 2% epidote, 1% hornblende (edenite to hastingsite), 1% titanite, and 1% oxides (primarily hematite). There is also minor pyrite, muscovite and zircon. Unlike 01 and 13, epidote is not associated with quartz-carbonate veins and is occasionally included in biotite. The sample is fairly coarse-grained, although large crystals (5-8 mm) are predominately plagioclase. Alkali feldspars are almost exclusively found rimming plagioclase.

Two zircon populations were found in this sample: large (500-200 μm), red-brown to pink cloudy crystals, and smaller (200-150 μm) clear transparent to pink grains. All of the grains have aspect rations from 1:1 to 1:3, with the small, clear grains closer to 1:1. All crystals, regardless of their size contain cores, and resorption shadows are common in both the cores and rims. Rims of these zircons are oscillatory-zoned or clear, and many contain inclusions, especially biotite. Several grains exhibit very thin (5-10 μm) additional rims, which were not dated. Textures within cores include oscillatory zoning, sector zoning, composite grains, and metamict textures, and inclusions, mainly sulphides, are common (**Fig. 13e**). For geochronology, 34 spots on 19 grains were analyzed. Thirteen of these spots from zircon rims yielded an age of 2731 ± 13 Ma, with a lower intercept of 54 ± 130 Ma (MSWD: 0.87). Seventeen of the spots from cores and resorption shadows in rims (2 spots) gave an age of 2853 ± 10 Ma, with a lower intercept of -225 ± 280 Ma (MSWD: 0.85). There were also three cores with an age of 2982 ± 23 Ma, with a lower intercept anchored at 0 Ma (MSWD: 0.99; **Fig. 10e**). One point from a resorption shadow was not included in any population because it gave a mixed age ($^{207}Pb/^{206}Pb$ age of 2790 ± 5 Ma).

Titanite grains are euhedral, and generally have few inclusions, which are mostly oxides and sulphides. Most grains are concentrically zoned, with BSE-dark cores and BSE-light rims. Cores can be unzoned, patchy-zoned, or oscillatory-zoned, but rims are either oscillatory-zoned or unzoned. Patchy to wormy textures are common at the contact between cores and rims. In thin section, the average size of titanite grains is 2 mm along the long axis, but broken, analyzed grains are between 200 and 500 μm. For geochronology, 14 spots on 11 grains were analyzed, and, like in the zircon, two populations emerged. Five spots from the rims had a concordant age of 2764 ± 7 Ma (MSWD: 0.95). Six spots from the cores of grains

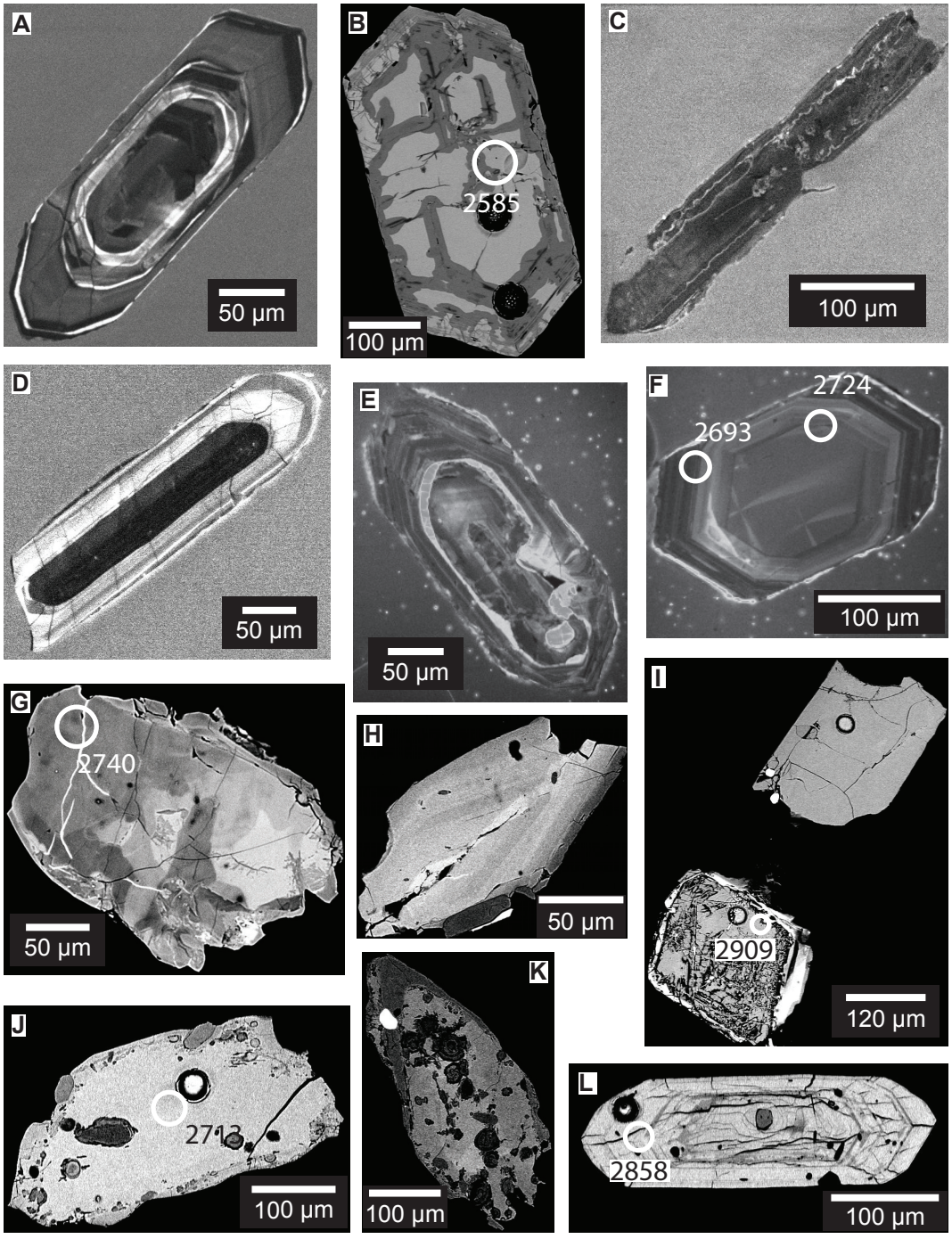

Figure 13: A. CL image of zircon (sample 48) with three age domains. B. BSE image of zircon (sample 54) showing metamict zircon from pegmatite with alteration along cracks. C. CL image of narrow zircon (sample 66) from an initially zircon-undersaturated melt. D. CL image of zircon (sample 63) with distinct cores and rims of a single age. E. CL image of zircon (sample 29) with an igneous core and hydrothermally altered rim. F. CL image of zircon (sample 45) with igneous core and rims of different ages. G. BSE image of titanite (sample 45) showing patchy zoning of a single age. H. BSE image of oscillatory-zoned igneous titanite (sample 51). I. BSE image of titanite (sample 1) showing uniform igneous titanite, both inclusion-free, and inclusion-rich with thin rims. J. BSE image of metamorphic titanite (sample 66). K. BSE image of inclusion-rich igneous titanite (sample 71). L. BSE image of oscillatory-zoned inclusion-rich zircon (sample 71).

yielded an age of 2822 ± 32 Ma, with a lower intercept of 1582 ± 1200 Ma (MSWD: 0.90; **Fig. 10f**). Three points were excluded for excess ^{204}Pb.

In zircons, 11 spots were analyzed for trace element concentrations. Six spots were from the 2731 Ma population, 4 spots were from the 2853 Ma, and one spot was on a xenocrystic core. Rims tended to have lower P and Th/U and higher Ti and REEs, as well as less pronounced Eu anomalies (Eu/Eu* = 0.86 in rims and 0.65 in cores). The xenocrystic core was chemically similar to the other cores, but had a less pronounced Eu anomaly (Eu/Eu* = 0.85). Both the xenocrystic core and the 2853 Ma populations have similar REE trends, with slight positive Ce (Ce/Ce* = 1.8) and negative Eu anomalies and a gentle positive slope in LREEs that plateaus in the MREEs before following the steep positive slope in the HREEs. The 2853 Ma population has higher concentrations of LREEs and MREEs than the xenocrystic core, but the inherited core has higher concentrations of HREEs (668 ppm). The 2731 Ma population has higher concentrations of LREEs and MREEs, and also lacks a Ce anomaly. The patterns in the REEs of the 2731 Ma population mirror the patterns in the 2853 Ma population, except for a negative slope between Gd and Dy, as the concentrations of HREEs are the same in the two populations (**Fig. 12**).

48: Weakly gneissic granite

This sample comes from the centre of the Southern batholith, ~20 km south of the NCGB, in a prominent magnetic low. In outcrop, it is texturally heterogeneous. This rock is generally gneissic, but banding is very localized, and complexly folded. Much of the rock has very poorly developed compositional banding and has a moderate fabric defined by biotite. This granite is composed of 30% alkali feldspar, 35% plagioclase, 30% quartz, 5% biotite, and minor apatite, muscovite, oxides, and pyrite. Alkali feldspar crystals are rather large (up to 2 cm), whereas other minerals rarely reach 5 mm. Plagioclase is commonly myrmekitic and has strongly sericite-altered cores.

Zircons in this sample are fairly homogeneous, between 150 and 350 μm long. All have aspect ratios between 1:2 and 1:3, and most contain cores, commonly with resorption shadows. Some cores are oscillatory- or sector-zoned, but most are inclusion-rich and metamict. Several cores appear to contain xenocrystic cores themselves. Rims generally lack inclusions and are oscillatory-zoned, but many contain cracks radiating from the core. Due to the multiple concentric layers within these zircons (**Fig. 13a**), clearly distinguishing growth

textures, and placing ablation spots in single domains was challenging and many spots showed variations in $^{207}Pb/^{206}Pb$ age over the duration of the run. For geochronology, 23 spots on 18 grains were analyzed; 13 of the spots were discarded due to ablation pits on cracks, inclusions or extremely metamict areas. Two populations emerged from the data. Three spots from rims had an upper intercept age of 2710 ± 33 Ma, with a lower intercept of 280 ± 300 Ma (MSWD: 0.08), whereas spots in zircon cores yielded an age of 2837 ± 15 Ma, with a lower intercept of 340 ± 560 Ma (MSWD: 0.51; **Fig. 10g**). Additionally, three spots with elevated ^{204}Pb concentrations from metamict, inclusion-rich cores have a upper intercept age of 3458 ± 17 Ma. As the high ^{204}Pb concentrations in these spots, as well as their textures, would result in their exclusion from a normal regression, this age is considered dubious.

Sixteen spots on zircons were analyzed for trace element concentrations. Nine spots were from the 2710 Ma population, and 7 were from the 2837 Ma population. Because these zircons were highly fractured and metamict, several of these spots were on areas that would have been excluded from the geochronology data set. The young population tends to have higher Ti and U and lower REEs and Th/U. On chondrite-normalized REE plots, there are two distinct patterns, which are not correlated with age or zircon morphology. However, zircons with higher concentrations of LREEs seem to have less radiation damage. Both trends show strong Eu anomalies (Eu/Eu* = 0.37) and similar concentrations of HREEs, but have LREE concentrations that differ by more than an order of magnitude. The low LREE population has a flat LREE profile and a positive slope through the MREEs and HREEs, along with a small positive Ce anomaly. Likewise, the high LREE group has a flat LREE profile, but a negative slope in the MREEs, which becomes a more typical positive slope in HREEs (**Fig. 12**).

3.4.2 Schade Lake gneissic complex

52: Gneissic tonalite

This tonalite (trondhjemite) sample is from the south-central part of the SLGC, to the west of the SLB. It is extremely heterogeneous with textures including well-developed gneissic banding, strong foliation, shear bands, relatively unfoliated patches, and apparent schlieren composed of fine-grained, biotite- and hornblende-rich material. Contacts are generally gradational except between schlieren and the surrounding rock. Outside of

schlieren, the rock is generally coarse-grained, even in areas of higher strain. It is composed of 45% plagioclase (An_{31}), 35% quartz, 15% biotite, 5% hornblende (hastingsite to ferropargasite), and trace alkali feldspar, pyrite, chlorite, and epidote, which are associated with quartz-carbonate veins and fractures. There is only minor sericite alteration of plagioclase and chlorite and epidote alteration of biotite and hornblende, but there are euhedral epidote inclusions in biotite as well. This sample is darker and has more calcic plagioclase than typical trondhjemites in this area.

Zircons generally have aspect ratios between 1:1 and 1:2, and are between 100-300 μm long. Most have cores and rims, with resorption shadows in the cores. There are occasional inclusions, almost exclusively in the cores, which are mostly oscillatory-zoned, although a couple are sector-zoned or metamict. For geochronology, 34 spots on 19 grains were analyzed, and two populations emerged. The younger population, consisting of 11 spots and found in rims and small grains is 2844 ± 15 Ma, with a lower intercept of 173 ± 170 Ma (MSWD: 0.98). The older population with 23 spots is 2886 ± 8 Ma with a lower intercept of -2 ± 350 Ma (MSWD: 0.23; **Fig. 10h**).

Trace element concentrations in zircon were obtained from 5 spots, and all were from the 2886 Ma population. In general, these zircons have negligible Ce and Eu anomalies, and the chondrite-normalized REE plots show a flat profile in the LREEs and a positive slope in the HREEs (**Fig. 12**).

53F/C: Heterogeneously deformed gneiss

This sample was obtained from the northern boundary of the SLGC, near the eastern-most extent of the Muskrat Dam Lake greenstone belt, from a small area with low magnetic susceptibility. It is strongly foliated, almost proto-mylonitic in places, and has well-developed gneissic banding, although strain is not homogeneously partitioned. There are prominent alkali feldspar augen, which are primarily albite and up to 4 cm, and some are fractured parallel to the shortening direction. It is a granite with a composition in dark bands of 20% alkali feldspar (primarily as augen, but also as small crystals in narrow, ~1 cm compositional bands), 25% plagioclase feldspar (~An_{20}), 25% quartz, 30% biotite, and trace pyrite and epidote associated with fractures and biotite alteration. Plagioclase is also sericite-altered near fractures. In the light bands, there is 5-10% biotite, and up to 40% alkali feldspars, which tend to be more K-rich. Because of the heterogeneous strain in this rock,

geochronology samples were divided into high- and low-strain groups, which correspond to grain-size, and are designated F (for fine-grained) and C (for coarse-grained), respectively (**Fig. 4h**).

Zircons from 53F tend to be narrow, with aspect ratios between 1:2 and 1:4, although there are a couple of grains with ratios closer to 1:1. They range in size from 150-250 μm. Zircons from 53C have more variety in aspect ratios, which typically fall between 1:1 and 1:3, with many grains clustering at either end of the range. They also tend to be larger, varying between 150-350 μm. In both samples, inclusions are common in both cores and rims (where they exist), and composite grains are common, although more prevalent in 53F. Most composite grains have parallel long axes, but there are a couple examples with different orientations. Resorption shadows are common, and most grains are at least partially metamict. Some sector and oscillatory zoning is present, but most has been obliterated by resorption shadows. Due to the number of inclusions, some analysis spots were on resorption shadows or metamict areas that were typically avoided. For 53F, 28 spots on 23 grains and for 53C, 21 spots on 17 grains were analyzed. When zircons from both samples are considered, three broad populations are present. The first is found in 30 spots from rims and cores of both size fractions and is 2642 ± 10 Ma, with a lower intercept of 318 ± 86 Ma (MSWD: 1.7). Twelve of the spots in this population have high concentrations of ^{204}Pb, and without these spots, the age is 2640 ± 9 Ma, with a lower intercept of 293 ± 150 Ma (MSWD: 1.03). The second population is defined by 7 spots from cores in 53F and has an age of 2715 ± 18 Ma, with a lower intercept of 8 ± 87 Ma (MSWD: 0.71). Two spots from cores of 53F have a ^{207}Pb/^{206}Pb weighted average age of 2841 ± 29 Ma, (MSWD: 5.0; **Fig. 10i**). Nine spots, not including those mentioned above, were excluded from analysis because the ablation pits were on cracks, inclusions, or areas with high ^{204}Pb, and one spot was excluded for yielding a likely mixed age.

Twenty spots on zircons were analyzed for trace element concentrations. Ten spots sampled zircon in the 2645 Ma population, 8 spots were from the 2726 Ma population, and 2 were from the 2841 Ma population. The youngest population tends to have lower Ti, LREEs (La-Gd), U, Th/U, and more pronounce Ce anomalies. The oldest population has high Ti, but is otherwise identical to the 2726 Ma population. Likewise, REE profiles of the inherited grains and the 2726 Ma population are similar, although grains from the 2726 Ma population

have higher concentrations of LREEs. These profiles have a slight positive Ce anomaly and a pronounce negative Eu anomaly, along with a concave-down pattern in the LREEs and MREEs and a positive slope in the HREEs. The 2645 Ma population has lower concentrations of LREEs with very small Ce and Eu anomalies. This population has a positive slope in LREEs, a flat plateau in MREEs, and a positive slope in HREEs (**Fig. 12**).

71 D/P: K-feldspar-flooded granodiorite

This sample was collected from the southwestern side of the SLGC, at the contact between the SLGC and the NCGB. It is highly strained with large (up to 1 cm) phenocrysts of plagioclase and K-feldspar that show evidence of rotation. There are also quartz- and K-feldspar-rich dykelets (1-10 cm wide) that are roughly parallel to foliation and frequently interfingered with the host rock. This is an unusual texture in pegmatites, which generally have clear contacts with the host rock. In addition, there are zones of sericite, hematite, and, most prominently, K-alteration surrounding epidote veins that crosscut the fabric of the rock. This sample is granodioritic to granitic (if the K-feldspar dykelets are included), with a composition of 15% alkali feldspars, 35% plagioclase feldspar (~An_{20}), 40% quartz, 8% biotite, 2% epidote, and trace titanite and muscovite. Biotite is occasionally chlorite-altered, especially near epidote veins, and plagioclase is sericite-altered. To determine if zircons from altered areas recorded the timing of the alteration, I divided the sample into host rock (D) and K-feldspar-rich areas (P), including both the dykelets and alteration halos, but because of the interfingered relationship between the host rock and the pegmatite, the division was imperfect (**Fig. 4g**).

These zircons have aspect ratios between 1:1 and 1:3 (200-300 μm along their long axis), and there is no difference in morphology between the zircons of 71D and 71P. Most of the zircons are inclusion-rich, and they are typically oscillatory-zoned. Only one grain observed had a clear resorption rim, and there are rare narrow rims (usually <10 μm wide), which are typically inclusion-free. Some zircons have inclusion-free cores or inclusion-free rims, and some cores are extremely metamict (**Fig. 13l**). For 71D, 28 spots on 23 grains and for 71P, 25 spots on 22 grains were analyzed. When data from both samples was combined, two populations emerged from the data. The youngest is defined by five spots on grains from 71P and is 2702 ± 57 Ma, with a lower intercept of 1063 ± 240 Ma (MSWD: 2.4). The older population is defined by 34 spots on grains from both 71D and 71P, and has an upper

intercept age of 2858 ± 5 Ma, with a lower intercept of 334 ± 140 Ma (MSWD: 1.7; **Fig. 10j**). Twelve discordant spots that apparently belong in the younger population were excluded because of extreme metamict textures and excessive ^{204}Pb, and two points were excluded for representing mixed ages.

Titanites are also inclusion-rich, although they contain fewer inclusions than those from sample 01. Patchy or sector zoning is sometimes observed, but grains are generally unzoned or exhibit gradational concentric zones, especially in 71P. However, several grains exhibit thin rims (**Fig. 13k**). Titanites were not observed in thin section associated with the dyklets or alteration, so both samples are combined for statistical analysis. For 71D, 20 spots on 19 grains and for 71P, 15 spots on 14 grains were analysed. One spot was excluded for low U concentrations. The remaining 34 spots, which clustered on concordia, yielded an age of 2854 ± 7 Ma, with a lower intercept anchored at 0 Ma (MSWD: 1.4; **Fig. 10k**).

Trace element concentrations were obtained from 20 spots on zircons: 6 spots were from the 2702 Ma population, and 14 were from the 2858 Ma population. The younger population tends to have lower Th/U and higher Ti, Hf, and U and exhibits more pronounced positive Ce and negative Eu anomalies. The older population has no Eu anomaly and a minor positive Ce anomaly (Ce/Ce* = 5.2). The REE patterns from both age populations are similar with flat LREE and MREEs and a positive slope in HREEs. Both populations have similar concentrations of LREEs, but the 2702 Ma population has higher HREE concentrations. In general, zircons from this sample have high LREE concentrations (**Fig. 12**).

3.4.3 Skinner Lake block

41: Tonalite containing blebby pegmatite

This sample is from the eastern edge of the Skinner Lake block. It is gneissic and strongly foliated, but is also crosscut by a metamorphosed diabase dyke and narrow epidote-rich veins and has many wormy pegmatitic enclaves (**Fig. 4c**). Gneissic bands are narrow (~1 mm), fairly gradational, and approximately planar, although there is some waviness in the banding. Compositionally, this sample is a tonalite, containing trace alkali feldspar, 50% plagioclase (An_{22}), 40% quartz, 10% biotite, and trace allanite with epidote rims, pyrite, and hornblende (magnesiohornblende). There is minor epidote and chlorite alteration of biotite and hornblende, which occurs with sericite alteration of plagioclase and is associated with epidote veins. Plagioclase is also myrmekitic.

Zircons have variable morphologies and sizes with aspect ratios from 1:1 to 1:3 and lengths between 450 and 150 μm. Many grains have xenocrystic cores with thin (~10 μm) resorption rims, and there are several compound grains. There are few inclusions and minor metamict areas, especially in cores. Most grains are generally oscillatory-zoned, although a couple are unzoned. For geochronology, 34 spots on 27 grains were analyzed. Three spots were excluded: one for high ^{204}Pb concentrations, one, which was on a resorption rim, for yielding a mixed age, and one that was extremely metamict. Two populations emerged from the data. The first, from 9 spots found in rims and in cores of two unzoned grains, had an age of 2828 ± 9 Ma, with a lower intercept of 113 ± 480 Ma (MSWD: 2.2). The second population of 19 spots from cores yielded an age of 2871 ± 6 Ma, with a lower intercept of 141 ± 450 Ma (MSWD: 1.9). The three remaining spots are also from cores and have $^{207}Pb/^{206}Pb$ ages of 2932 ± 8 Ma, 2955 ± 10 Ma, and 2996 ± 10 Ma (**Fig. 10l**).

Ten spots on zircons were analyzed for trace element concentrations. Four spots were from the 2828 Ma population, and 6 were from the 2871 Ma population. The younger spots are characterized by lower Ti, LREEs (La-Gd) and Th/U, as well as more pronounced positive Ce and negative Eu anomalies. These spots also have steeper HREE slopes. Both populations have similar trends in REE concentrations, with strong negative Eu anomalies and negligible positive Ce anomalies. Rims have flat LREE and MREE profile with a steep positive slope in HREEs, whereas cores have a slight positive slope in LREEs and MREEs with a steep positive slope in HREEs (**Fig. 12**).

43: K-feldspar augen gneiss

This sample is from the centre of the Skinner Lake block, about 12 km north of the eastern edge of the NCGB, in an area with abundant pegmatites. It is from an augen gneiss with plagioclase and alkali feldspar augen up to 2 cm in diameter. Gneissic bands are 1-5 cm wide, and are roughly planar, with only minor folding and undulation. Biotite-rich bands are strongly foliated and medium- to fine-grained, whereas felsic bands are coarse-grained and K-feldspar-rich. Compositionally, this sample is a granite, containing 25% alkali feldspar, 35% plagioclase (~An_{20}), 25% quartz, 15% biotite, and trace pyrite, magnetite, and zircon. Plagioclase commonly exhibits myrmekite and has many inclusions. Chlorite and sericite alteration is common.

Zircons tend to be long and narrow, with aspect ratios between 1:2 and 1:3 and sizes between 150 and 450 μm, with most grains ~250-300 μm. Many zircons contain xenocrystic cores, and some have extremely thin resorption rims (~10 μm). Some cores lack resorption rims, and instead are surrounded by inclusions, and some cores are surrounded by several concentric rims. Most of the zircons have inclusion-rich and metamict zones, which are usually, but not exclusively, located in cores. Outside of these areas, grains are generally oscillatory-zoned. For geochronology, 29 spots on 14 grains were analyzed, and three populations emerged. Twelve points formed the first population, which is found in rims and cores of three grains without xenocrystic cores, and their age is 2735 ± 7 Ma, with a lower intercept of 63 ± 180 Ma (MSWD: 0.95). The second population of 5 spots from cores and interior rims has an age of 2835 ± 13 Ma with a lower intercept of 17 ± 970 Ma (MSWD: 0.53). The final population is defined by 6 spots from cores and 1 from an interior rim, and yields an age of 2871 ± 9 Ma, with a lower intercept of -153 ± 1100 Ma (MSWD: 1.11; **Fig. 10m**). Five points were excluded for high ^{204}Pb concentrations.

Trace element concentrations were analyzed in 10 spots on zircons. 5 spots were from the 2735 Ma population, 4 were from the 2835 Ma population, and 1 was from the 2871 Ma population. Chemically, the two youngest populations are similar. These two younger populations have higher Hf, Th, U, lower Th/U, and more pronounce positive Ce anomalies. The older population had a negative Ce anomaly, but otherwise all three populations have similar REE profiles; they all have strong negative Eu anomalies, flat profiles in LREEs and MREEs, and steep positive slopes in HREEs (**Fig. 12**).

3.4.4 Wharram Lake block

55: Equigranular granodiorite

This sample is from the northeastern boundary of the Wharram Lake pluton and is coarse-grained, equigranular and isotropic. Although there is no fabric, quartz in this rock exhibits strong undulose extinction, and there are some centimeter-scale, irregularly shaped, unaligned, biotite-rich pockets. Compositionally, this rock is a granodiorite, containing 15% alkali feldspar, 45% plagioclase (~An_{20}), 30% quartz, 9% biotite, 1% magnetite, and trace titanite, apatite, muscovite, and pyrite. There is minor sericite alteration, and some biotite has been altered to chlorite.

Zircons have a variety of morphologies and sizes, ranging from 150-400 μm. They have aspect ratios between 1:1 and 1:5, and most are oscillatory zoned. Xenocrystic cores are common and are distinguished by disrupted zoning, since resorption rims are uncommon in these zircons. Composite grains are common, as are inclusions, especially in cores. Cores are also commonly metamict. For geochronology, 25 spots on 18 grains were analyzed, and three spots were excluded for high ^{204}Pb concentrations. Three populations emerged from the data, the first consisting of 9 spots from rims with an age of 2678 ± 18 Ma, with a lower intercept at -85 ± 470 Ma (MSWD: 2.0). The second population is formed by 10 spots from cores and yielded an age of 2928 ± 12 Ma, with a lower intercept of -876 ± 1200 Ma (MSWD: 0.87). The third population is defined by three spots from zircon cores and has an upper intercept age of 2976 ± 15 Ma, with a lower intercept fixed at 0 Ma (MSWD: 0.56; **Fig. 10n**).

Titanite grains are rare and relatively homogenous, with only minor concentric or patchy zoning. There are only minor inclusions and cracks, some of which are annealed. Most analyzed grains were broken, but titanite is typically ~0.5 mm long. For geochronology, 15 spots on 13 grains were analyzed, and the results cluster tightly on concordia. The resulting age is 2689 ± 13 Ma, with a lower intercept fixed at 0 Ma (MSWD: 0.85; **Fig. 10o**).

In zircons, 20 spots were analyzed for trace element concentrations. Ten spots are from the 2678 Ma population, 9 are from the 2967 Ma population, and one is from a xenocrystic core. The younger population is characterized by lower Th/U and higher La, Hf, and U. The inherited grain has a similar REE profile to the 2967 Ma population, with a very strong Eu anomaly, flat to negative slopes in LREEs and a strong positive slope in MREEs and HREEs, although the spot from the xenocrystic core has much higher concentrations of REEs. The chondrite-normalized REE patterns in the 2678 Ma population are similar to those from the pegmatite sample (54), but zircons from this population lack the prominent negative Eu anomaly of the pegmatites. This population has flat slopes in the LREEs, strong negative slopes through the MREEs and strong positive slopes in the HREEs. Concentrations of MREEs and HREEs are similar between the two populations, but the 2678 Ma zircons have higher concentrations of LREEs (**Fig. 12**).

3.4.5 North Caribou Lake batholith pluton

46: Foliated granodiorite

This sample is from the centre of the western edge of the NCB, near Musselwhite Mine. It is fairly strongly foliated, but the orientation of foliation is slightly variable, especially near contacts with pegmatitic dykes. The amount of strain is heterogeneous, and the rock ranges from fine to medium grained. Compositionally, it is a granodiorite containing 10% alkali feldspar, 50% plagioclase (~An_{20}), 30% quartz, 10% biotite, and trace magnetite, titanite, apatite, hornblende, allanite, and epidote. The hornblende is almost entirely altered to epidote, which also occurs as inclusions in biotite, rims on allanite, and as an alteration product of biotite. There is very minor sericite alteration of plagioclase near fractures.

Zircons are generally short and stout, with aspect ratios between 1:1 and 1:2 and lengths between 150-200 μm, but two grains are slightly narrower, with aspect ratios closer to 1:3 and lengths ~300 μm. They are generally inclusion-free and oscillatory-zoned, although about half have metamict cores that are CL dark, and a few have rounded CL-bright cores. Some zircons have disrupted zoning between rims and cores, but only 2 have resorption shadows, and most crystals only show compositional variation between rims and cores. For geochronology, 19 spots on 18 grains were analyzed, and one spot was excluded due to high ^{204}Pb concentrations. Sixteen spots from both rims and cores yielded an age of 2867 ± 9 Ma, with a lower intercept of -182 ± 380 Ma (MSWD: 1.8). Two spots from CL-bright cores had older $^{207}Pb/^{206}Pb$ ages of 2957 ± 4 Ma and 3005 ± 6 Ma (**Fig. 10p**).

Titanite grains are generally prismatic and homogeneous in BSE, but are subhedral and zoned toward their rims, which are low in U (<30 ppm). Grains from the mineral separate were broken, but the average size of whole crystals is 200-600 μm. For geochronology, 14 spots on 11 grains were analyzed. Four spots from rims were excluded because the U concentrations were too low for accurate analysis. The remaining grains formed two populations, which cluster on concordia. The younger, consisting of 6 spots, has an upper intercept age of 2742 ± 35 Ma, with a lower intercept fixed at 0 Ma (MSWD: 4.2). All of these spots, save 1, are concordant, and the concordia age is 2766 ± 18 Ma (MSWD: 3.0). Four grains form the older population, with an age of 2869 ± 15 Ma, a lower intercept fixed at 0 Ma (MSWD: 1.6; **Fig. 10q**).

Trace element concentrations were collected from 10 spots on zircons, 2 of which were on xenocrystic cores. Both the xenocrystic cores and the 2867 Ma population have similar REE patterns, with no Ce anomaly, a strong negative Eu anomaly, gentle positive slopes in LREEs and MREEs and steep positive slopes in HREEs. The inherited cores have higher concentrations of LREEs, but the concentrations of HREEs are similar between the two populations. In general, these zircons are characterized by high LREE concentrations (**Fig. 12**).

49: Leucocratic granodiorite

This sample is from the southeastern corner of the NCB, about 15 km north of the southern arm of the Windigo greenstone belt. This sample is generally gneissic, although banding, which is defined by relative amounts of quartz and feldspar, is difficult to follow in outcrop due to a scarcity of mafic minerals. Throughout the area are several, mostly aplitic, dykes. This rock is a granodiorite, with a composition of 20% alkali feldspar, 45% plagioclase (~An_{20}), 30% quartz, 4% biotite, and 1% muscovite, with trace amounts of apatite, zircon and epidote, which occurs as inclusions in biotite.

Zircons are short, with aspect ratios between 1:1 and 1:2, and lengths ~150-250 μm, with a couple larger grains from 300-400 μm. Xenocrystic cores are common, though not ubiquitous, and are surrounded by resorption shadows. Oscillatory zoning is common in both rims and cores, and most zircons a have a couple of inclusions in both their rims and cores. For geochronology, 25 spots on 23 grains were analyzed. Two spots were not included, one for high ^{204}Pb concentrations, and one, which fell on a resorption shadow, for yielding a mixed age. Three populations emerged; the youngest from 5 spots on the rims of zircons had an age of 2857 ± 9 Ma, a lower intercept of -1022 ± 460 Ma (MSWD: 0.10). The second population of 6 points from cores yielded an age of 3002 ± 14 Ma, with a lower intercept of 0 ± 24 Ma (MSWD: 1.4). The oldest population with 12 points, mostly from cores that had truncated oscillatory zoning, had an age of 3132 ± 7 Ma, a lower intercept of 35 ± 22 Ma (MSWD: 1.10; **Fig. 10r**).

In zircons, 10 spots were analyzed for trace element concentrations. Five spots were from the 2857 Ma population, and 5 were from the 3132 Ma population. The younger population had lower Ti, P, Hf, Th, LREE, and Th/U. Both populations have slight positive Ce anomalies and strong negative Eu anomalies. The younger population has lower

concentrations of LREEs and a gentle positive slope throughout the REE profile, whereas the older population has a flat to gentle positive slope in LREEs and MREEs (**Fig. 12**).

66: High-strain tonalite

This sample is from the centre of the NCBp, about 7 km southwest of sample 46. In outcrop, this rock is extremely heterogeneous, with fine-grained biotite-rich bands that are up to 30 cm wide and lighter, coarser-grained bands that can be greater than 50 cm wide. Biotite-rich bands tend to be fairly discrete, and contain cm-scale bands of lighter material that are generally compositionally similar to the light bands, although some are transposed quartz veins. Both light and dark material was strongly foliated, and dark bands were commonly boudinaged. Although exposure was fairly good in the area, individual outcrops were small, so it was difficult to determine whether the biotite-rich bands were strongly sheared inclusions or a product of gneissic banding. Aplitic to pegmatitic dykes were common. This sample is from a biotite-rich band, and is a tonalite containing: 45% plagioclase (An_{30}), 30% quartz, 15% hornblende (edenite), 10% biotite, and minor apatite, titanite, epidote, and K-feldspar. Epidote, typically an alteration product of biotite, and K-feldspar are associated with fractures and sericite alteration of plagioclase.

Only 7 zircons were recovered from this sample, and they are narrow, with aspect ratios ≥1:4 and lengths from 150-400 μm. Grains tend to have extremely metamict, inclusion-rich cores and thin (<10 μm thick) oscillatory-zoned rims. Three of the seven grains were compound or twinned zircon (**Fig. 13c**). Six spots on 6 grains were analyzed, and two spots were excluded for high ^{204}Pb concentrations. The remaining 4 spots form a discordia line with an age of 2829 ± 13 Ma, a lower intercept of 1009 ± 65 Ma (MSWD: 0.90; **Fig. 10s**).

Titanite grains tend to be round (**Fig. 4j**), and they have few inclusions, most of which are in a layer between the rims and cores. Rims are thin (<10 μm), and only preserved on a couple grains. Most grains analyzed for geochronology were broken, as titanites are typically 100-200 μm. In BSE, these grains are generally patchy, but many have concentric zones with lighter cores and darker rims, and a couple have remnant oscillatory zoning that is overprinted by patchy light and dark areas (**Fig. 13j**). For geochronology, 13 points on 12 grains were analyzed. Three points with low U (< 30ppm) and 2 spots with high ^{204}Pb

concentrations were discarded. The remaining 8 points cluster on concordia and have a upper intercept age of 2733 ± 33 Ma, with a lower intercept fixed at 0 Ma (MSWD: 2.5; **Fig. 10t**).

Trace element concentrations in zircon were obtained from 8 spots. Despite the homogeneity of the ages in this sample, there are two populations in the trace element data, much like sample 48. The first, with 5 spots, has a flat chondrite-normalized REE pattern, with a slight negative Eu anomaly (Eu/Eu* = 0.62) and no Ce anomaly, and the second, with 3 spots, has a flat LREE profile, with a steep positive slope in MREEs and HREEs and strong positive Ce (Ce/Ce* = 2.9) and weak negative Eu anomalies (Eu/Eu* = 0.53). The first population has higher LREEs and MREEs, but lower HREEs, along with higher Hf, lower Th, U, Th/U, and more pronounce positive Ce anomalies (**Fig. 12**).

3.4.6 North Caribou Lake batholith core

51: K-feldspar augen gneiss

This sample is from the south-central part of the batholith, near the southern boundary of the North Caribou batholith core. In outcrop, the rock is extremely heterogeneous, containing gneissic areas with complexly folded compositional bands, as well as areas with schlieren surrounded by weakly foliated leucogranite (**Fig. 4e**). There are also abundant wormy pegmatites and pegmatitic dykes. This sample is from the weakly foliated leucogranite. Compositionally, this sample is a granite containing 25% alkali feldspars, 35% plagioclase (~An_{20}), 25% quartz, 8% biotite, 5% titanite, 1% muscovite, 1% magnetite, and trace apatite and pyrite. Alkali feldspars are large (up to 2 cm) and commonly exhibit perthitic texture, and plagioclase is strongly sericite-altered, especially in cores.

Based on morphology, there are two zircon populations. The first has aspect ratios between 1:1 and 1:3 (150-400 μm long), and these zircons typically have xenocrystic, oscillatory-zoned cores surrounded by resorption rims. Rims have radial cracks, and a couple of these grains are composite. Zircons in the second population are thin, with aspect ratios between 1:4 and 1:7 (200-350 μm long). Grains in both populations are oscillatory zoned and have many inclusions. For geochronology, 16 spots on 16 grains were analyzed, and two populations emerged. The first population of 9 spots is associated with the narrow grains and rims on the wider grains, and yielded an age of 2693 ± 12 Ma with a lower intercept of 771 ± 910 Ma (MSWD: 1.6). The second age is found in xenocrystic cores and had an age of 2834 ± 32 Ma, a lower intercept of -823 ± 2800 Ma (MSWD: 2.5). Three spots were discarded:

two for high ^{204}Pb concentrations and one that landed on a resorption rim and yielded a mixed age (**Fig. 10u**).

Titanite is so abundant in this sample that it defines the foliation. Unbroken titanite grains are 0.2-2.5 mm long. Grains are euhedral and typically oscillatory zoned, although many grains have unzoned cores (**Fig. 13h**). For geochronology, 18 spots on 16 grains were analyzed, and the spots cluster tightly on concordia. Two of these spots, which are outliers, were on BSE-dark areas. Including these spots, the upper intercept age is 2810 ± 17 Ma with a lower intercept fixed at 0 Ma (MSWD: 2.8), but if these spots are excluded, the upper intercept is 2812 ± 10 Ma (MSWD: 1.4; **Fig. 10v**).

In zircons, 9 spots were analyzed for trace element concentrations. Five spots were from the 2693 Ma population, and 4 were from the 2834 Ma population. The older population has higher Hf, lower U/Th, and a less pronounce Ce anomaly. Both populations have flat chondrite-normalized REE profiles and very slight positive Ce and negative Eu anomalies. Additionally, both populations have similar concentrations of REEs and high LREE concentrations compared with zircons from other samples (**Fig. 12**).

61: Massive tonalite

This sample is from a magnetic low just west of the North Caribou batholith core. It is not in the pluton defined by Stott and Biczok (2010), but it has the same magnetic signature as the pluton. In outcrop, this sample looks like incipient gneiss, with some higher-strain areas that are more biotite-rich and finer-grained. There is no obvious fabric in either domain, although quartz is deformed, exhibiting undulose extinction to sub-grain formation. This sample is from the more massive, coarser-grained areas in the outcrop. Compositionally, it is a tonalite containing 5% alkali feldspar, 45% plagioclase (An_{26}), 40% quartz, 6% biotite, 3% hornblende (hastingsite), 1% magnetite, and trace apatite, epidote, titanite and pyrite. There is minor sericite alteration of plagioclase and epidote alteration of biotite and hornblende associated with fractures, but there are also euhedral epidote inclusions in biotite that appear to be in equilibrium.

Zircons have a variety of morphologies, with aspect ratios ranging from 1:1 to 1:5, but most are ~1:2. They are generally ~150-200 μm long, but range up to 350 μm long. Most have a few inclusions and are oscillatory zoned with CL-bright cores and CL-dark rims. There are also a few rounded xenocrystic cores with disrupted zoning, and occasional

metamict patches. For geochronology, 25 spots on 22 grains were analyzed, and two were discarded for falling on extremely metamict areas. Of the remaining spots, 20 formed a population with an age of 2833 ± 13 Ma, a lower intercept of 665 ± 660 Ma (MSWD: 2.0). Three spots from xenocrystic cores have an age of 2913 ± 11 Ma, with a lower intercept fixed at 0 Ma (MSWD: 1.4; **Fig. 10w**).

Titanite is sub- to anhedral, and typically occurs as round, rather than prismatic, crystals. Since there is no obvious fabric in the sample, it is impossible to tell if the titanite grains are aligned with foliation, but they do tend to occur along linear arrays. The grains are unzoned to patchy zoned, and one exhibits some oscillatory zoning. Typical crystals are 50-300 μm long. Most grains are full of micron-scale inclusions. For geochronology, 11 spots on 11 grains were analyzed, and they cluster tightly on concordia. The resulting upper intercept age is 2786 ± 14 Ma, with a lower intercept fixed at 0 Ma (MSWD: 2.2; **Fig. 10x**).

Trace element concentrations were analyzed in 10 spots on zircons. They have high LREE concentrations, a flat LREE and MREE profile and a steep positive slope in HREEs. There are weak positive Ce and negative Eu anomalies (**Fig. 12**).

62/63: Gneissic tonalite

These samples are from the same outcrop in the centre of the magnetic high that defines the North Caribou Lake batholith core. Sample 62 has a stronger foliation and a smaller grain-size than sample 63, but they are compositionally similar. The outcrop is weakly gneissic around sample 62, with some biotite- and hornblende-rich bands ~2 cm wide, but contact with the coarser-grained, weakly foliated rock (sample 63) is gradational, irregular, and crosscuts foliation. Both samples are tonalites, containing trace alkali feldspars, 50% plagioclase (An_{28}), 40% quartz, 8% biotite, 1% hornblende (magnesiohornblende), 1% magnetite, and trace apatite, pyrite, epidote, and chlorite. There is minor sericite alteration of plagioclase, which is associated with chlorite and, in sample 62, epidote-alteration of biotite and hornblende. All alteration is associated with fractures.

There is very little variation in zircon morphologies, and grains typically have aspect ratios between 1:2 and 1:3 and are between 150-400 μm long. All zircons have CL-dark cores and CL-bright rims, with sharp contacts between rims and cores. Grains are oscillatory zoned, with few inclusions, which are generally concentrated in cores, and occasional metamict textures. There are a few composite grains, and most grains contain radial cracks in

both rims and cores (**Fig. 13d**). For sample 62, 24 spots on 18 grains, and for sample 63, 21 spots on 19 grains were analyzed. As the ages were identical, the data from both samples were combined. Five spots were excluded from these results because of elevated ^{204}Pb concentrations. Of the remaining spots, 38 clustered around concordia and formed a population with an age of 2854 ± 8 Ma, with a lower intercept of 562 ± 480 Ma (MSWD: 1.8). Two spots from cores yielded much older ages, although there was no visible difference between these cores and cores in other grains. These $^{207}Pb/^{206}Pb$ ages were 2953 ± 10 Ma and 3094 ± 15 Ma (**Fig. 10y**).

Trace element concentrations were obtained from 20 spots. Eight spots were from cores, and 12 were from rims. Cores have higher Th, U, Ce, and REEs (Tb-Lu), whereas REE patterns are similar, with slight positive Ce (Ce/Ce* = 3.8) and Eu (Eu/Eu* = 1.1) anomalies. Chondrite-normalized REE plots have a slight positive slope in LREEs, a flat plateau in MREEs and a steep positive slope in HREEs. In general, these zircons have high concentrations of LREEs (**Fig. 12**).

3.4.7 Libert Lake pluton

45: Melanocratic granite

This sample is from the centre of the Libert Lake pluton as defined by the Ontario Geological Survey map (1991), although geophysical evidence suggests that if a discrete intrusion exists in this area, it is located further north, putting the location of this sample near its southern margin. This rock is heterogeneous, ranging from gneissic to strongly foliated and is generally medium-grained, with larger (5-10 mm) plagioclase and alkali feldspar crystals. Compositionally, it is a granite, containing 25% alkali feldspar, 30% plagioclase (~An_{20}), 25% quartz, 18% biotite, 1% apatite, 1% titanite, and trace magnetite, pyrite, and allanite with epidote rims. In addition to the gneissic banding and strong foliation, quartz grains have completed sub-grain formation and are polygonal. Plagioclase has myrmekitic textures and very little to no sericite alteration, and there is minor epidote alteration of biotite. Late pegmatites are common in this outcrop.

Zircons are generally stout, with aspect ratios between 1:1 and 1:2 and from 150-350 μm long. Most grains are oscillatory zoned, although some have minor sector zoning as well. There are also a few grains with xenocrystic cores and accompanying resorption rims. These zircons are rarely metamict, although metamict textures and abundant inclusions are more

common in the centres of grains (**Fig. 13i**). Most grains are also fractured. For geochronology, 30 spots on 14 grains were analyzed, and 9 spots were excluded due to high ^{204}Pb concentrations. Two additional spots from resorption rims were excluded for yielding likely mixed ages. Two concordant spots from rims yield a concordia age of 2700 ± 8 (MSWD: 1.9), and 15 spots from rims and cores yielded an age of 2730 ± 8 Ma, with a lower intercept of 7 ± 200 Ma (MSWD: 1.9). Two spots from xenocrystic cores had $^{207}Pb/^{206}Pb$ ages of 2872 ± 12 Ma and 2945 ± 9 Ma (**Fig. 10z**).

Titanite grains are strongly aligned with foliation and commonly rimmed with biotite. They are round and have obvious transparent rims. In BSE, they exhibit mottled to patchy cores and homogenous rims. There are very few inclusions and cracks, and there are healed fractures in the cores of some grains (**Fig. 13g**). Grains used for geochronology are broken, but titanite crystals are typically 0.3-1 mm long. For geochronology, 18 spots on 14 grains were analyzed, and three spots were excluded for high ^{204}Pb concentrations. Two populations emerged, and the first, consisting of 11 spots, yielded an age of 2700 ± 27 Ma, with a lower intercept fixed at 0 Ma (MSWD: 1.7). Four spots from titanite cores yielded an age of 2830 ± 51 Ma, with a lower intercept of 249 ± 3800 Ma (MSWD: 1.6; **Fig. 10aa**).

Trace element concentrations were analyzed in 5 spots on zircons. Three spots were from the 2730 Ma population, one was from the 2700 Ma, and one was from the 2945 Ma xenocrystic grain. The xenocrystic core is indistinguishable from the 2730 Ma population, except it has no Ce anomaly, whereas the spot from the 2700 Ma population has lower P and Th/U, and higher Ti, LREEs and U. It also has a less pronounced negative Eu anomaly. REE profiles for all of the spots are nearly identical, with a moderate negative Eu anomaly, a flat slope through the LREEs and MREEs, and steep positive slopes in the HREEs (**Fig. 12**).

3.4.8 Pegmatite

54: K-feldspar pegmatite

This single pegmatite sample with abundant zircon is from the SLGC and was collected from the same outcrop as 53C/F. Compositionally, it is fairly typical of K-feldspar pegmatites. In outcrop, it is not obviously deformed, and it intruded as brittle-ductile dykes. Grain size varies from aplitic to pegmatitic throughout the outcrop, and there is no correlation between grain size and the proximity of the contact with the country rock. However, pegmatitic areas are generally found in wider areas within the dykes. It contains

40% alkali feldspar, 25% plagioclase (~An_{20}), 30% quartz, 3% biotite, 2% muscovite, and trace zircon and pyrite. Alkali feldspars have perthitic textures, and quartz has very strong undulose extinction, and minor, small subgrains forming near its edges. Plagioclase is almost completely altered to sericite.

Zircons are large, up to 1 mm long, and fairly similar. Because of their size, zircons were extracted from mineral separates with diameters between 500 and 250 μm. They are prismatic and have aspect ratios ~1:2. Most zircons are extremely metamict and full of inclusions, and a couple have oscillatory-zoned patches, usually on the rims (**Fig. 13b**). For geochronology, 29 spots on 20 grains were analyzed, but due to the extreme radiation damage on these grains, all but 2 had excess ^{204}Pb, and most had experienced Pb-loss. Because of the metamict textures of these zircons, all exhibited $^{207}Pb/^{206}Pb$ ratios with multiple plateaus in Iolite. For other samples, intervals used for age determinations were chosen based on the longest plateau over pristine zircon, which was determined by ^{204}Pb concentrations and patterns in U and Zr concentrations. Since most of these zircons were no longer crystalline, that methodology was impractical, and intervals were chosen based on the proximity of each spot to others on a U-Pb concordia diagram. Although this method likely introduces extra bias into the data, it was the best way to find a reasonable age estimate for these zircons. Only 4 spots were concordant, and one of these is likely inherited. The 13 spots with the highest $^{207}Pb/^{206}Pb$ ages form a model 2 discordia line with an age of 2619 ± 14 Ma, a lower intercept of 546 ± 210 Ma (MSWD: 2.0; **Fig. 10ab**). Both of the points with no excess ^{204}Pb are in this population. When all of the points, except for 2 inherited points, are considered, the resulting age is 2623 ± 27 Ma, with a lower intercept of 950 ± 89 Ma (MSWD: 9.5). When the data were reduced using the longest plateau, as with the rest of the samples, the best age (from 10 out of 29 points) was 2588 ± 14 Ma, with a lower intercept of 497 ± 50 Ma (MSWD: 2.9). One of the inherited points is concordant, whereas the other is 26% discordant, and these two points have a $^{207}Pb/^{206}Pb$ weighted average age of 2758 ± 5 Ma (**Fig. 10ab**).

Trace element concentrations were collected from 12 spots. There are 2 spots on a xenocrystic zircon, and these spots exhibit a flatter REE pattern, but are otherwise chemically similar to the other spots. These zircons are characterized by high U concentrations (up to 16,000 ppm, about an order of magnitude greater than zircons from

other samples), high Hf, Th, HREEs (Gd-Lu), low Th/U, and variable LREEs (La-Sm). These zircons have a strong negative Eu anomaly, a flat to slightly negative slope in LREEs, and a strong positive slope in MREEs and HREEs (**Fig. 12**).

3.5 Thermobarometry

To illuminate the temperature and pressure conditions under which these intrusive rocks were emplaced, I applied several geothermometers, including Ti-in-zircon and amphibole-plagioclase, and one geobarometer, Al-in-hornblende to a suite of samples.

Amphibole and plagioclase compositions were acquired using a JEOL 8230 SuperProbe electron microprobe at the University of Ottawa, Ottawa, Canada and Camebax MBX electron microprobe at Carleton University, Ottawa, Canada. Analysis preformed at Carleton used a 1 μm spot size, with a 20 kV accelerating voltage and 15 second count times for all elements except Cl, F (both 45 seconds) and Si, which was measured to 40,000 counts. An in-house garnet standard was used for calibrations. Ni and Zn were not analyzed at Carleton, and Cl and F were only analyzed in 5 spots from each sample. At the University of Ottawa a 5 μm spot size was used with an accelerating voltage of 20 kV. Counting times were 10-30 seconds, depending on the element, and enstatite, diopside, hematite, albite, and sanidine standards were used for amphiboles, and albite, sanidine and barite standards were used for plagioclase. Plagioclase was only analyzed at the University of Ottawa. Spots from plagioclase grains were within 20 μm of the contact with adjacent amphiboles and were paired with spots on these amphiboles. In addition to spots on amphibole rims that are paired with plagioclase spots, spots were analyzed in the centres of amphiboles from some samples to confirm chemical homogeneity.

Ti-in-zircon thermometry was preformed on zircons from all of the geochronology samples. Titanium concentrations were collected with other trace elements using LA-ICP-MS at the University of New Brunswick, Fredericton, Canada. NIST 610 and 612 glasses were used as standards, along with the 91500 zircon, although this standard has been shown to have variable Ti concentrations (Fu *et al.*, 2008). Since all samples have at least 60 wt% SiO_2 and contain abundant quartz, SiO_2 saturation is assumed. Many samples are likely undersaturated in TiO_2, but since low αTiO_2 leads to underestimating temperatures, all of the calculated temperatures are maximum values. Moreover, Ferry & Watson (2007) demonstrated that calculations performed on low αTiO_2 rocks only underestimates

temperature by up to 100 °C. This thermometer is highly sensitive to small changes in Ti concentrations, as variations of 1-2 ppm Ti (the typical error associated with a single analysis) can yield temperatures that vary by up to 50 ºC. Additionally, as has been reported by other authors (e.g. Hofmann *et al.*, 2009), there can be extreme variations (> 10 ppm is not uncommon) in Ti concentrations within a single crystal. Due to this sensitivity and variability, most samples have errors around 100 °C, and therefore, rocks with low αTiO_2 would still yield Ti-in-zircon temperatures within calculated errors. Temperatures are calculated using the revised formula published by Ferry & Watson (2007). Trace element data were reduced using Iolite, and if Ti concentrations showed irregular patterns over the course of a single ablation (spikes, concave down curves, concentrations increasing throughout the duration of the analysis, etc.), data from those spots were not used for calculating temperatures. Weighted averages, which generally yielded values more consistent with probability density plots than the means did, were calculated using Isoplot. Reported errors are 2σ, and results are summarized in **Appendix H**.

Al-in-hornblende and plagioclase thermobarometry was performed on samples with hornblende that co-exists with quartz and plagioclase feldspar. In general, amphiboles are subhedral to euhedral. About half of the samples contained amphiboles with a uniform composition, which indicates that they are likely primary and not metamorphic, and about half have rims that are either grew or recrystallized during a subsequent thermal event. Amphibole crystals used for this analysis were not chlorite- or epidote-altered, although many were from samples with altered hornblende, especially near late veins. Johnson & Rutherford's (1989) experimental calibrations were based on a buffering assemblage of hornblende + biotite + plagioclase + K-feldspar + quartz + titanite + Ti and Fe-oxides. However, Anderson & Smith (1995) note that low $\alpha_{orthoclase}$ and $\alpha_{titanite}$ do not have a significant effect on the calculated pressures. In addition to the buffering assemblage, samples should have plagioclase with compositions below 35% An, and whole-rock SiO_2 from 60-68 wt%. Amphibole formulas were calculated using the methods outlined in Leake *et al.* (1997), and maximum and minimum quantities of Fe^{3+} were calculated. For all elements, apfu in amphiboles were calculated based on the average of these two Fe^{3+} values, and amphibole compositions are reported in **Appendix H** and displayed in **Figure 14**. Plagioclase is zoned in many samples, but plagioclase rims were essentially homogenous.

Table 3. Summary of hornblende and zircon thermobarometry

Sample		Hbl-Plag Therm B			550 °C (±50)		Hbl-Plag Therm A			Ti-in-hbl Thermometer			Gd/ Trondhj Solidi			Tonalite Solidus			Buffer	Fe/Fe	Fe-Mg hbl	Fe-Mg rock	SiO_2 rock	%An
		T	P	km	P	km	T	P	km	T	P	km	T	P	km	T	P	km						
01		610 ± 20	5.1 ± 0.2	19	--	--	**519 ± 7**	4.8 ± 0.2	18	**690 ± 40**	4.5 ± 0.4	17	620	5.1 ± 0.2	19	--	--	--	yes	0.18*	0.51	0.57	62	20
13	Cores	610 ± 10	6.3 ± 0.6	23	--	--	**560 ± 30**	6.3 ± 0.6	23	610 ± 40	6.3 ± 0.6	23	620	6.3 ± 0.6	23	--	--	--	yes	0.25*	0.54	0.59	61	23
	Rims	560 ± 10	3.6 ± 0.2	13	3.6 ± 0.2	13	505 ± 8	3.1 ± 0.3	11	**680 ± 50**	3.2 ± 0.3	12	--	--	--	--	--	--	yes	0.14*	0.47	0.59	61	16
15	Cores	610 ± 30	5.5 ± 0.6	20	--	--	**529 ± 9**	5.3 ± 0.7	20	560 ± 20	5.5 ± 0.6	20	620	5.6 ± 0.5	21	--	--	--	yes	0.36	0.51	0.59	61	22
	Rims	570 ± 20	3.6 ± 0.3	13	3.5 ± 0.3	13	505 ± 6	3.1 ± 0.3	11	526 ± 5	3.3 ± 0.3	12	--	--	--	--	--	--	yes	0.31	0.45	0.59	61	22
	Rims+	560 ± 20	1.8 ± 0.3	7	1.7 ± 0.5	6	**488 ± 5**	0.9 ± 0.6	3	508 ± 8	1.2 ± 0.6	5	--	--	--	--	--	--	yes	0.21*	0.41	0.59	61	22
13+15	Cores	610 ± 20	6.2 ± 0.7	23	--	--	**550 ± 26**	6.1 ± 0.7	23	600 ± 40	6.1 ± 0.7	23	620	6.2 ± 0.6	23	--	--	--	yes	0.27	0.54	0.59	61	22
	Rims	550 ± 10	3.6 ± 0.2	13	3.6 ± 0.2	13	506 ± 7	3.1 ± 0.3	12	660 ± 70	3.2 ± 0.3	12	--	--	--	--	--	--	yes	0.17*	0.47	0.59	61	22
	Rims+	560 ± 20	1.8 ± 0.3	7	1.7 ± 0.5	6	**488 ± 5**	0.9 ± 0.6	3	508 ± 8	1.2 ± 0.6	5	--	--	--	--	--	--	yes	0.21*	0.41	0.59	61	22
22	Cores	600 ± 20	5.8 ± 0.7	22	--	--	640 ± 40	5.6 ± 0.5	21	600 ± 60	5.7 ± 0.7	21	620	5.8 ± 0.7	22	**660**	5.6 ± 0.8	21	yes	0.18*	0.49	0.67	67	39*
	Rims	610 ± 10	7.9 ± 0.3	29	8.1 ± 0.3	30	**830 ± 40**	**3 ± 1**	**13**	**660 ± 30**	7.5 ± 0.4	28	--	--	--	--	--	--	yes	0.16*	0.54	0.67	67	39*
29	Cores	590 ± 30	6.5 ± 0.3	24	--	--	540 ± 10	6.4 ± 0.3	24	**700 ± 40**	5.6 ± 0.6	21	620	6.5 ± 0.2	24	--	--	--	yes	0.19*	0.56	0.57	65	15
	Rims	590 ± 30	5.4 ± 0.3	20	5.4 ± 0.3	20	517 ± 8	5.2 ± 0.4	19	630 ± 60	5.2 ± 0.6	19	--	--	--	--	--	--	yes	0.26*	0.52	0.57	65	15
36		**660 ± 10**	7.1 ± 0.3	26	7.6 ± 0.3	28	580 ± 10	7.6 ± 0.3	28	630 ± 20	7.4 ± 0.4	27	--	--	--	--	--	--	yes	0.31	0.61	0.62	64	26
40		570 ± 20	2.4 ± 0.4	9	2.2 ± 0.3	9	**489 ± 5**	1.5 ± 0.4	5	**680 ± 20**	2.3 ± 0.2	9	--	--	--	--	--	--	ttn*	0.23*	0.34*	0.67	66	22
52		640 ± 30	7.4 ± 0.3	27	--	--	680 ± 50	6.9 ± 0.9	25	700 ± 40	6.7 ± 0.8	25	610	7.7 ± 0.3	28	650	7.4 ± 0.3	27	ttn*	0.19*	0.61	0.65	65	31
61	Cores	640 ± 10	7.9 ± 0.3	29	--	--	620 ± 40	8.0 ± 0.3	29	620 ± 30	8.0 ± 0.4	29	610	8.1 ± 0.3	20	650	7.8 ± 0.3	29	yes	0.34	0.58	0.75	72*	26
	Rims	**640 ± 10**	7.1 ± 0.2	26	7.4 ± 0.2	27	580 ± 10	7.4 ± 0.2	27	**670 ± 40**	6.8 ± 0.5	25	--	--	--	--	--	--	yes	0.32	0.56	0.75	72*	26
62	Cores	660 ± 20	6.8 ± 0.4	25	--	--	640 ± 30	7.0 ± 0.2	26	630 ± 40	7.0 ± 0.6	26	610	7.2 ± 0.4	26	650	6.9 ± 0.4	25	K-spar*	0.45	0.45	0.74	69*	28
	Rims	**640 ± 20**	5.9 ± 0.3	22	6.0 ± 0.3	22	590 ± 20	6.1 ± 0.2	22	630 ± 30	5.9 ± 0.3	22	--	--	--	--	--	--	K-spar*	0.42	0.42	0.74	69*	28
64	Cores	640 ± 20	7.8 ± 0.4	29	--	--	**790 ± 60**	**5 ± 2**	**17**	620 ± 30	8.0 ± 0.4	29	610	8.1 ± 0.3	30	650	7.7 ± 0.3	28	K-spar*	0.33	0.52	0.71	61	28
	Rims	**640 ± 10**	6.6 ± 0.3	24	6.8 ± 0.3	25	**650 ± 30**	6.5 ± 0.2	24	**650 ± 30**	6.5 ± 0.4	24	--	--	--	--	--	--	K-spar*	0.33	0.49	0.71	61	28
65	Cores	610 ± 20	7.8 ± 0.3	29	--	--	**820 ± 20**	**3.8 ± 0.3**	**14**	490 ± 20	7.2 ± 0.8	26	610	7.9 ± 0.3	29	650	7.6 ± 0.3	28	K-spar*	0.37	0.53	0.77	67	28
	Rims	**620 ± 10**	6.6 ± 0.4	24	6.7 ± 0.4	25	**650 ± 50**	6.2 ± 0.6	23	520 ± 20	6.4 ± 0.5	24	--	--	--	--	--	--	K-spar*	0.40	0.50	0.77	67	28
64+65	Cores	630 ± 30	7.7 ± 0.3	28	--	--	**810 ± 50**	**4 ± 1**	**16**	580 ± 70	7.7 ± 0.6	28	610	8.0 ± 0.3	29	650	7.7 ± 0.3	28	K-spar*	0.34	0.52	0.74	64	28
	Rims	**640 ± 20**	6.6 ± 0.3	24	6.8 ± 0.3	25	**650 ± 30**	6.4 ± 0.4	23	600 ± 70	6.5 ± 0.4	24	--	--	--	--	--	--	K-spar*	0.36	0.49	0.74	64	28
66		600 ± 20	6.3 ± 0.2	23	6.3 ± 0.2	23	570 ± 10	6.3 ± 0.2	23	**680 ± 30**	**5.7 ± 0.3**	**21**	--	--	--	--	--	--	yes	0.22*	0.49	0.67	58	30
68		640 ± 10	7.6 ± 0.3	28	--	--	650 ± 20	7.4 ± 0.3	27	680 ± 20	7.1 ± 0.4	26	610	7.8 ± 0.3	29	650	7.5 ± 0.3	28	ttn*	0.26*	0.59	0.72	70*	27
69		630 ± 20	7.4 ± 0.3	27	--	--	650 ± 40	7.1 ± 0.5	26	**680 ± 20**	6.8 ± 0.3	25	610	7.5 ± 0.3	28	650	7.2 ± 0.3	27	ttn*	0.25*	0.57	0.72	70*	25
68+69		640 ± 20	7.5 ± 0.3	27	--	--	650 ± 30	7.3 ± 0.4	27	680 ± 20	7.0 ± 0.4	26	610	7.6 ± 0.3	28	650	7.3 ± 0.3	27	ttn*	0.26*	0.58	0.72	70*	26
Range of experimental calibrations (Al-in-hbl)																				≥ 0.27	0.40-0.65	> hbl	60-68	≤ 35

Notes:

T reported as °C and P reported as kbar

All T and P values reported as 1σ, except for Ti-in-zr reported as 2σ and solidi temperatures estimated at 5%

Bold values differ from prefered values (hbl-plag thermometer B for igneous hbl and 550 ºC for metamorphic hbl)

Depth in km calculated based on densities from Christensen & Mooney (1995)

*: Outside of the range of experimental calibration; see text for discussion

Fe/Fe: Fe^{3+}/Fe^{2+}; Fe-Mg: Fe/(Fe+Mg); minerals listed under "Buffer" are missing from the full buffering assemblage

Hbl: hornblende; Plag: plagioclase; Therm: geothermometer; Gd: granodiorite; Trondhj: trondhjemite; ttn: Ti-rich mineral (titanite, rutile, ilmenite, etc.); K-spar: K-feldspar

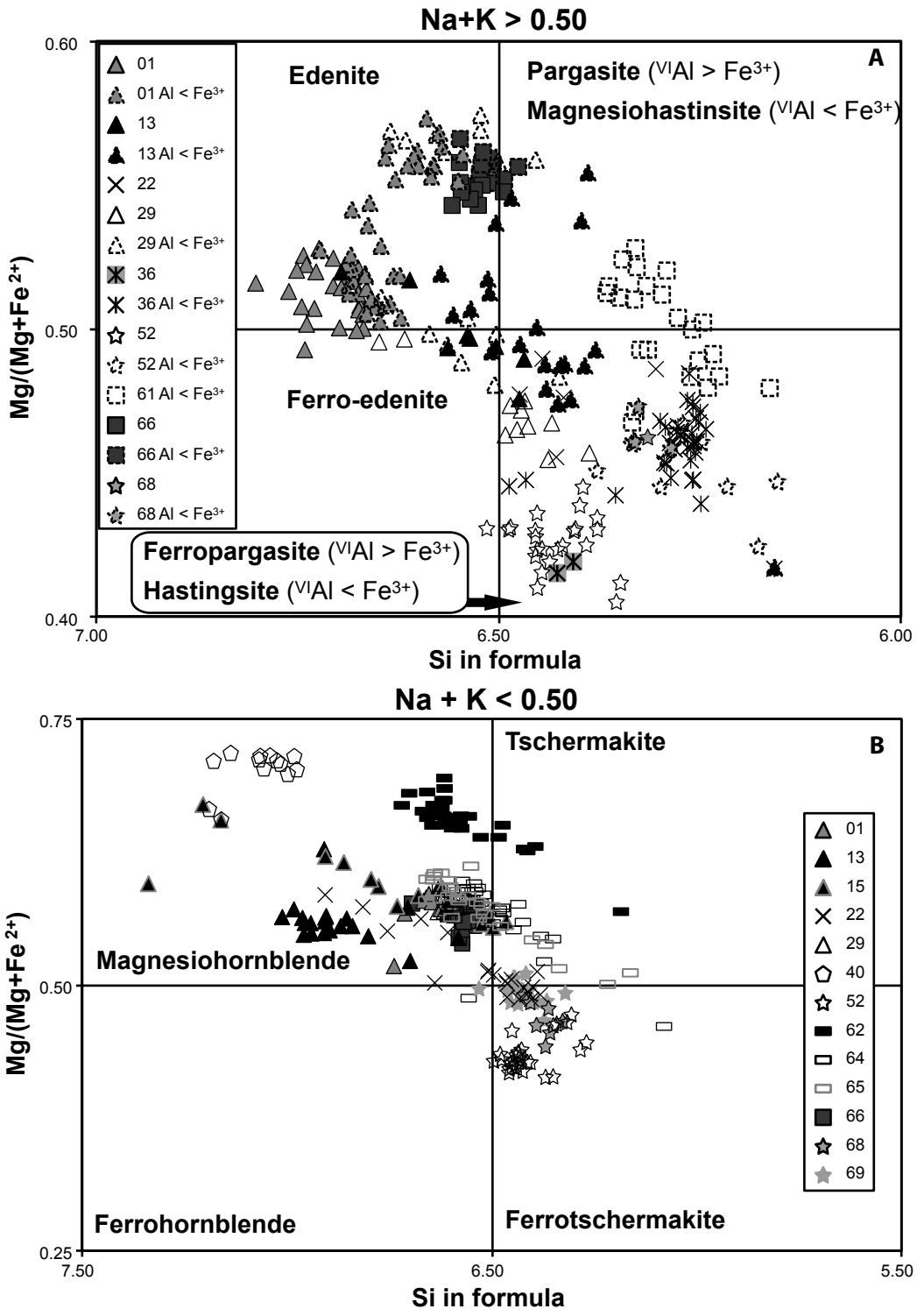

Figure 14: Amphibole compositions for calcic amphiboles. All amphiboles on these diagrams contain CaB ≥ 1.50, CaA < 0.50, and Ti < 0.50 apfu after Leake et al. (1997). Samples with metamorphic rims on igneous hornblende (i.e. 29) show distinct clusters of compositions.

plagioclase is extremely slow (Morse, 1984), so hornblende overgrowths that were not accompanied by recrystallization or new growth in plagioclase may not accurately record the temperatures associated with the overgrowth.

In addition to assuring the proper buffering assemblage for the barometer, other parameters, including f_{O2}, were examined to insure that the barometer would be correctly applied. Low f_{O2} rocks can yield anomalously high pressures, because Al will occupy sites typically filled by Fe^{3+}, so a sufficient supply of Fe^{3+} must be verified. Although f_{O2} was not determined for these rocks, Fe/Fe+Mg and Fe^{3+}/Fe^{2+} ratios, both of which are affected by f_{O2} (Anderson & Smith, 1995) were calculated. In all samples, the Fe/Fe+Mg ratios were below 0.65, and low-f_{O2} granitoids tend to have Fe/Fe+Mg ratios above 0.65. These amphiboles also have Fe/Fe+Mg ratios below that of the whole rock, which is consistent with high f_{O2}. Fe^{3+}/Fe^{2+} ratios use average Fe^{3+} and are between 0.43 and 0.17. Some of the Fe^{3+} ratios are in the range of those from low f_{O2} granites, but as these ratios are only estimates, they may not accurately represent the oxidation state. The analyses performed with the different microprobes also yield different Fe^{3+}/Fe^{2+} ratios, which suggests that this ratio is not a reliable proxy for f_{O2} in these rocks. Most rocks also have magnetite or hematite in them, indicating that the magmas were sufficiently buffered for the thermobarometer (Anderson & Smith, 1995). In general, the proxies for f_{O2} in the samples in this study indicate that oxidation conditions were appropriate for the application of the amphibole geobarometer.

The pressures were calculated using the temperature-corrected formula from Anderson & Smith (1995). Temperatures that are used with this geobarometer include the amphibole-plagioclase formulas A (for assemblages with quartz) and B (for assemblages with or without quartz) of Holland & Blundy (1994), and the Ti-in-hornblende thermometer of Colombi (1988) as reported by Otto (2002). A Ti-in-hornblende thermometer was developed in the 1980's by Spear (1981) and Raase *et al.* (1986), although neither published a specific formula for calculating temperature from Ti concentrations. The experimental studies of Spear (1981) show a strong correlation between temperature and Ti concentrations, with no dependence on pressure. This thermometer, however, is sensitive to f_{O2} and α_{Ti}, but a Ti phase, such as ilmenite or titanite, is sufficient to buffer the reaction (Spear, 1981; Raase *et al.*, 1986). These data were augmented and revised by experimental work by Ernst & Liu (1998), who also published a comprehensive list of amphibole

temperatures and Ti content from studies on synthesized amphiboles. This thermometer, however, is not widely used, and is only applied here to compare the results discussed here with those reported by Otto (2002).

I report temperatures calculated using both thermometers of Blundy & Holland (1990) and Holland & Blundy (1994), but the preferred temperature is from their B formulation (assemblages with or without quartz), as these temperatures and pressures are more consistent between samples. Ague & Brandon (1996) also found that this equation better matches the regional metamorphic patterns of their study area. The thermometers of Holland & Blundy (1994), which are dependant on pressure, were substituted into the temperature-dependent Al-in-hornblende barometer, and both temperature and pressure were calculated from the resulting equations.

Several of the temperatures calculated using the plagioclase thermometer are subsolidus, indicating that the plagioclase and amphiboles equilibrated at temperatures lower than the amphibole crystallization temperature. Because of this, water-saturated solidus temperatures were also used to estimate temperature and are based on work by Ebadi & Johannes (1991) for granites, Naney (1993) and Piwinskii (1968) for granodiorite, Johnston & Wyllie (1988) and van der Laan & Wyllie (1992) for trondhjemites, and Schmidt (1993) and Schmidt & Thompson (1996) for tonalite. All of the solidus temperatures were approximated iteratively using pressure estimates based on amphibole compositions, H_2O-saturated curves and compositions closest to that of the sample. Since the H_2O content of these rocks is unknown, and amphiboles frequently crystallize above the solidus, these temperatures may underestimate the temperatures at the time of crystallization (Stone, 2000). For samples with chemically distinct rims, pressures were also calculated at 550 °C, which is a temperature based on possible metamorphic conditions. Because of its accepted use in thermobarometry, the amphibole-plagioclase thermometer B is the source for the preferred temperature, except in overgrowths, where the estimated metamorphic temperature is preferred. In all of the samples with overgrowths on hornblende, the pressures calculated from the amphibole-plagioclase thermometer B are identical, within error, to the pressures calculated using 550 °C. Temperatures generated from the B thermometer also generally overlap those from the solidus curves and the Ti-in-hornblende thermometer, adding additional credence to its acceptability as the preferred temperature. Results are reported in

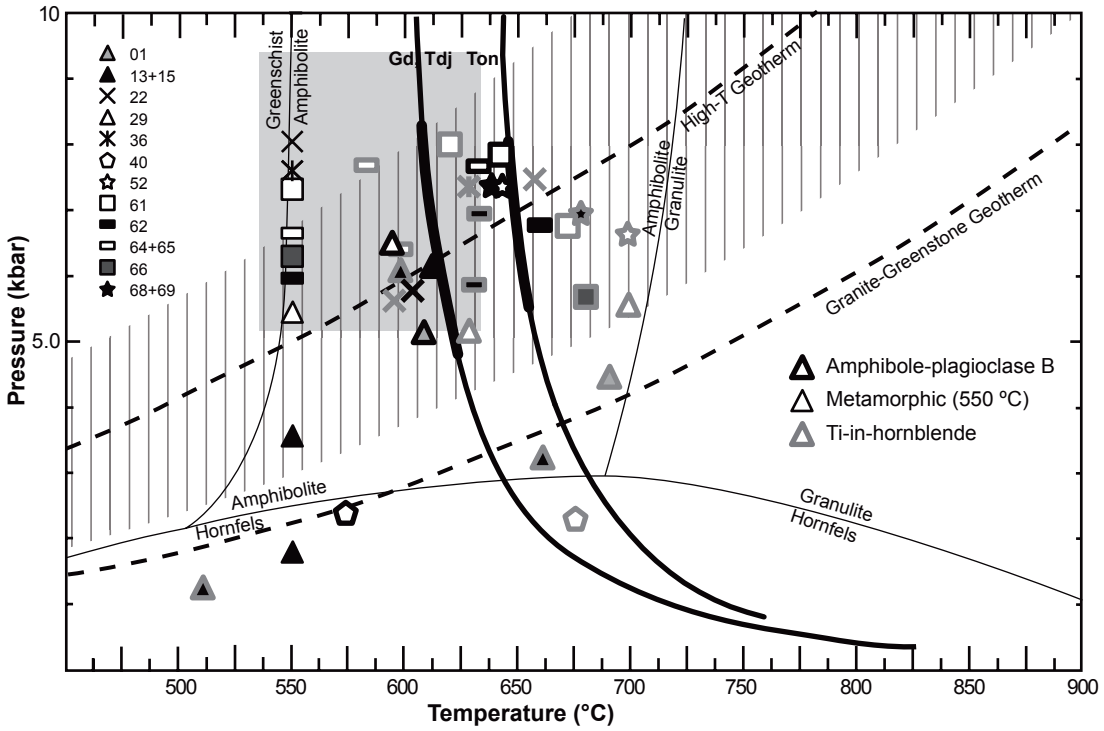

Figure 15: P-T diagram displaying average pressures and temperatures calculated in this study. Bold black outlines are P-T conditions calculated using the amphibole-plagioclase B thermometer of Holland and Blundy (1994), which are the preferred P-T conditions for igneous hornblende. Light black outlines are pressures from metamorphic rims, calculated at 550 ºC. Dark lines are granodiorite and trondhjemite (Gd, Tdj) and tonalite (Ton) H_2O-saturated solidi from Naney (1983), Johnston & Wyllie (1988), van der Laan & Wyllie (1992), Schmidt (1993), Schmidt and Thompson (1996), and Schmidt and Poli (2004). Bold sections highlight P-T estimates based on solidi temperatures. Archean granite-greenstone and high-temperature geothermal gradients are from Condie (1984). Striped area indicates the range of pressures and temperatures typically observed in high-temperature Archean terranes, also from Condie (1984). Thermobarometry shows a better fit with the high-temperatures geothermal gradient. Shaded box represents the temperatures and pressures calculated by Otto (2002) for metamorphic assemblage at Musselwhite mine. Many of the samples in this study yield pressures and temperatures within this range.

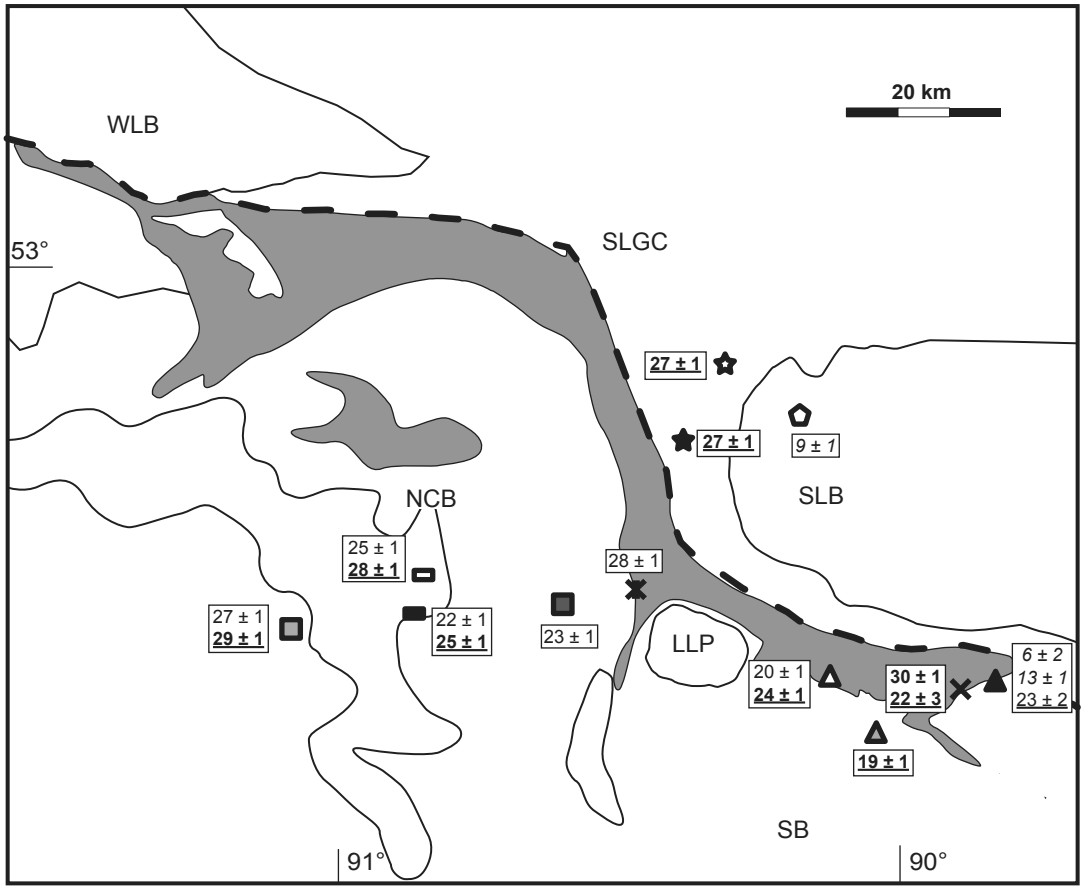

Figure 16: Maps of barometric results (km) calculated in this study. Underlined values denote primary magmatic depths, and bold values are associated with 2880 to 2830 Ma tectonic events. Values in normal font are associated with c. 2700 Ma deformation and alteration, and italics values denote later metamorphic or hydrothermal depths. See text for discussion. Depths calculated from barometry with average granodioritic crustal densities of Christensen & Mooney (1995).

Tables 6 and 10, and P-T data are displayed in **Figures 15** and **16**.

3.5.1 Southern batholith

01: Leucocratic granodiorite

For Ti-in-zircon thermometry, 4 spots from the 2860 Ma population and one from a xenocrystic core were analysed. One spot from the 2860 Ma population was excluded due to excessive Ti, likely from an inclusion. Temperatures for the two populations were identical, with the older core crystalizing at 721 ± 89 °C, and the younger zircon crystalizing at 742 ± 50 °C.

Amphiboles in this sample are approximately aligned with the foliation (**Fig. 4k**). Some have inclusions of quartz, plagioclase, and biotite. This sample contained the full buffering assemblage, in addition to containing magnetite. Other parameters are reported in **Table 3**. Sixty-seven spots were analyzed on 8 amphiboles, and 21 of these spots are on rims with plagioclase pairs. For plagioclase, 20 spots were analyzed on 19 grains, with one spot on an alkali feldspar. Chemically these amphiboles are fairly homogeneous. Rims have significantly lower Ti and K, and higher Mg and F concentrations and slightly higher Al. Generally, amphiboles are edenite, although cores tend toward magnesiohornblende. Feldspars are 20 ± 3% An. The one spot from an orthoclase grain was 93% potassic.

Aluminum in this sample is 1.63 ± 0.03 apfu, and Ti in cores is 0.11 ± 0.02 apfu, whereas rims contain 0.07 ± 0.02 apfu Ti. With the amphibole-plagioclase thermometer B, the temperatures and pressures are 607 ± 16 °C and 5.14 ± 0.16 kbar. Other temperatures and their associated pressure are reported in **Table 3**. Temperatures from the plagioclase thermometer B and the granodiorite solidus were similar, and pressures from both plagioclase thermometers, the Ti-in-hornblende thermometer, and the granodiorite solidus were similar.

13/15: Strongly foliated granodiorite

For Ti-in-zircon thermometry, 5 spots from sample 13 were analyzed. Two spots had irregular patterns during the analysis, and were excluded. The temperature from these zircons was calculated to be 735 ± 51 °C.

Both of these samples are from the same outcrop, and sample 13 is relatively unaltered, whereas sample 15 is from an area with quartz-carbonate-epidote veins. Amphiboles in sample 13 are weakly aligned with the foliation and contain small (50 μm)

very minor inclusions of quartz, plagioclase, and biotite. In sample 15, the amphibole textures are similar, but the grains are more strongly aligned with the foliation. Additionally, some amphiboles in sample 15 are epidote-altered (**Fig. 4l**). These samples contain the full buffering assemblage except magnetite, although they have some hematite. Sample 13 had 55 spots on 9 amphiboles, and 12 of these spots are on rims with plagioclase pairs. Sample 15 had 17 spots on 4 amphiboles, and all of these spots had plagioclase pairs. For plagioclase, 31 spots were analyzed, 14 spots on 12 grains in sample 13 and 17 spots on 11 grains in sample 15. Amphiboles in these samples show chemical zoning, which is related to strain, since cores and rims in strain shadows are chemically similar, with higher Al, Mg, Na, K, Fe and Fe/(Fe+Mg) and lower Si and Mg than rims parallel to foliation. In addition, sample 15 has another population of late rims, which are also parallel to foliation. When compared with the cores, these late rims differ compositionally in a similar manner as the other rims, but with more extreme enrichments or depletions in all elements except Ti. There are 40 spots from cores, 16 spots from rims, and three spots on late rims. Eight spots were excluded for representing a mix of rims and cores. Cores of amphiboles are edenite, and both sets of rims have a magnesiohornblende composition. %An in plagioclase ranges from 26-10%, with an average of 22 ± 4%.

In cores, Al is 1.83 ± 0.12 apfu, whereas rims are slightly less aluminous with 1.36 ± 0.03 apfu. Late rims have much less Al, with an average of 1.03 ± 0.08 apfu. Titanium in cores is 0.055 ± 0.016 apfu, and rims have 0.084 ± 0.032 apfu Ti, with late rims containing 0.022 ± 0.003 apfu Ti. With the amphibole-plagioclase thermometer B, the temperatures and pressures in cores are 611 ± 21 °C and 6.17 ± 0.65 kbar. When pressures from rims are calculated with possible metamorphic temperatures of 550 °C, they are 3.6 ± 0.2, and late rims are shallower, at 1.7 ± 0.5 kbar. In cores, temperatures from the plagioclase thermometer B, the Ti-in-hornblende thermometer, and the granodiorite solidus are similar, and the temperature from the plagioclase thermometer B is similar to that from the Ti-in-hornblende thermometer. All of the pressures are similar. In rims and the late rims, all of the pressures were similar.

22: Mylonitic augen gneiss

This sample is from the eastern edge of the NCGB, along the inferred Neawagank Lake fault. This sample is from a mylonitic augen gneiss and comes from a biotite-

hornblende band with ~1 cm plagioclase augen. Gneissic bands, which are perfectly planar and nearly vertical, range from 1 cm to ~20 cm, with an average around 10 cm for dark bands and around 2 cm for lighter bands. At the outcrop scale, this rock is compositionally a tonalite, containing 5% alkali feldspar, 45% plagioclase feldspar (An_{39}), 40% quartz, 10% biotite, and trace hornblende, titanite, sulphides, and magnetite. The foliation in this sample is primarily defined by hornblende, titanite, and quartz ribbons, whereas biotite, which occurs as very small grains, is more randomly oriented. There is some epidote alteration of hornblende, and in the high-strain areas, biotite is almost completely altered to chlorite.

Since this sample is so highly strained, amphiboles are nearly perfectly aligned with foliation. Amphiboles contain minor inclusions of quartz, plagioclase, biotite, titanite, and sulphides. Some amphiboles in this sample exhibit minor epidote or chlorite alteration (**Fig. 4p**). Twenty-five spots were analyzed on 7 amphiboles, and 23 spots were analyzed on 17 plagioclase grains. Six spots from cores and pressure shadows show higher Si and Mg, and lower Al, total Fe, Na, and K than foliation-parallel rims. In these amphiboles, the majority of the crystal has a rim composition, leaving only a small amount of core. One outlier from the population of rims was discarded. This sample contains the full buffering assemblage, in addition to containing magnetite. The cores of amphiboles are magnesiohornblende, whereas rims are ferrotschermakite. Plagioclase contains 39 ± 1 %An.

In the cores of amphiboles, Al is 1.77 ± 0.14 apfu, whereas rims have higher Al concentrations of 2.18 ± 0.05 apfu. Ti concentrations in cores are 0.053 ± 0.021 apfu, and in rims they are 0.075 ± 0.011 apfu. With the amphibole-plagioclase thermometer B, the temperatures and pressures in cores are 602 ± 21 °C and 5.84 ± 0.71 kbar. At 550 °C, the pressure from the rims would be 8.1 ± 0.3 kbar. In cores, all of the temperatures and pressures are similar, and in rims, all of the pressures, except those calculated with the plagioclase thermometer A, were similar.

29: Moderately foliated granodiorite

Ti concentrations for Ti-in-zircon thermometry were obtained from 7 spots from the 2731 Ma population, 3 spots from the 2853 Ma, and one spot on a xenocrystic core. Three spots from the younger population had irregular patterns in Ti concentrations and were excluded from the analysis. Younger zircons crystalized at 827 ± 38 °C, and 2853 Ma zircon crystalized at 705 ± 66 °C. The xenocrystic core crystallized at 766 ± 118 °C.

Amphiboles in this sample are weakly aligned with the foliation, which is primarily defined by biotite. A few amphibole grains are altered to epidote and/ or biotite, and in many places, amphibole and plagioclase react along contacts to form quartz. Amphiboles in this sample are generally inclusion-free, but most are complexly intergrown with biotite. Fifty-four spots on 6 amphiboles were analyzed, and 15 spots on plagioclase grains were analyzed, 2 of which fell on alkali feldspar grains. Two populations emerged from the analyses, with spots from cores and pressure shadows containing lower Si and Mg, and higher Al, total Fe, and K than spots from rims. Four spots from cores had Ca concentrations that were too high for the thermobarometric calculations, and they were excluded from the analyses. This sample contains the full buffering assemblage, but contains hematite rather than magnetite. The composition of amphibole cores is hastingsite, and rims have an edenite composition. Alkali feldspars are 95% orthoclase, 3% albite, and 2% Ba-feldspar, and plagioclase is 15 ± 5 %An.

In the cores of amphiboles, Al is 1.89 ± 0.04 apfu, and in rims, Al concentrations are 1.69 ± 0.06 apfu. Titanium concentrations in cores are 0.10 ± 0.03 apfu, and in rims they are 0.07 ± 0.04 apfu. With the amphibole-plagioclase thermometer B, the temperatures and pressures in cores are 593 ± 31 °C and 6.48 ± 0.27 kbar. The pressure from metamorphic (550 °C) rims is 5.4 ± 0.3 kbar. In cores, temperatures were similar between the plagioclase thermometer B and the granodiorite solidus, and all of the pressures were similar. Likewise, in rims, all of the pressures were similar.

48: Weakly gneissic granite

Titanium concentrations from 9 spots from 2710 Ma population and 7 spots from the 2837 Ma population were measured for Ti-in-zircon thermometry. Four spots from each population had irregular patterns in Ti concentration and were excluded from analysis. The younger population crystalized at 910 ± 51 °C, and the older population crystalized at 808 ± 51 °C.

3.5.2 Schade Lake gneissic complex

52: Gneissic tonalite

For Ti-in-zircon thermometry, 5 spots from the 2886 Ma population were analyzed. One spot was excluded for high Ti concentrations, and the zircons crystalized at 770 ± 90 °C.

Amphiboles in this sample are not aligned with foliation, but occur in clumps of mafic minerals in poorly developed gneissic banding. Many amphibole grains have experience chlorite and/ or epidote alteration, and most have minor quartz inclusions. A few grains also have biotite inclusions, especially in their rims. Sixty-three spots were analyzed on 4 amphiboles, and 18 of these spots have plagioclase pairs from 15 plagioclase grains. Out of the minerals in the buffering assemblage, this sample lacks a Ti-phase and only contains trace alkali feldspars. Amphiboles from this sample are fairly homogenous, although cores have slightly lower Al and slightly higher Si and Na than rims do. Amphiboles are ferrotschermakite; plagioclase contains 31 ± 1 %An.

Aluminum concentrations are 2.12 ± 0.06 apfu, and Ti is 0.10 ± 0.03 apfu. With the amphibole-plagioclase thermometer B, the temperatures and pressures are 642 ± 29 °C and 7.40 ± 0.31 kbar. Temperatures from plagioclase formulas A and B, as well as Ti-in-hornblende, and the tonalite solidus are similar, and all of the calculated pressures are similar.

53F/C: Heterogeneously deformed gneiss

Titanium concentrations were measured in 10 spots from the 2645 Ma population, 8 spots from the 2726 Ma population, and 2 spots from the 2841 Ma population for Ti-in-zircon thermometry. Two spots from the 2645 Ma population and one from the 2726 Ma population had irregular patterns in Ti concentrations and were excluded from the analysis. Zircons from the youngest population crystallized at 723 ± 44 °C; the 2841 Ma population crystallized at 774 ± 35 °C; and the oldest population crystallized at 878 ± 59 °C.

68/69: Heterogeneously deformed tonalite

These samples are from the western side of Wapuskeya Lake, about 3 km east of the Dinnick Lake Fault Zone. In outcrop, fabric varies from poorly developed gneissic banding to massive granitoid to strongly planar/ anastomosing foliation with a weak lineation. These samples are compositionally tonalites containing 45% plagioclase (An_{26}), 45% quartz, 4% biotite, 4% epidote, 2% hornblende, and trace alkali feldspar, sulphides, allanite, and apatite. Both samples are weakly gneissic, with mafic minerals occurring in clumps. Sample 69 is slightly less segregated, but has a stronger planar foliation. In both samples, the foliation is primarily defined by biotite and hornblende, although quartz is also elongated in the foliation

plane and has developed serrated boundaries. There is significant epidote alteration of biotite, and minor epidote and chlorite alteration of amphibole.

In both of these samples, amphibole grains are perfectly aligned with the foliation, and some grains show minor epidote and/ or chlorite alteration. Large (≥100 μm) inclusions of quartz, plagioclase, and biotite are common in larger crystals, but these amphiboles are otherwise inclusion-free. Some amphibole grains react with plagioclase to form quartz, much like in sample 29, but this reaction is observed less frequently in these samples. Twenty-nine spots on 9 grains were analyzed, 11 spots on 4 grains in sample 68 and 18 spots on 5 grains in sample 69, and 26 of these have plagioclase pairs. Thirty-five spots on plagioclase grains were analyzed, 17 spots on 12 grains in sample 68, and 18 spots on 10 grains in sample 69. Of the minerals required for the buffering assemblage, these samples lack a Ti-phase and only contain trace alkali feldspar. These amphiboles are extremely homogeneous ferrotschermakite. Plagioclase compositions have an average of 26 ± 4 %An. There is a significant K component in most of the plagioclase grains, with the percent orthoclase up to 10%, with an average of 1 ± 2%.

These samples have Al concentrations of 2.11 ± 0.06 apfu, and Ti is 0.09 ± 0.01 apfu. With the amphibole-plagioclase thermometer B, the temperatures and pressures are 637 ± 17 °C and 7.46 ± 0.30 kbar. Temperatures from plagioclase formulas A and B, as well as Ti-in-hornblende, and the tonalite solidus are similar, and all of the calculated pressures are similar.

71D/P: K-feldspar-flooded granodiorite

For Ti-in-zircon thermometry, 7 spots from the 2702 Ma population and 13 from the 2858 Ma population were analyzed. Six spots from the younger population and 4 from the older had irregular patterns in Ti concentrations. The younger population crystallized at 666 ± 104 °C and the older population crystallized at 792 ± 50 °C.

3.5.3 Skinner Lake block

40/41: Tonalite containing blebby pegmatite

Titanium concentrations in zircons were collected from 4 spots from the 2828 Ma population and 6 from the 2871 Ma population. One analysis from the older population was excluded for an irregular pattern in Ti concentrations. The younger population crystallized at 659 ± 69 °C, and the older crystallized at 708 ± 74 °C.

Amphiboles in this sample are not aligned with any fabric in the rock, but they occur within 2 m of a mafic dyke, which has been metamorphosed to an amphibolite. Consequently, it is possible that these grains are xenocrystic, hydrothermal, or a product of contact metamorphism. There is extensive biotite, chlorite, and/ or epidote alteration of some large (>1 mm) hornblende grains, but most are unaltered. There are a few small (~10 μm), round inclusions of quartz, plagioclase, and sulphides in these amphiboles, but they are generally inclusion-free (**Fig. 4n**). Fifteen spots were analyzed on 4 amphibole grains, and all have plagioclase pairs from 7 feldspar grains, of which 2 were K-feldspars. Of the required minerals for the buffering assemblage, this sample lacks a Ti-phase, but it does include magnetite. Fe/(Fe+Mg) ratios are 0.34 ± 0.01, which is a bit below the range used in experimental calibrations. Although high Fe/Fe+Mg ratios may indicate low f_{O2}, which leads to pressure-independent high Al concentrations, low Fe/Fe+Mg ratios likely do not impact the validity of the barometer. All of the spots on the amphibole grains had a magnesiohornblende composition, but cores had slightly higher Si and Na and lower Mg. Plagioclase compositions are 22 ± 4 %An. Alkali feldspar grains are 93 ± 1 % K-feldspar, 6 ± 1 % albite, and 1 % Ba-feldspar.

Average Al concentrations are 1.12 ± 0.06 apfu, and Ti is 0.08 ± 0.01 apfu. With the amphibole-plagioclase thermometer B, the temperatures and pressures are 574 ± 21 °C and 2.38 ± 0.36 kbar. Metamorphic temperatures were also calculated for this sample, as the hornblende may have grown during contact metamorphism, and the pressure at 550 °C is 2.2 ± 0.3 kbar. Temperatures from the amphibole-plagioclase B thermometer were similar to the estimated metamorphic temperature, and all of the pressures, except those calculated from the plagioclase thermometer A, are similar. However, pressures from plagioclase thermometer A are similar to those calculated using the tonalite solidus.

43: K-feldspar augen gneiss

Titanium concentrations in zircons were analyzed from 5 spots from the 2735 Ma population, 4 from the 2835 Ma population, and 1 from the 2871 Ma population. Two spots from the youngest population were excluded for irregular patterns in Ti concentrations. The youngest population crystallized at 728 ± 230 °C, the middle population crystallized at 754 ± 190 °C, and the oldest crystallized at 723 ± 92 °C.

3.5.4 Wharram Lake block

55: Equigranular granodiorite

For Ti-in-zircon thermometry, 10 spots from the 2678 Ma population, 9 from the 2967 Ma population, and one from a xenocrystic core were analyzed. Ten spots were excluded due to irregular patterns in Ti concentration, including 3 from the youngest population, 6 from 2967 Ma population, and the xenocrystic spot. The temperatures for the two populations were within error of eachother, with the younger crystallizing at 804 ± 63 °C, and the older at 709 ± 53 °C.

3.5.5 North Caribou Lake batholith pluton

36: Strongly foliated tonalite

This sample is from the western side of the Libert Lake arm of the NCGB, only 10's of metres from the contact between the NCLB and metavolcanic rocks of the NCGB. In outcrop, this rock was strongly foliated with occasional cm-scale shear zones, and this sample is from one of those shear zones. Compositionally, this rock is a tonalite, containing 5% alkali feldspars, 40% plagioclase (An_{26}), 40% quartz, 10% biotite, 4% hornblende, 1% epidote, and trace titanite, sulphide, apatite, and allanite. The foliation is primarily defined by biotite, hornblende, and quartz ribbons, which have formed subgrains. There is some sericite alteration of plagioclase and epidote alteration of hornblende and biotite near quartz veins, but elsewhere, this rock is unaltered, and epidote is euhedral and in equilibrium with biotite.

Amphiboles in this sample are perfectly aligned with foliation, and are essentially unaltered. There are minor inclusions of sulphides, quartz, and biotite (**Fig. 4m**). Thirty-seven spots were analyzed on 10 amphibole grains, and 33 had plagioclase pairs, with a total of 35 spots on 28 plagioclase grains. This sample contains the full buffering assemblage in addition to magnetite. Amphiboles have hastingsite compositions, but cores have slightly higher Si, Mg, and Na, and slightly lower Al and total Fe. Average plagioclase compositions are 26 ± 1 %An.

Aluminum concentrations are 2.09 ± 0.06 apfu, and Ti is 0.06 ± 0.01 apfu. With the amphibole-plagioclase thermometer B, the temperatures and pressures are 660 ± 12 °C and 7.13 ± 0.25 kbar. Because of the alignment of the hornblende with foliation, pressures from potential metamorphism were calculated, with an average of 7.6 ± 0.3 kbar at 550 °C. Temperatures and pressures from all thermometers are similar.

46: Foliated granodiorite

Titanium concentrations were measured in 8 spots from the 2867 Ma population and 2 spots from xenocrystic cores. Four spots, including one from a xenocrystic core, were excluded for irregular pattern in Ti concentrations. The xenocrystic core crystallized at 739 ± 127 °C, and the rest of the zircon crystallized at 829 ± 78 °C.

49: Leucocratic granodiorite

For Ti-in-zircon thermometry, 5 spots from the 2857 Ma population and 5 from the 3132 Ma population were analyzed. One spot from each population was excluded for irregular patterns in Ti concentrations. The younger population crystallized at 797 ± 67 °C, and the older population crystallized at 921 ± 130 °C.

66: High-strain tonalite

This sample had two populations of zircon based on trace element patterns, but the Ti-in-zircon temperatures in these groups are the same. Two spot were excluded for irregular patterns of Ti concentrations. These zircons crystallized at 892 ± 65 °C.

Amphiboles define the foliation in this sample, are euhedral, and are unaltered. There are minor inclusions of quartz, plagioclase, biotite, titanite, and sulphides, and inclusions tend to be large and discrete. Thirty-five spots on 23 amphibole grains were analyzed, and all but 4 have plagioclase pairs, with 35 spots on 33 plagioclase grains. This sample lacks an Fe-oxide and only contains trace K-feldspar for the full buffering assemblage. Amphiboles have an edenite composition, and plagioclase is 30 ± 1 %An.

Aluminum concentrations are 1.85 ± 0.04 apfu, whereas Ti is 0.09 ± 0.02 apfu. With the amphibole-plagioclase thermometer B, the temperatures and pressures are 604 ± 16 °C and 6.30 ± 0.22 kbar. Because the amphiboles are aligned with foliation, pressures from potential metamorphic conditions were also calculated, yielding an average pressure of 6.3 ± 0.2 kbar at 550 °C. Temperatures from plagioclase formula B and metamorphic conditions are similar. All pressures are similar.

3.5.6 North Caribou Lake batholith core

51: K-feldspar augen gneiss

Titanium concentrations in zircon were analyzed in 5 spots from the 2693 Ma population and 4 from the 2834 Ma population. Two spots from the younger population were

excluded for irregular patterns in Ti concentrations. The younger population crystallized at 811 ± 54 °C, and the older population crystallized at 794 ± 140 °C.

61: Massive tonalite

Titanium concentrations in 10 spots from 2833 Ma zircons were measured, and 4 were excluded for irregular patterns in Ti concentrations. These zircons crystallized at 784 ± 46 °C.

Amphiboles from this sample are randomly oriented, and this sample has no obvious fabric. There is minor epidote alteration of hornblende near fractures, but otherwise, amphiboles in this sample are pristine, although they are inclusion-rich, containing quartz, plagioclase, biotite, titanite, and sulphides of various sizes. Twenty-four spots were analyzed on 8 amphibole grains, and all of the spots have plagioclase pairs, with a total of 24 spots on feldspars, 23 on plagioclase, and one on an alkali feldspar. Two populations of amphiboles emerged from the data: 10 spots from cores and pressure shadows and 14 from rims. This sample contains the full buffering assemblage, including magnetite. Spots from cores have slightly lower Si and Mg, and slightly higher Al. Compositionally, spots from cores were hastingsite, and those on rims were magnesiohastingsite. Plagioclase is 26 ± 1 %An, and K-feldspar contains 92% K-feldspar, 3% Ba-feldspar, and 4% albite.

In the cores of amphiboles, average Al concentrations are 2.20 ± 0.06 apfu, and in rims, Al is 2.05 ± 0.03 apfu. Ti concentrations in cores are 0.06 ± 0.01 apfu, and in rims, they are higher, with an average of 0.08 ± 0.02 apfu. With the amphibole-plagioclase thermometer B, the temperatures and pressures in cores are 639 ± 12 °C and 7.89 ± 0.30 kbar. Under metamorphic conditions (550 °C), the pressure from the rims is 7.4 ± 0.2 kbar. In cores, both plagioclase temperatures, as well as the tonalite solidus temperature are similar. Ti-in-hornblende and trondhjemite temperatures are also similar to the plagioclase temperatures. All of the pressures in cores are similar. Likewise, all of the pressures in rims are similar.

62/63: Gneissic tonalite

Zircons from this sample have clearly zoned rims and cores, which yielded a single age. Titanium concentrations were measured in 20 spots, and 9 spots were excluded for irregular patterns in Ti concentrations. Despite the chemical zoning in the rims and cores, both areas have the same crystallization temperature of 718 ± 28 °C.

Amphiboles in sample 62 are roughly aligned with the weak fabric, whereas 63 has no obvious fabric. There is minor chlorite, biotite, and epidote alteration of hornblende associated with fractures, and most grains are inclusion-rich, containing quartz, biotite, plagioclase, and sulphides. Analyses were preformed on 30 spots on 8 amphiboles and all of the spots but one had plagioclase pairs, with 29 total spots analyzed on plagioclase. There are two populations of amphiboles; 6 spots were from cores, which have lower Si and Mg, and higher Al, Fe^{2+}, total Fe, K, and Cl, and 23 spots on rims. Out of the required buffering assemblage, this sample lacks K-feldspar and contains very little titanite, but it does contain magnetite. Amphibole compositions in cores are variable between tschermakite and magnesiohornblende, whereas rims are all tschermakitic. Plagioclase compositions average 28 ± 1 %An and are completely void of K-feldspar.

In the cores of amphiboles, average Al concentrations are 2.02 ± 0.07 apfu, and in rims, they are lower at 1.80 ± 0.05 apfu. Ti concentrations in cores are 0.07 ± 0.01 apfu, and in rims they are 0.07 ± 0.01 apfu. With the amphibole-plagioclase thermometer B, the temperatures and pressures in cores average 659 ± 24 °C and 6.78 ± 0.37 kbar. With metamorphic temperatures, (550 °C), the pressures from the rims average 6.0 ± 0.3 kbar, slightly lower than the pressures in cores. In cores, both plagioclase temperatures, as well as the Ti-in-hornblende thermometer and the tonalite solidus temperature are similar. The trondhjemite solidus temperature is similar to the Ti-in-hornblende temperature and the temperatures from the plagioclase thermometer A. All of the pressures are similar. In rims, all of the temperatures, except the amphibole-plagioclase thermometer B are similar, and all of the pressures are similar.

64/65: Weakly gneissic tonalite

These samples are from the centre of the North Caribou Lake batholith, about 30 km west of Musselwhite Mine. In outcrop, these samples are from a weakly foliated, poorly developed gneiss, with heterogeneous strain and grain size. There are also brittle-ductile amphibolite enclaves in outcrop (**Fig. 4f**). Sample 64 is finer-grained and more strongly foliated than sample 65, which is massive, but neither sample exhibits obvious fabric in thin section. Compositionally, these samples are tonalites containing 60% plagioclase (An_{28}), and 30% and 35% quartz respectively, with trace sulphides, apatite, magnetite, and either ilmenite or rutile. For mafic minerals, sample 64 has 9% hornblende and 1% biotite, and

sample 65 has 3% biotite, 2% sulphides and oxides, and only trace hornblende. There is minor sericite alteration of plagioclase in cores and along some twinning planes. Quartz in sample 64 exhibits undulose extinction to sub-grain formation, whereas sample 65 has quartz with well-developed sub-grains and very little undulose extinction.

Since fabric is so poorly developed in these samples, it is difficult to tell if individual amphiboles are aligned with foliation, but in hand sample they are generally aligned with the fabric in the rock. In both of these samples, hornblende is unaltered, but in sample 65 grains are riddled with inclusions of primarily quartz, with some plagioclase, sulphides, and oxides. Inclusions are almost exclusively in the cores of grains, and most inclusion-rich cores are completely surrounded by inclusion-free rims (**Fig. 4o**). Most amphiboles from sample 64 are essentially inclusion-free. Sixty-five spots on 16 amphiboles were analyzed, 38 on 11 grains from sample 64 and 27 on 5 grains from sample 65. Two populations of amphiboles emerged from the analyses, with cores containing lower Si and Mg, and higher Al and K. There were 7 spots from cores in sample 64 and 3 from sample 65. A total of 68 spots were analyzed on plagioclase grains. Of the minerals required for the buffering assemblage, these samples lack K-feldspar, and sample 65 lacks a Ti-phase, but both contain magnetite. Cores have an average tschermakite composition, whereas rims tend toward magnesiohornblende. Plagioclase compositions average 28 ± 1 %An.

In the cores of amphiboles, average Al compositions are 2.18 ± 0.06 apfu, and in rims, Al is 1.94 ± 0.06 apfu. Titanium concentrations in cores average 0.05 ± 0.03 apfu, and in rims they are 0.05 ± 0.03 apfu. With the amphibole-plagioclase thermometer B, the temperatures and pressures in cores are 631 ± 28 °C and 7.72 ± 0.33 kbar. Under metamorphic temperatures of 550 °C, the pressures from the rims are 6.8 ± 0.3 kbar, slightly lower than pressures in cores. In cores, the plagioclase thermometer B, the Ti-in-hornblende thermometer, and the trondhjemite solidus yield similar temperatures. Additionally, the tonalite solidus temperature is similar to the temperature from the plagioclase thermometer B. All of the pressures, except that calculated from the plagioclase thermometer A, are similar. In rims, metamorphic and Ti-in-hornblende temperatures are similar, along with all of the pressures.

3.5.7 Libert Lake pluton

45: Melanocratic granite

In this sample, Ti concentrations were collected from 1 spot from 2700 Ma population, 3 spots from the 2730 Ma population, and one spot from a 2945 Ma xenocrystic core. The spot from the youngest population was excluded for an irregular pattern in Ti concentration. The xenocrystic core crystalized at 691 ± 113 °C, and the 2730 Ma population crystallized at 715 ± 62 °C.

3.5.8 Pegmatite

54: K-feldspar pegmatite

Ti concentrations were measured in 12 spots, two of which were on a xenocrystic core. Three spots were excluded for irregular patterns in Ti concentrations, and the resulting crystallization temperature was 624 ± 46 °C.

4. DISCUSSION

4.1 Geochronology

The geochronology conducted in this study has improved our understanding of the timing and tempo of magmatism recorded within the North Caribou Terrane, and the resulting ages are consistent with those that have been previously reported (cf. Biczok *et al*., 2012 and references therein). There are four broad categories of ages (**Fig. 17**): i) pre-2900 Ma that is mostly from inherited cores; ii) 2890-2830 Ma, which is the dominant age of magmatism in the area; iii) 2760-2680 Ma, which is mostly analyses from titanite and rims on zircon; and iv) pegmatites, which are likely around 2620 Ma. Some titanite ages fall between ii) and iii) populations, but this likely reflects titanite's lower closure temperature (660-700 °C) and greater tendency to recrystallize (Scott & St-Onge, 1995). Notably, the spatial distribution of these ages cannot be easily reconciled to lithotype nor readily correlated with any specific aeromagnetic signature.

In addition to the broad age groups, different interpretations of these ages arise from textures, chemistry, and distributions of ages within individual crystals as well as their host rocks. These patterns lead to three interpretations: rocks with a single igneous age, igneous rocks that have been hydrothermally altered, and igneous rocks that have older and younger igneous components.

4.1.1 Samples with a single igneous age

The first group, containing samples with a single igneous age in zircons, includes samples: 01, 13, 46, 66, 61, and 62/63. Most ages from these samples range from 2867 to 2829 Ma, but one sample (13) is much younger, at 2727 Ma. Additionally, zircons in all of them, except samples 13 and 66, have inherited cores. Zircons from samples 13 and 66 are also scarce (only seven grains were recovered from each sample) and narrow, with aspect ratios frequently less than 1:4. Both of these traits are common in zircons grown in liquids that are generally under-saturated in zircon (Corfu *et al.*, 2003), and if these zircons had grown under these conditions, no inherited cores would be preserved. Both of these samples also contain high concentrations of mafic minerals (biotite and hornblende), which leads to low zircon saturation temperatures, making zircon under-saturation plausible (Hanchar & Watson, 2003).

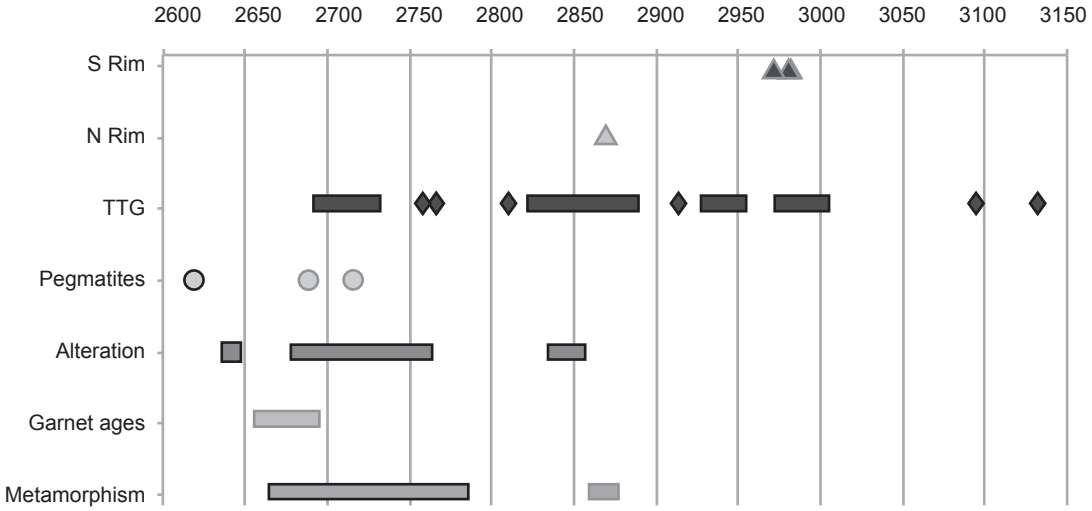

Figure 17: A timeline of the magmatic and metamorphic events affecting the rocks in this study area. Black outlines are data reported here, while grey outlines are data from Biczok et al., 2012, and Kalbfleisch, 2012.

Of the samples containing titanite, all, except sample 01, have titanite with young ages (2786-2733 Ma), similar to the age of sample 13. Although no geon-27 age was found in sample 01, titanite did have thin, undated rims, which mirrors the complexity seen in other samples in this group. In several samples, (01, 13, 46), older (2860-2890 Ma) titanite is preserved. In samples 01 and 46, this old titanite is the same age as the zircon, and records a crystallization age, and in sample 13, the old titanite shows that there was an inherited component in this rock, despite the lack of inheritance in zircon.

In all of theses samples, the zircon ages are clearly igneous, and in samples with titanite ages that match zircon ages, titanite is interpreted as igneous as well (01, 13, 46). The titanite that is younger than zircon is interpreted as metamorphic (rims on 46, 66, 61). This interpretation is consistent with the titanite morphologies in samples 66 and 61, which are small, round, anhedral crystals as opposed to the more typical prismatic morphology of igneous titanite. The low U concentrations from the rims of titanite in sample 46 are also consistent with metamorphic overgrowths (Frost *et al*., 2000). This set of samples records fairly simple igneous activity followed by metamorphism.

4.1.2 Samples with hydrothermal overgrowths

The second group of samples (29, 48, 43, 55, and 49) contains zircons with igneous cores and altered rims. I use alteration here to describe zircons that crystallized from a magma, but subsequently interacted with fluids that changed the chemistry of the rims without dissolving or precipitating significant amounts of zircon. This definition is similar to the processes reported by Pidgeon *et al*. (1966), Pidgeon (1992), Pidgeon *et al*. (1998), Rayer *et al*. (2005), and Geisler *et al.* (2007). An alteration interpretation for these samples is favoured for several reasons, including: textures in outcrop, trace element patterns in the cores and rims of altered zircons, and accompanying alteration of other minerals within the rock.

For the precipitation of young rims from a magmatic source, the rocks must have been flooded with magma ~40-250 My (the age difference between cores and rims) after they were emplaced. Because magmas solidify in less than 10 My (Pitcher, 1993), the original rocks would have been completely crystalized before the zircon rims grew and would, therefore, exhibit textural evidence for a later intrusion. Some samples (52, 53, 71, 41, 43, 51, and 45) do have complex outcrop-scale textures and patterns in age distribution,

morphology, and chemistry that could be consistent with multiple magmatic events, but these samples are in the third group and will be discussed below. The textures in the rocks within this group, however, are not consistent with renewed magmatism, and as the alteration age is solely recorded in the rims of zircon and titanite, it could easily be a remnant of fluid infiltration and alteration.

It can be difficult to distinguish hydrothermal alteration from igneous, metamorphic, or hydrothermal overgrowths in zircon. Chemically, the only consistent difference between them occurs in Th/U ratios (<0.1 in metamorphic and hydrothermal zircon and >0.5 in igneous zircon; Rubatto, 2002; Hoskin & Schaltegger, 2003). Textures are likewise ambiguous, as the disrupted zoning and resorption rims found in grains in this study are found in zircons with altered rims or magmatic and metamorphic overgrowths (Corfu *et al.*, 2003; Geisler *et al*., 2007). However, hydrothermally precipitated zircon tends to be very texturally distinctive, exhibiting spongy patterns as a result of substantial fluid and mineral inclusions (Schaltegger, 2007). The zircons in this study do not have spongy textures, and are therefore not interpreted as hydrothermal precipitates. Zircon morphologies are slightly less ambiguous, as hydrothermally precipitated and metamorphic zircons tend to be anhedral, whereas igneous zircons are typically prismatic (Corfu *et al.*, 2003). Conversely, morphologies of overgrowths and hydrothermally altered zircon are dependant on the shape of the original zircon (Geisler *et al*., 2007). The zircons in these samples are prismatic, typical of igneous zircons, but the morphologies are not helpful for distinguishing between overgrowths and hydrothermally altered rims. Although chemistry, textures, and morphology can not unambiguously distinguish the conditions for the formation of the zircon rims, none of the characteristics of the zircons in this group are inconsistent with hydrothermally altered rims.

In addition to the outcrop- and crystal-scale textural evidence consistent with an alteration origin for these ages, chemistry of the zircons also supports an alteration interpretation. In the zircons within this group, Th/U ratios are lower in rims than cores. This is a common pattern in altered zircon, as Th is less compatible than U in the zircon structure (**Fig. 18**; Geisler *et al.*, 2007). However, the Th/U ratios in rims are much higher than typical values for metamorphic overgrowths (<0.07; Rubatto, 2002). Trace elements in zircon also support a re-equilibration model, since rims and cores have similar patterns in REEs, with

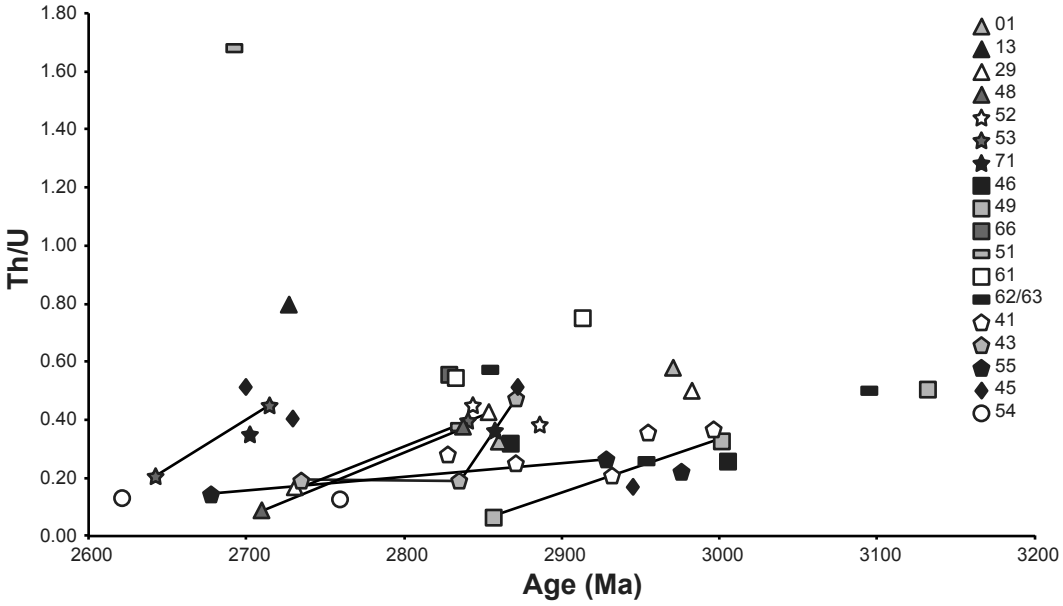

Figure 18: Median Th/U values in zircon versus age (Ma). Samples with hydrothermal rims show a decrease in Th/U ratios over time (29, 48, 53, 43, 55, 49; lines connect cores and rims), where samples with multiple igneous ages (45, 51, 71, 52, 41, 49) show little variation in Th/U ratios.

identical concentrations of HREEs, but variable concentrations of less-compatible LREEs (McBirney, 1993). If the rims are overgrowths from a magmatic or metamorphic source, the trace element trends in rims would not necessarily mimic those from cores, which is a pattern observed in some of the xenocrystic cores of zircons in this study (e.g. Sample 01; **Fig. 12b**). Experimental results discussed by Geisler *et al.* (2007) indicate that original oscillatory zoning, which is commonly observed in zircon rims in this study, can be preserved in zircons altered by high-temperature (600 °C) fluids. Zircon altered under these conditions can lose or gain Zr, Si, Hf, REE, U, Th, and Pb at variable rates depending on the composition of the fluid. Although the zircons in this study were likely altered at slightly lower temperatures (400-500 °C from thermometry at Musselwhite), these zircons preserve of original zoning and experienced variable chemical changes, indicating that these alteration traits may occur at lower temperatures.

If the age recorded by zircon rims in this group reflects a hydrothermal event, the altered parts of zircons must have lost nearly all of their radiogenic Pb to produce the discordia patterns observed. Partial Pb-loss should result in discordia between the original crystallization age and the time of re-setting, whereas the radiogenic ages of these samples has been completely re-set and no discordia is observed. Although zircon altered at high temperatures (>600 °C) readily incorporates compatible trace elements into its structure (Hf, REE, U, Th), this system, especially the fluid composition, is too poorly understood to determine if diffusion of Pb is efficient enough to completely purge the altered areas, or if these traits require additional precipitation of zircon. However, the textures, composition and isotopic data from the samples in this study suggest the Pb-loss due to hydrothermal alteration was efficient enough to completely reset the isotopic clocks in the zircon rims.

Additional support for an alteration source for these zircon rims comes from overgrowths on other minerals in the same rocks as these zircons. In some samples (e.g. 29), K-feldspars have grown as rims on plagioclase, and an increase in K is strongly correlated with zircons with young rims (**Fig. 19a**). The K-feldspar rims could, however, just represent a late-crystallizing phase. Another possible explanation for the correlation between more K-rich magmas and zircons with young rims arises from the greater susceptibility of radiation-damaged zircon to hydrothermal alteration (Ayers *et al.*, 2012; Geisler *et al.*, 2007). Granitic melts, with higher concentrations of K, tend to have higher concentrations of U than more

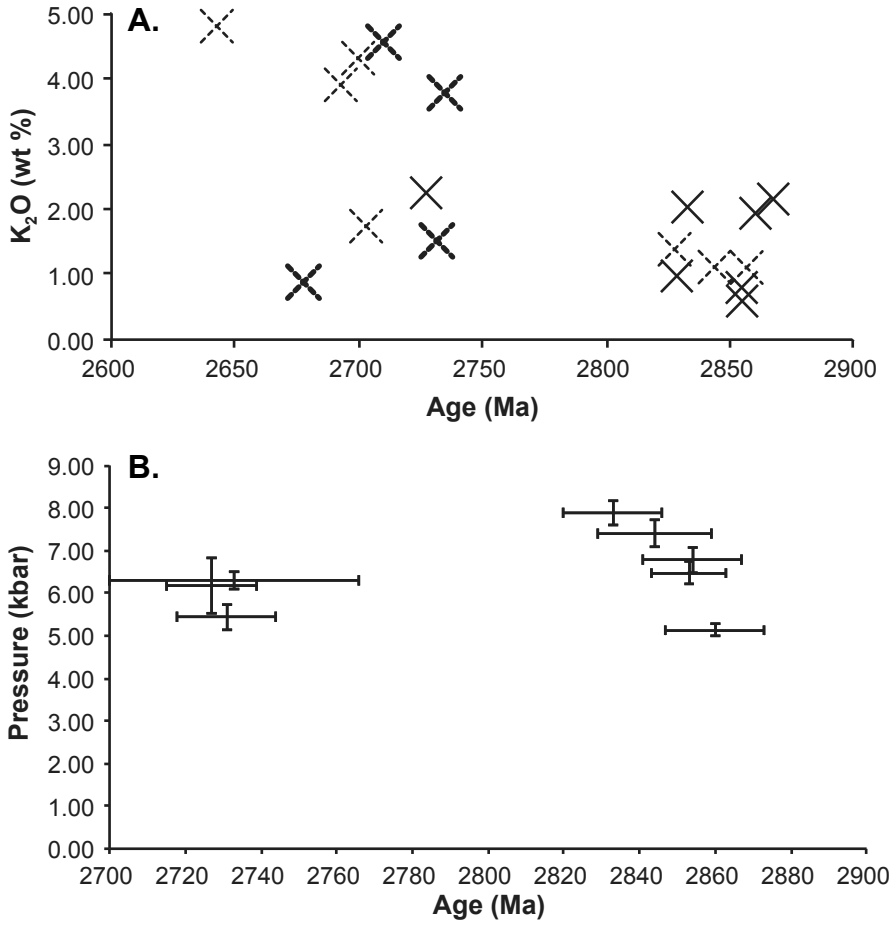

Figure 19: A. Plot of whole-rock weight % K_2O versus age (Ma). Altered samples bolded, and dashed lines are young ages from samples with multiple ages. Note the marked increase in weight % K_2O after 2750 Ma. B. Plot of preferred pressures from this study versus age (Ma). Igneous hornblende and zircon were paired as were zircon rims and rims on hornblende. Note the deeper pressure from 2860 Ma to 2830 Ma, and the cluster of ages and pressures c. 2730 Ma.

primitive melts (cf. Arth, 1976; McDonough & Sun, 1995). Zircons from granites may subsequently have higher concentrations of U and are more likely to suffer radiation damage, making them more susceptible to alteration. This may explain the young rims on samples 48 and 55, which have high U concentrations (1059 and 879 ppm respectively) and metamict cores in their zircons. Additionally, all of the samples in this group that also contain hornblende show overgrowths on the hornblende as well, and sample 29 also has titanite with overgrowths that are the same age as the hydrothermal rims on zircon. Hydrothermal rims on titanite have been reported elsewhere in the NCT (Corfu & Stone, 1998*b*), although a metamorphic source for the rims on the titanite is also possible. Fluid alteration of zircon rims may have been contemporaneous with metamorphism that could supply a source for the altering fluids and could explain the rim overgrowths on the hornblende.

Metamorphism is the most efficient mechanism for generating mobile fluids in the mid-crust and is implicated in Au-mineralization in orogenic deposits (Phillips & Powell, 2010). Because the ages from the rims of these zircons are likely recording an alteration event involving metamorphic fluids, they are also likely dating a regional increase in temperature that initiated the metamorphism. Fluids infiltration can also lower the melting temperature of affected rocks (Phillips & Powell, 2009), promoting, at higher temperatures, the development of migmatitic textures that are observed in the samples with several igneous zircon populations. As fluids are more mobile at greenschist facies (Phillips & Powell, 2009), these zircons are recording moderate-temperature alteration, which was followed by higher temperature metamorphism, a common pattern in amphibolite-grade Au deposits (Powell & Phillips, 2009).

A hydrothermal alteration source for zircon rims requires a re-evaluation of the Ti-in-zircon temperatures. This thermometer is relatively new (Ferry & Watson, 2007), and there has not been any work published on its applicability to hydrothermally altered zircon. Since the ion exchange between zircon and hydrothermal fluids is difficult to characterize, and depends so heavily of fluid composition (Geisler *et al.*, 2007), it is likely that the temperatures calculated from the zircon rims are inaccurate and do not have any geologic significance.

4.1.3 Samples with several igneous zircon populations

Samples in the third group (52, 53, 71, 41, 43, 51, and 45) have zircons with young rims, as well as young zircons, and are characterized by complex, outcrop-scale compositional variation that could be a result of multiple intrusions or partial melting. Regardless of age or grain morphology, zircon populations from the same sample typically have similar Th/U ratios, which are within the range of the igneous zircons in this study. All of the samples in this group, except 52, have granitic pegmatitic intrusions, and samples 53 and 71 show a correlation between alkali feldspar-rich areas and young zircon. Additionally, there are typically only a few zircons in each sample that record the younger age, except in the samples that are dominated by granitic gneissic banding (53, 43, 51). Trace elements in zircons from different age populations tend to show similar patterns, but they have much more variation in concentrations of REEs than is typical in altered zircon (e.g. 71). Consequently, unlike the altered zircons, zircon age populations in this group do not show a chemical affinity for each other. Titanite in these samples generally does not have ages that correspond with the younger event, although the age of the titanite in sample 45 overlaps with both of the zircon ages.

Because the young zircons in this group show several traits that are consistent with an igneous origin (high Th/U ratios, young zircons, pegmatitic intrusions, migmatitic textures), they are interpreted as directly precipitating from a melt. The samples in the group, except 71, record young ages that are slightly younger than the alteration ages of geographically proximal samples containing altered zircons, although the ages frequently overlap within analytical uncertainty. This is consistent with observations by Phillips & Powell (2009) from metamorphism of altered rocks. Fluid infiltration and alteration occurs at lower temperatures (500 °C maximum), and higher temperature metamorphism can later cause partial melting of the hydrated rocks (Phillips & Powell, 2009). This interpretation suggests that there have been several stages of highly evolved magmatism, as the one dated brittle pegmatitic dyke is significantly younger than any of the complexly deformed granitic intrusions. This pegmatite cross-cuts a slightly older gneiss with felsic bands that are compositionally identical to the pegmatite. The young zircons in this group are recording partial-melt and intrusions following alteration of the zircons in the second group.

4.2 Geothermobarometry

4.2.1 Geothermometry

The thermometers used in this study: Ti-in-zircon, granitoid solidi, Ti-in-hornblende, and both Holland & Blundy (1994) plagioclase-hornblende thermometers, fundamentally record temperatures from two distinct episodes of the rock's evolution: its high-temperature history and near- to sub-solidus conditions. None of the thermometers used in this study are well suited for estimating alteration or metamorphic temperatures, although the Ti-in-hornblende thermometer could, in theory, be used to calculate metamorphic temperatures.

The rocks' high-temperature history is recorded in zircon crystallization temperatures, which are typically higher than the temperatures from the other thermometers. This is consistent with previous studies that show that in most felsic rocks zircon can be saturated at high temperatures (c.f. Hanchar & Watson, 2003). Temperatures calculated with the Ti-in-zircon thermometer are probably reliable in the original igneous zircons, but are probably not meaningful in the altered zircons. Temperatures from the young zircons from partially melted host rocks should be treated with caution, since the lack of Ti minerals suggests that there was low αTi in the melt pockets.

The other thermometers generally record near- to subsolidus conditions, and due to similarities in mineralogy, there is significant overlap in the temperatures from these thermometers. The solidus estimates are based on whole rock compositions, thus, assuming that the melt was saturated in water, these temperatures should accurately reflect the solidus temperatures of the rocks. If the melts were undersaturated in water, which is realistic in the more evolved compositions, the true crystallization temperature would be higher than the estimated value. As pressure estimates for these intrusions indicate that they were emplaced at midcrustal levels, they likely contained more water, which supports the use of the H_2O-saturated solidus curve for estimating solidus conditions (Hyndman, 1981). The solidus thermometers should not be significantly influenced by metamorphism or alteration, as rock type was ascertained disregarding obvious alteration features (veins, bleaching, etc.). Although the solidus temperatures are estimates based on mineralogy, the temperatures obtained from them generally agree well with the temperatures calculated using other thermometers.

The remaining thermometers are based on mineral compositions, and they all require the interpretation of amphibole textures. Amphiboles from most of the samples (1, 13/15, 22, 29, 52, 68/69, 61, 62, 64/65) were sub- to euhedral and were likely originally igneous and crystallized at or above the solidus temperatures. Cores of these grains should, therefore yield temperatures higher than the solidus, and that is generally true for the Ti-in-hornblende thermometer, but not for the amphibole-plagioclase thermometers (**Fig. 20**). Many samples (13/15, 22, 29, 61, 62, 64/65) contain hornblende with compositional zoning, which typically parallels fabric in the rock. The rims of these grains are interpreted as metamorphic overgrowths based on deformational textures, compositional changes, and variations in Al concentrations. In addition to the metamorphic coronae on the igneous hornblende, there are three samples (36, 66, 41) that contain only metamorphic hornblende. Amphibole crystals in 36 and 66 are chemically homogenous, long (up to 3 cm), disarticulated and parallel to foliation, whereas the amphiboles in 41 occur within 50 cm of a mafic dyke. In sample 15, there is also evidence for alteration of hornblende associated with quartz-epidote veins.

The preferred temperature for crystallization temperatures is calculated from the amphibole-plagioclase thermometer B of Holland & Blundy (1994), since it yields the most consistent and unfluctuating temperatures for this data set and is the most commonly utilized (cf. Anderson *et al*., 2008; Stone, 2000; Anderson & Smith, 1995). Although the applicability of the amphibole-plagioclase thermometers to igneous rocks has been well documented (cf. Anderson *et al.*, 2008 and references therein), their relevance to metamorphic and hydrothermal systems is thus far unproven (Essene, 2009). Although the amphiboles in these rocks are clearly chemically zoned (**Fig. 3o)**, zoning in plagioclase is poorly documented, and it is difficult to correlate zoning in amphiboles with zoning in plagioclase. Additionally, diffusion in plagioclase without significant alteration is very inefficient (Morse, 1984). However, some authors have demonstrated that high-temperature hydrous fluids can re-set amphibole-plagioclase compositions (Anderson *et al*., 2008), and new hornblende-plagioclase-quartz thermobarometers have been calibrated for metamorphic systems (Bhadra & Bhattacharya, 2007). I report the calculated temperatures from both amphibole-plagioclase thermometers for igneous and metamorphic hornblende. However, the calculated metamorphic temperatures should be used cautiously, and the preferred temperature for the metamorphic hornblende is 550 °C, which was chosen based on

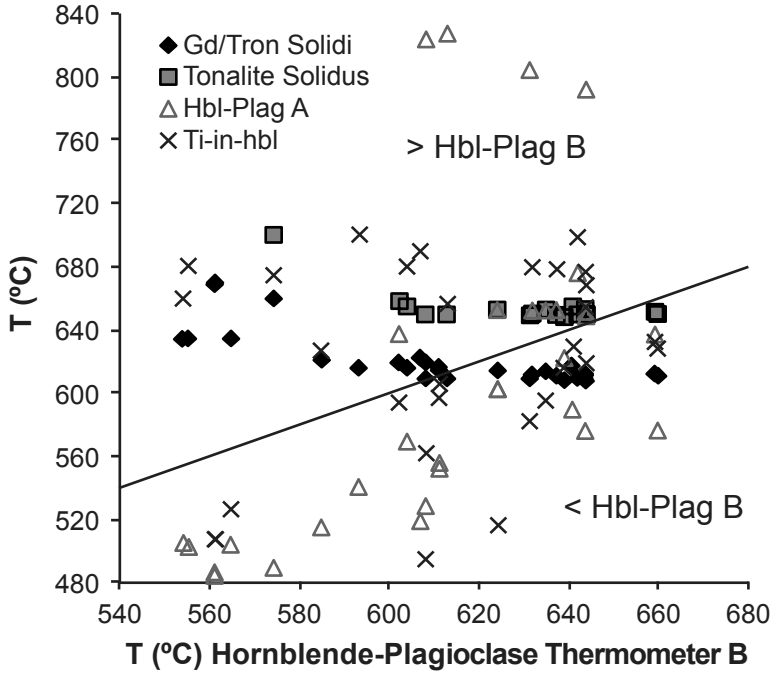

Figure 20: Plot comparing the results from the different thermometers used in this study. Symbols above the line have temperatures higher than the preferred temperature (hornblende-plagioclase thermometer B), while those below the line had lower temperatures. Temperatures from the hornblende-plagioclase thermometer A are generally lower than those from the B thermometer, while the other thermometers yield temperatures that are near or slightly above the preferred temperature. Temperatures from the solidi are roughly linear because there is less scatter in the solidi estimates than the other thermometers.

thermometry from Musselwhite (Otto, 2002; Hall & Rigg, 1986), as well as the metamorphic conditions required for the growth of hornblende. For all of the samples, there is no difference between the pressures calculated with the temperatures from the amphibole-plagioclase thermometer and those calculated from the temperature estimated from metamorphic conditions elsewhere in the belt. However, for metamorphic hornblende, both temperatures are merely estimates.

The temperatures calculated using the amphibole-plagioclase plagioclase thermometer B are consistently higher than those from the A thermometer (**Fig. 20**). Holland & Blundy (1994) argue that if B is lower than A, the system must have been undersaturated with quartz when the hornblende and plagioclase equilibrated, but temperatures from the B thermometer should not be higher than those calculated with the A thermometer, which is the case in several of the samples in this study. If the temperatures from the B thermometer are higher than those from the A thermometer, there might be a problem with the allocation of ferric iron or the plagioclase and hornblende were not in equilibrium (Holland & Blundy, 1994). Most of the samples with lower temperatures from the A thermometers were analyzed on the microprobe at Carleton University, and have much higher amounts of calculated ferric iron than amphibole analyses on the University of Ottawa microprobe. The rest of the analyses with lower A temperatures are from metamorphic hornblende, which may not have chemically re-equilibrated with plagioclase during metamorphism. This suggests that the temperatures calculated with the amphibole-plagioclase thermometer for the metamorphic hornblende are inaccurate, but the temperatures calculated from the igneous amphibole-plagioclase pairs are in agreement with expected results.

The Ti-in-hornblende thermometer has not been fully evaluated, but in this study, it yields reasonable temperatures compared to the other thermometers (70% of igneous samples have identical Ti-in-hornblende and amphibole-plagioclase B temperatures). Where the temperatures from the Ti-in-hornblende thermometer differ from the amphibole-plagioclase thermometer B, they tend to agree with the estimated solidus temperatures (**Fig. 20**). Titanium concentrations, however, are fairly heterogeneous within single hornblende grains (for example, 0.21 to 0.03 apfu in grain 2 from sample 52), and, more disconcertingly, between different grains in the same sample (0.09 to 0.13 in sample 1). Low Ti concentrations and high errors on the analyses can explain some of the variability and the

large errors associated with the temperatures, but the inter-crystal variation suggests that Ti distribution in the melt was not homogenous, and, perhaps, Ti partitioning in hornblende is sensitive to small changes in amphibole composition. The results presented here suggest that the amphiboles were crystallizing above, but near the solidus temperatures, which is consistent with the grain morphology and previous work (cf. Anderson & Smith, 1995, and references therein). If the thermodynamics of this system can be better constrained, a Ti-in-hornblende thermometer would be an ideal complement to the Al-in-hornblende barometer, since temperature could be ascertained from the same phase as the pressure.

4.2.2 Geobarometry

All of the pressure estimates in this study are based on the Al-in-hornblende barometer of Anderson & Smith (1995). The barometer is temperature sensitive, so temperatures from all of the thermometers, except Ti-in-zircon, were used to calculate the pressures, generally with similar results regardless of the thermometer used. Like the plagioclase-amphibole thermometers, the Al-in-hornblende barometer may not be applicable to metamorphic hornblende (Essene, 2009), so pressures calculated from metamorphic and altered grains should be considered with care. For the samples in this study, all of the metamorphic pressures are similar to pressures from samples with igneous hornblende of a similar age, except, possibly, for the rims on 22. The intense deformation recorded by the mylonitic textures in sample 22 may have disturbed the Al concentrations in these amphiboles, or sample 22 could be recording c. 2830 Ma deformation, as the pressures are similar to igneous hornblende of this age. I favour the latter interpretation (c. 2830 Ma deformation), because deformation should encourage Al to migrate out of the hornblende lattice, and this sample has higher Al concentrations in the rims. Additionally, the pressures from the contact-metamorphic hornblende in sample 40 and the hydrothermally altered hornblende in sample 15 cannot be verified against other samples, so the pressures from these samples are also of questionable validity. The igneous pressures calculated from hornblende in these rocks range from 5 to 8 kbar, which is within the range of pressures calculated from metamorphic assemblages at Musselwhite Mine by Otto (2002). These pressures also agree with magmatic epidote in some samples (29, 36, 46, 49, 61). The epidote in these samples occurs as inclusions in biotite without showing signs of disequilibrium, and magmatic epidote is stable between 5 and 8 kbar (Schmidt & Poli, 2004).

The new thermobarometry from the granitoids agrees well with several independent evaluations, and when considered with geochronology, adds greater resolution on the pressure changes that these rocks experience through time.

Results from the geobarometry (**Fig 19b**) show two age-depths populations that correspond with the two main age populations. The first, from 2880 to 2830 Ma, shows an increase in pressure with age, from 5 to 8 kbar, and this pattern is interpreted to represent crustal thickening during this time. The second depth population is from metamorphic hornblende, and is a tight cluster of pressures of 5.5-6.5 kbar at c. 2700 Ma. Because this hornblende is metamorphic, the period between 2830 and 2700 Ma was likely a time of significant unroofing, followed by re-burial at c. 2700 Ma.

4.3 Petrogenesis

The granitoids surrounding the North Caribou greenstone belt have been interpreted as arc rocks based on their specific geochemical signature (Wyman *et al.*, 2011), and the results of this study are consistent with this model, since the rocks I have studied have identical geochemical signatures to those reported previously (Wyman *et al.*, 2011; Biczok *et al.*, 2012).

My additional whole-rock geochemical data show that all of the felsic intrusive rocks within the area, regardless of age, follow a single, consistent trend in Harker-style major element diagrams, which strongly supports the idea that they represent a single magmatic series (Moyen & Martin, 2012). The c. 300 My spread in ages, however, prohibits a single melting episode, and this pattern likely indicates that partial-melting of 2890 Ma (or older) TTGs was the source for the younger intrusions. The Sm-Nd isotope data of Wyman *et al.* (2011) are consistent with this interpretation, as they show a strong relationship between decreasing εNd and decreasing crystallization age. Isotopic studies from elsewhere in the NCT (i.e. Stevenson *et al.*, 2009) show a significant component of old (~3.0 Ga) crust, which is consistent with the data presented here. The progressive evolution of bulk magma composition through time, predominantly tonalite in the oldest rocks, though granodiorites and granites in the 2760-2680 Ma population, culminating with granitic pegmatites, supports this hypothesis, as do the similar trends in trace elements throughout the area. It is also striking that the only rocks that indicate a possible sedimentary source are pegmatites intruding metasediments of the NCGB, and these S-type pegmatites could represent melting

of the sediments. Because intrusions of all ages have a similar geochemical signature, I will primarily be discussing the provenance of the original magmas.

Wyman *et al.* (2011) discuss in depth the prominent adakite signature of the rocks of the NCGB environs, and this study confirms that these rocks fall into the adakite fields of traditional discrimination diagrams. On the K/Rb v. SiO_2/MgO diagram of Martin *et al.* (2005), these rocks plot in the high-silica adakite field, which, in modern settings includes magmas derived from melting the subducted slab in the presence of free H_2O once it has reached amphibolite facies metamorphic conditions (**Fig. 21a**). This signature is nearly ubiquitous in Archean TTGs from around the world (Martin *et al.*, 2005; Moyen & Martin, 2012). There are also a strong, negative Ta-Nb anomalies in the primitive-mantle-normalized spider diagrams (**Fig. 6**), which is a signature of subduction-related melting in general, and is also found in modern adakites (Martin *et al.*, 2005). The negative slope from LREEs to HREEs also suggests a deep (at least 15 kbar pressure, or ~45 km depth) melting source for TTGs, as garnet and amphibole in the melt residue will fractionate HREEs (Moyen & Matrin, 2012). Additionally, the lack of Eu and Sr anomalies suggests that little to no plagioclase remained in the melt residue (Moyen & Martin, 2012). Again, these are fairly common patterns in TTGs (Barker & Arth, 1976; Moyen & Martin, 2012). There is also a correlation between lower Yb/Gd ratios and older rocks, suggesting that the original garnet-residue signature was dampened with continued crustal reworking, as younger rocks have less strongly fractionated REE patterns (**Fig. 21b**).

Although the characteristics of these rocks are consistent with the interpretation of Wyman *et al.* (2011) that these are subduction-related rocks, there could be additional settings that would generate the same characteristics. The adakite signature and Nb-Ta anomalies only require partial melting of a rock with a basaltic composition within the garnet stability field in the presence of free water. Subduction is the most efficient method to deliver both basalt and free water to the depths required to generate these melts, but there is debate over the nature or existence of subduction during the Mesoarchean (Foley, 2008; Dhuime *et al.*, 2012). Additional, non-subduction models for growth of Archean crust may also account for the geochemical signatures of TTGs, as long as they can provide sufficient sources of free water, heat, and basalt at 45 km depths.

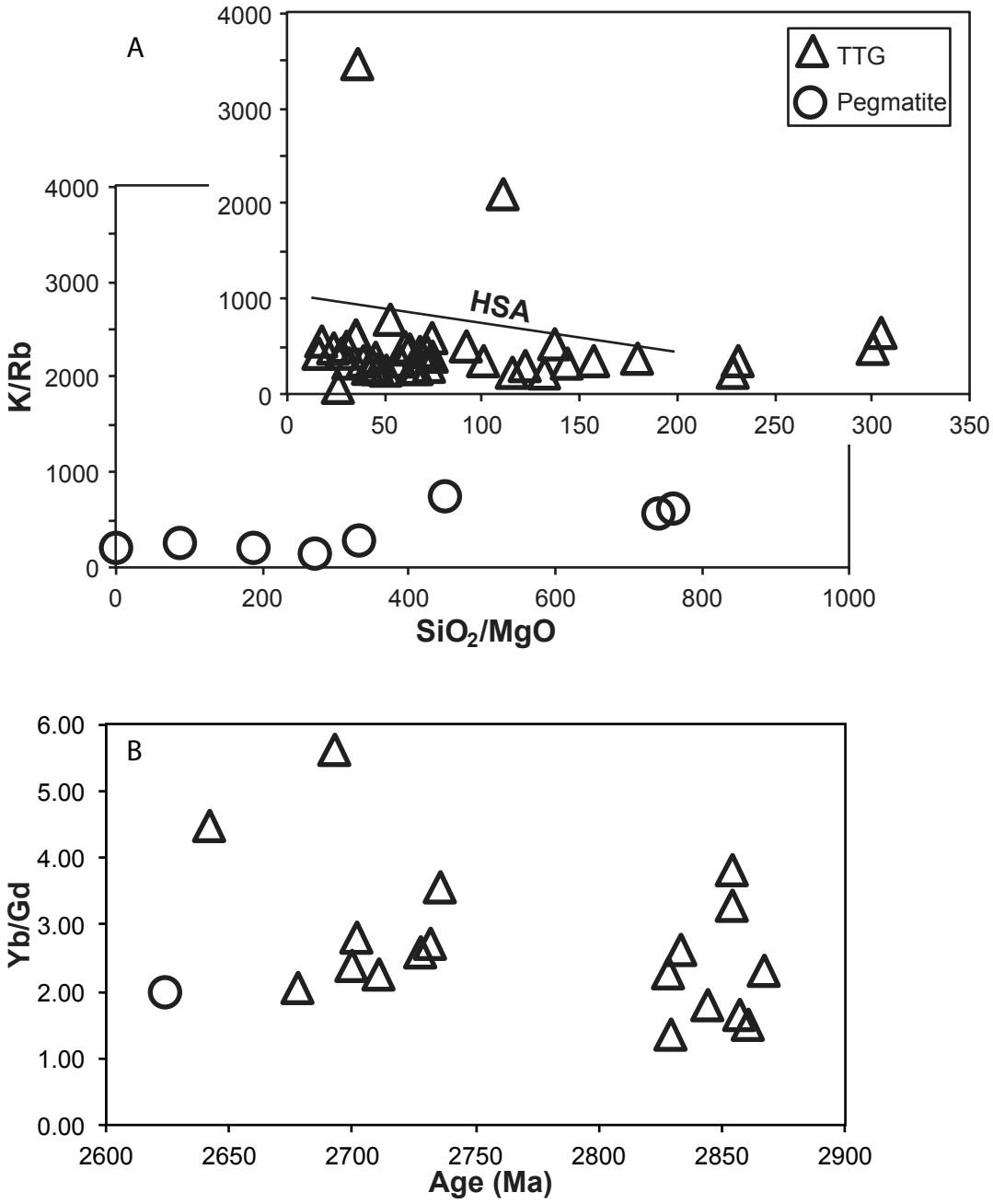

Figure 21: A. Adakite discrimination diagram. Samples below the line fall in the high silica adakite (HSA) field, which includes typical TTG compositions after Martin et al. 2005. Most samples from this study have typical HSA and TTG compositions. B. Diagram showing potential garnet influence on whole-rock trace element concentrations. A decrease in MREE/HREE concentrations over time indicates a stronger garnet influence over the older melts, possibly indicating a garnet-rich melt residue.

4.4 The status of the crescentic North Caribou pluton

The data presented here provide limited evidence supporting the crescent pluton model of the NCBp. The shape of the NCGB, the magnetic signature of the NCBp, and the structural data from previous workers are similar to the observations of crescentic plutons in other greenstone belts (Stott & Biczok, 2010). Additionally, the model requires an intrusive contact between the crescent plutons and the supracrustal rocks, and the contact metamorphic aureole and interfingered TTG and amphibolites at the contact between the NCBp and the NCGB are indicative of an intrusive contact. Major, minor, and trace element geochemistry from the NCBp is less variable than that from the NCBc, despite a wide range of SiO_2 concentrations (**Figs. 5 & 6**). This suggests that the rocks in the NCBp are more similar to each other than those in the NCBc. These observations, however, do not provide the required data to validate the crescentic pluton model, as there are many models that can explain these data.

Significantly, I report data that cannot be resolved within a late crescent pluton model. Critically, zircon U-Pb ages in the NCBp range from 2870-2858 Ma, which is slightly older than the ages from the NCBc (2852-2833 Ma). The late crescentic pluton would have to be younger than the core of the North Caribou batholith, and the rocks of the NCB are older close to the contact with the greenstone belt. There is also no difference between the textures in the pluton and the batholith, as both contain gneisses and isotropic granitoids. Additionally, temperatures and pressures are indistinguishable across the contact between the NCBp and the NCBc (**Fig. 16**), and REE patterns from zircons are indistinguishable between the NCBp and the NCBc (**Fig. 12**). This suggests the source and the level of emplacement of all of the rocks within the North Caribou batholith (both NCBc and NCBp) were more or less identical.

The older zircon ages in the NCBp indicate that it represents the initial magmatic pulse in what would become the NCB rather than a late intrusion. The kinematics and structures presented in Stott and Biczok (2010) suggest that the emplacement of the NCB folded the NCGB. However, the contemporaneous magmatism in the NCB and NRV require folding to post-date the emplacement of the NCB, which is similar to models proposed for the Yilgarn craton of Australia (Chen *et al*., 2001). Therefore, no ballooning model for the emplacement of the NCB can explain the deformation within the NCGB. Further studies of the NCB,

including fabric analysis, could better constrain the dynamics of the intrusion of the NCB and evaluate its relationship with the geometry of the NCGB.

4.5 Is there a domain boundary between the SLGC and the NCGB?

There are two primary arguments for placing a domain boundary between the SLGC and the NCGB: 1) there are significant shear zones bordering the NCGB to the north and 2) some rocks within the ILD are younger than most of the rocks of the NCC (Stott *et al*., 2010). Many authors have documented the shear zones separating the ILD and the NCC (cf. Breaks *et al*., 2001), but it is impossible to define a distinct terrane based solely on the existence of shear zones. Therefore, the critical distinction between the ILD and the NCC is their ages, and Nd-model ages of some ILD rocks are younger than the 3.0 Ga model ages of NCC rocks (Stevenson & Turek, 1992).

Because geochemistry, geochronology, and rock textures are not significantly different between the rocks in the SLGC and those from the south, the most relevant piece of evidence that I can add to this debate is the unique geochronologic signatures of some of the rocks in the SLGC. These geochronologic signatures include: 2830 Ma hydrothermal alteration of and magmatic overgrowths on zircon in some samples and an absence of inherited zircon outside of the SLB and WLB. Although the hydrothermal and igneous rims indicate that the rocks of the SLGC experienced a significant hydrothermal episode not recorded in the rocks south of the NCGB, the patterns in inherited zircons could indicate several things about the history of rocks within the SLGC.

The sequestration of inherited grains within specific domains of the SLGC could indicate that these blocks are remnants of older crust, while the surrounding rocks are more juvenile, as one might find in modern-day active continental margin. Nd isotopic data from Wyman *et al.* (2011) show a wide range between the rocks within the SLB (εNd: +0.5) and those outside of the SLB (εNd: +3.3), and these data suggest that the rocks outside of the SLB and WLB are from a more depleted source or have less crustal contamination than those within these two crustal blocks. However, the isotopic data set is only based on one sample from the SLGC and one from the SLB, so more data are necessary to confirm this correlation. However, these data would support the division of the ILD and NCC as two separate terranes with distinct histories based on the age of primitive melts.

Other scenarios would not necessarily require a terrane boundary. A lack of inherited grains could also be the result of a sampling bias. This is unlikely, because the rocks from the SLGC were among the most intensely analyzed in this study. Additionally, about 65% of samples from the WLB and SLB have inherited cores, which is similar to the distribution in the SB and NCB, while there are no samples (out of 3) with inherited zircon from the SLGC outside of the WB and SB. Additional mapping and analysis of rocks within the SLGC, especially further from the NCGB, would be needed to eliminate a potential sampling bias.

Another possible scenario for an absence of inherited zircon is the dissolution of older grains during younger melting episodes. The similarity in major and trace element patterns within the SLGC, including both the SLB and the WLB, are indistinguishable, suggesting that different zircon solubility within these magmas could not arise from compositional differences in the melts. Although temperature and pressure differences also impact zircon solubility (Hanchar & Watson, 2003), the geothermobarometry data presented here do not suggest that the rocks of the SLGC outside of the SLB and WLB experienced significantly different conditions than those within the SLB and WLB.

Although the isotopic data might support the separation of the NCC and the ILD, the similarities in geochemical signatures suggest that the magmas in the different domains shared a common source. If the ILD was near or at the northern margin of the NCC from 2880 to 2860 Ma both terranes could have sampled the same melt source. A collision between the ILD and NCC could also explain the patterns observed with pressure increases from 2860-2830 Ma rocks and the hydrothermal alteration of zircon in the SLGC at 2830 Ma (**Fig. 19b**). However, the data presented in this study are not sufficient to determine if the northern boundary of the NCGB is unequivocally a terrane boundary between the NCC and ILD.

4.6 Tectonic history

4.6.1 Pre-2890 Ma

The pre-2890 Ma rock record from the NCC is scant. The only previously reported pre-2890 Ma intrusive rocks in this area are from the Weagamow batholith at 2990 Ma (Biczok *et al.*, 2012). What is preserved from this time period are primarily xenocrystic cores of zircon, which are found in about 70% of samples south of the NCGB. Additionally, two rocks, one from the Wharram Lake block and one from the NCB, are within this age range.

Based on these two samples, magmatism at this time was tonalitic to granodioritic in composition. Despite the poor preservation of pre-2890 Ma rocks, the ubiquity of older zircons, especially ~3000 Ma, throughout the study area suggests that there must have been significant amounts of zircon-bearing crust in the NCC from at least 3000 Ma. The oldest zircons in this study are 3130 Ma, which is consistent with previously reported data (e.g. Percival *et al*., 2006*b*). Although there is evidence for significant 3000 Ma crust in the NCC, there are fewer, younger inherited grains from the SLGC, which is consistent with patterns seen elsewhere in the ILD suggesting that the ILD is slightly younger than the NCC (Percival *et al.*, 2006*b*). Despite the significant reworking of the pre-2890 Ma rocks, the information preserved in xenocrystic zircons and a few rocks suggests protracted tonalitic and granodioritic magmatism starting at least by 3130 Ma, with pulses of magmatic activity at c. 2940 and c. 2990 Ma (**Fig. 17**). Sm-Nd isotopic studies by other authors indicate that despite the poor preservation of rocks of this age, pre-2980 Ma magmatic rocks may be source for the subsequent intrusions of TTGs (i. e. Stevenson *et al.*, 2009).

4.6.2 2890-2830 Ma

The rocks surrounding the NCGB record a complex tectonomagmatic history from 2890 to 2830 Ma, an interval of time marked by a voluminous magmatism. All of the samples dated here, as well as the North Rim Volcanics (NRV) have a zircon or titanite ages within this time period. This suggests that the NRV must be—at least temporally—related to the major magmatic bodies surrounding the NCGB (Biczok *et al.*, 2012) and must have been juxtaposed against the intrusive rocks of the Schade Lake gneissic complex after deposition at 2870 ± 2 Ma.

The rocks formed during this interval are chemically similar to the older TTGs with compositions between tonalite to granodiorite. Additionally, the whole-rock geochemistry shows coherent trends in both major and trace elements, suggesting that all of the magmas emplaced during this time originated from a similar source.

Although the apparent timing of magmatism during this major period of crustal growth is within a 60 My window, there are two notable age populations. Most of the magmatic activity occurred between 2870-2855 Ma, with a second pulse from 2840-2835 Ma. Some samples from the SLGC contain zircons with 2870 Ma cores and 2830 Ma magmatic/ hydrothermal rims. Additionally, thermobarometry from these samples shows an

increasing emplacement depth through time, from about 5 to 8 kbar between 2860 and 2830 Ma, with the deepest emplacement depths occurring c. 2830 Ma (**Fig. 19b**). This change in emplacement depths is likely the result of tectonic thickening during crustal accretion and collision. Tectonism during this time is independently recorded in the detrital age populations from Eyapamikama metasediments (J. Duff, *personal communication*) that would suggest basin development and unroofing during collision, coeval with metamorphism in deeper parts of the orogen based on ages from foliation-parallel zircons within the greenstone belt (Kalbfleisch, 2012). The simplest explanation for the patterns in the zircon ages, the increase in emplacement pressure through time, and the tectonic juxtaposition of the SLGC along the northern border of the NCGB is a collision between the NCC and the ILD or another more northerly domain. The peak of collision and the thickening likely postdates most of the magmatism in the area, although several intrusions in the NCB would be syntectonic. In summary, the data suggest that from 2890-2830 Ma, there was wide-spread magmatism from 2870-2855 Ma followed by crustal thickening, possibly from collision with the Island Lake Domain, and renewed magmatic activity from 2840-2835.

4.6.3 2760-2680 Ma

The ~70 My period between 2830 and 2760 Ma is not recorded by zircons or titanite in this study of the North Caribou, but detrital evidence from in the Eyapamikama sediments suggests that it was a period of erosion and deposition (Duff, *personal communication*). Commencing at 2760 Ma is a more cryptic tectonomagmatic event, recorded in about two-thirds of the samples, primarily as rims on zircon or in metamorphic titanite grains. This is coincident with the effusive magmatism of the Berens River subprovince to the southwest and the inception of the Uchi orogeny (Percival *et al*., 2006*b*) and is similar to Sm-Nd ages from garnet at Musselwhite that are thought to be contemporaneous with mineralization (Biczok *et al.*, 2012). Rocks exhibiting this age signature are found throughout the study area, although less commonly in the NCB, and there is a general pattern of decreasing ages from east to west. Although most rocks of this age record hydrothermal alteration, there are several samples with igneous zircons (13, 45, 53, 71, 43, 51). All of the samples with igneous zircons are granodiorites or granites, and an increase in K concentrations is also observed in some samples with hydrothermal zircon rims (**Fig. 18**). However, other than an increase in K, there is very little geochemical difference between rocks from the 2890-2830

events and the younger TTGs. This geochemical signature suggests that the rocks with igneous zircons formed either by partial melting of a similar source as the TTGs or of the TTGs themselves.

The prevalence of hydrothermal ages along with infrequent igneous ages suggests that the second main tectonomagmatic event recorded by the granitoids surrounding the NCGB was primarily a hydrothermal and metamorphic event, with limited magmatism that was more evolved than the magmas from the 2890-2830 Ma time period. Because of limited fluid mobility at amphibolite-grade metamorphic conditions, the fluid influx probably slightly predated metamorphism of titanite and hornblende, and extra volatile content likely fuelled partial melting in the granitoids with multiple igneous zircon populations. This is apparent in zircon ages; most altered zircons slightly pre-date the formation of the secondary magmatic zircon populations. Hornblende thermobarometry indicates that these rocks were ~20 km deep during metamorphism, which is similar to some of the geobarometric results from the ore zone at Musselwhite (Otto, 2002).

A source for the heat and fluids required in this scenario is not obvious from the TTGs. However, sedimentary sequences from the Island Lake domain and the Heaton Metasediments in the NCGB (Duff, *personal communication*) suggest that preceding the onset of magmatic activity, there was erosion and sedimentation that is regionally linked to the Uchi orogeny (2748-2708 Ma; Percival *et al.*, 2006*b*). The Uchi orogeny is also associated with the prolific magmas of the Berens River area, and the sedimentation in the NCGB confirms that the rocks surrounding the NCGB were also affected by the Uchi orogeny. Accordingly, it is likely that the accretion of the Winnipeg River Terrane and the resulting orogeny provided sufficient heat to initiate metamorphism. Metamorphism in the NCT added fluids to the volatiles produced by the magmatic activity in the Berens River intrusions, providing sufficient fluids to produce the observed alteration characteristics. Metamorphic fluids at greenschist facies carrying Au-mineralizing fluids followed by higher-grade metamorphism is a common pattern in orogenic Au deposits (Phillips & Powell, 2009), and this would suggest that Au-mineralization occurred during this time period.

4.6.4 Post-2680 Ma

The final magmatic event in the NCGB region is recorded in pervasive pegmatitic to aplitic brittle-ductile dykes. The single pegmatite sample containing zircon yielded an age of

2619 ± 14 Ma, indicating a ~60 My gap between the cessation of the 2790-2680 Ma event and the intrusion of pegmatites. These pegmatites have highly evolved compositions, with abundant K-feldspar, muscovite and biotite along with garnet, fluorite, and tourmaline in S-type pegmatites that cross-cut the metasedimentary sequences. The brittle-ductile intrusive textures exhibited by the pegmatites (**Figs. 4a,b**) indicate that they must have been emplaced near the brittle-ductile transition, at about 12-15 km depths under typical crustal conditions (Scholtz, 1988), and possibly shallower with higher heat flow conditions of the Archean. This depth is similar to that from metamorphic hornblende in sample 13/15, which developed a strong fabric post-2730 Ma. Hornblende from this sample shows fabric-parallel overgrowths with pressures of 3.6 kbar, which correspond to a depth of ~13 km. The high Mn concentrations (25-50 mol%) of the pegmatitic garnets also correspond with depths near or above 12 km (Green, 1977).

There is also some evidence for tectonism subsequent to the emplacement of the pegmatites. All of the samples of pegmatites are deformed, exhibiting undulose extinction in quartz. There is also abundant evidence for syn- to post-pegmatitic fluid infiltration, with many planar quartz-carbonate-(epidote) veins cross-cutting pegmatitic dykes. Hornblende from sample 15 shows overgrowths associated with quartz veins, and these overgrowths yield pressures around 1.8 kbar. Additionally, hornblende in sample 41 grew as a result of contact metamorphism with a mafic dyke that yields a similar pressure of 2.4 kbar. There are several Proterozoic dyke swarms in the area, and it is likely that this intrusion is a member of one of these swarms (Ontario Geological Survey, 2011). The vein quartz also exhibits undulose extinction, pointing to an extended period of deformation within the core of the Superior Province, which has been confirmed by recent work on monazite (Kalbfleisch *et al.*, 2011).

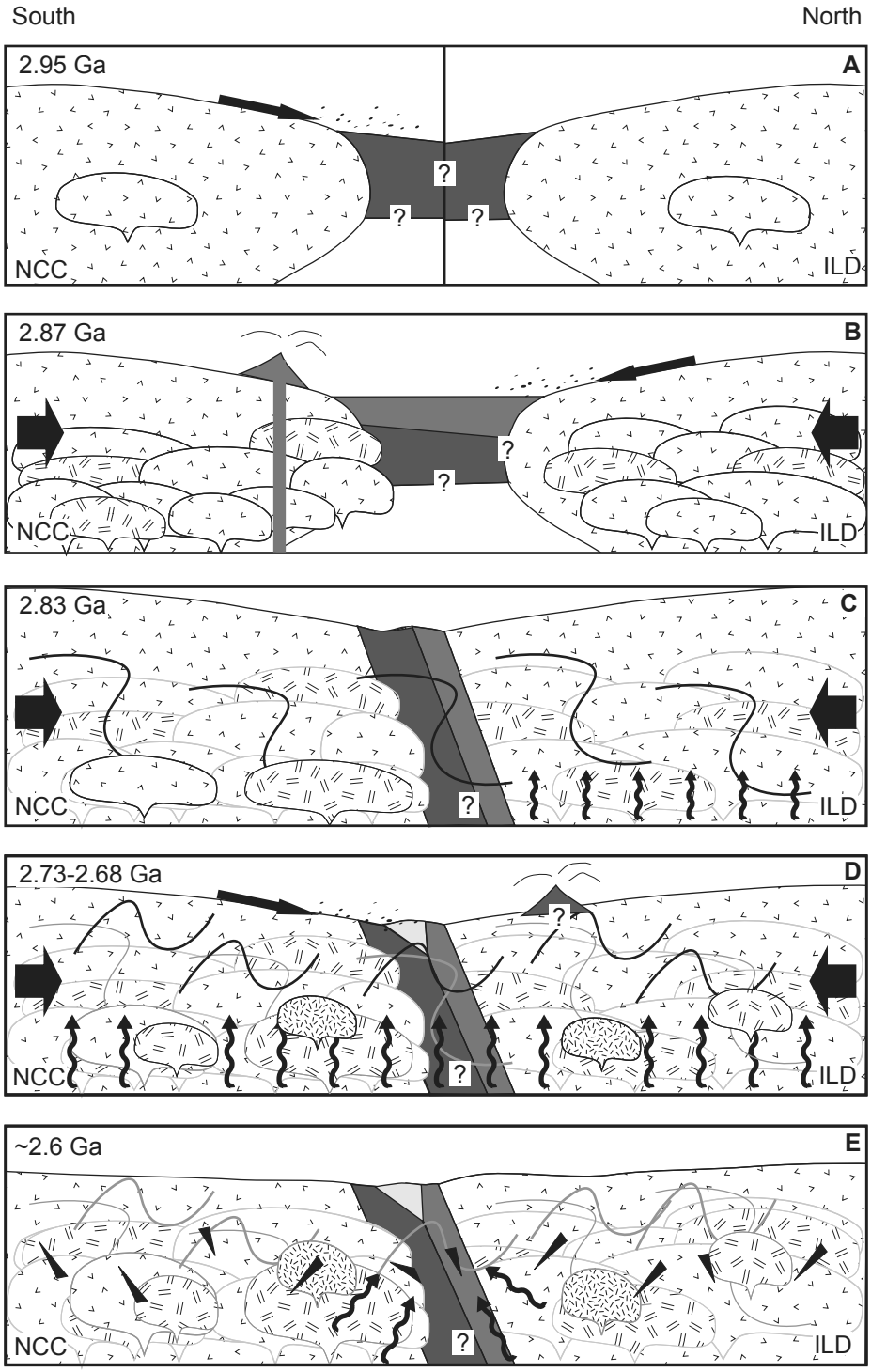

Figure 22: Schematic north-south cross-sections across the NCGB. NCC: North Caribou core, ILD: Island Lake domain. Large amplitude waves indicate deformation, bold arrows indicate compression, and squiggly arrows indicate hydrothermal alteration. A. Formation of SRV accompanied by tonalitic magmatism and erosion. B. Major tonalitic and granodioritic magmatism and the formation of the NRV. C. Collision of the ILD with the NCC. Minor tonalitic and granodioritic magmatism accompanied by deformation and hydrothermal activity in the ILD. D. Minor magmatism in both the NCC and ILD along with intense hydrothermal activity, deformation, formation of the Heaton Metasediments, and volcanic activity in the ILD. Possilble Au-mineralization. E. Emplacement of brittle-ductile pegmatitic dykes and possible Au-mineralization.

5. SUMMARY

Granitoids surrounding the NCGB are diverse in age and composition, and they record tectonic activity from > 3100 to < 2600 Ma.

1. Pre-2890 Ma (**Fig. 22a**): The oldest period of magmatic activity is preserved in some tonalites and inherited cores of zircons (the oldest of which is 3132 ± 7 Ma). Rocks of this age likely represent the original continental crust in the NCC.

2. 2880-2850 Ma (**Fig. 22b**): The major intrusive complexes (SLGC, SB and NCB) formed during this time. These rocks are tonalitic to granodioritic and exhibit deformation styles ranging from weak foliation to strong gneissic banding. Thermobarometry suggests that 2880-2850 Ma intrusions were emplaced at 20 km depths, and the geochemistry suggests that they or their precursor crustal rocks were derived from a deep (≥ 45 km) source. Additionally, geochronology shows that there is no discrete pluton on the northern and western boundaries of the NCB. Rocks from this period represent the main magmatic pulse in the area, during which 1000s of km^3 of magma was emplaced at mid-crustal levels.

3. c. 2830 Ma (**Fig. 22c**): Rocks of this age record a second pulse of magmatism, accompanied by hydrothermal alteration of zircon in the SLGC, shortly following the main magmatic event. Thermobarometry records an increase in emplacement depths, corresponding to levels up to 30 km deep. Although the geochronology and geochemistry do not absolutely resolve a terrane boundary between the SLGC and the rocks to the south, these data are consistent with a collision between the ILD and the NCC between 2840 and 2830 Ma. The 2830 Ma rocks likely record the growth of the North Caribou Core prior to the accretion of the rest of the Western Superior Province.

4. 2760-2680 Ma (**Fig. 22d**): The ca. 2700 event is primarily recorded by alteration of older rocks along with volumetrically minor intrusions. The alteration associated with this event affected the rims of zircon, resulted in K enrichment, and moved from east to west through time. The alteration event was followed by metamorphism of titanite and hornblende, along with partial melting of some altered rocks that reached higher temperatures. This alteration may be contemporaneous with mineralization at Musselwhite (Biczok *et al.*, 2012). Igneous rocks emplaced during this time are more evolved than the older rocks, with compositions between granodiorite and granite. These intrusions were likely emplaced at depths around 20 km. Magmatism and fluid infiltration from 2760 to 2680

Ma is likely related to the Uchi orogeny at ca. 2730, as well as the Berens River Intrusive Complex further to the west (Percival *et al.*, 2006*b*).

5. Pegmatites (**Fig. 22e**): The final felsic magmatic episode of the NCGB occurs as ubiquitous brittle-ductile pegmatitic to aplitic dykes. These late pegmatites have granitic (*sensu stricto*) compositions, and may include garnet, muscovite, biotite, and fluorite as accessory minerals. The only date acquired from one of these pegmatites is 2619 ± 14 Ma, which is similar to recent monazite ages from sheer zones within the NCGB (Kalbfleisch *et al.*, 2011; Kalbfleisch, 2012). Late pegmatites are found throughout the Superior Province and suggest widespread, volumetrically minor, post-orogeny crustal anatexis (Percival *et al.*, 2006*b*; Wyman *et al.*, 2011).

The granitic rocks from the North Caribou Terrane demonstrate that cratonization and crustal growth is a long-lived process, as geochronology performed in this study highlights more than 500 My of magmatic activity. Geochemistry shows that it involves substantial reworking and modification of older crustal material, and thermobarometry indicates that these rocks underwent several cycles of burial and exhumation before becoming the stable core of North America.

6. REFERENCES

Ague J. J. & Brandon, M. T. (1996). Regional tilt of the Mount Stuart batholith, Washington, determined using aluminum-in-hornblende barometry: Implications for the northward translation of Baja British Columbia. *Geological Society of America Bulletin* **108**, 471-488.

Anderson, J. L., Barth, A. P., Wooden, J. L. & Mazdab, F. (2008). Thermometers and thermobarometers in granitic systems. *Reviews in Mineralogy & Geochemistry* **69**, 121-142.

Anderson, J. L. & Smith, D. R. (1995). The effects of temperature and f_{O2} on the Al-in-hornblende barometer. *American Mineralogist* **80**, 549-559.

Arth, J. G. (1976). Behavior of trace elements during magmatic processes - a summary of theoretical models and their applications. *Journal of Research of the U. S. Geological Survey* **4**, 41-47.

Arth, J. G. & Barker, F. (1976). Rare-earth partitioning between hornblende and dacitic liquid and implications for the genesis of trondhjemitic-tonalitic magmas. *Geology* **4**, 534-536.

Ayers, J. C., Zhang, L., Luo, Y., & Peters, T. J. (2012). Zircon solubility in alkaline aqueous fluids at upper crustal conditions. *Geochimica et Cosmochimica Acta* **96**, 18-28.

Barker, F. (1979). Trondhjemites, Dacites, and Related Rocks. Elsevier: New York, 676 p.

Barker, F. & Arth, J. G. (1976). Generation of trondhjemitic-tonalitic liquids and Archean bimodal trondhjemite-basalt suites. *Geology* **4**, 596-600.

Bartlett, J. R., Breaks, F. W., de Kemp, E. A. & Shields, H. N. (1985). Precambrian geology of Eyapamikama Lake area (Opapimiskan Lake Project), Kenora District (Patricia Portion). *Ontario Geological Survey*, **Map P.2834**.

Bhadra, S. & Bhattacharya, A. (2007). The barometer tremolite + tschermakite + 2 albite = 2 pargasite + 8 quartz: Constraints from experimental data at unit silica activity, with application to garnet-free natural assemblages. *American Mineralogist* **92**, 491-502.

Biczok, J., Hollings, P., Klipfel, P., Heaman, L., Maas, R., Hamilton, M., Kamo, S. & Friedman, R. (2012). Geochronology of the North Caribou greenstone belt, Superior Province Canada: Implications for tectonic history and gold mineralization at the Musselwhite mine. *Precambrian Research* **192-195**, 209-230.

Blundy, J. D. & Holland, T. J. B. (1990). Calcic amphibole equilibria and a new amphibole-plagioclase geothermometer. *Contributions to Mineralogy and Petrology* **104**, 208-224.

Breaks, F. W. & Bartlett, J. R. (1991). Geology of the Eyapamikama Lake area. *Ontario Geological Survey Open File Report* **5792**, 131 p.

Breaks, F. W., Bartlett, J. R., de Kemp, E. A., Finamore, P. F., Jones, G. R., Macdonald, A. J., Shields, H. N. & Wallace, H. (1984). Precambrian geology, quaternary geology, and mineral deposits of the North Caribou Lake area, District of Kenora, Patricia Portion. *Ontario Geological Survey Miscellaneous Report* **119**, 258-273.

Breaks, F. W., Bartlett, J. R., de Kemp, E. A. & Osmani, I. A. (1991). Geology of the Doubtful-Akow Lakes area, District of Kenora. *Ontario Geological Survey Open File Report* **5795**. 130 p.

Breaks, F. W., Bartlett, J. R., de Kemp, E. A. & Osmani, I. A. (1986). Precambrian geology of the Doubtful-Akow Lakes area (Opapimiskan Lake Project), Kenora District (Patricia Portion). *Ontario Geological Survey*, **Map P.2965**.

Breaks, F. W., Osmani, I. A. & de Kemp, E. A. (2001). Geology of the North Caribou Lake area, northwestern Ontario. *Ontario Geological Survey Open File Report* **6023**. 80 p.

Breaks, F. W., Osmani, I. A. & de Kemp, E. A. (1987*a*). Precambrian geology of the Opapimiskan-Neawagank Lakes area, eastern part (Opapimiskan Lake Project), Kenora District (Patricia Portion). *Ontario Geological Survey*, **Map P.3081**.

Breaks, F. W., Osmani, I. A. & de Kemp, E. A. (1987*b*). Precambrian geology of the Opapimiskan-Neawagank Lakes area, western part (Opapimiskan Lake Project), Kenora District (Patricia Portion). *Ontario Geological Survey*, **Map P.3080**.

Card, K. D. & Ciesielski, A. (1986). DNAG # 1. Subdivisions of the Superior Province of the Canadian Shield. *Geoscience Canada* **13**, 5-13.

Chen, S. F., Libby, J. W., Greenfield, J. E., Wyche, S. & Riganti, A. (2001). Geometry and Kinematics of large arcuate structures formed by impingement of rigid granitoids into greenstone belts during progressive shortening. *Geology* **29**, 283-286.

Christensen, N. I. & Mooney, W. D. (1995). Seismic velocity structure and composition of the continental crust: A global view. *Journal of Geophysical Research: Solid Earth* **100**, 9761-9788.

Claiborne, L. L., Miller, C. F., Walker, B. A., Wooden, J. L., Mazdab, F. K. & Bea, F. (2006). Tracking magmatic processes through Zr/Hf ratios in rocks and Hf and Ti zoning in zircons: An example from the Spirit Mountain batholith, Nevada. *Mineralogical Magazine* **70**, 517-543.

Colombi, A. (1988). Métamorphisme et géochimie des roche mafiques des Alpes oust-centrales (géoprofil Viège-Domodossola-Locarno). *Unpublished PhD thesis*, University of Lausanne 216 p.

Condie, K. C. (1984). Archean geotherms and supracrustal assemblages. *Tectonophysics* **105**, 29-41.

Condie, K. C. & Kröner, A. (2008). When did plate tectonics begin? Evidence from the geologic record. *Geological Society of America Special Paper* **440**, 281-294.

Corfu, F., Hanchar, J. M., Hoskin, P. W. O. & Kinny P. (2003). Atlas of zircon textures. *Reviews in Mineralogy and Geochemistry* **53**, 469-500.

Corfu, F. & Lin, S. (2000). Geology and U-Pb geochronology of the Island Lake greenstone belt, northwestern Superior Province, Manitoba. *Canadian Journal of Earth Sciences* **37**, 1275-1286.

Corfu, F. & Stone, D. (1998*a*). Age structure and orogenic significance of the Berens River composite batholiths, western Superior Province. *Canadian Journal of Earth Sciences* **35**, 1089-1109.

Corfu, F. & Stone, D. (1998*b*). The significance of titanite and apatite U-Pb ages: Constraints for the post-magmatic thermal-hydrothermal evolution of a batholithic complex, Berens River area, northwestern Superior Province, Canada. *Geochimica et Cosmochimica Acta* **62**, 2979-2995.

Davis, D. W., Amelin, Y., Nowell, G. M. & Parrish, R. R. (2005). Hf isotopes in zircon from the western Superior Province, Canada: Implications for Archean crustal development and evolution of the depleted mantle reservoir. *Precambrian Research* **140**, 132-156.

Davis, D. W. & Stott, G. M. (2001). Project Unit 89-47. Geochronology of several greenstone belts in the Sachigo Subprovince, northwestern Ontario. *Ontario Geological Survey Open File Report* **6070**, 18-1-18-13.

deKemp, E. A. (1987). Stratigraphy, provenance, and geochronology of Archean supracrustal rocks of western Eyapamikama Lake area, Northwestern Ontario. *Unpublished MSc thesis*, Carleton University 98 pp.

Dhuime, B., Hawkesworth, C. J., Cawood, P. A. & Storey, C. D. (2012). A change in the geodynamics of continental growth 3 billion years ago. *Science* **335**,1334-1336.

Donaldson, J. A. & de Kemp, E. A. (1998). Archaean quartz arenites in the Canadian Shield: examples from the Superior and Churchill Provinces. *Sedimentary Geology* **120**, 153-176.

Douglas, R. J. W. (1973). *Geological Provinces*. In: *The National Atlas of Canada, 4th edition*. Ottawa: Department of Energy, Mines and Resources, 27-28.

Duff, J., Hattori, K., Schneider, D. A., Cossette, É., Jackson, S. & Biczok, J. (2012). Garnet as a tracer for the mineralization in a banded-iron formation-hosted orogenic gold

deposit, North Caribou greenstone belt, western Superior Province. *Geological Association of Canada/ Mineralogical Association of Canada Annual Meeting Abstracts* **35**, 37.

Easton, R. M. (2000). Metamorphism of the Canadian shield, Ontario, Canada. I. The Superior Province. *The Canadian Mineralogist* **38**, 287-317.

Ebadi, A. & Johannes, W. (1991). Beginning of melting and composition of first melts in the system Qz-Ab-Or-H_2O-CO_2. *Contributions to Mineralogy and Petrology* **106**, 286-295.

Ernst, W. G. & Liu, J. (1998). Experimental phase equilibrium study of Al- and Ti-contents of calcic amphibole in MORB—A semiquantitative thermobarometer. *American Mineralogist* **83**, 952-969.

Essene, E. J. (2009). *Thermobarometry gone astray*. In: Gupta, A. K. & Dasgupts, S. (eds.) *Physics and Chemistry of the Earth's Interior*. New Delhi: Indian National Science Academy, 101-133.

Ferry, J. M. & Watson, E. B. (2007). New thermodynamic models and revised calibrations for the Ti-in-zircon and Zr-in-rutile thermometers. *Contributions to Mineralogy and Petrology* **154**, 429-437.

Foley, S. (2008). A trace element perspective on Archean crust formation and on the presence or absence of Archean subduction. *Geological Society of America Special Paper* **440**, 31-50.

Frost, B. R., Barnes, C. G., Collins, W. J., Arculus, R. J., Ellis, D. J. & Frost, C. D. (2001). A geochemical classification for granitic rocks. *Journal of Petrology* **42**, 2033-2048.

Frost, B. R., Chamberlain, K. R. & Schumacher, J. C. (2000). Sphene (titanite): phase relations and role as a geochronometer. *Chemical Geology* **172**, 131-148.

Fu, B., Page, F. Z., Cavosie, A. J., Fournelle, J., Kita, N. T., Lackey, J. S., Wilde, S. A. & Valley, J. W. (2008). Ti-in-zircon thermometry: applications and limitations. *Contributions to Mineralogy and Petrology* **156**, 197-215.

Geisler, T., Schaltegger, U., Tomaschek, F. (2007). Re-equilibration of zircon in aqueous fluids and melts. *Elements* **3**, 43-50.

Green, T. H. (1977). Garnet in silicic liquids and its possible use as a P-T indicator. *Contributions in Mineralogy and Petrology* **65**, 59-67.

Hanchar, J. M. & Watson, E. B. (2003). Zircon saturation thermometry. *Reviews in Mineralogy and Geochemistry* **53**, 89-112.

Hofmann, A. E., Valley, J. W., Watson, E. B., Cavosie, A. J. & Eiler, J. M. (2009). Sub-micron scale distributions of trace elements in zircon. *Contributions in Mineralogy and Petrology* **158**, 317-335.

Hoisch, T. (1990). Empirical calibration of six geobarometers for the mineral assemblage quartz + muscovite + biotite + plagioclase + garnet. *Contributions to Mineralogy and Petrology* **104**, 225-234.

Holland, T. & Blundy, J. (1994). Non-ideal interactions in calcic amphiboles and their bearing on amphibole thermometry. *Contributions in Mineralogy and Petrology* **116**, 433-447.

Hollings, P. & Kerrich, R. (1999). Trace element systematics of ultramafic and mafic volcanic rocks from the 3 Ga North Caribou greenstone belt, northwestern Superior Province. *Precambrian Research* **93**, 257-279.

Hoskin, P. W. O. & Schaltegger, U. (2003). The composition of zircon and igneous and metamorphic petrogenesis. *Reviews in Mineralogy & Geochemistry* **53**, 27-62.

Hyndman, D. W. (1981). Controls on source and depth of emplacement of granitic magma. *Geology* **9**, 244-249.

Iolite Users' Manual. (2012). url: http://iolite.earthsci.unimelb.edu.au/wiki/doku.php?id=manual_page. Last updated: 4 April, 2012

Irvine, T. N. & Baragar, W. R. A. (1971). A guide to the chemical classification of the common volcanic rocks. *The Canadian Journal of Earth Sciences* **8**, 523-548.

Isaac, C. (2008). Stable isotope (N, O, H) geochemistry, petrology and compositions of biotite of the Musselwhite Mine, Ontario: implications for mineralization. *Unpublished MSc. thesis*, Lakehead University 104 p.

Johannes, W. (1984). Beginning of melting in the granite system Qz-Or-Ab-An-H_2O. *Contributions to Mineralogy and Petrology* **86**, 264-273.

Johnson, M. C. & Rutherford, M. J. (1989). Experimental calibration of the aluminum-in-hornblende geobarometer with application to Long Valley Caldera (California) volcanic rocks. *Geology* **17**, 837-841.

Johnston, A. D. & Wyllie, P. J. (1988). Constraints on the origin of Archean trondhjemites based on phase relationships of Nûk gneiss with H_2O at 15 kbar. *Contributions to Mineralogy and Petrology* **100**, 35-46.

Kalbfleisch, T. (2012). Crustal-scale shear zones recording 400 M.Y. of tectonic activity in the North Caribou greenstone belt, western superior Province of Canada. *Unpublished MSc. thesis*, University of Ottawa 95 p.

Kalbfleisch, T., Duff, J., Schneider, D. A., Hattori, K. & Biczok, J. (2011). Evidence for 2.45 Ga tectonism recorded in the North Caribou greenstone belt, northwestern Ontario. *Geological Society of America Annual Meeting Abstracts with Programs* **43**, 471.

Kelsey, C. H. (1965). Calculation of the C.I.P.W. norm. *The Mineralogical Magazine* **34**, 276-282.

Kohn, M. J. & Spear, F. S. (1990). Two new geobarometers for garnet amphibolites, with applications to southeastern Vermont. *American Mineralogist* **75**, 89-96.

Leake, B. E., Woolley, A. R., Arps, C. E. S., Birch, W. D., Gilbert, M. C., Grice, J. D., Hawthorne, F. C., Kato, A., Kisch, H. J., Krivovichev, V. G., Linthout, K., Laird, J., Mandarino, J. A., Maresch, W. V., Nickel, E. H., Rock, N. M. S., Schumacher, J. C., Smith, D. C., Stephenson, N. C. N., Ungaretti, L., Whittaker, E. J. W. & Yuozhi, G. (1997). Nomenclature of amphiboles: report of the subcommittee on amphiboles of the international mineralogical association, commission on new minerals and mineral names. *The Canadian Mineralogist* **35**, 219-246.

Lin, S & Corfu, F. (2002). Structural setting and geochronology and auriferous quartz veins at the High Rock Island gold deposit, Northwestern Superior Province, Manitoba, Canada. *Economic Geology* **97**, 43-57.

Lin, S., Davis, D. W., Rotenberg, E., Corkery, M. T. & Bailes, A. H. (2006). Geological evolution of the northwestern Superior Province: Clues from geology, kinematics, and geochronology in the Gods Lake Narrows area, Oxford-Stull Terrane, Manitoba. *Canadian Journal of Earth Science* **43**, 749-765.

Ludwig, K. R. (2012). User's Manual for Isoplot 3.75: Geochronological Toolkit for Microsoft *Excel*. Berkeley Geochronology Center Special Publication No. 5.

Maniar, P. D. & Piccoli, P. M. (1989). Tectonic discrimination of granitoids. *Geological Society of America Bulletin* **101**, 635-643.

Martin, H., Smithies, R. H., Rapp, R., Moyen, J. –F. & Champion, D. (2005). An overview of adakite, tonalite-trondhjemite-granodiorite (TTG), and sanukitoid: relationships and some implications for crustal evolution. *Lithos* **79**, 1-24.

McBirney, A. R. (1993). *Igneous Petrology*: Jones and Bartlett Publishers, 511 p.

McDonough, W. F. & Sun, S. S. (1995). The composition of the Earth. *Chemical Geology* **120**, 223-253.

Miller, C. F. (1985). Are strongly peraluminous magmas derived from politic sedimentary sources? *Journal of Geology* **93**, 673-689.

Morse, S. A. (1984). Cation diffusion in plagioclase feldspar. *Science* **225**, 504-505.

Moyen, J. -F. & Martin, H. (2012). Forty years of TTG research. *Lithos* **148**, 312-336.

Naney, M. T. (1983). Phase equilibria of rock-forming ferromagnesian silicates in granitic systems. *American Journal of Science* **283**, 993-1033.

Ontario Geological Survey. (2011). 1: 250 000 scale bedrock geology of Ontario. *Ontario Geological Survey, Miscellaneous Release* **Data 126-Revision 1.**

Ontario Geological Survey. (1991). Bedrock Geology of Ontario, northern sheet. *Ontario Geological Survey Map* **2541**.

Otto, A. (2002). Ore forming processes in the BIF-hosted gold deposit Musselwhite Mine, Ontario, Canada. *Unpublished MSc. thesi*s, Freiberg University of Mining and Technology 86 p.

Paces, J. B. & Miller, J. D., Jr. (1993). Precise U-Pb ages of Duluth Complex and related mafic intrusions, northeastern Minnesota: Geochronological insights to physical, petrogenetic, paleomagnetic, and tectonomagmatic processes associated with the 1.1 Midcontinent Rift System. *Journal of Geophysical Research* **98B**, 13997-14013.

Parks, J., Lin, S., Davis, D. & Corkery, T. (2006). New high-precision U-Pb ages for the Island Lake greenstone belt, northwestern Superior Province: Implications for regional stratigraphy and the extent of the North Caribou Terrane. *Canadian Journal of Earth Sciences* **43**, 789-803.

Paton, C., Woodhead, J. D., Hellstrom, J. C., Hergt, J. M., Greig, A. & Maas, R. (2010). Improved laser ablation U-Pb zircon geochronology through robust downhole fractionation correction. *Geochemistry, Geophysics, Geosystems* **11**, Q0AA06.

Percival, J. A. (2007). Geology and Metallogeny of the Superior Province, Canada. In: Goodfellow, W. D. (ed.). *Mineral Deposits of Canada: A Synthesis of Major Deposit-Types, District Metallogeny, the Evolution of Geological Provinces, and Exploration Methods*. Geological Association of Canada, Mineral Deposits Divisions, Special Publication **5**, 903-928.

Percival, J. A., McNicoll, V. & Bailes, A. H. (2006*a*). Strike-slip juxtaposition of ca. 2.72 Ga juvenile arc and >2.98 Ga continent margin sequences and its implications for Archean terrane accretion, western Superior Province, Canada. *Canadian Journal of Earth Sciences* **43**, 895-927.

Percival, J. A., Sanborn-Barrie, M., Skulski, T., Stott, G. M., Helmstaedt, H. & White, D. J. (2006*b*). Tectonic evolution of the western Superior Province from NATMAP and Lithoprobe studies. *Canadian Journal of Earth Sciences* **43**, 1085-1117.

Phillips, G. N. & Powell, R. (2010). Formation of gold deposits: A metamorphic devolatilization model. *Journal of Metamorphic Geology* **28**, 689-718.

Phillips, G. N. & Powell, R. (2009). Formation of gold deposits: Review and evaluation of the continuum model. *Earth-Science Reviews* **94**, 1-21.

Pidgeon, R. T. (1992). Recrystallization of oscillatory zoned zircon: some geochronological and petrological implications. *Contributions to Mineralogy and Petrology* **110**, 463-472.

Pidgeon, R. T., O'Neil, J. R. & Silver, L. T. (1966). Uranium and lead isotopic stability in a metamict zircon under experimental hydrothermal conditions. Science **154**, 1538-1540.

Pidgeon, R. T., Nemchin, A. A. & Hitchen, G. J. (1998). Internal structures of zircon from Archean granites from the Darling Range batholith: implications for zircon stability and the interpretation of zircon U-Pb ages. *Contributions to Mineralogy and Petrology* **132** 288-299.

Piroshco, D. W., Breaks, F. W. & Osmani, I. A. (1989). The geology of gold prospects in the North Caribou Lake greenstone belt, District of Kenora, northwestern Ontario. *Ontario Geological Survey Open File Report* **5698**, 94 p.

Pitcher, W. S. (1993). On the rates of emplacement, crystallization and cooling. In: Pitcher, W. S. *The Nature and Origin of Granites*. Glasgow: Blackie Academic & Professional, 182-192.

Piwiniskii, A. J. (1968). Experimental studies of igneous rock series Central Sierra Nevada batholith, California. *Journal of Geology* **76**, 548-570.

Pollack, H. (1986). Cratonization and thermal evolution of the mantle. *Earth and Planetary Science Letters* **80**, 175-182.

Raase, P., Raith, M., Ackermand, D. & Lal, R. K. (1986). Progressive metamorphism of mafic rocks from greenschist to granulite facies in the Dharwar Craton of South India. *Journal of Geology* **94**, 261-282.

Rayer, N., Stern R. A. & Carr, S. D. (2005). Grain-scale variations in trace element composition of fluid-altered zircon, Acasta Gneiss Complex, northwestern Canada. *Contributions to Mineralogy and Petrology* **148**, 721-734.

Rubatto, D. (2002). Zircon trace element geochemistry: partitioning with garnet and the link between U-Pb ages and metamorphism. *Chemical Geology* **184**, 123-138.

Satterly, J. (1941). Geology of the Windigo-North Caribou Lakes Area. *Ontario Department of Mines Annual Reports* **48** (Part 9). 32 p.

Schaltegger, U. (2007). Hydrothermal zircon. *Elements* **3**, 51-52.

Scherer, E. E., Whitehouse, M. J. & Münker, C. (2007). Zircon as a monitor of crustal growth. *Elements* **3**, 19-24.

Schmidt, M. W. (1993). Phase relations and compositions in tonalite as a function of pressure: an experimental study at 650 ºC. *American Journal of Science* **293**, 1011-1060.

Schmidt, M. W. & Poli, S. (2004). Magmatic epidote. *Reviews in Mineralogy & Geochemistry* **56**, 399-430.

Schmidt, M. W. & Thompson, A. B. (1996). Epidote in calc-alkaline magmas: An experimental study of stability, phase relationships, and the role of epidote in magmatic evolution. *American Mineralogist* **81**, 462-474.

Scholz, C. H. (1988). The brittle-plastic transition and depth of seismic faulting. *Geologische Rundscau* **77**, 319-328.

Schwerdtner, W. M., Stott, G. M. & Sutcliffe, R. H. (1983). Strain patterns of crescentic granitoid plutons in the Archean greenstone terrain of Ontario. *Journal of Structural Geology* **5**, 419-430.

Scott, D. J. & St-Onge, M. R. (1995). Constraints of Pb closure temperature in titanite based on rocks from the Ungava orogen, Canada: Implications for U-Pb geochronology and P-T-t path determinations. *Geology* **23**, 1123-1126.

Shirey, S. B. & Hanson, G. N. (1984). Mantle-derived Archean monzodiorites and trachyandesites. *Nature* **310**, 222-224.

Spear, F. S. (1981). An experimental study of hornblende stability and compositional variability in amphibolite. *American Journal of Science* **281**, 697-734.

Stevenson, R. (1995). Crust and mantle evolution in the Late Archean: Evidence from a Sm-Nd isotopic study of the North Spirit Lake greenstone belt, northwestern Ontario, Canada. *Geological Society of America Bulletin* **107**, 1458-1467.

Stevenson, R. K., Henry, P. & Gariépy, C. (2009). Isotopic and geochemical evidence for differentiation and crustal contamination from granitoids of the Berens River subprovince, Superior Province, Canada. *Precambrian Research* **168**, 123-133.

Stevenson, R. K. & Turek, A. (1992). An isotopic study of the Island Lake Greenstone Belt, Manitoba: crustal evolution and progressive cratonization in the late Archean. *Canadian Journal of Earth Sciences* **29**, 2200-2210.

Stockwell, C. H. (1982). Proposals for time classification and correlation of Precambrian rocks and events in Canada and adjacent areas of the Canadian Shield, Part 1: A time classification of Precambrian rocks and events. *Geological Survey of Canada Paper* **80-19**, 135 p.

Stone, D. (2005). Geology of the Northern Superior Area, Ontario. *Ontario Geological Survey Open File Report 6140*. 94 p.

Stone, D. (2000). Temperature and pressure variations in suites of Archean felsic plutonic rocks, Berens River area, northwest Superior Province, Ontario, Canada. *The Canadian Mineralogist* **38**, 455-470.

Stott, G. M. & Biczok, J. (2010). North Caribou greenstone belt: Gold and its possible relation to the North Caribou pluton emplacement—A belt-wide contact-strain aureole? *Ontario Geological Survey, Open File Report* **6260**, 22-1-22-12.

Stott, G. M., Corkery, M. T., Percival, J. A., Simard, M. & Goutier, J. (2010). A Revised Terrane Subdivision of the Superior Province. *Ontario Geological Survey, Open File Report* **6260**, 20-1-20-10.

Streckeisen, A. (1976). To each plutonic rock its proper name. *Earth-Science Reviews* **12**, 1-33.

Thurston, P. C., Osmani, I. A. & Stone, D. (1991). Northwestern Superior Province: Review and terrane Analysis. In: Thurston, P. C., Williams, H. R., Sutsliffe, R. H. & Stott, G. M. (eds.). *Geology of Ontario, Ontario Geological Survey Special Volume 4, Part 1*. Toronto: Ministry of Northern Development and Mines, 81-142.

Thurston, P. C., Sage, R. P. & Siragusa, G. M. (1979). Geology of the Winisk Lake Area, District of Kenora, Patricia Portion. *Ontario Geological Survey Report* **193**, 169 p.

van der Laan, S. R. & Wyllie, P. J. (1992). Constraints of Archean Trondhjemite Genesis from Hydrous Crystallization Experiments on Nûk Gneiss at 10-17 kbar. *Journal of Geology* **100**, 57-68.

Wyman, D. A., Hollings, P. & Biczok, J. (2011). Crustal evolution in a cratonic nucleus: Granitoids and felsic volcanic rocks of the North Caribou Terrane, Superior Province Canada. *Lithos* **123**, 37-49.

Appendix A. Whole-rock XRF results from granitoids surrounding the NCGB

Analyses performed at Memorial University

	SiO_2	Al_2O_3	CaO	K_2O	MgO	MnO	Na_2O	P_2O_5	Fe_2O_3T	Zn	TiO_2	Ba	Ga	Ni
	wt%	wt%	wt%	wt%	wt%	wt%	wt%	wt%	wt%	ppm	wt%	ppm	ppm	ppm
01	62.18	15.53	3.57	1.93	2.55	0.05	4.35	0.19	3.40	28	0.51	686	18	9
02	77.29	15.94	0.78	4.91	0.05	0.01	4.35	0.02	0.53	< 6	0.06	203	22	< 4
05	76.00	15.53	1.50	5.31	< 0.03	0.01	4.27	0.01	0.35	27	0.12	239	17	< 4
08	72.88	18.09	0.25	8.33	< 0.03	0.01	3.45	0.02	0.15	< 6	< 0.008	< 40	28	12
09	65.82	16.49	2.77	2.64	2.09	0.03	4.44	0.13	2.26	18	0.32	1069	20	5
10	76.14	15.72	0.81	5.63	0.03	0.01	3.76	0.05	0.44	< 6	0.04	42	13	4
11	65.34	15.74	2.53	3.01	2.26	0.04	3.94	0.15	2.54	20	0.39	987	20	8
14	61.23	15.72	4.35	2.26	3.60	0.08	4.02	0.17	5.12	30	0.56	777	21	17
16	81.10	12.58	1.52	2.22	0.40	0.03	3.40	0.02	0.63	12	0.11	945	12	< 4
18	68.99	15.64	2.19	4.16	1.18	0.03	3.45	0.08	2.17	15	0.28	1094	17	< 4
19	72.03	15.55	1.01	5.15	0.50	0.02	3.05	0.06	1.97	10	0.22	1312	14	< 4
21	67.30	16.14	3.22	2.33	1.49	0.06	4.10	0.16	3.03	18	0.34	344	17	< 4
26	74.33	16.57	0.94	3.98	< 0.03	0.03	5.23	0.02	0.45	< 6	0.02	< 40	26	4
28	72.95	17.17	2.27	3.76	0.04	0.01	4.26	0.01	0.37	< 6	0.04	1690	16	< 4
29	65.11	16.40	3.33	1.52	1.86	0.04	5.70	0.10	2.48	21	0.29	856	21	6
31	68.96	16.46	2.41	2.33	1.10	0.02	5.25	0.11	1.86	21	0.30	730	20	< 4
32	72.51	16.81	0.61	4.68	< 0.03	0.09	5.22	0.06	0.38	< 6	0.01	< 40	33	12
35	78.24	14.13	1.09	0.49	< 0.03	0.10	6.53	0.02	0.61	< 6	0.03	48	15	< 4
36	63.68	16.56	3.45	1.47	2.36	0.07	4.57	0.17	3.84	30	0.44	617	20	12
37	88.22	9.55	0.15	3.25	< 0.03	0.02	2.88	0.04	0.49	< 6	0.01	49	20	6
38	73.42	15.10	1.66	2.32	0.32	0.03	4.90	0.02	1.21	6	0.17	883	16	< 4
40	66.03	15.69	3.23	1.53	1.42	0.03	4.52	0.11	2.83	13	0.36	402	18	< 4
41	64.92	15.62	3.27	1.39	1.46	0.04	4.47	0.10	3.03	17	0.38	267	18	< 4
42D	66.89	15.88	3.08	1.85	1.60	0.05	4.24	0.11	3.14	22	0.36	366	16	< 4
42l	78.32	16.69	2.23	3.50	0.10	0.01	4.09	0.02	0.41	< 6	0.04	1230	15	< 4
43	69.29	15.56	2.12	3.79	1.16	0.02	3.52	0.08	2.16	13	0.24	993	15	5
44	73.46	15.11	1.13	4.74	0.32	0.03	3.59	0.04	1.19	8	0.13	414	20	8
45	69.55	15.75	2.30	4.30	0.98	0.04	3.31	0.09	2.59	19	0.37	1242	18	6
46	64.85	15.82	3.15	2.17	1.63	0.04	4.03	0.13	3.26	23	0.41	543	20	< 4
47	68.80	15.78	2.46	1.83	1.36	0.07	4.24	0.09	2.86	19	0.34	303	19	5
48	71.26	16.17	1.62	4.52	0.40	0.03	3.71	0.04	1.06	9	0.12	734	19	< 4
49	70.70	16.38	2.82	1.11	0.58	0.02	5.20	0.04	1.25	6	0.15	267	18	< 4
50	74.39	16.38	1.14	4.41	< 0.03	0.01	4.62	0.01	0.56	< 6	0.05	41	27	< 4
51	64.35	16.40	2.71	3.90	1.84	0.05	3.74	0.29	3.58	33	0.69	2631	20	6
52	65.08	15.84	4.47	1.09	2.14	0.05	4.00	0.14	3.96	22	0.48	378	19	6

Appendix A. (cont)

Analyses performed at Memorial University

	Pb	Rb	Sr	Th	U	V	Y	Zr	Nb	Cr	Ce	S	Cl	Sc	Cu	As	Co	La	Nd	LOI
	ppm	ppm	ppm	ppm	ppm	ppm	ppm	ppm	ppm	ppm	ppm	ppm	ppm	ppm	ppm	ppm	ppm	ppm	ppm	wt%
01	16	41	762	9	< 4	51	7	160	6	28	93	167	64	< 7	13	< 15				
02	24	218	50	20	6	< 9	8	71	13	< 7	45	117	59	< 7	< 5	< 15				
05	41	188	69	24	< 4	9	14	98	33	< 7	62	207	194	< 7	18	< 15				
08	67	807	15	12	5	< 9	3	9	5	< 7	< 24	115	86	< 7	< 5	< 15				
09	19	83	662	5	< 4	34	3	107	2	20	60	115	58	< 7	< 5	< 15				
10	43	196	55	16	9	< 9	19	20	8	8	< 24	118	67	< 7	< 5	< 15				
11	18	75	594	10	4	38	3	117	3	23	63	149	81	< 7	< 5	< 15				
14	14	57	598	5	< 4	81	7	106	5	58	< 24	157	95	8	15	< 15				
16	16	57	193	13	< 4	< 9	21	102	9	10	63	111	< 38	< 7	< 5	15				
18	20	120	395	7	< 4	25	5	73	6	8	< 24	146	64	< 7	6	< 15				
19	23	178	151	23	5	9	5	188	5	< 7	74	120	115	< 7	< 5	< 15				
21	8	65	205	7	< 4	33	7	114	8	< 7	24	139	56	< 7	< 5	< 15				
26	42	192	20	16	18	< 9	44	54	3	< 7	< 24	130	66	< 7	< 5	< 15				
28	26	97	493	< 4	< 4	< 9	4	60	1	< 7	< 24	238	62	< 7	8	< 15				
29	12	24	871	4	< 4	37	6	125	4	20	54	333	38	< 7	7	< 15				
31	16	47	701	6	< 4	21	3	140	2	11	64	130	< 38	< 7	< 5	< 15				
32	31	371	12	14	13	< 9	45	31	37	< 7	< 24	114	75	< 7	< 5	< 15				
35	15	8	35	8	6	< 9	18	35	6	< 7	< 24	124	46	< 7	< 5	< 15				
36	12	356	535	11	< 4	59	7	125	4	23	< 24	218	< 38	< 7	14	< 15				
37	9	410	20	9	4	< 9	3	8	20	< 7	< 24	124	172	< 7	< 5	< 15				
38	19	69	291	19	< 4	< 9	6	87	6	< 7	86	121	< 38	< 7	< 5	< 15				
40	11	58	382	6	< 4	25	2	112	4	< 7	71	130	89	< 7	5	< 15				
41	8	48	281	< 4	< 4	24	3	121	4	8	42	166	139	< 7	< 5	< 15				
42D	10	66	266	< 4	< 4	27	3	119	6	11	46	168	205	< 7	< 5	< 15				
42l	14	57	274	< 4	< 4	< 9	< 1	68	< 1	< 7	< 24	157	127	< 7	< 5	< 15				
43	15	76	202	8	< 4	12	2	170	5	10	87	139	137	< 7	< 5	< 15				
44	30	228	90	20	5	< 9	13	94	13	< 7	69	123	53	9	< 5	< 15				
45	17	96	198	19	< 4	15	9	246	11	10	205	132	62	< 7	< 5	< 15				
46	12	59	425	8	< 4	35	4	142	5	15	98	161	69	< 7	8	< 15				
47	9	78	179	7	< 4	20	7	120	6	20	< 24	142	104	8	< 5	< 15				
48	35	123	270	9	5	< 9	4	73	5	< 7	< 24	136	103	< 7	< 5	< 15				
49	14	38	458	< 4	< 4	10	2	75	5	< 7	< 24	124	85	< 7	< 5	< 15				
50	37	147	40	20	11	< 9	4	100	7	< 7	< 24	121	62	8	< 5	< 15				
51	14	67	897	8	< 4	41	9	271	10	12	230	280	135	8	26	< 15				
52	8	22	327	< 4	< 4	45	9	144	5	20	54	152	150	9	5	< 15				

Appendix A. (cont)

Analyses performed at the University of Ottawa

	SiO_2	Al_2O_3	CaO	K_2O	MgO	MnO	Na_2O	P_2O_5	Fe_2O_3T	Zn	TiO_2	Ba	Ga	Ni
	wt%	wt%	wt%	wt%	wt%	wt%	wt%	wt%	wt%	ppm	wt%	ppm	ppm	ppm
53	72.80	14.78	1.52	4.76	0.53	0.03	3.37	0.05	2.05	27	0.21	1041	9	22
54	72.78	13.52	1.60	2.99	0.39	0.02	3.86	0.02	2.15	31	0.23	98	5	42
55	70.59	15.45	3.03	0.89	0.61	0.02	5.04	0.04	1.51	34	0.18	81	9	< 4
56	71.52	14.54	2.18	2.75	0.54	0.04	4.07	0.06	2.07	38	0.23	693	7	8
58	68.23	16.00	3.50	1.00	0.74	0.03	4.89	0.11	2.67	44	0.30	401	1	11
59	69.75	16.05	3.65	0.86	0.93	0.03	4.52	0.11	2.91	45	0.34	359	10	< 4
60	73.18	14.69	1.85	2.04	0.24	0.02	5.08	0.02	0.86	31	0.08	597	8	< 4
61	72.28	14.57	1.84	2.03	0.24	0.02	5.06	0.02	0.71	31	0.08	612	11	12
62	68.71	16.26	3.69	0.79	1.00	0.02	4.64	0.12	2.88	46	0.41	783	10	12
63	64.67	16.86	4.39	0.61	1.22	0.05	5.09	0.20	3.87	56	0.49	405	7	8
64	61.01	18.81	5.89	0.29	1.69	0.05	5.64	0.24	4.20	56	0.62	254	11	16
65	67.43	17.58	4.15	0.42	0.61	0.03	5.35	0.10	2.00	29	0.34	290	12	< 4
66	57.88	17.35	6.98	0.98	3.29	0.09	4.42	0.12	6.63	68	0.60	260	8	49
67	72.03	14.09	0.75	7.64	0.16	0.01	2.26	0.03	0.68	11	0.07	2587	3	< 4
69	69.68	15.50	3.52	0.86	0.93	0.03	4.49	0.06	2.44	42	0.30	299	10	6
70	73.30	14.42	0.75	3.66	0.22	0.01	4.20	0.05	0.85	17	0.18	527	16	< 4
71D	70.52	15.67	3.36	1.77	0.96	0.05	4.68	0.13	3.31	55	0.37	508	12	28
71P	65.89	14.05	1.41	2.58	0.76	0.04	4.88	0.09	2.18	31	0.28	488	9	< 4
72	73.57	14.81	1.10	2.27	0.27	0.02	4.58	0.06	0.82	22	0.22	225	14	< 4
73	46.86	15.48	7.23	2.87	4.29	0.18	2.19	0.54	14.37	155	1.42	596	11	27
74A	74.19	14.51	2.12	1.36	0.47	0.03	5.13	0.04	1.65	31	0.24	1004	8	< 4
74B	74.13	13.15	0.95	3.85	0.10	0.01	4.07	0.02	0.52	8	0.05	296	4	< 4
75	69.72	15.60	2.48	2.36	0.69	0.03	4.68	0.07	2.23	40	0.24	622	11	5
T-06	69.49	14.86	1.07	2.69	1.04	0.05	5.07	0.09	2.97	24	0.33	702	9	7
T-07	68.67	15.70	2.59	2.40	1.06	0.05	4.44	0.14	3.45	46	0.39	693	10	4
T-25	72.49	14.57	0.35	8.49	0.05	0.05	2.56	0.01	0.18	5	0.02	113	3	< 4

Appendix A. (cont)

Analyses performed at the University of Ottawa

	Pb	Rb	Sr	Th	U	V	Y	Zr	Nb	Cr	Ce	S	Cl	Sc	Cu	As	Co	La	Nd	LOI
	ppm	ppm	ppm	ppm	ppm	ppm	ppm	ppm	ppm	ppm	ppm	ppm	ppm	ppm	ppm	ppm	ppm	ppm	ppm	wt%
53	39	99	191	42	9	11	3	167	3	6	106						4	55	35	1.53
54	79	157	101	477	80	6	13	478	11	39	63						3	< 1	28	1.74
55	27	46	322	20	7	17	< 2	123	2	6	26						7	< 1	15	2.57
56	26	132	233	23	5	23	14	134	6	33	59						9	42	17	2.03
58	20	23	518	14	5	27	< 2	138	2	11	52						10	19	10	1.37
59	13	24	396	8	1	31	< 2	135	3	4	38						12	1	7	1.76
60	30	38	357	11	6	7	< 2	60	1	5	< 1						2	1	< 4	1.09
61	23	36	350	9	4	2	< 2	61	2	18	1						3	1	4	1.73
62	1	18	538	1	< 1	41	< 2	151	1	9	25						9	21	6	1.36
63	18	11	593	11	5	47	< 2	113	4	14	68						11	46	26	1.13
64	13	3	370	14	3	77	13	96	10	9	41						18	5	23	1.34
65	6	2	519	3	< 1	21	< 2	130	1	5	18						6	10	12	1.61
66	24	24	199	19	7	155	16	136	5	65	31						30	32	18	1.77
67	44	108	301	26	10	17	3	80	3	1	16						2	< 1	14	2.40
69	8	17	382	10	3	25	< 2	119	4	16	36						9	25	10	1.60
70	28	137	390	26	17	10	< 2	101	6	2	64						4	21	27	2.48
71D	30	68	341	25	8	38	2	172	5	21	71						10	50	22	1.47
71P	26	112	197	22	9	22	5	124	7	8	36						8	10	21	2.86
72	31	142	345	23	12	9	5	167	16	3	104						1	31	25	2.25
73	11	80	717	3	1	232	26	135	14	37	84						49	38	40	3.71
74A	17	44	393	27	7	10	6	187	6	< 1	157						4	86	46	1.65
74B	44	74	116	28	13	3	8	33	5	< 1	< 1						2	< 1	< 4	1.46
75	18	68	444	10	3	25	2	112	3	6	50						9	15	13	1.44
T-06	15	114	172	22	10	26	6	118	4	9	31						12	28	18	1.79
T-07	22	100	317	18	5	37	2	138	6	5	39						15	23	20	1.68
T-25	75	404	43	25	16	< 2	28	23	21	6	10						1	5	8	1.00

Notes:
< x: Below the detection limit (x)

Appendix B. Whole-rock ICP-MS results from granitoids surrounding the NCGB

	Cu	Ni	Cr	Co	Se	Zn	Pb	Ag	As	Sn	Sb	Mo	B	Li	Be	V	Mn	Ga
	ppm	ppm	ppm	ppm	ppm	ppm	ppm	ppm	ppm	ppm	ppm	ppm	ppm	ppm	ppm	ppm	ppm	ppm
01	13	10	< 30	7.3	< 0.8	70	14.9	< 10	< 5	1.6	< 2	< 1	< 10	69	< 3	62	313	18.7
02	< 2	60	< 30	0.4	1.9	< 30	28.7	< 10	< 5	1.7	< 2	< 1	20	16	< 3	19	136	20.2
05	28	< 10	< 30	2.2	< 0.8	60	57.0	30	18	1.0	< 2	7	40	6	< 3	25	80	16.2
08	< 2	< 10	< 30	< 0.2	< 0.8	< 30	67.9	< 10	< 5	1.1	< 2	< 1	20	9	< 3	27	61	23.1
09	< 2	< 10	< 30	5.4	< 0.8	50	24.7	< 10	< 5	0.7	< 2	< 1	10	81	< 3	61	224	19.1
10	< 2	< 10	< 30	0.3	< 0.8	< 30	56.9	< 10	< 5	2.0	< 2	< 1	20	12	< 3	37	76	14.3
11	2	80	< 30	6.0	< 0.8	50	20.1	< 10	< 5	0.5	< 2	68	40	93	< 3	64	249	18.9
14	16	40	40	14.3	1.0	80	13.6	< 10	< 5	1.1	< 2	< 1	30	31	< 3	117	574	19.0
16	2	140	< 30	1.4	2.0	40	18.9	< 10	9	1.6	< 2	< 1	20	12	< 3	33	241	11.6
18	6	< 10	< 30	4.9	< 0.8	50	27.1	< 10	< 5	1.5	< 2	< 1	30	70	< 3	50	274	17.0
19	< 2	< 10	< 30	1.5	< 0.8	40	24.8	< 10	< 5	1.2	< 2	< 1	20	34	< 3	18	152	14.5
21	2	< 10	< 30	5.6	< 0.8	50	11.6	< 10	12	1.5	< 2	< 1	< 10	52	< 3	48	383	17.0
26	5	140	< 30	0.3	0.8	< 30	56.8	< 10	< 5	3.0	< 2	< 1	10	7	< 3	16	348	21.5
28	9	< 10	< 30	1.2	1.1	< 30	30.0	< 10	8	0.6	< 2	< 1	30	20	< 3	18	100	15.3
29	8	< 10	< 30	5.7	< 0.8	60	17.1	< 10	< 5	1.4	< 2	< 1	30	21	< 3	60	273	19.2
31	< 2	< 10	< 30	3.9	0.9	60	19.3	< 10	< 5	1.0	< 2	< 1	10	72	< 3	40	167	19.7
32	< 2	< 10	< 30	0.2	0.8	< 30	37.2	< 10	< 5	4.3	< 2	< 1	40	16	< 3	11	1300	27.1
35	< 2	< 10	< 30	0.8	1.8	< 30	31.7	< 10	24	0.7	< 2	< 1	30	8	< 3	19	1230	14.2
36	13	20	< 30	9.1	0.8	80	12.4	< 10	< 5	2.7	< 2	< 1	20	251	4	79	563	19.0
37	< 2	< 10	< 30	< 0.2	< 0.8	< 30	9.2	< 10	< 5	4.0	< 2	< 1	20	< 3	< 3	13	158	16.9
38	3	< 10	< 30	0.9	1.1	30	18.8	< 10	18	1.2	< 2	< 1	40	41	< 3	13	215	14.6
40	8	< 10	< 30	5.0	1.5	40	13.6	< 10	< 5	< 0.5	< 2	< 1	< 10	18	< 3	8	201	17.6
41	< 2	< 10	< 30	4.9	1.6	50	8.6	< 10	< 5	< 0.5	< 2	< 1	10	40	< 3	10	278	17.8
42D	8	< 10	< 30	5.4	2.0	60	11.3	< 10	< 5	< 0.5	< 2	< 1	20	40	< 3	13	315	18.5
42l	7	< 10	< 30	0.9	< 0.8	< 30	15.2	< 10	< 5	5.8	< 2	< 1	20	5	< 3	< 5	104	13.4
43	14	100	560	4.0	1.8	50	14.4	< 10	< 5	1.3	< 2	< 1	10	24	< 3	< 5	195	16.1
44	< 2	< 10	< 30	1.2	1.8	30	34.0	< 10	< 5	< 0.5	< 2	< 1	30	81	< 3	< 5	251	18.4
45	4	< 10	< 30	3.9	1.1	60	16.8	< 10	< 5	48.8	< 2	< 1	60	74	< 3	6	260	19.0
46	7	< 10	< 30	5.9	1.8	70	9.4	< 10	< 5	< 0.5	< 2	< 1	20	45	< 3	17	321	19.2
47	< 2	< 10	< 30	4.6	1.4	50	8.0	< 10	< 5	< 0.5	< 2	< 1	40	32	< 3	8	437	17.3
48	4	40	< 30	1.7	2.3	30	47.4	< 10	< 5	22.8	< 2	8	30	30	< 3	< 5	184	16.2
49	3	< 10	< 30	1.7	< 0.8	30	18.5	< 10	< 5	< 0.5	< 2	< 1	20	40	< 3	< 5	142	18.0
50	< 2	< 10	< 30	< 0.2	1.8	< 30	47.5	< 10	40	1.2	< 2	< 1	40	12	3	< 5	102	22.6
51	29	< 10	< 30	7.5	1.4	80	13.6	< 10	< 5	8.6	< 2	< 1	10	21	< 3	29	342	20.8
52	7	< 10	< 30	8.1	1.7	50	4.7	< 10	< 5	< 0.5	< 2	< 1	20	34	< 3	33	353	18.1

Appendix B. (cont)

	Ge	Rb	Sr	Y	Nb	Cs	Ba	La	Ce	Pr	Nd	Sm	Eu	Gd	Tb	Dy	Ho	Er
	ppm	ppm	ppm	ppm	ppm	ppm	ppm	ppm	ppm	ppm	ppm	ppm	ppm	ppm	ppm	ppm	ppm	ppm
01	2.4	43.5	754	7.4	4.5	1.5	610	15.3	42.2	4.1	14.8	2.8	0.7	2.0	0.3	1.5	0.3	0.9
02	2.1	233.0	56	9.4	12.0	5.2	210	8.9	19.6	2.3	8.0	2.2	0.2	1.9	0.3	1.8	0.3	1.0
05	1.6	199.0	97	14.2	25.9	2.2	274	28.4	57.3	6.4	21.1	4.3	0.7	3.9	0.6	3.2	0.5	1.2
08	2.4	847.0	15	3.7	4.9	14.1	9	1.7	2.7	0.3	0.9	0.3	< 0.1	0.4	< 0.1	0.6	< 0.2	0.3
09	1.9	88.0	660	3.6	< 2.4	5.4	944	21.5	40.8	4.3	13.9	2.0	0.6	1.4	0.1	0.7	< 0.2	0.4
10	1.8	216.0	64	21.3	6.0	3.7	52	6.0	11.8	1.3	4.3	1.5	0.2	2.1	0.5	3.4	0.7	1.9
11	1.8	78.3	610	3.8	< 2.4	4.8	863	20.8	41.7	4.3	14.2	2.1	0.6	1.4	0.1	0.8	< 0.2	0.3
14	2.7	60.0	612	7.9	3.6	1.5	737	25.3	49.2	5.7	20.1	3.4	1.0	2.5	0.3	1.6	0.3	0.8
16	1.9	62.9	214	21.0	6.2	1.5	1010	37.1	68.1	7.1	21.5	3.6	0.5	2.9	0.4	3.1	0.7	2.2
18	1.6	132.0	415	6.0	4.4	4.4	1040	8.9	17.0	2.0	7.3	1.4	0.3	1.2	0.2	1.2	0.2	0.7
19	1.9	184.0	156	4.6	3.6	5.8	1190	34.2	61.5	5.8	17.0	2.5	0.5	1.5	0.2	0.8	< 0.2	0.5
21	2.2	66.7	210	9.1	6.6	1.7	304	5.8	11.7	1.2	4.1	1.2	0.4	1.3	0.2	1.6	0.3	1.0
26	2.6	207.0	25	56.3	2.4	1.3	13	7.8	16.1	1.9	7.1	2.9	0.1	4.4	1.0	7.5	1.8	5.6
28	2.2	107.0	520	3.4	< 2.4	1.7	1750	5.0	9.2	1.0	3.7	0.8	0.4	0.6	< 0.1	0.6	< 0.2	0.4
29	2.6	27.5	902	7.1	3.8	1.3	746	24.5	50.6	5.8	19.7	3.2	0.8	2.3	0.2	1.3	0.2	0.7
31	2.5	52.3	720	3.7	< 2.4	1.5	706	27.0	50.1	5.5	18.1	2.9	0.7	1.9	0.2	0.8	< 0.2	0.4
32	3.3	402.0	24	63.0	32.2	8.5	17	12.5	24.9	3.0	11.0	3.9	< 0.1	4.6	1.1	8.4	1.9	6.8
35	2.8	9.4	45	22.0	4.3	0.7	55	7.7	17.4	2.0	6.3	1.8	0.1	1.9	0.4	3.1	0.7	2.2
36	2.7	396.0	553	6.9	4.3	72.5	619	20.2	43.5	4.1	13.3	2.1	0.7	1.5	0.2	1.3	0.2	0.7
37	3.4	445.0	22	2.9	15.7	10.3	50	1.5	3.1	0.4	1.6	0.6	< 0.1	0.6	< 0.1	0.5	< 0.2	0.2
38	2.8	75.6	323	7.1	4.3	4.1	838	46.3	92.6	9.1	27.3	4.0	0.9	2.5	0.3	1.5	0.3	0.7
40	2.1	63.5	399	2.5	< 2.4	1.5	357	30.8	57.3	5.3	16.3	2.4	0.6	1.4	0.1	0.5	< 0.2	0.2
41	1.9	53.5	299	4.0	3.0	1.7	208	11.0	23.3	2.2	7.1	1.3	0.5	1.1	0.1	0.8	< 0.2	0.4
42D	2.1	76.6	287	3.1	4.6	1.8	334	22.1	38.4	3.9	12.3	1.8	0.5	1.3	0.1	0.7	< 0.2	0.3
42l	1.3	60.0	282	0.6	< 2.4	0.4	1260	6.3	11.0	1.1	3.6	0.5	0.4	0.4	< 0.1	< 0.3	< 0.2	< 0.1
43	2.0	82.9	216	2.7	3.5	0.5	910	23.0	46.5	4.2	12.9	1.9	0.5	1.3	0.1	0.6	< 0.2	0.3
44	2.1	245.0	94	13.3	11.6	6.3	386	13.5	30.5	2.7	8.4	1.8	0.2	1.7	0.3	2.1	0.4	1.3
45	2.8	104.0	211	10.2	9.7	4.1	1140	80.8	140.0	14.7	42.6	5.4	0.8	3.5	0.3	1.9	0.3	1.0
46	2.3	68.4	444	5.0	3.6	1.1	467	15.7	36.7	3.2	10.6	1.9	0.6	1.4	0.2	1.0	< 0.2	0.5
47	2.2	84.7	186	7.8	4.8	3.3	257	7.5	14.6	1.4	4.4	0.9	0.4	1.0	0.2	1.3	0.3	0.8
48	1.7	131.0	281	4.4	2.9	1.9	674	12.9	23.9	2.5	8.0	1.4	0.3	1.1	0.1	0.8	< 0.2	0.4
49	1.4	43.4	474	3.0	3.4	1.6	243	6.6	15.0	1.2	3.7	0.7	0.5	0.6	< 0.1	0.5	< 0.2	0.3
50	2.1	152.0	38	3.6	5.6	1.9	47	4.7	11.4	1.5	5.5	1.3	0.3	1.0	0.1	0.6	< 0.2	0.4
51	3.5	70.8	895	11.4	9.4	0.7	2530	99.4	200.0	23.7	77.8	10.5	2.2	6.2	0.5	2.5	0.4	1.1
52	2.4	24.4	344	10.4	3.4	1.2	329	12.8	24.8	3.0	11.6	2.5	0.9	2.4	0.3	2.0	0.4	1.1

Appendix B. (cont)

	Tm	Yb	Hf	Ta	W	Tl	Bi	Th	U	Al	Ca	Fe	K	Mg	P	S	Si	Ti
	ppm	ppm	ppm	ppm	ppm	ppm	ppm	ppm	ppm	%	%	%	%	%	%	%	%	%
01	0.1	1.1	< 10	0.7	< 0.7	0.7	< 2	7.4	1.5	8.45	2.44	1.98	1.4	0.79	0.063	0.01	31.5	0.21
02	0.2	1.1	< 10	1.2	1.0	3.5	< 2	18.8	6.0	7.12	0.53	0.43	3.8	0.06	0.008	< 0.01	31.8	0.04
05	0.2	1.0	< 10	1.6	3.7	2.6	< 2	24.3	4.1	7.21	0.77	0.23	4.4	0.04	0.005	0.02	31.1	0.06
08	< 0.1	0.3	< 10	1.9	< 0.7	12.6	5	2.9	1.7	8.18	0.16	0.09	6.8	0.01	0.015	< 0.01	29.4	< 0.01
09	< 0.1	0.3	< 10	< 0.2	2.2	1.4	< 2	7.4	2.2	8.25	1.85	1.37	1.8	0.51	0.046	< 0.01	32.3	0.16
10	0.3	2.4	< 10	1.0	0.9	2.9	< 2	13.8	7.9	7.13	0.56	0.32	4.5	0.04	0.021	< 0.01	29.8	0.02
11	< 0.1	0.4	< 10	< 0.2	< 0.7	1.2	< 2	10.4	2.4	8.06	1.82	1.54	2.1	0.59	0.051	0.02	32.1	0.18
14	0.1	0.8	< 10	0.3	< 0.7	1.0	< 2	5.3	1.4	8.84	3.08	3.37	1.8	1.35	0.069	0.04	30.0	0.33
16	0.3	2.3	< 10	0.6	1.3	0.8	< 2	14.5	3.2	5.64	0.84	0.40	1.7	0.16	0.009	0.01	32.4	0.07
18	< 0.1	0.7	< 10	1.0	1.0	1.9	< 2	6.4	4.5	7.62	1.58	1.55	3.3	0.43	0.031	< 0.01	32.7	0.13
19	< 0.1	0.5	< 10	0.6	1.0	2.4	< 2	26.6	3.9	7.09	0.69	1.28	3.8	0.20	0.028	< 0.01	33.1	0.11
21	0.1	1.0	< 10	0.7	2.9	0.8	< 2	5.3	1.3	7.83	2.21	1.92	1.7	0.50	0.053	0.02	31.9	0.18
26	0.9	7.0	< 10	0.3	0.9	2.8	< 2	16.4	13.8	7.40	0.64	0.33	3.0	0.03	0.007	0.01	32.8	< 0.01
28	< 0.1	0.5	< 10	< 0.2	< 0.7	1.3	< 2	2.1	1.0	7.90	1.55	0.23	2.8	0.07	0.007	0.02	29.1	0.02
29	< 0.1	0.7	< 10	0.4	1.8	0.4	< 2	6.9	1.4	8.52	2.38	1.58	1.1	0.62	0.041	0.05	30.9	0.16
31	< 0.1	0.3	< 10	0.2	0.7	1.0	< 2	6.3	12.2	8.00	1.66	1.19	1.8	0.42	0.045	< 0.01	32.7	0.17
32	1.3	10.8	< 10	8.6	< 0.7	5.8	6	12.6	9.9	7.76	0.44	0.37	3.7	0.02	0.022	< 0.01	30.8	< 0.01
35	0.4	2.9	< 10	1.0	1.8	0.1	< 2	8.9	7.4	6.36	0.71	0.47	0.3	0.05	0.008	< 0.01	32.8	0.02
36	0.1	0.8	< 10	1.1	< 0.7	7.7	< 2	7.9	1.4	8.39	2.40	2.65	1.2	0.87	0.072	0.03	31.1	0.24
37	< 0.1	0.3	< 10	6.5	1.8	6.4	< 2	4.7	1.9	3.91	0.10	0.37	2.4	0.02	0.014	< 0.01	35.9	< 0.01
38	0.1	0.8	< 10	0.4	< 0.7	1.0	< 2	25.7	2.1	7.07	1.13	0.75	1.6	0.17	0.010	< 0.01	30.4	0.09
40	< 0.1	0.2	< 10	< 0.2	< 0.7	0.9	< 2	11.4	0.2	8.07	2.29	1.85	1.1	0.46	0.039	0.02	32.3	0.17
41	< 0.1	0.4	< 10	0.3	2.1	0.7	< 2	2.1	0.3	8.19	2.43	1.82	0.9	0.45	0.038	0.01	32.6	0.17
42D	< 0.1	0.3	< 10	0.4	< 0.7	1.1	< 2	6.2	0.4	8.17	2.20	1.98	1.4	0.52	0.043	0.01	32.8	0.17
42l	< 0.1	0.1	< 10	< 0.2	< 0.7	0.7	< 2	2.4	0.8	7.73	1.52	0.29	2.7	0.07	0.008	0.01	35.0	0.02
43	< 0.1	0.3	< 10	0.4	1.1	1.0	< 2	11.6	0.5	7.70	1.48	1.30	2.9	0.36	0.024	0.03	32.4	0.11
44	0.2	1.5	< 10	2.1	< 0.7	3.4	< 2	22.1	4.0	7.43	0.80	0.77	3.7	0.13	0.012	< 0.01	34.8	0.06
45	0.2	1.2	< 10	4.5	3.8	1.6	3	20.7	1.8	7.95	1.55	1.76	3.4	0.39	0.041	< 0.01	32.7	0.20
46	< 0.1	0.5	< 10	0.2	< 0.7	0.9	< 2	6.2	0.5	8.38	2.34	2.14	1.6	0.54	0.046	0.01	31.9	0.22
47	0.1	1.0	< 10	0.4	1.6	1.0	< 2	6.1	1.3	7.83	1.71	1.87	1.4	0.44	0.033	0.01	31.0	0.16
48	< 0.1	0.4	< 10	0.4	< 0.7	1.6	< 2	8.1	2.4	7.69	1.18	0.71	3.5	0.16	0.018	< 0.01	32.8	0.06
49	< 0.1	0.3	< 10	0.6	< 0.7	0.6	< 2	3.6	0.8	8.08	2.05	0.77	0.8	0.21	0.013	< 0.01	32.3	0.07
50	< 0.1	0.5	< 10	0.4	3.7	2.1	< 2	20.5	7.7	7.28	0.77	0.51	3.2	0.02	< 0.005	< 0.01	33.7	0.03
51	0.1	0.9	< 10	3.9	1.9	1.0	< 2	10.3	1.1	8.33	1.90	2.62	3.1	0.68	0.113	0.03	30.8	0.40
52	0.1	1.1	< 10	0.2	< 0.7	0.3	< 2	0.8	0.3	8.46	3.33	2.54	0.8	0.74	0.055	0.01	31.1	0.23

Appendix B. (cont)

	Cu	Ni	Cr	Co	Se	Zn	Pb	Ag	As	Sn	Sb	Mo	B	Li	Be	V	Mn	Ga
	ppm	ppm	ppm	ppm	ppm	ppm	ppm	ppm	ppm	ppm	ppm	ppm	ppm	ppm	ppm	ppm	ppm	ppm
53	< 2	< 10	< 30	3.6	< 0.8	30	24.5	< 10	< 5	< 0.5	< 2	< 1	< 10	20	< 3	< 5	184	14.9
54	10	< 10	< 30	2.3	1.6	30	73.9	< 10	< 5	1.5	< 2	< 1	20	21	< 3	< 5	173	19.4
55	4	< 10	< 30	3.4	1.7	40	11.7	< 10	< 5	< 0.5	< 2	< 1	< 10	36	< 3	< 5	159	19.1
56	< 2	< 10	< 30	3.7	1.4	40	20.7	< 10	< 5	0.9	< 2	< 1	< 10	74	< 3	< 5	273	17.1
58	2	< 10	< 30	4.8	< 0.8	60	5.4	< 10	< 5	4.3	2800	< 1	20	23	< 3	< 5	233	18.4
59	< 2	< 10	< 30	6.7	1.7	50	4.8	< 10	< 5	< 0.5	< 2	< 1	< 10	8	< 3	< 5	239	17.6
60	< 2	< 10	< 30	0.5	< 0.8	30	13.8	< 10	< 5	< 0.5	< 2	< 1	< 10	12	< 3	< 5	117	17.0
61	5	10	< 30	10.5	1.9	70	7.3	< 10	< 5	1.2	< 2	< 1	< 10	23	< 3	25	439	20.2
62	14	10	< 30	6.4	< 0.8	50	3.7	< 10	< 5	1.3	< 2	< 1	< 10	10	< 3	7	164	17.6
63	25	< 10	< 30	7.0	1.9	60	4.2	< 10	< 5	1.0	< 2	< 1	< 10	4	< 3	6	369	18.8
64	6	10	< 30	11.7	< 0.8	60	8.3	< 10	< 5	1.4	< 2	< 1	< 10	< 3	< 3	45	396	21.2
65	18	10	< 30	4.3	< 0.8	40	6.1	10	< 5	1.2	< 2	< 1	< 10	3	< 3	< 5	198	18.4
66	52	60	40	20.9	1.9	90	6.0	< 10	< 5	0.8	< 2	< 1	< 10	9	< 3	144	654	17.9
67	17	< 10	< 30	1.0	1.7	< 30	20.4	< 10	< 5	< 0.5	< 2	< 1	< 10	< 3	< 3	< 5	54	14.0
69	< 2	< 10	< 30	6.1	2.7	40	3.9	< 10	< 5	< 0.5	< 2	< 1	20	22	< 3	< 5	221	16.9
70	37	< 10	< 30	0.6	< 0.8	< 30	26.7	< 10	< 5	2.6	544	< 1	30	39	4	< 5	63	23.9
71D	15	< 10	< 30	7.0	1.9	60	10.9	< 10	< 5	0.8	< 2	< 1	< 10	58	< 3	8	348	19.6
71P	5	20	< 30	4.7	1.1	30	8.4	< 10	< 5	0.5	< 2	< 1	< 10	28	< 3	< 5	284	16.4
72	< 2	< 10	< 30	0.6	1.4	< 30	30.3	< 10	< 5	1.1	< 2	< 1	10	35	5	< 5	104	22.3
73	80	50	< 30	42.7	2.3	170	13.3	< 10	< 5	2.0	< 2	< 1	< 10	44	< 3	261	1330	22.2
74A	4	< 10	< 30	2.3	< 0.8	40	15.9	< 10	< 5	2.8	< 2	< 1	< 10	< 3	< 3	< 5	192	16.0
74B	< 2	< 10	< 30	0.4	< 0.8	< 30	25.7	< 10	< 5	1.5	< 2	< 1	< 10	< 3	< 3	< 5	58	16.4
75	9	< 10	< 30	4.5	1.6	40	18.6	< 10	< 5	< 0.5	< 2	< 1	< 10	27	< 3	37	240	17.8
T-06	6	10	100	6.3	< 0.8	30	4.9	< 10	< 5	4.7	< 2	< 1	< 10	29	< 3	< 5	366	15.8
T-07	10	< 10	< 30	8.4	< 0.8	50	12.8	< 10	< 5	2.6	< 2	< 1	< 10	18	< 3	11	379	18.2
T-25	14	< 10	< 30	0.4	2.1	< 30	51.1	< 10	< 5	3.0	< 2	< 1	< 10	< 3	< 3	< 5	329	19.2

Appendix B. (cont)

	Ge	Rb	Sr	Y	Nb	Cs	Ba	La	Ce	Pr	Nd	Sm	Eu	Gd	Tb	Dy	Ho	Er
	ppm	ppm	ppm	ppm	ppm	ppm	ppm	ppm	ppm	ppm	ppm	ppm	ppm	ppm	ppm	ppm	ppm	ppm
53	1.1	96.4	208	6.0	2.6	0.8	1050	47.2	87.6	8.8	29.7	3.8	0.8	2.2	0.3	1.2	0.2	0.6
54	0.9	154.0	108	17.7	18.3	1.4	118	12.2	54.6	5.8	23.9	6.8	0.5	4.4	0.7	3.5	0.7	2.1
55	< 0.7	44.1	354	1.2	< 2.4	1.0	92	22.7	34.6	3.5	10.5	1.1	0.3	0.5	< 0.1	< 0.3	< 0.2	0.1
56	1.3	139.0	259	16.5	4.4	3.5	715	38.9	63.3	7.2	23.9	3.6	0.7	2.9	0.4	2.0	0.4	1.0
58	< 0.7	21.5	583	2.9	< 2.4	0.6	427	23.1	39.7	4.3	15.0	1.9	0.7	1.2	0.1	0.6	< 0.2	0.3
59	< 0.7	23.7	426	3.7	< 2.4	0.2	355	11.6	20.8	2.3	8.0	1.2	0.7	0.8	0.1	0.6	< 0.2	0.4
60	< 0.7	35.4	381	1.3	< 2.4	1.1	642	3.3	6.5	0.8	3.0	0.6	0.2	0.4	< 0.1	< 0.3	< 0.2	0.1
61	1.1	47.2	531	7.6	< 2.4	0.9	600	24.4	51.3	4.5	16.0	2.6	0.8	1.9	0.3	1.6	0.3	0.8
62	< 0.7	18.5	588	2.3	< 2.4	0.5	804	19.0	37.2	3.4	12.1	1.3	1.1	0.8	< 0.1	0.4	< 0.2	0.2
63	0.9	8.3	654	3.3	< 2.4	< 0.1	429	31.6	55.9	5.9	20.0	2.4	1.2	1.4	0.1	0.7	< 0.2	0.4
64	1.8	0.9	399	15.8	8.1	< 0.1	250	19.5	41.4	5.1	20.5	4.2	1.3	3.5	0.6	3.1	0.6	1.6
65	< 0.7	2.1	592	1.6	< 2.4	< 0.1	297	9.8	14.9	1.5	5.2	0.7	1.0	0.5	< 0.1	< 0.3	< 0.2	0.2
66	2.0	18.7	216	16.0	3.1	0.3	267	9.9	23.8	3.0	12.4	2.6	0.8	2.3	0.4	2.7	0.6	1.7
67	< 0.7	110.0	326	4.7	< 2.4	0.9	2630	13.1	26.3	2.9	10.3	1.9	0.7	1.1	0.2	0.9	< 0.2	0.4
69	< 0.7	15.8	414	2.1	< 2.4	0.6	305	11.0	20.8	1.9	6.3	0.8	0.6	0.6	< 0.1	0.4	< 0.2	0.2
70	< 0.7	137.0	416	1.4	4.9	2.6	551	15.0	33.7	3.9	13.7	1.8	0.5	0.7	< 0.1	< 0.3	< 0.2	0.1
71D	1.4	66.7	380	5.9	4.7	1.8	548	40.7	65.6	6.8	21.7	2.6	0.8	1.7	0.2	1.1	0.2	0.6
71P	0.7	112.0	211	6.1	5.2	0.8	503	19.2	37.7	3.6	12.1	1.9	0.5	1.4	0.2	1.1	0.2	0.6
72	< 0.7	146.0	370	6.3	14.7	3.2	234	32.6	65.2	6.8	21.6	2.3	0.6	1.4	0.2	1.1	< 0.2	0.5
73	6.0	86.6	813	28.3	8.0	2.3	629	35.1	90.1	12.2	51.3	8.7	2.4	6.5	1.0	5.6	1.1	2.9
74A	< 0.7	43.5	422	9.5	6.4	1.1	1010	78.4	137.0	13.0	39.5	4.6	1.1	2.8	0.3	1.8	0.3	1.0
74B	< 0.7	70.7	124	9.8	4.3	0.3	305	9.2	17.6	2.0	7.0	1.5	0.3	1.3	0.3	1.6	0.3	1.1
75	1.8	74.8	474	3.8	< 2.4	2.2	615	18.1	30.3	3.0	9.3	1.5	0.5	1.0	0.1	0.7	< 0.2	0.4
T-06	< 0.7	115.0	193	9.8	4.4	1.6	715	23.2	41.8	4.4	15.1	2.4	0.8	1.8	0.3	1.6	0.3	1.0
T-07	1.3	101.0	348	5.2	4.5	5.8	681	13.9	29.2	2.7	9.3	1.5	0.5	0.9	0.2	0.9	< 0.2	0.6
T-25	< 0.7	409.0	42	23.6	17.6	7.3	120	0.9	1.8	0.2	0.8	0.8	0.1	1.3	0.5	3.6	0.8	2.8

Appendix B. (cont)

	Tm	Yb	Hf	Ta	W	Tl	Bi	Th	U	Al	Ca	Fe	K	Mg	P	S	Si	Ti
	ppm	ppm	ppm	ppm	ppm	ppm	ppm	ppm	ppm	%	%	%	%	%	%	%	%	%
53	< 0.1	0.4	< 10	< 0.2	< 0.7	0.6	< 2	25.3	1.7	10.20	1.07	1.24	4.0	0.29	0.026	< 0.01	40.5	0.14
54	0.3	2.2	20	1.3	< 0.7	1.1	< 2	387.0	53.0	9.92	1.14	1.50	2.6	0.21	0.010	0.02	36.9	0.15
55	< 0.1	0.2	< 10	< 0.2	< 0.7	0.3	< 2	6.9	0.5	11.30	2.23	1.16	0.8	0.35	0.017	< 0.01	45.0	0.12
56	< 0.1	0.6	< 10	0.3	< 0.7	0.9	< 2	14.1	0.9	8.14	1.54	1.60	2.3	0.30	0.028	< 0.01	32.3	0.13
58	< 0.1	0.2	< 10	< 0.2	< 0.7	0.1	< 2	3.2	< 0.1	9.16	2.48	1.68	0.8	0.41	0.042	0.04	33.8	0.18
59	< 0.1	0.4	< 10	0.3	< 0.7	0.1	< 2	0.9	0.1	11.20	2.62	1.97	0.8	0.55	0.048	< 0.01	35.1	0.22
60	< 0.1	0.1	< 10	< 0.2	< 0.7	0.3	< 2	0.7	0.3	10.30	1.33	0.50	1.7	0.13	0.009	< 0.01	39.0	0.05
61	< 0.1	0.6	< 10	< 0.2	< 0.7	0.3	< 2	4.5	0.5	11.60	2.87	3.04	1.5	1.02	0.083	< 0.01	41.7	0.31
62	< 0.1	0.2	< 10	0.3	< 0.7	0.2	6	1.2	0.1	11.00	2.67	1.87	0.7	0.61	0.053	< 0.01	37.4	0.27
63	< 0.1	0.3	< 10	0.2	< 0.7	< 0.1	< 2	1.4	< 0.1	11.40	3.15	2.61	0.5	0.72	0.090	0.06	32.4	0.30
64	0.2	1.2	< 10	1.3	< 0.7	< 0.1	< 2	5.3	0.9	14.20	4.22	2.87	0.3	1.01	0.107	0.03	32.0	0.42
65	< 0.1	0.1	< 10	< 0.2	< 0.7	< 0.1	< 2	0.3	< 0.1	10.20	2.96	0.88	0.3	0.39	0.044	0.03	34.4	0.22
66	0.2	1.4	< 10	0.3	< 0.7	0.1	< 2	1.8	0.4	9.91	4.89	3.61	0.8	1.96	0.052	< 0.01	35.7	0.39
67	< 0.1	0.4	< 10	2.8	< 0.7	0.6	< 2	8.9	1.1	8.07	0.54	0.50	6.2	0.10	0.011	< 0.01	47.0	0.04
69	< 0.1	0.2	< 10	< 0.2	< 0.7	< 0.1	< 2	1.5	0.2	10.40	1.37	0.92	0.8	0.54	0.026	< 0.01	44.4	0.13
70	< 0.1	0.1	< 10	0.7	7.2	0.9	< 2	17.1	12.0	8.35	0.51	0.53	3.1	0.11	0.023	0.07	35.5	0.12
71D	< 0.1	0.5	< 10	0.6	< 0.7	0.4	< 2	8.6	1.1	9.27	2.31	2.06	1.5	0.53	0.053	< 0.01	34.4	0.23
71P	< 0.1	0.5	< 10	1.1	< 0.7	0.6	< 2	6.2	1.3	8.90	0.99	1.44	2.2	0.43	0.038	< 0.01	33.7	0.17
72	< 0.1	0.3	< 10	2.2	1.6	0.8	< 2	12.9	4.9	8.44	0.69	0.45	1.9	0.14	0.024	< 0.01	39.1	0.13
73	0.4	2.1	< 10	0.7	< 0.7	0.6	< 2	3.0	0.7	9.33	5.15	9.77	2.4	2.60	0.241	0.27	23.1	0.78
74A	0.1	0.9	< 10	0.8	< 0.7	0.2	< 2	18.4	2.8	8.22	1.44	1.03	1.1	0.26	0.020	< 0.01	33.8	0.15
74B	0.2	1.1	< 10	1.0	< 0.7	0.3	< 2	9.1	3.0	7.34	0.51	0.32	3.2	0.04	0.006	< 0.01	47.0	0.02
75	< 0.1	0.4	< 10	< 0.2	< 0.7	0.5	< 2	6.7	1.7	9.74	1.66	1.08	2.0	0.38	0.031	< 0.01	39.8	0.13
T-06	0.1	0.8	< 10	1.1	4.6	0.5	< 2	8.1	2.9	8.68	0.66	1.82	2.2	0.59	0.040	< 0.01	40.0	0.21
T-07	< 0.1	0.5	< 10	1.0	< 0.7	0.5	< 2	8.5	1.9	9.24	1.76	2.25	2.0	0.61	0.062	< 0.01	33.2	0.25
T-25	0.5	3.2	< 10	4.0	< 0.7	2.6	< 2	4.5	2.3	8.90	0.17	0.08	7.1	0.01	< 0.005	< 0.01	31.7	< 0.01

Notes:

< x: Below the limit of detection (x)

Appendix C. EMPA results for igneous garnet from pegmatites

	SiO_2	TiO_2	Al_2O_3	Cr_2O_3	MgO	CaO	MnO	FeO	Total	D
8: Pegmatitic leucogranite intruding basalt										
08-1-A-1	31.72	0.06	17.85	0.00	0.19	0.36	17.52	24.79	92.48	0
08-1-A-2	39.47	0.04	15.78	0.00	1.04	0.20	3.36	29.27	89.17	59
08-1-A-3	35.82	0.07	20.71	0.00	0.19	0.20	21.33	22.20	100.51	101
08-1-A-4	33.84	0.03	21.82	0.02	4.49	0.15	0.60	26.13	87.07	148
08-1-A-5	35.72	0.06	20.68	0.01	0.21	0.18	21.17	22.31	100.34	181
08-1-A-6	30.08	0.06	17.00	0.01	0.26	0.32	15.19	21.35	84.28	357
08-1-A-7	34.03	0.04	19.40	0.00	0.15	0.24	19.93	22.61	96.40	374
08-1-A-8	30.90	0.08	17.59	0.01	0.17	0.32	16.55	25.80	91.42	449
08-1-A-9	33.83	0.05	19.22	0.00	0.18	0.23	18.82	25.09	97.42	543
08-1-A-10	35.33	0.01	20.75	0.01	0.21	0.22	20.59	22.98	100.10	505
08-1-A-11	29.86	0.08	16.19	0.00	0.25	0.24	13.42	32.80	92.84	664
08-1-A-12	35.49	0.02	20.57	0.06	0.25	0.19	18.46	25.19	100.24	725
08-1-A-13	35.49	0.05	20.57	0.00	0.39	0.22	15.66	27.74	100.11	811
08-1-A-14	35.75	0.05	20.66	0.00	0.55	0.31	12.14	31.27	100.74	964
08-1-A-15	35.75	0.00	20.82	0.00	0.67	0.40	9.88	32.43	99.94	1055
08-1-B-1	33.81	0.03	19.34	0.00	0.17	0.35	19.56	22.73	96.00	0
08-1-B-2	26.11	0.11	17.58	0.00	1.35	1.35	7.61	32.35	86.47	145
08-1-B-3	30.90	0.07	17.55	0.02	0.15	0.33	15.18	28.18	92.38	290
08-1-B-4	34.22	0.06	19.30	0.00	0.23	0.33	18.05	23.99	96.16	436
08-1-B-5	34.60	0.08	19.90	0.01	0.19	0.32	20.04	22.12	97.25	582
08-1-B-6	35.69	0.00	20.71	0.00	0.16	0.19	21.45	21.66	99.86	728
08-1-B-7	26.71	0.06	16.08	0.03	0.11	0.25	16.70	33.00	92.92	874
08-1-B-8	35.59	0.00	20.79	0.01	0.17	0.17	21.58	21.64	99.94	1020
08-1-B-9	35.62	0.03	20.68	0.02	0.18	0.17	21.20	21.91	99.81	1167
08-1-B-10	35.40	0.01	20.18	0.01	0.16	0.22	20.20	22.58	98.76	1314
08-1-B-11	35.42	0.03	20.64	0.02	0.17	0.18	20.99	22.58	100.03	1461
08-1-B-12	35.44	0.04	20.59	0.03	0.19	0.21	20.37	23.02	99.89	1608
08-1-B-13	35.40	0.05	20.66	0.00	0.23	0.20	19.26	24.04	99.84	1755
08-1-B-14	36.12	0.03	20.77	0.02	0.26	0.24	17.80	25.53	100.76	1903
08-1-B-15	36.07	0.04	20.44	0.05	0.31	0.28	16.32	27.15	100.65	2051
08-1-B-16	39.31	0.09	22.23	0.01	2.04	0.21	5.97	21.58	91.44	2198
08-1-B-17	36.20	0.00	20.50	0.00	0.40	0.30	14.08	29.66	101.12	2347
08-1-B-18	36.19	0.07	20.48	0.02	0.41	0.31	13.40	29.81	100.67	2495
08-1-B-19	36.31	0.02	20.54	0.00	0.46	0.40	13.02	30.10	100.85	2643
08-1-B-20	36.22	0.02	20.36	0.03	0.45	0.44	12.31	30.23	100.05	2792
08-1-B-21	36.37	0.01	20.46	0.02	0.52	0.38	12.06	31.09	100.90	2941
08-1-B-22	36.21	0.05	20.42	0.00	0.61	0.28	10.84	32.39	100.80	3090
08-1-B-23	36.44	0.02	20.32	0.00	0.68	0.39	9.45	33.50	100.80	3239
08-1-B-24	36.52	0.03	20.69	0.00	0.83	0.32	8.05	34.99	101.43	3388
08-1-B-25	36.03	0.02	20.18	0.00	0.56	0.33	12.42	29.87	99.41	3538

Appendix C. (cont)

	SiO_2	TiO_2	Al_2O_3	Cr_2O_3	MgO	CaO	MnO	FeO	Total	D
08-2-1	35.73	0.02	20.69	0.00	0.22	0.20	19.20	24.62	100.67	0
08-2-2	35.63	0.18	20.59	0.00	0.24	0.21	19.99	23.82	100.66	151
08-2-3	35.21	0.01	20.74	0.00	0.20	0.26	20.09	23.49	100.00	326
08-2-4	35.35	0.02	20.69	0.02	0.20	0.25	20.44	23.08	100.07	434
08-2-5	35.22	0.01	20.55	0.01	0.20	0.29	19.80	23.26	99.33	584
08-2-6	35.38	0.05	20.75	0.00	0.18	0.22	20.03	23.53	100.14	820
08-2-7	33.90	0.05	19.95	0.02	0.22	0.24	18.09	25.14	97.62	954
08-2-8	32.90	0.04	19.70	0.01	0.25	0.26	17.18	25.83	96.18	1209
08-2-9	35.30	0.01	20.71	0.04	0.24	0.23	18.56	24.21	99.31	1315
08-2-10	35.25	0.05	20.71	0.00	0.22	0.23	19.74	23.37	99.55	1490
08-2-11	33.94	0.02	19.92	0.03	0.21	0.22	18.47	22.99	95.81	1553
08-2-12	35.99	0.00	20.92	0.01	0.33	0.15	16.39	26.96	100.73	1898
08-2-13	35.46	0.00	20.37	0.00	0.28	0.33	16.13	27.22	99.79	2178
08-2-14	35.54	0.04	20.69	0.00	0.33	0.29	14.50	29.21	100.60	2325
08-2-15	35.96	0.00	20.63	0.02	0.35	0.23	15.08	28.38	100.65	2526
08-2-16	35.98	0.01	20.59	0.03	0.40	0.44	13.43	29.99	100.85	2691
08-2-17	35.81	0.03	20.73	0.05	0.48	0.43	12.66	30.86	101.04	2843
08-2-18	36.04	0.02	20.70	0.01	0.43	0.46	12.57	31.10	101.32	2988
08-2-19	35.85	0.03	20.61	0.00	0.51	0.38	10.90	31.98	100.27	3154
08-2-20	36.00	0.03	20.64	0.01	0.59	0.40	9.95	33.35	100.98	3312
08-2-21	35.95	0.05	20.68	0.02	0.63	0.41	9.50	33.67	100.91	3409
08-2-22	35.96	0.01	20.81	0.03	0.67	0.39	8.79	33.90	100.55	3529
08-2-23	35.84	0.01	20.80	0.03	0.73	0.37	8.35	34.61	100.73	3636
08-2-24	36.01	0.00	20.91	0.00	0.82	0.42	8.03	34.97	101.16	3744
08-2-25	36.08	0.00	20.73	0.03	0.70	0.34	10.36	32.02	100.24	3873

Appendix C. (cont)

	SiO_2	TiO_2	Al_2O_3	Cr_2O_3	MgO	CaO	MnO	FeO	Total	D
32: Pegmatitic leucogranite										
32-1-1	35.72	0.07	20.10	0.00	0.83	0.40	14.94	26.08	98.13	0
32-1-2	35.55	0.04	20.22	0.00	0.84	0.41	14.69	26.05	97.80	74
32-1-3	35.59	0.02	20.37	0.01	0.84	0.38	14.62	26.46	98.31	148
32-1-4	35.45	0.05	20.06	0.02	0.86	0.42	14.49	26.56	97.91	223
32-1-5	35.52	0.00	20.20	0.01	0.86	0.45	14.29	26.40	97.73	297
32-1-6	35.58	0.01	20.41	0.03	0.89	0.44	14.02	26.57	97.94	371
32-1-7	35.48	0.03	20.22	0.01	0.87	0.38	14.06	26.93	97.98	446
32-1-8	35.75	0.05	20.26	0.05	0.93	0.43	14.20	26.54	98.20	521
32-1-9	35.73	0.00	20.17	0.00	0.93	0.43	13.87	26.59	97.71	595
32-1-10	35.63	0.01	20.28	0.00	0.92	0.41	13.88	26.89	98.02	670
32-1-11	35.62	0.05	20.11	0.00	0.97	0.44	13.92	27.10	98.22	745
32-1-12	35.41	0.05	20.18	0.02	0.96	0.44	13.53	27.34	97.93	820
32-1-13	35.52	0.05	20.27	0.00	0.97	0.43	13.44	27.30	97.97	895
32-1-14	35.43	0.06	20.16	0.06	0.99	0.41	13.42	27.39	97.91	970
32-1-15	35.56	0.05	20.02	0.01	0.99	0.41	13.23	27.51	97.78	1045
32-1-16	35.51	0.04	20.22	0.00	1.01	0.38	13.02	27.66	97.84	1120
32-1-17	35.74	0.05	20.51	0.00	1.04	0.39	12.91	27.95	98.58	1196
32-1-18	35.80	0.04	20.48	0.00	1.08	0.48	13.03	28.03	98.95	1271
32-1-19	35.69	0.02	20.45	0.03	1.13	0.64	12.55	28.53	99.03	1347
32-1-20	35.82	0.02	20.29	0.01	0.54	0.35	14.53	26.88	98.43	1422
32-2-1	35.78	0.02	20.26	0.02	0.82	0.45	13.49	28.07	98.91	0
32-2-2	35.91	0.06	20.22	0.01	1.09	0.39	12.66	28.02	98.37	83
32-2-3	35.81	0.02	20.32	0.03	1.13	0.39	12.57	27.97	98.25	165
32-2-4	35.75	0.07	20.33	0.03	1.08	0.39	12.50	28.08	98.23	248
32-2-5	35.78	0.08	20.57	0.00	0.96	0.42	13.03	28.22	99.06	330
32-2-6	35.46	0.03	20.29	0.00	0.93	0.40	13.12	27.71	97.93	413
32-2-7	35.61	0.05	20.27	0.04	1.02	0.38	13.20	27.72	98.29	495
32-2-8	35.72	0.06	20.19	0.00	1.07	0.40	12.81	27.80	98.04	578
32-2-9	35.63	0.05	20.27	0.00	1.10	0.42	13.05	27.39	97.91	660
32-2-10	35.44	0.02	20.27	0.00	1.13	0.41	13.09	27.49	97.84	743
32-2-11	35.67	0.01	20.47	0.00	1.07	0.40	12.99	27.66	98.27	825
32-2-12	35.08	0.04	20.15	0.00	1.06	0.47	12.36	27.82	96.97	907
32-2-13	35.68	0.04	20.57	0.00	1.17	0.46	12.47	28.33	98.72	989
32-2-14	35.62	0.03	20.57	0.05	1.16	0.47	12.14	28.66	98.70	1072
32-2-15	35.62	0.01	20.49	0.00	0.69	0.48	13.74	27.25	98.27	1154
32-3-1	35.68	0.00	20.42	0.02	1.13	0.44	12.25	28.52	98.46	0
32-3-2	35.85	0.00	20.35	0.00	1.19	0.52	12.11	28.69	98.70	20
32-3-3	36.68	0.01	20.80	0.02	1.17	0.50	12.85	30.02	102.04	41
32-3-4	35.84	0.04	20.63	0.03	1.15	0.49	12.31	28.67	99.16	61
32-3-5	35.73	0.00	20.34	0.01	1.15	0.46	12.17	28.56	98.41	82
32-3-6	36.05	0.00	20.53	0.00	1.17	0.54	12.06	28.57	98.93	102
32-3-7	35.80	0.06	20.45	0.00	1.13	0.56	12.14	28.48	98.61	123
32-3-8	35.85	0.01	20.50	0.00	1.15	0.51	12.35	28.70	99.07	143
32-3-9	35.62	0.00	20.47	0.00	0.98	0.48	12.24	28.54	98.34	163
32-3-10	35.81	0.00	20.30	0.01	0.56	0.36	14.24	26.93	98.21	184

Appendix C. (cont)

	SiO_2	TiO_2	Al_2O_3	Cr_2O_3	MgO	CaO	MnO	FeO	Total	D
32-4-1	35.62	0.05	20.15	0.00	1.18	0.40	11.52	28.80	97.72	0
32-4-2	35.52	0.03	20.37	0.00	1.19	0.38	11.58	28.83	97.89	37
32-4-3	35.37	0.06	20.11	0.03	1.17	0.41	11.64	28.54	97.33	74
32-4-4	35.12	0.09	20.06	0.00	1.48	0.36	11.01	28.65	96.78	111
32-4-5	35.58	0.05	20.27	0.00	1.19	0.41	11.52	28.72	97.74	148
32-4-6	35.77	0.06	20.21	0.02	1.22	0.43	11.45	28.90	98.05	185
32-4-7	35.72	0.02	20.47	0.01	1.23	0.44	11.42	28.81	98.12	222
32-4-8	35.98	0.02	20.58	0.02	1.09	0.40	11.79	28.89	98.78	259
32-4-9	35.80	0.04	20.43	0.04	0.42	0.57	14.11	26.89	98.29	296
32-4-10	99.07	0.01	0.01	0.02	0.00	0.02	0.08	0.20	99.39	332
32-5-1	35.84	0.06	20.45	0.00	1.08	0.41	11.64	28.70	98.17	0
32-5-2	35.66	0.01	20.22	0.00	1.04	0.41	11.83	28.70	97.86	11
32-5-3	35.55	0.04	20.33	0.00	1.02	0.39	11.89	28.66	97.87	22
32-5-4	35.72	0.05	20.30	0.01	1.02	0.40	11.87	28.86	98.23	34
32-5-5	35.54	0.05	20.24	0.02	1.00	0.41	11.86	28.31	97.43	45
32-5-6	35.48	0.00	20.18	0.02	0.99	0.40	12.00	28.66	97.73	56
32-5-7	35.32	0.05	20.32	0.00	0.98	0.47	12.07	28.22	97.42	68
32-5-8	35.64	0.00	20.63	0.00	0.88	0.46	12.24	28.57	98.42	79
32-5-9	35.44	0.05	20.51	0.00	0.80	0.49	12.65	28.37	98.31	90
32-5-10	35.20	0.03	20.48	0.01	0.43	0.47	14.96	26.95	98.53	102
32-6-1	35.81	0.07	20.27	0.01	1.16	0.43	12.13	28.29	98.18	0
32-6-2	35.75	0.07	20.52	0.00	1.21	0.46	12.23	28.44	98.68	47
32-6-3	35.67	0.04	20.39	0.01	1.14	0.46	11.98	28.33	98.02	95
32-6-4	35.64	0.03	20.48	0.00	1.17	0.40	12.16	28.47	98.35	142
32-6-5	35.56	0.07	20.40	0.03	1.20	0.40	12.03	28.43	98.12	190
32-6-6	35.79	0.05	20.24	0.00	1.16	0.39	11.75	28.63	98.02	237
32-6-7	35.68	0.04	20.36	0.00	1.17	0.39	12.07	28.62	98.33	285
32-6-8	35.72	0.07	20.39	0.00	1.14	0.41	11.89	28.61	98.23	332
32-6-9	35.94	0.01	20.56	0.01	1.10	0.47	11.92	28.61	98.62	380
32-6-10	35.97	0.00	20.80	0.00	0.49	0.60	14.42	27.02	99.29	427

Notes:
All results reported as weight %
D: The distance from the first spot analyzed (μm)

Appendix D. LA-ICP-MS results for REEs in igneous garnets from pegmatites

	La	Ce	Pr	Nd	Sm	Eu	Gd	Tb	Dy	Ho	Er	Tm	Yb	Lu
08: Pegmatitic leucogranite intruding basalt; cores														
08-3	24.470	27.220	45.720	88.04	433.08	1.050	526.60	604.90	587.54	438.98	453.58	508.07	569.66	509.38
08-4	11.050	20.220	59.810	114.53	508.65	0.334	678.74	823.48	837.71	664.23	717.12	828.25	938.42	852.78
08-7	0.299	4.220	25.600	84.15	811.13	0.042	1,212.42	1,501.47	1,487.09	1,118.59	1,204.19	1,466.38	1,768.48	1,634.35
08-8	0.716	7.240	36.400	95.39	648.68	< 0.04	891.81	1,095.62	1,092.20	849.80	924.75	1,099.95	1,275.38	1,192.33
rims														
08-1	< 0.003	0.009	0.062	0.38	20.88	0.102	118.66	249.83	343.11	322.89	367.28	408.95	432.20	396.75
08-2	0.007	0.047	0.392	1.88	55.74	0.051	344.75	729.16	959.22	734.00	633.24	578.23	516.70	345.00
08-5	< 0.003	0.005	0.057	0.49	17.96	0.049	140.33	368.96	674.34	837.16	1,179.25	1,615.43	2,085.59	2,063.92
08-6	< 0.003	0.016	0.225	1.12	38.10	0.105	148.43	232.84	250.12	183.66	172.95	175.28	177.80	135.49
32: Pegmatitic leucogranite; cores														
32-1	0.022	0.026	0.067	0.24	25.41	0.151	349.13	941.24	1,730.45	2,187.49	3,276.76	4,790.85	6,415.57	6,636.91
32-6	0.025	0.032	0.181	1.43	48.64	0.280	341.47	825.75	1,501.48	1,913.27	2,832.33	4,099.28	5,549.12	5,710.85
32-10	0.025	0.024	0.036	0.39	18.11	0.050	218.75	627.38	1,270.94	1,803.17	2,930.64	4,522.54	6,561.13	7,457.82
?														
32-5	0.003	0.010	0.074	0.67	32.76	0.124	292.21	734.84	1,297.91	1,492.56	1,847.32	2,220.20	2,473.09	2,125.70
32-7	< 0.003	0.009	0.114	0.86	38.17	0.157	311.23	789.90	1,380.03	1,567.38	1,997.47	2,448.88	2,837.03	2,436.63
rims														
32-2	< 0.003	0.002	0.019	0.33	16.64	0.088	210.00	551.93	997.07	1,189.97	1,461.13	1,654.08	1,760.06	1,572.38
32-3	< 0.003	0.004	0.027	0.25	9.42	< 0.04	100.67	283.93	583.46	837.02	1,260.58	1,706.88	2,141.80	2,203.39
32-4	0.033	0.109	0.114	0.37	17.81	0.086	183.08	480.78	918.35	1,240.84	1,743.26	2,262.63	2,827.66	3,204.98
32-8	< 0.003	0.004	0.039	0.18	6.17	0.046	56.92	165.20	347.21	500.33	794.23	1,155.43	1,542.56	1,620.04
32-9	< 0.003	0.003	0.017	0.21	8.42	0.072	87.23	257.93	560.09	850.34	1,324.50	1,779.64	2,247.13	2,404.96

Notes:
< x: Below detection limit (x)
All results reported in ppm

Appendix E. LA-ICP-MS results for U-Pb geochronology of zircons from granitoids surrounding the NCGB

			Isotope ratios							Age (Ma)					
	Th/U	^{204}Pb	^{207*}Pb/^{206*}Pb	2σ	^{207*}Pb/^{235}U	2σ	^{206*}Pb/^{238}U	2σ	Err. Corr.	^{207*}Pb/^{206*}Pb	2σ	^{206*}Pb/^{238}U	2σ	^{207*}Pb/^{235}U	2σ
Southern batholith															
01: Leucocratic granodiorite															
01-4-r	0.16	309.0	0.1788	0.0015	8.14	0.25	0.3301	0.0096	0.9246	2642	6	1838	45	2245	27
01-24-r	0.18	142.0	0.1800	0.0020	9.35	0.35	0.3690	0.0130	0.5733	2660	14	2024	59	2372	31
01-2-c	0.20	212.0	0.1884	0.0015	9.38	0.30	0.3645	0.0110	0.8354	2728	5	2003	51	2378	29
01-12-r	0.10	154.0	0.1894	0.0020	11.65	0.41	0.4452	0.0140	0.6004	2738	14	2373	63	2576	30
01-6-r	0.16	93.0	0.1985	0.0025	13.17	0.51	0.4840	0.0160	0.5254	2809	27	2542	77	2691	48
01-11-r	0.82	129.0	0.1984	0.0026	11.60	0.54	0.4280	0.0180	0.7449	2811	15	2296	84	2572	45
01-1-r	0.12	59.0	0.1997	0.0018	14.17	0.72	0.5249	0.0270	0.4474	2824	14	2720	130	2761	68
01-24-c	0.48	103.0	0.1996	0.0029	14.50	0.45	0.5263	0.0150	0.3968	2826	11	2725	63	2783	29
01-24-m	0.79	41.0	0.2001	0.0026	15.03	0.45	0.5425	0.0150	0.5483	2828	13	2793	64	2816	29
01-12-m	0.44	-3.0	0.2013	0.0019	15.41	0.44	0.5532	0.0150	0.6374	2840	8	2838	63	2841	28
01-20-r	0.44	112.0	0.2016	0.0019	13.28	0.40	0.4756	0.0140	0.7245	2840	8	2508	59	2699	28
01-17-r	0.10	-2.0	0.2013	0.0020	14.83	0.43	0.5342	0.0150	0.6229	2841	8	2758	61	2804	28
01-8-m	0.33	113.0	0.2024	0.0022	15.07	0.43	0.5442	0.0150	0.4441	2843	10	2800	63	2820	27
01-12-c	0.50	47.0	0.2020	0.0020	14.01	0.41	0.5031	0.0140	0.7936	2844	8	2626	62	2750	28
01-3-c	0.31	4.0	0.2026	0.0026	14.95	0.44	0.5398	0.0150	0.3514	2847	11	2782	62	2814	27
01-17-c	0.58	89.0	0.2018	0.0029	15.07	0.46	0.5390	0.0150	0.4955	2850	13	2778	62	2818	29
01-4-c	0.34	33.0	0.2038	0.0020	15.60	0.45	0.5566	0.0150	0.7134	2850	10	2852	62	2854	28
01-16-c	0.33	10.0	0.2030	0.0023	14.02	0.45	0.5012	0.0150	0.6043	2856	13	2619	64	2750	29
01-20-c	0.24	11.0	0.2029	0.0021	15.67	0.45	0.5559	0.0150	0.4580	2857	8	2851	61	2856	28
0L1-17-m	0.08	-16.0	0.2039	0.0023	13.61	0.45	0.4828	0.0160	0.6030	2860	14	2543	70	2722	34
01-2-r	0.23	83.0	0.2042	0.0017	14.24	0.41	0.5118	0.0140	0.6725	2860	5	2664	58	2767	26
01-1-c	0.27	-9.0	0.2045	0.0018	14.73	0.44	0.5311	0.0150	0.8466	2861	7	2745	63	2797	28
01-16-r	0.24	34.0	0.2044	0.0020	15.31	0.50	0.5416	0.0160	0.7177	2868	12	2789	68	2834	34
01-6-c	0.54	132.0	0.2183	0.0020	14.84	0.45	0.4949	0.0140	0.8702	2971	6	2591	60	2806	28
01-11-c	0.62	-35.0	0.2182	0.0025	17.65	0.51	0.5818	0.0160	0.5434	2972	14	2960	65	2970	29

Appendix E. (cont)

		Isotope ratios								Age (Ma)					
	Th/U	^{204}Pb	^{207*}Pb/^{206*}Pb	2σ	^{207*}Pb/^{235}U	2σ	^{206*}Pb/^{238}U	2σ	Err. Corr.	^{207*}Pb/^{206*}Pb	2σ	^{206*}Pb/^{238}U	2σ	^{207*}Pb/^{235}U	2σ
13: Strongly foliated granodiorite															
13-z4-c*	1.45	390.0	0.1730	0.0037	8.17	0.33	0.3448	0.0110	0.9664	2585	7	1909	55	2248	35
13-z5-r	0.47	22.0	0.1822	0.0042	11.63	0.53	0.4610	0.0210	0.6627	2688	17	2443	100	2573	56
13-z1-r2	1.08	110.0	0.1869	0.0038	12.64	0.30	0.4880	0.0110	0.8624	2708	12	2560	50	2652	25
13-z3-c2	0.19	110.0	0.1866	0.0043	13.54	0.42	0.5240	0.0150	0.6854	2709	13	2714	62	2716	28
13-z1-r	1.07	34.0	0.1861	0.0041	13.51	0.59	0.5239	0.0220	0.8898	2710	7	2715	92	2715	36
13-z2-r2	1.26	149.0	0.1871	0.0039	11.37	0.29	0.4438	0.0110	0.8242	2716	7	2367	49	2554	23
13-z6-c	0.31	-22.0	0.1871	0.0041	13.49	0.34	0.5230	0.0120	0.7567	2721	10	2711	53	2715	24
13-z6-r	0.23	29.0	0.1881	0.0047	13.23	0.36	0.5111	0.0120	0.2190	2727	14	2661	52	2694	26
13-z5-c	1.51	152.0	0.1892	0.0040	12.59	0.33	0.4833	0.0120	0.7571	2728	11	2547	52	2651	25
13-z3-c	0.98	6.0	0.1885	0.0040	13.68	0.34	0.5270	0.0130	0.6954	2729	9	2728	53	2729	24
13-z6-r2	0.13	-18.0	0.1873	0.0046	12.40	0.36	0.4758	0.0120	0.5685	2731	14	2508	51	2632	27
13-z2-c	0.97	50.0	0.1886	0.0043	13.16	0.38	0.5078	0.0140	0.6298	2731	18	2646	59	2693	28
13-z1-c	0.92	142.0	0.1888	0.0040	13.69	0.35	0.5270	0.0130	0.7671	2732	8	2730	55	2728	24
13-z7-c	0.48	170.0	0.1901	0.0043	12.88	0.34	0.4979	0.0120	0.5990	2748	15	2604	50	2671	25
13-z2-r	1.51	373.0	0.1927	0.0041	11.70	0.40	0.4380	0.0130	0.9174	2767	14	2347	59	2581	36

Appendix E. (cont)

			Isotope ratios							Age (Ma)					
	Th/U	^{204}Pb	^{207*}Pb/^{206*}Pb	2σ	^{207*}Pb/^{235}U	2σ	^{206*}Pb/^{238}U	2σ	Err. Corr.	^{207*}Pb/^{206*}Pb	2σ	^{206*}Pb/^{238}U	2σ	^{207*}Pb/^{235}U	2σ
29: Moderately foliated granodiorite															
29-z9-r	0.10	-7.0	0.1804	0.0023	9.11	0.29	0.3568	0.0140	0.8650	2662	11	1966	66	2348	30
29-z10-r	0.24	603.0	0.1870	0.0022	10.80	0.35	0.4128	0.0160	0.9724	2717	7	2227	76	2506	34
29-z3-r	0.08	17.0	0.1892	0.0025	13.17	0.34	0.5103	0.0170	0.3987	2728	11	2658	75	2696	25
29-z13-r	0.29	225.0	0.1889	0.0025	9.03	0.40	0.3514	0.0170	0.9372	2729	11	1940	76	2343	34
29-z21-r	0.09	104.0	0.1887	0.0023	13.35	0.35	0.5179	0.0180	0.7691	2733	8	2690	79	2705	26
29-z4-r	0.07	25.0	0.1890	0.0025	11.69	0.32	0.4490	0.0170	0.7610	2733	11	2390	74	2579	25
29-z7-r	0.24	78.0	0.1892	0.0023	13.93	0.37	0.5304	0.0190	0.6949	2735	7	2743	79	2746	25
29-z17-r	0.07	121.0	0.1897	0.0025	14.21	0.40	0.5548	0.0210	0.4606	2736	11	2845	83	2764	25
29-z23-r	0.19	52.0	0.1894	0.0028	12.97	0.37	0.5023	0.0190	0.7176	2738	12	2622	81	2676	27
29-z24-r2	0.09	-14.0	0.1899	0.0024	13.77	0.37	0.5295	0.0190	0.9209	2742	10	2739	80	2736	26
29-z6-r	0.34	166.0	0.1906	0.0024	11.08	0.30	0.4237	0.0150	0.8965	2748	8	2276	69	2531	25
29-z20-r	0.10	-6.0	0.1917	0.0024	14.32	0.47	0.5585	0.0210	0.6538	2754	7	2860	86	2771	28
29-z16-r	0.26	52.0	0.1926	0.0024	12.90	0.38	0.4977	0.0180	0.8017	2764	10	2609	79	2671	29
29-z9-c*	0.04	11.0	0.1957	0.0024	13.75	0.37	0.5022	0.0180	0.6653	2790	5	2623	77	2733	25
29-z27-r	1.08	74.0	0.1991	0.0032	15.66	0.45	0.5563	0.0210	0.4247	2834	22	2850	86	2855	27
29-z19-c	0.39	99.0	0.2008	0.0026	13.64	0.39	0.4985	0.0180	0.6185	2835	13	2607	79	2724	30
29-z24-r1	0.17	-33.0	0.2020	0.0027	15.75	0.42	0.5699	0.0210	0.4571	2843	10	2912	83	2861	25
29-z26-c	0.23	34.0	0.2024	0.0030	14.84	0.45	0.5330	0.0210	0.8409	2844	12	2751	87	2802	29
29-z27-c	0.73	-42.0	0.2029	0.0035	15.61	0.45	0.5560	0.0210	0.3062	2846	14	2849	86	2853	28
29-z11-r	0.11	51.0	0.2023	0.0026	14.56	0.39	0.5202	0.0190	0.7178	2848	9	2699	79	2786	25
29-z15-c	0.47	46.0	0.2028	0.0028	15.53	0.43	0.5620	0.0200	0.5942	2849	11	2874	83	2848	29
29-z10-c	0.34	3.0	0.2029	0.0025	15.70	0.49	0.5570	0.0220	0.9544	2849	6	2855	90	2860	31
29-z23-c	0.54	14.0	0.2038	0.0031	15.41	0.42	0.5550	0.0200	0.2086	2854	15	2845	82	2844	27
29-z5-c	0.76	-5.0	0.2038	0.0029	15.61	0.45	0.5572	0.0210	0.6772	2854	14	2853	85	2852	29
29-z7-c	0.41	110.0	0.2039	0.0027	15.04	0.40	0.5305	0.0190	0.5323	2856	14	2743	82	2817	26
29-z26-r	0.11	24.0	0.2042	0.0028	14.63	0.52	0.5180	0.0230	0.8915	2860	13	2698	96	2793	33
29-z11-c	0.49	170.0	0.2038	0.0027	12.19	0.37	0.4283	0.0160	0.8840	2862	10	2296	75	2620	28
29-z3-c	0.59	80.0	0.2059	0.0026	13.69	0.39	0.4859	0.0190	0.8679	2866	7	2553	78	2728	29
29-z20-c	0.32	32.0	0.2038	0.0028	15.59	0.46	0.5602	0.0210	0.7343	2868	14	2871	88	2849	30
29-z24-c	0.21	113.0	0.2054	0.0028	15.80	0.45	0.5603	0.0210	0.7476	2872	11	2867	87	2863	28
29-z4-c	0.25	117.0	0.2103	0.0027	13.87	0.40	0.4815	0.0180	0.7880	2904	12	2533	79	2742	26
29-z21-c	0.35	22.0	0.2193	0.0028	17.41	0.49	0.5811	0.0210	0.7520	2977	8	2952	86	2956	27
29-z13-c	0.60	-50.0	0.2215	0.0029	18.17	0.48	0.5924	0.0200	0.6569	2995	15	2999	84	2998	26
29-z6-c	0.55	13.0	0.2229	0.0031	17.10	0.46	0.5605	0.0200	0.6401	3000	13	2868	85	2940	27

Appendix E. (cont)

			Isotope ratios							Age (Ma)					
	Th/U	^{204}Pb	^{207*}Pb/^{206*}Pb	2σ	^{207*}Pb/^{235}U	2σ	^{206*}Pb/^{238}U	2σ	Err. Corr.	^{207*}Pb/^{206*}Pb	2σ	^{206*}Pb/^{238}U	2σ	^{207*}Pb/^{235}U	2σ
48: Weakly gneissic granite															
48z-8r*	0.13	4.4	0.1339	0.0022	4.47	0.11	0.2412	0.0063	0.9706	2154	6	1392	33	1719	23
48z-24c*	0.15	89.0	0.1379	0.0039	3.51	0.30	0.1871	0.0110	0.9360	2194	11	1105	56	1526	51
48z-22c*	0.05	15.6	0.1526	0.0027	5.81	0.25	0.2753	0.0097	0.8929	2381	4	1568	47	1948	32
48z-19c*	0.38	46.5	0.1811	0.0033	8.58	0.46	0.3447	0.0140	0.9369	2667	6	1908	65	2292	42
48z-23c2	0.04	8.3	0.1820	0.0043	9.98	0.52	0.3980	0.0150	0.8824	2668	12	2156	70	2441	49
48z-5r	0.10	3.7	0.1830	0.0032	9.87	0.27	0.3925	0.0080	0.8667	2685	7	2134	38	2421	27
48z-4r	0.11	1.8	0.1850	0.0032	11.85	0.20	0.4650	0.0053	0.7387	2699	4	2461	23	2592	15
48z-2c*	0.56	48.3	0.1907	0.0034	11.34	0.30	0.4322	0.0093	0.8645	2750	7	2315	41	2550	23
48z-14r*	0.17	14.3	0.1926	0.0031	13.76	0.19	0.5201	0.0070	0.8350	2763	5	2702	30	2732	13
48z-16r*	0.29	17.1	0.1923	0.0032	13.40	0.33	0.5046	0.0120	0.9255	2767	7	2633	56	2708	27
48z-5c	0.47	0.6	0.2004	0.0035	14.98	0.67	0.5496	0.0230	0.7005	2829	13	2823	100	2812	58
48z-17c	0.19	1.6	0.2008	0.0033	15.86	0.29	0.5726	0.0099	0.4245	2830	4	2918	42	2868	18
48z-8c	0.69	1.8	0.2013	0.0038	14.38	0.49	0.5214	0.0140	0.8152	2837	10	2705	61	2774	38
48z-21c	0.68	0.9	0.2024	0.0042	15.57	0.32	0.5569	0.0083	0.4162	2841	14	2853	34	2851	20
48z-14c	0.11	10.8	0.2023	0.0034	16.88	0.26	0.6051	0.0088	0.7277	2842	5	3050	36	2928	18
48z-25c	0.42	14.1	0.2011	0.0043	16.13	0.29	0.5760	0.0067	0.4866	2845	8	2936	27	2885	18
48z-23c1	0.03	7.0	0.2007	0.0053	15.63	0.90	0.5570	0.0200	0.6667	2847	13	2852	76	2850	45
48z-24r*	0.16	107.6	0.2539	0.0064	5.10	0.33	0.1456	0.0140	0.5306	3219	12	876	73	1834	44
48z-12c*	0.45	158.0	0.2740	0.0160	28.90	1.20	0.7800	0.0280	0.4570	3314	25	3715	100	3450	42
48z-25r*	0.47	171.0	0.2706	0.0054	24.76	0.45	0.6670	0.0110	0.8016	3317	8	3293	40	3297	18
48z-18c*	0.38	264.0	0.2818	0.0062	19.53	0.43	0.5010	0.0084	0.9502	3379	5	2617	36	3067	22
48z-10r*	0.80	374.0	0.2985	0.0055	29.11	0.58	0.7120	0.0120	0.8045	3466	11	3463	45	3459	20
48z-20r*	0.60	219.2	0.3044	0.0054	31.65	1.30	0.7540	0.0310	0.8340	3493	6	3621	110	3542	47

Appendix E. (cont)

			Isotope ratios							Age (Ma)					
	Th/U	^{204}Pb	^{207*}Pb/^{206*}Pb	2σ	^{207*}Pb/^{235}U	2σ	^{206*}Pb/^{238}U	2σ	Err. Corr.	^{207*}Pb/^{206*}Pb	2σ	^{206*}Pb/^{238}U	2σ	^{207*}Pb/^{235}U	2σ
Schade Lake gneissic complex															
52: Gneissic tonalite															
52-36-c	0.53	286.0	0.2001	0.0024	13.36	0.30	0.4861	0.0110	0.8495	2826	10	2553	49	2704	21
52-37-r1	0.66	123.0	0.2010	0.0026	10.98	0.29	0.4002	0.0110	0.7603	2831	10	2169	50	2522	23
52-36-r2	0.44	400.0	0.2004	0.0025	10.20	0.25	0.3697	0.0100	0.6630	2831	8	2028	46	2453	22
52-37-c	0.65	220.0	0.2006	0.0024	12.20	0.34	0.4446	0.0120	0.7689	2833	6	2371	57	2619	29
52-31-r	0.29	20.0	0.2010	0.0026	15.11	0.33	0.5417	0.0120	0.2192	2836	12	2790	51	2824	21
52-33-r	0.37	56.0	0.2006	0.0026	15.44	0.34	0.5552	0.0130	0.6828	2841	10	2846	55	2842	22
52-30-r	0.18	7.0	0.2019	0.0026	14.19	0.31	0.5044	0.0120	0.3532	2842	7	2632	49	2763	20
52-25-r	0.86	43.0	0.2012	0.0025	13.99	0.31	0.4998	0.0120	0.2948	2842	8	2613	50	2749	21
52-36-r	0.37	92.0	0.2021	0.0025	14.02	0.31	0.5088	0.0120	0.5554	2844	9	2651	50	2751	21
52-37-r2	0.32	123.0	0.2033	0.0028	15.41	0.41	0.5548	0.0150	0.5200	2844	14	2844	59	2842	24
52-42-r	0.33	27.0	0.2050	0.0026	14.88	0.33	0.5249	0.0130	0.6806	2869	8	2719	53	2808	21
52-22-c	0.32	72.0	0.2062	0.0025	15.87	0.34	0.5588	0.0130	0.7601	2875	6	2861	52	2870	20
52-28-r	0.46	64.0	0.2062	0.0025	15.71	0.35	0.5495	0.0130	0.4897	2877	6	2823	52	2859	20
52-39-c	0.30	2.0	0.2067	0.0025	16.02	0.35	0.5626	0.0130	0.7202	2878	6	2879	53	2877	21
52-31-c	0.59	30.0	0.2074	0.0025	14.05	0.30	0.4881	0.0110	0.6367	2879	8	2562	50	2753	21
52-25-c	0.35	23.0	0.2077	0.0026	15.76	0.34	0.5506	0.0120	0.5632	2882	7	2827	52	2862	21
52-42-c	0.35	25.0	0.2070	0.0027	16.05	0.35	0.5630	0.0130	0.6026	2882	7	2879	53	2881	21
52-23-c	0.35	47.0	0.2063	0.0025	14.62	0.38	0.5148	0.0130	0.4371	2883	7	2677	59	2791	27
52-28-c	0.43	13.0	0.2074	0.0024	16.53	0.35	0.5748	0.0130	0.6643	2883	5	2929	53	2908	20
52-33-c	0.28	95.0	0.2063	0.0028	14.63	0.34	0.5113	0.0120	0.6176	2883	10	2662	52	2792	22
52-30-m	0.43	-37.0	0.2072	0.0024	15.75	0.33	0.5470	0.0120	0.4758	2885	8	2812	51	2862	20
52-40-c	0.33	129.0	0.2069	0.0026	15.50	0.33	0.5439	0.0120	0.4364	2885	14	2799	52	2846	20
52-40-r	0.31	58.0	0.2075	0.0025	15.96	0.36	0.5629	0.0130	0.4508	2885	10	2878	55	2874	23
52-30-c	0.38	-20.0	0.2078	0.0025	16.11	0.34	0.5614	0.0130	0.3847	2887	7	2872	53	2883	21
52-3-r	0.20	57.0	0.2084	0.0030	15.68	0.38	0.5449	0.0140	0.6184	2888	10	2803	60	2856	24
52-18-c	0.36	63.0	0.2075	0.0024	15.68	0.32	0.5481	0.0120	0.5424	2888	10	2817	51	2857	20
52-11-c	0.47	92.0	0.2077	0.0026	14.02	0.31	0.4894	0.0120	0.7479	2888	6	2567	50	2751	22
52-2-c	0.32	31.0	0.2071	0.0030	16.20	0.38	0.5670	0.0150	0.6637	2889	17	2893	60	2888	22
52-5-c	0.34	13.0	0.2083	0.0028	15.61	0.36	0.5438	0.0130	0.5307	2889	7	2799	54	2853	21
52-3-c	0.68	134.0	0.2069	0.0029	14.38	0.37	0.5054	0.0140	0.8126	2890	7	2636	57	2776	24
52-8-r	0.32	76.0	0.2078	0.0027	15.74	0.35	0.5475	0.0130	0.6299	2891	8	2814	53	2862	21
52-34-c	0.38	68.0	0.2082	0.0026	15.90	0.36	0.5546	0.0130	0.6612	2892	12	2844	54	2873	22
52-8-c	0.33	55.0	0.2086	0.0025	16.08	0.35	0.5597	0.0130	0.6853	2892	8	2865	52	2881	21
52-42-c	0.55	231.0	0.2082	0.0024	16.24	0.36	0.5672	0.0130	0.8905	2894	5	2896	54	2891	22

Appendix E. (cont)

	Isotope ratios									Age (Ma)					
	Th/U	^{204}Pb	^{207*}Pb/^{206*}Pb	2σ	^{207*}Pb/^{235}U	2σ	^{206*}Pb/^{238}U	2σ	Err. Corr.	^{207*}Pb/^{206*}Pb	2σ	^{206*}Pb/^{238}U	2σ	^{207*}Pb/^{235}U	2σ
53: Heterogeneously deformed gneiss															
53Cz-24c*	0.18	119.0	0.0923	0.0058	1.60	0.04	0.1234	0.0055	0.8717	1474	23	750	32	971	17
53Fz-33c*	1.45	124.4	0.1326	0.0027	3.40	0.43	0.1862	0.0210	0.6656	2136	36	1101	110	1503	74
53Cz-12c*	1.25	19.3	0.1463	0.0033	3.56	0.48	0.1731	0.0170	0.8852	2303	20	1029	90	1538	76
53Fz-34c*	0.25	32.7	0.1520	0.0028	7.05	0.34	0.3381	0.0130	0.5649	2371	18	1877	63	2116	49
53Cz-1r*	0.29	74.7	0.1540	0.0022	5.35	0.13	0.2495	0.0040	0.6975	2392	15	1436	21	1877	21
53Fz-38r*	1.47	323.0	0.1562	0.0049	6.84	0.34	0.3200	0.0150	0.9420	2419	16	1790	79	2084	56
53Fz-22r*	0.06	12.6	0.1581	0.0026	5.27	0.24	0.2442	0.0077	0.5325	2446	20	1408	40	1862	34
53Cz-16c*	0.10	5.3	0.1642	0.0029	9.94	0.45	0.4370	0.0150	0.9335	2496	13	2335	71	2425	54
53Fz-29c	0.49	32.6	0.1662	0.0023	7.35	0.22	0.3201	0.0075	0.7348	2517	14	1790	37	2154	30
53Cz-12r	0.11	10.0	0.1689	0.0019	7.83	0.27	0.3340	0.0100	0.5550	2552	14	1858	49	2210	29
53Cz-32r	0.13	5.6	0.1698	0.0026	9.63	0.39	0.4120	0.0130	0.7212	2556	18	2224	64	2397	43
53Fz-20c	0.10	26.9	0.1710	0.0025	8.17	0.22	0.3474	0.0096	0.0212	2564	16	1922	44	2249	26
53Cz-30c	1.16	77.1	0.1711	0.0028	9.12	0.34	0.3832	0.0100	0.4370	2573	19	2091	47	2349	31
53Fz-29r	0.44	57.5	0.1718	0.0017	8.50	0.22	0.3599	0.0089	0.9194	2577	8	1981	43	2284	22
53Cz-20c	0.26	64.7	0.1732	0.0025	8.01	0.20	0.3407	0.0054	0.2829	2579	37	1890	25	2229	26
53Cz-28c	0.04	11.4	0.1729	0.0026	8.13	0.33	0.3440	0.0120	0.4681	2586	18	1905	55	2243	33
53Cz-26c	0.41	234.0	0.1740	0.0045	7.03	0.34	0.2908	0.0076	0.8455	2595	17	1645	37	2114	36
53Fz-3r	0.12	113.0	0.1752	0.0026	7.98	0.37	0.3308	0.0130	0.8092	2610	17	1842	65	2234	44
53Fz-6c	0.07	6.7	0.1761	0.0025	9.99	0.24	0.4128	0.0068	0.8794	2614	13	2227	31	2433	23
53Cz-1c	0.04	13.3	0.1771	0.0031	10.69	0.32	0.4335	0.0096	0.6969	2625	16	2321	44	2494	28
53Fz-5c	0.05	2.4	0.1773	0.0027	11.80	0.40	0.4817	0.0140	0.7974	2626	14	2534	63	2587	36
53Fz-21c	0.49	10.7	0.1765	0.0032	9.97	0.27	0.4078	0.0071	0.5640	2627	16	2211	33	2431	25
53Fz-33r	0.09	10.3	0.1767	0.0083	10.21	0.38	0.4243	0.0098	0.4026	2627	18	2279	45	2452	29
53Fz-32r	0.03	1.1	0.1774	0.0029	12.37	0.30	0.5033	0.0082	0.5206	2629	15	2628	36	2631	23
53Fz-35c	0.07	0.3	0.1776	0.0026	13.51	0.28	0.5536	0.0068	0.5167	2634	10	2840	28	2718	20
53Cz-25c	0.17	0.2	0.1783	0.0029	13.10	0.30	0.5382	0.0067	0.2197	2638	13	2778	28	2685	21
53Cz-9c	0.11	72.0	0.1773	0.0068	8.59	0.47	0.3577	0.0079	0.4716	2640	23	1971	36	2301	43
53Cz-4c	0.19	1.1	0.1790	0.0025	12.53	0.46	0.5060	0.0150	0.8850	2641	11	2637	66	2644	37
53Fz-17r	0.04	1.8	0.1786	0.0032	12.65	0.34	0.5081	0.0090	0.7184	2648	14	2647	40	2650	26
53Fz-14r	0.19	100.8	0.1792	0.0025	11.18	0.27	0.4510	0.0081	0.5536	2649	13	2399	35	2541	22
53Cz-3r	0.02	1.2	0.1795	0.0030	13.49	0.31	0.5452	0.0071	0.3992	2649	13	2805	30	2713	22
53Cz-2r	0.04	1.5	0.1803	0.0033	13.17	0.31	0.5294	0.0083	0.3822	2650	13	2739	35	2689	22
53Cz-5c	0.02	0.4	0.1807	0.0028	13.92	0.35	0.5615	0.0080	0.6152	2659	13	2872	33	2742	24
53Fz-4c	0.30	5.8	0.1807	0.0030	12.04	0.32	0.4872	0.0093	0.6380	2663	14	2558	39	2604	25
53Fz-18r	0.05	1.9	0.1814	0.0034	13.65	0.30	0.5474	0.0073	0.0181	2665	16	2814	30	2724	21

Appendix E. (cont)

	Isotope ratios									Age (Ma)					
	Th/U	^{204}Pb	^{207*}Pb/^{206*}Pb	2σ	^{207*}Pb/^{235}U	2σ	^{206*}Pb/^{238}U	2σ	Err. Corr.	^{207*}Pb/^{206*}Pb	2σ	^{206*}Pb/^{238}U	2σ	^{207*}Pb/^{235}U	2σ
53Cz-32c	0.08	0.7	0.1813	0.0032	12.54	0.62	0.5090	0.0190	0.8861	2669	21	2649	85	2646	48
53Fz-8c	0.02	3.1	0.1819	0.0040	13.87	0.38	0.5580	0.0088	0.0837	2672	21	2858	37	2737	27
53Cz-6c	0.70	20.8	0.1832	0.0031	11.91	0.35	0.4741	0.0130	0.8374	2682	12	2499	54	2597	28
53Fz-24c	0.45	13.0	0.1846	0.0035	9.08	0.37	0.3599	0.0084	0.6597	2688	17	1981	40	2349	35
53Fz-17c	1.41	59.7	0.1849	0.0021	9.04	0.34	0.3541	0.0130	0.7316	2699	11	1954	63	2342	38
53Fz-37c	0.12	31.6	0.1858	0.0051	11.45	0.50	0.4450	0.0230	0.6463	2710	20	2373	100	2559	49
53Fz-7r	0.14	5.4	0.1871	0.0023	13.53	0.27	0.5252	0.0063	0.3009	2718	8	2721	27	2716	19
53Fz-12c	0.15	56.6	0.1889	0.0043	4.48	0.50	0.1722	0.0150	0.9488	2734	13	1023	78	1720	69
53Fz-38c	0.35	0.2	0.1914	0.0034	13.73	0.33	0.5276	0.0086	0.4107	2747	12	2731	29	2731	24
53Fz-1c	0.53	1.7	0.1907	0.0029	13.43	0.30	0.5187	0.0073	0.4429	2750	17	2693	31	2712	22
53Cz-31c*	0.49	14.1	0.1936	0.0032	13.82	0.39	0.5138	0.0100	0.5143	2771	14	2673	46	2741	28
53Fz-22c	0.66	5.6	0.1999	0.0032	13.85	0.30	0.5058	0.0071	0.4162	2831	13	2638	30	2738	20
53Fz-27c	0.14	4.4	0.2032	0.0029	13.56	0.30	0.4854	0.0073	0.5588	2850	11	2550	32	2718	21
53Cz-31r*	0.89	283.0	0.4180	0.0099	3.63	0.84	0.0645	0.0200	0.8472	3964	19	403	110	1560	110

Appendix E. (cont)

			Isotope ratios							Age (Ma)					
	Th/U	^{204}Pb	^{207*}Pb/^{206*}Pb	2σ	^{207*}Pb/^{235}U	2σ	^{206*}Pb/^{238}U	2σ	Err. Corr.	^{207*}Pb/^{206*}Pb	2σ	^{206*}Pb/^{238}U	2σ	^{207*}Pb/^{235}U	2σ
71: K-feldspar-flooded granodiorite															
71Pz-2c*	0.22	39.8	0.1202	0.0047	3.49	0.91	0.2115	0.0350	0.4907	1957	16	1237	160	1523	110
71Pz-31c*	0.53	21.6	0.1276	0.0022	4.63	0.13	0.2646	0.0054	0.7024	2060	12	1513	27	1756	23
71Pz-9c*	0.29	86.0	0.1408	0.0026	5.81	0.22	0.2986	0.0093	0.9599	2230	13	1684	46	1947	32
71Dz-14c*	0.30	13.6	0.1461	0.0025	6.33	0.15	0.3135	0.0054	0.9114	2298	11	1757	27	2020	23
71Pz-23c*	0.54	35.6	0.1503	0.0025	6.28	0.19	0.3032	0.0072	0.8739	2350	5	1707	35	2015	24
71Dz-6c*	0.32	5.5	0.1553	0.0023	7.23	0.18	0.3348	0.0076	0.9160	2407	7	1861	37	2139	24
71Pz-5c*	0.21	64.4	0.1568	0.0027	6.09	0.16	0.2784	0.0056	0.9303	2421	13	1587	28	1986	22
71Pz-18c*	0.46	3.9	0.1580	0.0022	7.16	0.13	0.3262	0.0056	0.7882	2433	8	1820	27	2131	16
71Pz-6c	0.31	6.8	0.1576	0.0032	7.80	0.33	0.3592	0.0110	0.8704	2433	13	1977	49	2206	34
71Pz-12c	0.44	4.6	0.1590	0.0025	7.74	0.24	0.3539	0.0083	0.9341	2446	12	1956	39	2199	27
71Pz-32c*	0.35	49.8	0.1686	0.0028	6.67	0.30	0.2857	0.0120	0.8224	2545	16	1620	57	2067	34
71Pz-24c	0.31	4.5	0.1724	0.0025	10.16	0.17	0.4279	0.0073	0.6982	2581	6	2296	31	2449	15
71Dz-5c2	0.40	7.4	0.1802	0.0029	11.52	0.37	0.4610	0.0130	0.8900	2652	12	2449	57	2567	33
71Dz-25c1*	0.49	19.3	0.1813	0.0028	12.13	0.35	0.4800	0.0130	0.9313	2665	7	2525	56	2610	27
71Pz-23r	0.30	2.5	0.1858	0.0029	13.84	0.23	0.5396	0.0067	0.6527	2710	8	2782	28	2740	15
71Pz-11c*	0.17	17.0	0.1867	0.0032	12.59	0.30	0.4878	0.0100	0.8480	2713	11	2559	45	2649	22
71Dz-25c3*	0.62	20.9	0.1876	0.0029	13.75	0.18	0.5278	0.0061	0.5983	2723	7	2732	26	2732	13
71Dz-25c2*	0.17	8.9	0.1902	0.0032	12.75	0.21	0.4843	0.0072	0.7529	2750	10	2545	31	2660	15
71Dz-34c*	0.22	0.2	0.1928	0.0049	13.50	0.69	0.5010	0.0210	0.8858	2764	27	2617	94	2710	64
71Dz-5c1	0.44	4.0	0.1969	0.0032	12.32	0.18	0.4503	0.0067	0.7282	2794	10	2396	28	2629	14
71Pz-29r	0.31	6.3	0.1982	0.0032	13.51	0.22	0.4969	0.0068	0.5140	2811	10	2600	29	2715	16
71Dz-27r	0.49	5.5	0.1999	0.0030	13.09	0.26	0.4733	0.0088	0.9281	2823	6	2496	39	2684	18
71Dz-18c	0.47	1.3	0.2016	0.0033	14.09	0.24	0.5083	0.0083	0.8131	2836	10	2654	35	2754	16
71Pz-7r	0.25	1.7	0.2027	0.0029	15.41	0.24	0.5492	0.0086	0.6701	2841	8	2821	36	2840	16
71Dz-15r	0.30	1.2	0.2025	0.0033	15.62	0.23	0.5540	0.0077	0.7720	2843	12	2841	32	2854	16
71Pz-16c	0.52	1.5	0.2028	0.0039	16.55	0.34	0.5924	0.0110	0.7161	2844	12	2997	44	2909	20
71Pz-17r	0.38	2.1	0.2015	0.0036	15.51	0.26	0.5556	0.0078	0.6226	2844	10	2848	33	2848	16
71Dz-1c2	0.21	1.5	0.2024	0.0038	15.38	0.33	0.5531	0.0099	0.8792	2846	13	2837	41	2840	20
71Dz-29c	0.45	3.4	0.2024	0.0032	13.99	0.23	0.5010	0.0080	0.6096	2847	11	2618	34	2748	15
71Pz-22c	0.32	3.3	0.2015	0.0034	13.88	0.36	0.4922	0.0110	0.6751	2847	11	2579	47	2739	26
71Pz-26c	0.42	0.4	0.2039	0.0035	16.31	0.23	0.5808	0.0079	0.4397	2854	9	2955	32	2896	14
71Dz-22c	0.39	4.6	0.2045	0.0034	15.66	0.34	0.5550	0.0110	0.9248	2856	7	2845	45	2857	21
71Dz-7c	0.29	0.8	0.2036	0.0034	15.76	0.25	0.5584	0.0089	0.6426	2857	9	2859	37	2860	15
71Dz-8r	0.30	2.5	0.2037	0.0035	16.30	0.34	0.5770	0.0110	0.8464	2857	8	2934	47	2891	20
71Dz-24c	0.30	0.7	0.2042	0.0034	14.19	0.33	0.5007	0.0100	0.4735	2858	10	2616	45	2762	24

Appendix E. (cont)

	Isotope ratios									Age (Ma)					
	Th/U	^{204}Pb	^{207*}Pb/^{206*}Pb	2σ	^{207*}Pb/^{235}U	2σ	^{206*}Pb/^{238}U	2σ	Err. Corr.	^{207*}Pb/^{206*}Pb	2σ	^{206*}Pb/^{238}U	2σ	^{207*}Pb/^{235}U	2σ
71Dz-33r	0.30	1.1	0.2040	0.0029	15.86	0.18	0.5631	0.0073	0.8099	2858	6	2883	30	2867	11
71Dz-20r	0.47	1.0	0.2042	0.0034	16.39	0.29	0.5823	0.0086	0.8686	2859	7	2962	36	2898	16
71Dz-23c	0.37	0.8	0.2039	0.0029	16.35	0.19	0.5792	0.0080	0.7496	2859	5	2945	33	2899	12
71Pz-30c	0.45	1.5	0.2041	0.0033	17.75	0.44	0.6293	0.0150	0.7784	2859	8	3151	61	2974	25
71Dz-13c	0.35	0.0	0.2039	0.0034	15.84	0.22	0.5611	0.0071	0.5670	2859	7	2871	27	2866	13
71Dz-28c	0.36	1.7	0.2049	0.0032	15.60	0.39	0.5549	0.0130	0.6226	2860	10	2845	56	2852	27
71Pz-8r	0.35	1.3	0.2037	0.0033	15.80	0.33	0.5611	0.0110	0.7576	2860	9	2870	46	2863	21
71Pz-4c	0.23	0.8	0.2043	0.0033	16.64	0.24	0.5914	0.0094	0.4171	2861	9	2998	36	2914	14
71Dz-10c	0.38	1.2	0.2047	0.0032	15.83	0.18	0.5602	0.0067	0.6626	2863	7	2867	28	2866	11
71Pz-3c	0.21	1.1	0.2043	0.0035	16.61	0.25	0.5910	0.0075	0.6508	2863	10	2993	31	2911	14
71Dz-26c	0.46	2.6	0.2045	0.0036	15.85	0.27	0.5658	0.0092	0.6186	2864	8	2890	39	2869	17
71Dz-24r	0.37	4.0	0.2050	0.0032	15.00	0.19	0.5304	0.0068	0.6746	2865	6	2747	29	2814	12
71Dz-32r	0.32	1.0	0.2056	0.0029	15.82	0.19	0.5608	0.0066	0.6467	2866	6	2870	26	2865	11
71Dz-1c1	0.27	0.7	0.2052	0.0039	15.87	0.25	0.5651	0.0069	0.4300	2867	10	2887	28	2871	15
71Pz-14c	0.69	9.2	0.2058	0.0038	14.35	0.36	0.5093	0.0100	0.0331	2868	18	2653	47	2776	26
71Pz-29c	0.22	5.2	0.2052	0.0037	13.39	0.25	0.4653	0.0064	0.4259	2868	11	2463	28	2706	18
71Pz-32r	0.25	7.7	0.2073	0.0036	15.05	0.33	0.5312	0.0085	0.5779	2879	11	2746	34	2818	20
71Dz-11c	0.36	2.9	0.2073	0.0039	15.74	0.35	0.5564	0.0100	0.4511	2886	12	2851	42	2859	22

Appendix E. (cont)

			Isotope ratios							Age (Ma)					
	Th/U	^{204}Pb	^{207*}Pb/^{206*}Pb	2σ	^{207*}Pb/^{235}U	2σ	^{206*}Pb/^{238}U	2σ	Err. Corr.	^{207*}Pb/^{206*}Pb	2σ	^{206*}Pb/^{238}U	2σ	^{207*}Pb/^{235}U	2σ
Skinner Lake block															
41: Tonalite containing bleby pegmatite															
41z-30c*	0.13	2.4	0.1905	0.0026	12.69	0.29	0.4896	0.0098	0.7341	2746	9	2568	41	2656	22
41z-24r1	0.02	2.4	0.1994	0.0022	14.99	0.31	0.5470	0.0110	0.8362	2818	9	2810	45	2813	20
41z-3r	0.23	2.1	0.1986	0.0023	14.93	0.25	0.5471	0.0082	0.8808	2823	8	2813	35	2810	15
41z-32c	0.33	0.5	0.2008	0.0018	13.61	0.35	0.4919	0.0130	0.8080	2828	9	2585	54	2727	23
41z-36c	0.37	0.7	0.2001	0.0016	15.90	0.13	0.5762	0.0040	0.6347	2829	5	2933	16	2870	8
41z-9r	0.38	-0.3	0.2010	0.0024	16.21	0.22	0.5845	0.0062	0.6919	2833	8	2967	25	2891	13
41z-34r	0.30	3.3	0.2016	0.0017	15.22	0.18	0.5502	0.0067	0.8978	2834	6	2832	28	2831	12
41z-30r2	0.53	1.5	0.2018	0.0019	16.04	0.16	0.5760	0.0054	0.5990	2841	7	2932	22	2879	9
41z-21r1	0.29	0.8	0.2003	0.0027	15.43	0.22	0.5571	0.0058	0.4285	2844	10	2857	24	2842	14
41z-12r	0.07	1.9	0.2029	0.0029	12.27	0.32	0.4420	0.0100	0.5567	2849	12	2359	45	2624	22
41z-35r*	0.33	0.6	0.2030	0.0015	15.64	0.11	0.5588	0.0043	0.5982	2850	9	2862	18	2855	7
41z-16c	0.31	1.8	0.2033	0.0031	15.79	0.27	0.5627	0.0060	0.5612	2855	12	2878	25	2863	16
41z-34c	0.08	5.6	0.2044	0.0016	14.66	0.20	0.5195	0.0073	0.8200	2858	6	2697	31	2793	13
41z-1c	0.16	0.6	0.2049	0.0022	16.29	0.16	0.5781	0.0065	0.5741	2862	7	2940	25	2893	9
41z-22	0.22	2.2	0.2047	0.0029	15.84	0.33	0.5624	0.0095	0.5602	2863	11	2876	38	2866	19
41z-13r1	0.14	1.1	0.2052	0.0025	16.09	0.23	0.5732	0.0056	0.7467	2869	18	2920	23	2880	13
41z-7r2	0.08	2.2	0.2054	0.0020	15.97	0.17	0.5645	0.0058	0.5671	2871	9	2885	23	2875	10
41z-10c	0.25	0.5	0.2068	0.0026	15.98	0.24	0.5608	0.0073	0.7075	2879	9	2875	31	2874	14
41z-8c	0.09	4.5	0.2067	0.0028	15.76	0.35	0.5537	0.0120	0.5662	2879	14	2840	50	2861	23
41z-18c	0.12	1.1	0.2067	0.0025	15.41	0.17	0.5453	0.0048	0.3522	2880	8	2805	20	2842	10
41z-27c	0.30	1.6	0.2072	0.0023	16.07	0.21	0.5646	0.0059	0.5157	2884	10	2885	24	2886	12
41z-13c	0.50	2.1	0.2075	0.0028	16.29	0.31	0.5770	0.0080	0.4078	2886	21	2936	32	2893	18
41z-4c	0.46	1.5	0.2069	0.0020	16.11	0.17	0.5677	0.0062	0.5422	2887	9	2898	26	2883	10
41z-14c	0.09	2.7	0.2074	0.0029	14.87	0.32	0.5221	0.0082	0.8115	2889	10	2707	35	2807	20
41z-25c	0.69	2.2	0.2087	0.0028	15.08	0.24	0.5267	0.0063	0.3431	2891	10	2727	23	2819	15
41z-2r	0.07	12.8	0.2080	0.0021	16.05	0.24	0.5653	0.0088	0.8750	2893	8	2888	37	2883	15
41z-20c	0.44	0.8	0.2086	0.0027	15.86	0.32	0.5640	0.0089	0.8819	2894	10	2880	37	2866	18
41z-15	0.27	2.2	0.2077	0.0029	16.35	0.23	0.5669	0.0056	0.4634	2897	10	2895	23	2898	13
41z-28	0.42	0.3	0.2084	0.0023	16.34	0.18	0.5693	0.0065	0.4959	2898	8	2905	27	2896	11
41z-3c	0.08	0.0	0.2094	0.0022	17.36	0.29	0.6041	0.0099	0.6949	2899	10	3046	41	2960	17
41z-7r1	0.21	9.4	0.2139	0.0023	16.72	0.24	0.5704	0.0090	0.6658	2932	8	2909	37	2918	14
41z-11c	0.36	0.6	0.2151	0.0030	17.36	0.24	0.5817	0.0070	0.5457	2955	10	2955	29	2956	13
41z-7c	0.37	5.6	0.2225	0.0023	18.16	0.22	0.5915	0.0072	0.7114	2996	10	2995	29	2997	12
41z-35c*	0.46	9.9	0.2366	0.0024	15.96	0.16	0.4939	0.0064	0.2540	3087	15	2587	27	2874	9

Appendix E. (cont)

			Isotope ratios							Age (Ma)					
	Th/U	^{204}Pb	^{207*}Pb/^{206*}Pb	2σ	^{207*}Pb/^{235}U	2σ	^{206*}Pb/^{238}U	2σ	Err. Corr.	^{207*}Pb/^{206*}Pb	2σ	^{206*}Pb/^{238}U	2σ	^{207*}Pb/^{235}U	2σ
43: K-feldspar augen gneiss															
43-3-r*	0.20	308.0	0.1384	0.0015	4.64	0.07	0.2448	0.0031	0.8871	2206	7	1412	16	1755	13
43-20-c*	0.53	600.0	0.1440	0.0022	5.71	0.21	0.2877	0.0078	0.8970	2278	10	1630	38	1933	30
43-13-r2*	0.19	287.0	0.1610	0.0017	6.28	0.13	0.2819	0.0053	0.9215	2465	5	1602	26	2015	17
43-23-c*	0.05	121.0	0.1704	0.0019	7.72	0.14	0.3287	0.0045	0.8500	2560	4	1832	22	2199	16
43-20-r*	0.20	364.0	0.1761	0.0021	9.43	0.22	0.3896	0.0074	0.7048	2611	7	2120	33	2380	20
43-10-r	0.12	190.0	0.1876	0.0026	12.23	0.38	0.4753	0.0120	0.7557	2717	9	2507	55	2622	37
43-6-c	0.11	190.0	0.1867	0.0026	14.71	0.54	0.5717	0.0170	0.5948	2718	17	2914	74	2796	43
43-6-r	0.28	-51.0	0.1870	0.0024	13.60	0.22	0.5272	0.0066	0.3770	2723	17	2729	27	2722	14
43-21-r	0.07	208.0	0.1882	0.0026	9.61	0.54	0.3714	0.0160	0.9299	2727	9	2035	73	2397	44
43-13-r1	0.13	19.0	0.1878	0.0022	14.31	0.27	0.5496	0.0077	0.8768	2733	7	2823	33	2769	19
43-22-r	0.32	110.0	0.1897	0.0022	12.34	0.25	0.4743	0.0081	0.9348	2735	6	2502	36	2632	19
43-19-r2	0.12	219.0	0.1891	0.0022	12.58	0.32	0.4806	0.0110	0.9179	2736	8	2529	45	2648	22
43-3-c	0.13	-3.0	0.1888	0.0029	13.37	0.50	0.5119	0.0130	0.5813	2737	12	2664	56	2706	37
43-10-c	0.06	46.0	0.1896	0.0029	13.38	0.48	0.5110	0.0140	0.5865	2737	8	2661	63	2707	43
43-21-c	0.67	32.0	0.1898	0.0025	13.81	0.54	0.5300	0.0180	0.9696	2741	14	2735	82	2736	46
43-16-r	0.15	-11.0	0.1903	0.0023	13.84	0.28	0.5289	0.0098	0.7441	2746	12	2736	43	2738	20
43-15-r	0.11	9.0	0.1909	0.0022	14.15	0.28	0.5339	0.0086	0.6035	2765	13	2758	35	2764	18
43-13-c	0.54	7.0	0.1995	0.0024	15.14	0.23	0.5488	0.0058	0.6198	2820	6	2820	24	2823	14
43-22-c	0.09	71.0	0.2000	0.0021	16.00	0.22	0.5778	0.0059	0.7087	2827	4	2940	24	2877	13
43-14-r	0.12	8.0	0.2009	0.0021	16.00	0.22	0.5774	0.0058	0.7811	2833	4	2938	23	2879	13
43-24-r	0.07	-25.0	0.2011	0.0022	16.08	0.23	0.5795	0.0063	0.6192	2836	5	2947	26	2881	14
43-24-rb	0.11	49.0	0.2014	0.0024	15.44	0.22	0.5541	0.0065	0.6487	2841	8	2842	27	2842	14
43-8-r	0.19	94.0	0.2035	0.0021	15.67	0.22	0.5570	0.0064	0.7743	2852	10	2854	26	2857	13
43-16-c	1.11	90.0	0.2059	0.0041	16.94	0.58	0.5969	0.0110	0.7434	2869	10	3017	44	2930	30
43-19-c	0.24	144.0	0.2061	0.0023	15.98	0.52	0.5629	0.0160	0.8334	2872	9	2877	69	2874	37
43-14-c	0.06	328.0	0.2067	0.0025	14.94	0.35	0.5274	0.0120	0.4074	2878	11	2730	50	2811	21
43-8-c	0.35	-64.0	0.2069	0.0023	16.02	0.27	0.5610	0.0077	0.6527	2878	27	2890	31	2877	15
43-15-c	0.40	210.0	0.2067	0.0023	15.58	0.26	0.5468	0.0079	0.8587	2879	6	2815	33	2850	16
43-24-c	0.97	170.0	0.2071	0.0032	15.08	0.32	0.5311	0.0099	0.2189	2883	18	2749	43	2821	22

Appendix E. (cont)

			Isotope ratios							Age (Ma)					
	Th/U	^{204}Pb	^{207*}Pb/^{206*}Pb	2σ	^{207*}Pb/^{235}U	2σ	^{206*}Pb/^{238}U	2σ	Err. Corr.	^{207*}Pb/^{206*}Pb	2σ	^{206*}Pb/^{238}U	2σ	^{207*}Pb/^{235}U	2σ
Wharram Lake block															
55: Equigranular granodiorite															
55z-4r	0.18	0.6	0.1814	0.0039	13.25	0.25	0.5319	0.0096	0.4272	2664	14	2749	41	2697	18
55z-1c	0.13	1.9	0.1814	0.0042	11.56	0.33	0.4580	0.0120	0.7279	2670	16	2432	52	2567	27
55z-27r	0.07	1.0	0.1822	0.0033	12.82	0.63	0.5110	0.0220	0.7116	2672	17	2672	100	2666	55
55z-15r	0.15	2.3	0.1823	0.0030	14.20	0.22	0.5707	0.0077	0.6348	2676	9	2910	32	2762	15
55z-25c	0.24	8.8	0.1834	0.0046	8.12	1.20	0.3240	0.0400	0.9667	2683	18	1807	180	2242	110
55z-6r	0.10	5.9	0.1836	0.0033	13.17	0.26	0.5232	0.0079	0.6376	2692	13	2717	34	2690	19
55z-10r	0.12	1.1	0.1866	0.0032	13.41	0.22	0.5229	0.0100	0.5889	2713	11	2711	42	2708	15
55z-26r	0.17	1.8	0.1873	0.0050	13.39	0.62	0.5222	0.0150	0.4684	2725	18	2708	60	2706	39
55z-22c	0.09	2.9	0.1901	0.0040	13.60	0.68	0.5250	0.0160	0.8673	2736	14	2718	68	2721	44
55z-14r*	0.16	3.4	0.1904	0.0030	13.90	0.36	0.5316	0.0110	0.8578	2747	9	2748	48	2742	24
55z-13r*	0.05	3.0	0.1976	0.0035	14.99	0.27	0.5483	0.0098	0.6436	2818	11	2817	40	2814	17
55z-3r1*	0.21	5.5	0.2073	0.0041	15.85	0.52	0.5630	0.0140	0.8888	2877	13	2875	58	2870	32
55z-7r	0.12	2.9	0.2094	0.0039	19.41	0.76	0.6714	0.0200	0.6690	2905	17	3311	78	3062	43
55z-18r	0.36	2.7	0.2118	0.0041	16.74	0.28	0.5777	0.0071	0.1399	2917	17	2939	29	2920	17
55z-21c1	0.43	1.7	0.2109	0.0035	17.50	0.46	0.6040	0.0180	0.7377	2923	16	3043	71	2961	26
55z-8c	0.29	2.5	0.2116	0.0039	17.29	0.34	0.5990	0.0110	0.5756	2925	11	3025	46	2950	19
55z-6c	0.11	3.4	0.2131	0.0037	17.45	0.36	0.5979	0.0100	0.7364	2931	10	3021	42	2959	17
55z-12c	0.39	0.3	0.2133	0.0042	17.48	0.26	0.5976	0.0085	0.4709	2936	15	3020	27	2961	14
55z-19c	0.27	0.6	0.2147	0.0038	17.72	0.38	0.6071	0.0130	0.6101	2938	13	3058	45	2974	18
55z-21r	0.10	1.6	0.2139	0.0039	17.75	0.33	0.6085	0.0110	0.6942	2938	11	3063	43	2978	17
55z-21c2	0.42	1.1	0.2147	0.0045	16.71	0.39	0.5630	0.0120	0.7130	2943	14	2877	50	2916	23
55z-4c	0.14	-0.8	0.2163	0.0048	17.22	0.32	0.5798	0.0100	0.3230	2945	14	2947	41	2946	18
55z-15c	0.21	0.7	0.2190	0.0032	18.06	0.20	0.5976	0.0096	0.6044	2966	6	3020	38	2993	10
55z-25r	0.17	21.7	0.2195	0.0049	17.34	0.58	0.5801	0.0120	0.5417	2968	17	2949	50	2953	36
55z-27c	0.30	10.1	0.2200	0.0034	17.91	0.34	0.5890	0.0120	0.6360	2977	18	2985	50	2984	18

Appendix E. (cont)

			Isotope ratios							Age (Ma)					
	Th/U	^{204}Pb	^{207*}Pb/^{206*}Pb	2σ	^{207*}Pb/^{235}U	2σ	^{206*}Pb/^{238}U	2σ	Err. Corr.	^{207*}Pb/^{206*}Pb	2σ	^{206*}Pb/^{238}U	2σ	^{207*}Pb/^{235}U	2σ
North Caribou batholith "pluton"															
46: Foliated granodiorite															
46z-18c	0.52	3.7	0.2021	0.0033	18.55	0.36	0.6631	0.0120	0.9218	2842	4	3278	46	3019	20
46z-21r	0.22	3.9	0.2024	0.0034	15.56	0.26	0.5578	0.0076	0.7940	2849	5	2857	32	2852	16
46z-20c	0.20	1.3	0.2027	0.0037	15.88	0.45	0.5678	0.0120	0.7854	2854	5	2899	52	2869	31
46z-8c	0.24	2.1	0.2033	0.0036	16.16	0.25	0.5761	0.0071	0.6464	2857	5	2932	29	2886	15
46z-17c	0.43	9.3	0.2043	0.0034	15.71	0.24	0.5597	0.0068	0.6999	2862	6	2865	26	2861	15
46z-19c	0.57	1.0	0.2050	0.0035	15.78	0.31	0.5599	0.0078	0.8903	2864	7	2866	32	2862	18
46z-2c	0.55	1.1	0.2053	0.0046	16.71	0.31	0.5878	0.0084	0.4634	2870	8	2979	34	2916	18
46z-2r	0.16	1.2	0.2053	0.0045	16.59	0.36	0.5858	0.0073	0.5325	2872	7	2972	30	2911	20
46z-27c	0.16	1.0	0.2052	0.0034	16.79	0.26	0.5902	0.0090	0.8201	2872	5	2989	36	2923	15
46z-9c	0.36	2.5	0.2058	0.0035	17.49	0.29	0.6178	0.0075	0.7302	2873	5	3100	30	2961	15
46z-22c	0.21	1.7	0.2064	0.0034	16.01	0.28	0.5634	0.0073	0.7307	2878	4	2880	30	2876	16
46z-4c	0.31	-0.7	0.2079	0.0049	15.92	0.46	0.5617	0.0097	0.4373	2879	10	2874	39	2871	25
46z-15c	0.19	1.9	0.2073	0.0035	16.59	0.28	0.5853	0.0120	0.7717	2880	5	2970	41	2913	17
46z-11c	0.34	0.0	0.2076	0.0037	17.01	0.25	0.6001	0.0069	0.5766	2883	7	3030	28	2935	14
46z-1r	0.32	3.2	0.2075	0.0040	16.91	0.35	0.5926	0.0099	0.7599	2889	4	2999	40	2928	20
46z-5r	0.28	14.7	0.2099	0.0046	14.86	0.39	0.5170	0.0100	0.7709	2905	5	2690	42	2801	25
46z-23r*	0.29	7.0	0.2110	0.0035	15.20	0.29	0.5230	0.0089	0.7640	2916	6	2711	39	2827	19
46z-25c*	0.18	0.0	0.2164	0.0035	18.45	0.24	0.6192	0.0059	0.6848	2957	4	3107	22	3013	13
46z-16c	0.26	2.2	0.2227	0.0036	18.29	0.26	0.5935	0.0073	0.7787	3005	6	3003	30	3004	13

Appendix E. (cont)

			Isotope ratios							Age (Ma)					
	Th/U	^{204}Pb	^{207*}Pb/^{206*}Pb	2σ	^{207*}Pb/^{235}U	2σ	^{206*}Pb/^{238}U	2σ	Err. Corr.	^{207*}Pb/^{206*}Pb	2σ	^{206*}Pb/^{238}U	2σ	^{207*}Pb/^{235}U	2σ
49: Leucocratic granodiorite															
49z-1r*	0.15	21.0	0.1754	0.0045	8.31	0.39	0.3511	0.0110	0.8384	2615	18	1940	51	2280	38
49z-31r	0.07	0.4	0.2039	0.0019	16.16	0.23	0.5788	0.0096	0.6426	2859	6	2949	39	2886	14
49z-16r	0.03	1.6	0.2050	0.0022	16.03	0.23	0.5719	0.0110	0.6885	2873	10	2915	45	2878	14
49z-26r	0.05	9.5	0.2069	0.0018	14.86	0.27	0.5237	0.0120	0.8590	2886	7	2714	48	2808	14
49z-2r	0.06	19.0	0.2100	0.0024	14.77	0.42	0.5168	0.0150	0.6831	2904	9	2685	64	2800	26
49z-14r	0.11	6.0	0.2162	0.0028	13.28	0.22	0.4537	0.0081	0.5868	2940	9	2411	36	2700	15
49z-10r	0.02	48.0	0.2183	0.0035	17.15	0.68	0.5800	0.0270	0.5048	2964	28	2947	120	2943	44
49z-23c	0.45	1.6	0.2223	0.0026	15.02	0.43	0.4937	0.0120	0.6704	2998	9	2586	53	2819	25
49z-25c	0.60	3.3	0.2264	0.0024	15.61	0.23	0.5045	0.0085	0.7097	3026	7	2633	37	2855	14
49z-22c	0.31	5.7	0.2287	0.0038	15.32	0.53	0.5000	0.0160	0.8403	3044	11	2612	72	2835	36
49z-9c	0.25	0.9	0.2298	0.0024	10.47	0.51	0.3381	0.0190	0.7324	3049	9	1877	90	2477	40
49z-17c*	1.06	25.5	0.2293	0.0025	1.43	0.59	0.0466	0.0190	0.9896	3049	14	293	110	895	150
49z-31c*	0.53	3.8	0.2342	0.0039	18.84	0.37	0.5911	0.0100	0.2267	3077	19	2994	41	3033	19
49z-18c	0.22	3.3	0.2377	0.0026	4.40	1.30	0.1381	0.0400	0.9821	3103	21	833	200	1709	130
49z-18r	0.30	7.9	0.2420	0.0026	9.08	0.29	0.2803	0.0087	0.5854	3124	11	1593	41	2346	30
49z-30c	0.49	2.0	0.2409	0.0023	20.74	0.40	0.6252	0.0130	0.8321	3134	9	3130	52	3125	18
49z-15c	0.88	8.6	0.2426	0.0024	19.78	0.82	0.5980	0.0270	0.9397	3137	8	3020	110	3080	41
49z-7c	0.38	0.6	0.2427	0.0028	20.97	0.34	0.6350	0.0100	0.7763	3139	15	3167	40	3136	15
49z-5c	0.78	10.2	0.2439	0.0028	9.16	1.60	0.2760	0.0460	0.9953	3140	8	1570	210	2340	110
49z-29c	0.32	2.9	0.2440	0.0025	18.52	0.33	0.5557	0.0130	0.8249	3145	10	2848	51	3016	18
49z-11c	0.62	1.6	0.2444	0.0020	21.08	0.25	0.6298	0.0100	0.8273	3150	6	3149	40	3142	12
49z-12c	0.75	1.5	0.2444	0.0025	21.18	0.37	0.6318	0.0120	0.8653	3151	8	3156	48	3146	17
49z-24c	0.49	3.4	0.2460	0.0031	14.65	0.75	0.4380	0.0220	0.7562	3160	12	2341	100	2791	63
49z-27c	0.46	7.8	0.2467	0.0091	11.45	1.00	0.3384	0.0310	0.7162	3172	24	1878	140	2559	67
49z-6c	0.39	7.3	0.2496	0.0029	18.56	0.61	0.5510	0.0180	0.8801	3178	11	2841	75	3017	30
66: High-strain tonalite															
66z-3c*	0.26	52.0	0.1765	0.0032	7.68	0.39	0.3161	0.0140	0.7287	2614	13	1770	65	2193	39
66z-5c	1.34	15.0	0.1671	0.0031	7.89	0.21	0.3447	0.0087	0.9324	2525	9	1907	41	2214	23
66z-6c*	1.54	21.3	0.1584	0.0026	7.91	0.12	0.3639	0.0055	0.9031	2437	6	2000	26	2219	15
66z-2c	0.56	2.7	0.1849	0.0034	10.51	0.22	0.4157	0.0084	0.7372	2694	7	2240	38	2478	20
66z-7c	0.26	4.5	0.1958	0.0047	13.96	0.27	0.5209	0.0140	0.6323	2784	7	2703	59	2748	19
66z-1c	0.07	0.9	0.2018	0.0039	15.29	0.27	0.5529	0.0065	0.9265	2837	5	2837	27	2837	17

Appendix E. (cont)

			Isotope ratios							Age (Ma)					
	Th/U	^{204}Pb	^{207*}Pb/^{206*}Pb	2σ	^{207*}Pb/^{235}U	2σ	^{206*}Pb/^{238}U	2σ	Err. Corr.	^{207*}Pb/^{206*}Pb	2σ	^{206*}Pb/^{238}U	2σ	^{207*}Pb/^{235}U	2σ
North Caribou batholith "core"															
51: K-feldspar augen gneiss															
51z-2c	1.96	13.1	0.1695	0.0022	7.75	0.26	0.3432	0.0099	0.9562	2552	16	1902	47	2202	27
51z-17c	3.39	1.8	0.1819	0.0019	12.45	0.50	0.5069	0.0210	0.7345	2682	11	2643	92	2642	35
51z-12r	0.63	7.3	0.1886	0.0048	12.87	0.39	0.4996	0.0120	0.4129	2734	34	2612	51	2668	27
51z-13c	0.16	1.1	0.1841	0.0019	13.17	0.23	0.5194	0.0093	0.7893	2695	11	2696	39	2691	17
51z-16c	0.68	1.2	0.1854	0.0023	13.20	0.26	0.5187	0.0130	0.7790	2698	11	2692	55	2692	19
51z-4c	2.18	0.8	0.1855	0.0020	13.24	0.21	0.5229	0.0094	0.7518	2701	11	2711	40	2696	15
51z-9r	1.78	3.7	0.1876	0.0020	13.28	0.21	0.5185	0.0088	0.6199	2721	11	2692	37	2699	15
51z-22c	2.56	3.2	0.1871	0.0019	13.31	0.22	0.5192	0.0110	0.7164	2717	10	2695	39	2701	16
51z-8c	1.75	4.2	0.1885	0.0022	13.63	0.32	0.5256	0.0120	0.6995	2731	10	2722	52	2724	23
51z-15c	1.71	1.0	0.1849	0.0022	13.83	0.27	0.5431	0.0100	0.8032	2694	12	2795	43	2737	19
51z-21c*	0.79	0.6	0.1892	0.0023	13.93	0.21	0.5304	0.0100	0.8222	2741	10	2743	44	2744	15
51z-14r*	0.82	1.7	0.1892	0.0055	13.94	0.31	0.5300	0.0160	0.8568	2737	20	2738	69	2743	19
51z-3c	0.43	1.2	0.2046	0.0025	14.08	0.51	0.5086	0.0190	0.8431	2869	7	2650	82	2755	38
51z-20r	0.29	3.0	0.2039	0.0018	15.37	0.20	0.5533	0.0076	0.6787	2854	6	2839	32	2838	13
51z-6c	0.50	-0.1	0.2037	0.0017	15.51	0.21	0.5563	0.0093	0.6790	2856	9	2851	39	2847	13
51z-19c	0.29	0.9	0.2001	0.0019	16.57	0.17	0.6101	0.0130	0.8267	2827	6	3070	52	2913	10

Appendix E. (cont)

			Isotope ratios							Age (Ma)					
	Th/U	^{204}Pb	^{207*}Pb/^{206*}Pb	2σ	^{207*}Pb/^{235}U	2σ	^{206*}Pb/^{238}U	2σ	Err. Corr.	^{207*}Pb/^{206*}Pb	2σ	^{206*}Pb/^{238}U	2σ	^{207*}Pb/^{235}U	2σ
61: Massive tonalite															
61z-15c	0.53	1.3	0.1979	0.0036	14.68	0.33	0.5410	0.0120	0.8547	2808	11	2787	50	2797	21
61z-26c	0.41	2.1	0.1980	0.0048	15.42	0.32	0.5584	0.0100	0.5636	2816	14	2859	43	2840	20
61z-24r	0.47	0.6	0.1992	0.0063	16.04	0.48	0.5830	0.0150	0.2622	2825	20	2959	61	2887	29
61z-19c	0.50	0.4	0.1998	0.0036	14.76	0.26	0.5347	0.0088	0.4496	2826	11	2761	38	2799	17
61z-18c	0.75	1.9	0.1989	0.0046	16.53	0.57	0.6070	0.0260	0.1873	2827	28	3058	99	2907	30
61z-3c	0.48	2.1	0.1996	0.0032	16.11	0.29	0.5841	0.0120	0.5575	2828	11	2965	50	2885	16
61z-5r	0.39	1.9	0.2010	0.0038	14.44	0.49	0.5240	0.0160	0.7904	2833	23	2716	71	2786	35
61z-28c	0.49	1.6	0.2003	0.0037	16.33	0.35	0.5865	0.0110	0.5159	2834	13	2975	46	2896	20
61z-11c	0.68	-0.1	0.2007	0.0040	15.39	0.37	0.5535	0.0088	0.3280	2835	16	2839	36	2839	21
61z-28r*	0.49	1.0	0.1991	0.0051	16.56	12.00	0.6010	0.0720	0.7092	2835	21	3031	240	2909	140
61z-7r	0.24	0.3	0.2019	0.0038	15.17	0.26	0.5513	0.0086	0.3135	2836	14	2830	36	2825	17
61z-22r	0.42	0.4	0.2036	0.0049	15.29	0.61	0.5520	0.0260	0.7176	2837	19	2829	110	2831	42
61z-16c	0.61	1.3	0.2019	0.0041	16.59	0.39	0.6000	0.0120	0.6465	2839	14	3035	51	2910	23
61z-4c	0.43	2.3	0.2013	0.0032	15.90	0.33	0.5712	0.0120	0.7628	2840	10	2912	49	2870	20
61z-17c	1.57	0.1	0.2025	0.0041	15.67	0.33	0.5657	0.0100	0.5014	2840	13	2889	41	2862	20
61z-6c	0.78	-0.6	0.2030	0.0038	15.60	0.28	0.5553	0.0140	0.0675	2843	21	2847	57	2852	17
61z-1c	0.35	1.1	0.2030	0.0041	15.58	0.25	0.5566	0.0084	0.7651	2846	12	2852	34	2851	15
61z-23c*	0.52	1.6	0.2017	0.0042	14.00	0.46	0.4940	0.0130	0.7835	2847	14	2588	58	2748	34
61z-13c	0.75	1.8	0.2026	0.0037	16.46	0.48	0.5940	0.0170	0.8373	2847	12	3014	69	2901	27
61z-7c	0.35	1.3	0.2036	0.0053	14.96	0.44	0.5420	0.0200	0.7579	2850	16	2788	85	2811	27
61z-25c	0.38	3.9	0.2061	0.0037	15.99	0.27	0.5609	0.0087	0.7183	2872	7	2870	36	2876	16
61z-2c	0.29	0.4	0.2057	0.0041	15.83	0.30	0.5621	0.0170	0.7085	2873	16	2874	68	2866	18
61z-27c	0.42	1.1	0.2096	0.0033	17.47	0.26	0.6061	0.0099	0.6544	2899	11	3054	40	2960	14
61z-20c	0.91	5.1	0.2127	0.0042	15.19	0.34	0.5210	0.0110	0.8828	2931	12	2702	48	2826	22
61z-27r	0.92	0.8	0.2140	0.0043	18.67	0.34	0.6380	0.0110	0.6609	2935	11	3181	43	3027	18

Appendix E. (cont)

	Isotope ratios									Age (Ma)					
	Th/U	^{204}Pb	^{207*}Pb/^{206*}Pb	2σ	^{207*}Pb/^{235}U	2σ	^{206*}Pb/^{238}U	2σ	Err. Corr.	^{207*}Pb/^{206*}Pb	2σ	^{206*}Pb/^{238}U	2σ	^{207*}Pb/^{235}U	2σ
62/63: Gneissic tonalite															
63z-4c*	0.18	4.5	0.1514	0.0014	7.55	0.11	0.3630	0.0072	0.8985	2362	6	1996	34	2180	13
62z-7c*	0.02	22.0	0.1639	0.0021	8.85	0.15	0.3929	0.0071	0.8557	2501	9	2136	33	2321	15
62z-27c*	0.08	5.6	0.1767	0.0028	11.53	0.15	0.4776	0.0073	0.1611	2622	11	2520	34	2567	12
62z-5r*	0.49	3.3	0.1929	0.0020	12.99	0.25	0.4867	0.0093	0.8993	2776	7	2556	40	2678	19
63z-7c*	0.17	0.8	0.1955	0.0031	14.20	0.29	0.5348	0.0098	0.6964	2786	14	2761	41	2761	20
63z-26r1	0.65	0.5	0.1992	0.0037	15.08	0.25	0.5554	0.0100	0.3702	2824	14	2851	42	2818	16
63z-2c	0.30	0.9	0.2013	0.0044	15.41	0.38	0.5574	0.0090	0.3007	2833	17	2856	37	2840	23
62z-18c	0.63	0.9	0.2014	0.0033	15.87	0.27	0.5733	0.0100	0.8345	2833	17	2921	42	2869	16
63z-26r2	0.49	0.1	0.2017	0.0035	15.48	0.27	0.5597	0.0100	0.3843	2834	13	2869	41	2848	17
63z-22r	0.52	0.4	0.2019	0.0044	15.52	0.26	0.5559	0.0100	0.1362	2848	17	2853	44	2849	17
63z-15r	0.66	0.8	0.2028	0.0039	15.45	0.25	0.5553	0.0095	0.3436	2851	14	2847	40	2844	16
62z-19c	0.48	3.1	0.2027	0.0026	14.50	0.22	0.5191	0.0100	0.7420	2851	8	2698	42	2786	14
62z-14c	0.27	2.8	0.2029	0.0036	15.69	0.23	0.5608	0.0095	0.5282	2852	12	2870	39	2858	14
63z-14c	0.70	0.7	0.2040	0.0039	16.32	0.29	0.5865	0.0100	0.3953	2853	13	2975	41	2902	17
62z-25r	0.58	0.0	0.2052	0.0046	15.84	0.27	0.5650	0.0110	0.3054	2854	16	2886	46	2866	16
62z-15r	0.63	0.0	0.2038	0.0027	15.07	0.18	0.5418	0.0089	0.4717	2855	11	2790	37	2818	11
63z-11c	0.20	0.3	0.2037	0.0025	16.01	0.20	0.5738	0.0092	0.5073	2856	8	2923	38	2878	12
62z-4r	0.53	1.0	0.2032	0.0065	15.83	0.49	0.5639	0.0120	0.2324	2856	24	2882	47	2863	30
63z-6r	0.54	0.9	0.2024	0.0036	15.77	0.33	0.5588	0.0120	0.6056	2857	13	2866	47	2866	20
63z-13r	0.67	0.3	0.2035	0.0035	15.71	0.25	0.5586	0.0093	0.1640	2861	13	2861	38	2858	15
62z-12r	0.68	1.5	0.2055	0.0057	15.32	0.45	0.5510	0.0140	0.4361	2862	27	2830	58	2833	28
62z-24c	0.32	1.2	0.2042	0.0030	16.28	0.21	0.5840	0.0097	0.3908	2863	9	2965	39	2892	12
62z-1r	0.68	0.6	0.2054	0.0032	16.09	0.24	0.5727	0.0110	0.4904	2863	13	2918	44	2881	14
62z-3c	0.13	0.2	0.2037	0.0027	16.63	0.19	0.5900	0.0095	0.4406	2864	9	2989	39	2913	11
62z-6c	0.27	3.2	0.2047	0.0026	17.00	0.19	0.6058	0.0097	0.4161	2865	9	3053	39	2934	11
62z-6r	0.57	1.0	0.2054	0.0049	15.58	0.46	0.5516	0.0100	0.5504	2866	18	2831	43	2846	29
63z-10c	0.75	0.9	0.2048	0.0029	16.20	0.22	0.5762	0.0087	0.3029	2867	10	2933	36	2887	13
62z-4c	0.36	1.2	0.2054	0.0029	15.77	0.20	0.5612	0.0088	0.4694	2869	9	2871	36	2863	13
63z-5c	0.62	4.3	0.2054	0.0021	15.83	0.13	0.5603	0.0087	0.6922	2870	7	2867	36	2866	8
62z-24r	0.65	0.6	0.2052	0.0045	15.55	0.25	0.5547	0.0100	0.0843	2870	16	2844	43	2849	15
62z-11r	0.54	1.0	0.2064	0.0035	15.72	0.43	0.5540	0.0160	0.8331	2870	12	2836	68	2854	26
62z-26c	0.34	1.9	0.2060	0.0023	15.62	0.19	0.5555	0.0086	0.6161	2871	8	2848	36	2855	11
63z-20r	0.62	0.7	0.2049	0.0037	15.12	0.26	0.5358	0.0095	0.3934	2871	13	2765	40	2823	17
63z-25c	1.49	2.2	0.2064	0.0047	16.03	0.37	0.5657	0.0097	0.5044	2876	16	2890	40	2877	22
63z-19r	0.59	1.0	0.2071	0.0039	15.60	0.24	0.5484	0.0096	0.1679	2880	13	2818	40	2851	15

Appendix E. (cont)

			Isotope ratios							Age (Ma)					
	Th/U	^{204}Pb	^{207*}Pb/^{206*}Pb	2σ	^{207*}Pb/^{235}U	2σ	^{206*}Pb/^{238}U	2σ	Err. Corr.	^{207*}Pb/^{206*}Pb	2σ	^{206*}Pb/^{238}U	2σ	^{207*}Pb/^{235}U	2σ
62z-27r	0.69	1.1	0.2054	0.0039	15.73	0.32	0.5601	0.0100	0.3676	2880	15	2871	45	2859	19
63z-16r	0.91	0.7	0.2052	0.0044	16.05	0.40	0.5648	0.0110	0.5808	2881	14	2886	46	2880	25
62z-26r	0.38	0.9	0.2063	0.0043	15.29	0.35	0.5397	0.0091	0.5713	2882	13	2782	38	2831	22
62z-2r	0.72	1.1	0.2061	0.0054	16.35	0.39	0.5820	0.0130	0.6334	2885	20	2956	55	2895	23
63z-23r	0.47	0.8	0.2077	0.0046	17.32	0.37	0.6048	0.0120	0.2812	2887	19	3048	47	2950	21
62z-23r	0.49	1.4	0.2090	0.0044	15.96	0.35	0.5560	0.0140	0.5098	2895	21	2850	58	2873	21
63z-9c	1.08	8.6	0.2092	0.0024	16.37	0.51	0.5690	0.0190	0.9492	2900	7	2903	78	2897	30
63z-25r	0.56	2.3	0.2104	0.0059	16.05	0.42	0.5535	0.0120	0.3804	2902	19	2839	51	2878	25
62z-1c	0.26	1.2	0.2170	0.0033	18.19	0.24	0.6086	0.0100	0.5136	2953	10	3064	42	2999	13
63z-24c	0.50	0.3	0.2348	0.0046	21.23	0.41	0.6541	0.0120	0.2680	3094	15	3243	45	3147	19

Appendix E. (cont)

			Isotope ratios							Age (Ma)					
	Th/U	^{204}Pb	^{207*}Pb/^{206*}Pb	2σ	^{207*}Pb/^{235}U	2σ	^{206*}Pb/^{238}U	2σ	Err. Corr.	^{207*}Pb/^{206*}Pb	2σ	^{206*}Pb/^{238}U	2σ	^{207*}Pb/^{235}U	2σ
Libert Lake pluton															
45: Melanocratic granite															
45-z13-c*	0.14	258.0	0.0842	0.0006	2.33	0.06	0.2004	0.0055	0.5004	1295	20	1177	30	1220	21
45-z14-c*	0.12	388.0	0.0897	0.0010	2.30	0.06	0.1860	0.0044	0.3431	1407	31	1100	25	1211	20
45-z7-r*	0.27	496.0	0.1458	0.0009	4.71	0.15	0.2344	0.0071	0.9596	2296	5	1357	36	1767	24
45-z8-r2*	0.74	3120.0	0.1808	0.0007	7.66	0.14	0.3081	0.0066	0.9748	2658	4	1730	33	2191	17
45-z5-r	0.54	67.0	0.1840	0.0013	13.09	0.23	0.5185	0.0095	0.7431	2693	8	2692	41	2688	17
45-z4-c	0.49	80.0	0.1855	0.0013	13.33	0.13	0.5202	0.0073	0.7469	2701	13	2700	31	2702	9
45-z11-c	0.59	30.0	0.1861	0.0012	13.65	0.12	0.5280	0.0075	0.4076	2704	21	2731	31	2725	8
45-z4-r	0.36	5.0	0.1863	0.0015	14.38	0.12	0.5576	0.0079	0.5949	2709	9	2856	33	2774	8
45-z1-r1	0.43	-50.0	0.1877	0.0021	13.76	0.19	0.5282	0.0079	0.2213	2710	22	2734	33	2732	13
45-z1-c2	0.30	25.0	0.1877	0.0017	14.01	0.15	0.5454	0.0076	0.5747	2714	9	2805	32	2751	11
45-z3-c	0.37	-23.0	0.1877	0.0017	14.66	0.13	0.5634	0.0081	0.4626	2723	8	2880	33	2793	9
45-z5-c	0.61	70.0	0.1875	0.0019	13.66	0.16	0.5270	0.0086	0.6577	2724	12	2726	36	2726	10
45-z8-r1	0.58	980.0	0.1884	0.0011	11.50	0.16	0.4432	0.0074	0.9206	2725	11	2363	33	2562	14
45-z9-r	0.26	234.0	0.1881	0.0019	11.46	0.27	0.4390	0.0094	0.8757	2726	25	2344	41	2564	19
45-z10-c	0.45	10.0	0.1876	0.0015	13.85	0.13	0.5317	0.0079	0.1635	2726	17	2748	33	2739	9
45-z11-r	0.61	4.0	0.1877	0.0014	14.53	0.19	0.5636	0.0096	0.4127	2727	14	2881	39	2785	12
45-z1-c1	0.40	0.0	0.1881	0.0021	14.34	0.16	0.5539	0.0081	0.4813	2729	11	2840	34	2772	11
45-z3-r	0.37	102.0	0.1880	0.0015	13.65	0.12	0.5249	0.0075	0.7143	2732	12	2727	31	2725	9
45-z2-r1	0.07	40.0	0.1883	0.0020	14.41	0.15	0.5522	0.0087	0.4145	2732	10	2834	36	2777	10
45-z10-r	0.49	30.0	0.1893	0.0017	13.99	0.14	0.5320	0.0078	0.5954	2739	12	2751	32	2748	9
45-z2-r2	0.17	80.0	0.1909	0.0013	14.19	0.11	0.5352	0.0075	0.5054	2748	6	2763	31	2762	8
45-z6-r*	0.59	80.0	0.1924	0.0017	14.29	0.29	0.5340	0.0120	0.9487	2762	8	2758	49	2767	19
45-z2-r2b*	0.38	444.0	0.1922	0.0012	14.17	0.12	0.5340	0.0073	0.7043	2764	5	2758	31	2762	8
45-z12-r*	0.26	747.0	0.1959	0.0010	11.31	0.18	0.4202	0.0076	0.5619	2788	10	2261	35	2552	16
45-z9-r1*	0.21	225.0	0.1994	0.0013	13.51	0.14	0.4876	0.0072	0.8176	2821	6	2560	31	2715	10
45-z8-c*	0.65	816.0	0.2002	0.0018	12.96	0.15	0.4700	0.0076	0.7084	2830	7	2483	33	2678	11
45-z9-c	0.51	133.0	0.2057	0.0018	15.59	0.21	0.5490	0.0092	0.4798	2872	12	2825	39	2851	13
45-z2-c	0.17	171.0	0.2144	0.0022	17.23	0.35	0.5790	0.0130	0.8499	2945	9	2945	52	2945	19
45-z7-c*	0.29	2460.0	0.2395	0.0042	17.15	0.48	0.5126	0.0100	0.7664	3120	16	2667	43	2942	32
45-z7-r1*	0.41	2690.0	0.2926	0.0050	22.90	0.47	0.5593	0.0100	0.5893	3437	19	2863	42	3221	19

Appendix E. (cont)

			Isotope ratios							Age (Ma)					
	Th/U	^{204}Pb	^{207*}Pb/^{206*}Pb	2σ	^{207*}Pb/^{235}U	2σ	^{206*}Pb/^{238}U	2σ	Err. Corr.	^{207*}Pb/^{206*}Pb	2σ	^{206*}Pb/^{238}U	2σ	^{207*}Pb/^{235}U	2σ
Pegmatites															
54: K-feldspar pegmatite; adapted methodology															
54z-14c*	0.16	22.4	0.1201	0.0019	3.95	0.17	0.2386	0.0081	0.8665	1951	19	1379	30	1624	15
54z-5r*	0.16	36.0	0.1182	0.0010	4.05	0.18	0.2490	0.0110	0.8170	1932	22	1433	23	1645	14
54z-28c*	0.16	64.3	0.1353	0.0013	4.65	0.22	0.2490	0.0120	0.8799	2171	17	1434	19	1758	12
54z-4*	0.15	64.0	0.1441	0.0013	5.14	0.20	0.2600	0.0120	0.6161	2300	23	1492	26	1841	20
54z-12*	0.14	38.0	0.1398	0.0020	6.45	0.21	0.3340	0.0100	0.9806	2230	8	1855	69	2038	51
54z-1*	0.12	16.8	0.1485	0.0013	6.46	0.42	0.3160	0.0230	0.9286	2322	37	1770	24	2039	16
54z-19c1*	0.11	8.5	0.1466	0.0016	6.49	0.30	0.3210	0.0110	0.7689	2320	24	1795	27	2044	18
54z-5c*	0.15	26.5	0.1466	0.0012	6.61	0.26	0.3290	0.0110	0.4161	2299	29	1834	20	2060	12
54z-19c2*	0.14	6.5	0.1496	0.0019	6.62	0.33	0.3230	0.0150	0.7709	2349	41	1802	33	2061	28
54z-14r*	0.16	18.0	0.1459	0.0013	6.75	0.29	0.3360	0.0130	0.8109	2301	15	1866	29	2079	19
54z-10r*	0.14	12.6	0.1586	0.0013	7.15	0.29	0.3270	0.0100	0.9340	2441	13	1824	24	2130	15
54z-13r*	0.17	5.4	0.1538	0.0014	7.70	0.25	0.3630	0.0120	0.4672	2388	26	1997	21	2196	10
54z-23r*	0.13	24.0	0.1642	0.0016	8.78	0.25	0.3900	0.0110	0.9703	2501	5	2119	56	2311	29
54z-29r*	0.15	23.7	0.1633	0.0026	8.82	0.42	0.3930	0.0100	0.8586	2475	23	2135	43	2319	35
54z-6c	0.09	-0.3	0.1710	0.0017	8.97	0.77	0.3820	0.0180	0.3389	2544	54	2087	41	2332	22
54z-24c	0.14	20.4	0.1685	0.0016	9.80	0.53	0.4240	0.0140	0.5557	2539	31	2277	37	2415	20
54z-9c	0.14	23.3	0.1710	0.0016	10.15	0.38	0.4310	0.0160	0.9044	2568	11	2309	38	2447	20
54z-20r	0.14	56.2	0.1736	0.0018	10.39	0.41	0.4360	0.0120	0.9032	2592	13	2333	30	2475	14
54z-10c2	0.14	7.9	0.1764	0.0019	11.11	0.43	0.4570	0.0130	0.8415	2618	16	2425	75	2531	47
54z-10c1	0.09	1.6	0.1778	0.0018	11.26	0.23	0.4646	0.0054	0.0900	2631	18	2460	43	2545	24
54z-13c	0.15	7.2	0.1716	0.0017	11.30	0.24	0.4687	0.0083	0.8003	2574	9	2478	31	2548	15
54z-21r	0.16	15.0	0.1780	0.0021	11.92	0.42	0.4860	0.0130	0.7351	2638	16	2552	61	2597	27
54z-15c	0.13	42.9	0.1756	0.0016	12.18	0.36	0.5020	0.0140	0.9726	2610	6	2623	56	2617	24
54z-18c	0.11	11.9	0.1760	0.0020	12.29	0.21	0.5059	0.0085	0.4756	2611	12	2639	33	2627	15
54z-2c	0.13	79.6	0.1749	0.0016	12.77	0.21	0.5302	0.0085	0.9382	2603	6	2741	46	2662	18
54z-23c	0.16	13.6	0.1803	0.0019	13.51	0.27	0.5464	0.0083	0.5674	2667	14	2810	79	2716	43
54z-26r	0.13	55.7	0.1790	0.0016	13.56	0.31	0.5500	0.0120	0.6915	2642	15	2824	38	2719	14
54z-28r	0.11	76.9	0.1921	0.0018	14.23	0.28	0.5370	0.0130	0.9771	2758	6	2770	36	2765	16
54z-2r	0.14	40.1	0.1918	0.0016	20.50	1.10	0.7760	0.0350	0.9714	2761	11	3700	69	3114	22

Appendix E. (cont)

			Isotope ratios							Age (Ma)					
	Th/U	^{204}Pb	^{207*}Pb/^{206*}Pb	2σ	^{207*}Pb/^{235}U	2σ	^{206*}Pb/^{238}U	2σ	Err. Corr.	^{207*}Pb/^{206*}Pb	2σ	^{206*}Pb/^{238}U	2σ	^{207*}Pb/^{235}U	2σ
54: K-feldspar pegmatite; traditional methodology															
54z-5r*	0.14	28.9	0.1176	0.0009	3.56	0.07	0.2198	0.0043	0.9711	1921	4	1280	23	1540	14
54z-14c*	0.16	26.2	0.1191	0.0017	3.79	0.07	0.2329	0.0057	0.9169	1948	7	1349	30	1589	15
54z-19c2*	0.19	20.1	0.1314	0.0018	4.50	0.18	0.2494	0.0065	0.9174	2117	11	1435	33	1731	28
54z-28c*	0.17	56.3	0.1340	0.0012	4.08	0.07	0.2214	0.0034	0.9567	2154	5	1289	18	1649	12
54z-12*	0.13	37.3	0.1390	0.0019	6.04	0.29	0.3170	0.0140	0.9809	2215	6	1775	69	1981	50
54z-5c*	0.11	28.1	0.1388	0.0011	5.65	0.08	0.2955	0.0039	0.9282	2217	5	1669	19	1924	12
54z-4*	0.14	69.1	0.1413	0.0011	4.08	0.11	0.2088	0.0048	0.9266	2247	5	1222	26	1650	20
54z-14r*	0.22	26.5	0.1446	0.0011	5.96	0.13	0.2988	0.0058	0.9234	2285	6	1688	29	1968	18
54z-1*	0.13	18.6	0.1465	0.0011	5.76	0.11	0.2854	0.0046	0.9647	2302	7	1618	23	1939	16
54z-19c1*	0.13	9.7	0.1466	0.0015	6.52	0.14	0.3227	0.0055	0.8338	2307	8	1803	26	2048	18
54z-10r*	0.12	9.0	0.1527	0.0011	5.93	0.10	0.2823	0.0047	0.8457	2377	5	1603	23	1965	14
54z-13r*	0.15	6.9	0.1535	0.0013	7.49	0.08	0.3544	0.0042	0.9097	2386	5	1955	20	2171	10
54z-29r*	0.13	28.7	0.1595	0.0026	8.51	0.28	0.3867	0.0090	0.8379	2460	8	2107	42	2290	35
54z-23r	0.13	23.0	0.1640	0.0014	8.39	0.28	0.3715	0.0120	0.9122	2496	7	2043	55	2273	29
54z-10c2	0.14	10.4	0.1642	0.0017	6.62	0.43	0.2920	0.0160	0.6612	2503	6	1651	75	2062	46
54z-24c	0.13	29.2	0.1645	0.0014	8.41	0.19	0.3687	0.0079	0.9585	2507	6	2022	37	2275	20
54z-6c*	0.05	2.7	0.1649	0.0016	9.82	0.22	0.4325	0.0087	0.9175	2508	7	2316	40	2421	22
54z-10c1	0.10	11.5	0.1660	0.0016	8.48	0.25	0.3714	0.0093	0.8873	2519	6	2036	43	2283	24
54z-23c	0.12	23.9	0.1665	0.0018	8.20	0.48	0.3576	0.0170	0.9742	2524	7	1970	78	2252	43
54z-9c	0.14	20.7	0.1694	0.0014	9.26	0.19	0.3952	0.0080	0.9534	2554	5	2146	37	2363	19
54z-20r	0.13	40.9	0.1704	0.0016	9.41	0.15	0.4020	0.0064	0.7882	2566	7	2178	29	2381	14
54z-13c	0.15	4.1	0.1730	0.0015	11.68	0.16	0.4903	0.0058	0.7806	2585	15	2571	26	2578	13
54z-2c	0.13	81.1	0.1736	0.0013	12.69	0.26	0.5313	0.0110	0.9574	2592	5	2746	45	2656	18
54z-15c	0.22	50.9	0.1758	0.0014	10.79	0.29	0.4520	0.0130	0.9636	2614	5	2402	55	2509	23
54z-18c	0.16	4.5	0.1788	0.0018	12.62	0.21	0.5100	0.0075	0.8638	2641	11	2655	32	2650	15
54z-26r	0.13	55.9	0.1793	0.0014	14.00	0.20	0.5675	0.0088	0.8677	2645	6	2896	36	2750	13
54z-21r	0.17	14.8	0.1804	0.0019	11.72	0.39	0.4758	0.0140	0.8473	2655	7	2508	60	2585	27
54z-28r	0.11	77.2	0.1909	0.0015	13.98	0.21	0.5330	0.0080	0.9746	2752	5	2755	35	2747	16
54z-2r	0.14	44.1	0.1917	0.0014	21.19	0.37	0.8040	0.0130	0.9848	2755	5	3801	47	3146	17

Notes:

^{204}Pb (ppm)

*: Samples not used in age calculations

All Pb values (except ^{204}Pb) are radiogenic Pb

Appendix F. LA-ICP-MS results for U-Pb geochronology of titanite from granitoids surrounding the NCGB

	Isotope ratios								Age (Ma)					
	^{204}Pb	$^{207*}Pb/^{206*}Pb$	2σ	$^{207*}Pb/^{235}U$	2σ	$^{206*}Pb/^{238}U$	2σ	Err. Corr.	$^{207*}Pb/^{206*}Pb$	2σ	$^{206*}Pb/^{238}U$	2σ	$^{207*}Pb/^{235}U$	2σ
Southern batholith														
01: Leucocratic granodiorite														
01t-10m	3.6	0.1984	0.0070	15.07	0.68	0.5478	0.0200	0.16661	2827	51	2815	82	2813	37
01t-9m	2.8	0.2047	0.0069	15.18	0.69	0.5513	0.0250	0.34698	2864	25	2829	96	2831	40
01t-2d	15.9	0.2322	0.0085	16.40	2.90	0.5410	0.0600	0.36403	3073	34	2786	220	2894	100
01t-8m	3.6	0.2080	0.0071	16.43	0.71	0.5670	0.0180	0.55065	2911	33	2892	74	2895	42
01t-3m	10.2	0.2092	0.0062	16.58	0.58	0.5710	0.0160	0.56608	2909	31	2909	66	2910	34
01t-7m2*	5.6	0.2240	0.0140	18.30	1.00	0.5740	0.0210	0.70963	3044	61	2923	87	2999	51
01t-6m*	20.0	0.2430	0.0140	20.60	5.30	0.6180	0.0900	0.83987	3135	36	3100	300	3115	140
01t-7m1*	12.6	0.2442	0.0097	20.60	1.90	0.6250	0.0390	0.69974	3144	34	3130	140	3117	65
01t-13m*	7.1	0.2490	0.0140	22.00	1.00	0.6410	0.0250	0.27393	3179	74	3191	100	3173	48
01t-21*	208.0	0.3279	0.0079	24.60	1.60	0.5500	0.0300	0.86326	3613	19	2823	120	3289	51
01t-4d*	43.3	0.2860	0.0120	25.90	5.10	0.6630	0.0830	0.61268	3414	5	3277	270	3343	110
01t-5m*	23.0	0.2580	0.0076	28.40	2.10	0.8030	0.0440	0.43139	3257	39	3798	150	3430	63
01t-1d*	544.0	0.3524	0.0074	141.70	7.20	2.9440	0.1300	0.83043	no value	N/A	8842	200	5041	45
01t-12m*	no value	no value	N/A	no value	N/A	no value	N/A	N/A	no value	N/A	no value	N/A	no value	N/A
01t-11d*	no value	no value	N/A	no value	N/A	no value	N/A	N/A	no value	N/A	no value	N/A	no value	N/A

Appendix F. (cont)

	Isotope ratios								Age (Ma)					
	^{204}Pb	$^{207*}Pb/^{206*}Pb$	2σ	$^{207*}Pb/^{235}U$	2σ	$^{206*}Pb/^{238}U$	2σ	Err. Corr.	$^{207*}Pb/^{206*}Pb$	2σ	$^{206*}Pb/^{238}U$	2σ	$^{207*}Pb/^{235}U$	2σ
13: Strongly foliated granodiorite														
13-t7-1	186	0.1883	0.0024	13.72	0.17	0.5281	0.0043	0.25402	2735	19	2733	18	2730	12
13-t9-1	194	0.1890	0.0029	13.90	0.21	0.5328	0.0045	0.22873	2738	9	2753	19	2742	14
13-t15-1	194	0.1910	0.0025	14.04	0.18	0.5321	0.0045	0.49078	2749	10	2750	19	2752	13
13-t11-2	191	0.1914	0.0024	14.58	0.19	0.5553	0.0041	0.31610	2750	8	2847	17	2789	12
13-t5-1	181	0.1918	0.0027	14.30	0.19	0.5404	0.0046	0.01981	2754	13	2785	19	2769	13
13-t12-1	169	0.1923	0.0028	14.43	0.21	0.5458	0.0047	0.43729	2756	9	2807	19	2777	14
13-t7-2	187	0.1917	0.0027	14.25	0.19	0.5368	0.0047	0.24569	2758	11	2770	20	2766	13
13-t3-3	190	0.1919	0.0025	14.63	0.21	0.5527	0.0047	0.40213	2759	8	2836	19	2791	14
13-t3-2	183	0.1919	0.0027	14.44	0.26	0.5466	0.0063	0.17739	2762	10	2811	26	2778	16
13-t4-2	212	0.1928	0.0027	14.68	0.24	0.5511	0.0060	0.49804	2762	9	2830	24	2794	15
13-t13-2	202	0.1926	0.0027	14.17	0.21	0.5357	0.0047	0.28722	2763	11	2765	19	2760	14
13-t6-2	188	0.1921	0.0028	14.38	0.20	0.5418	0.0038	0.17657	2763	9	2791	16	2774	13
13-t3-1	175	0.1926	0.0027	14.34	0.23	0.5376	0.0060	0.61661	2768	10	2772	25	2771	15
13-t11-1	163	0.1935	0.0028	14.22	0.20	0.5348	0.0047	0.21300	2771	11	2761	19	2765	13
13-t9-2	193	0.1936	0.0029	14.14	0.22	0.5274	0.0050	0.40901	2772	11	2730	21	2759	14
13-t15-2	189	0.1923	0.0027	14.32	0.19	0.5364	0.0050	0.35416	2773	11	2768	21	2770	13
13-t13-1	193	0.1932	0.0024	14.32	0.17	0.5361	0.0048	0.64410	2773	10	2767	20	2771	12
13-t1-2	200	0.1958	0.0052	14.40	0.25	0.5384	0.0110	0.17002	2777	18	2776	47	2776	17
13-t4-3	222	0.1929	0.0037	14.70	0.36	0.5514	0.0063	0.51593	2778	9	2831	26	2795	21
13-t6-1	189	0.1946	0.0028	14.12	0.19	0.5266	0.0050	0.03808	2781	10	2727	21	2757	13
13-t16-1	173	0.1953	0.0029	14.47	0.23	0.5393	0.0061	0.22255	2781	11	2780	24	2780	15
13-t16-2	169	0.1946	0.0030	14.51	0.22	0.5410	0.0050	0.51877	2784	14	2787	21	2785	14
13-t8-1	229	0.1954	0.0028	14.62	0.21	0.5446	0.0040	0.30219	2788	13	2802	17	2791	14
13-t12-2	184	0.1983	0.0029	14.92	0.23	0.5467	0.0050	0.35510	2811	9	2811	21	2809	14
13-t1-1*	205	0.1986	0.0028	15.09	0.23	0.5497	0.0045	0.43346	2819	11	2824	19	2819	14
13-t4-4*	244	0.1997	0.0260	15.20	13.00	0.5511	0.1500	0.07482	2822	24	2829	410	2827	190
13-t4-1	274	0.2073	0.0034	16.22	0.28	0.5673	0.0058	0.31989	2889	16	2896	23	2893	16

Appendix F. (cont)

	Isotope ratios								Age (Ma)					
	^{204}Pb	$^{207*}Pb/^{206*}Pb$	2σ	$^{207*}Pb/^{235}U$	2σ	$^{206*}Pb/^{238}U$	2σ	Err. Corr.	$^{207*}Pb/^{206*}Pb$	2σ	$^{206*}Pb/^{238}U$	2σ	$^{207*}Pb/^{235}U$	2σ
29: Moderately foliated granodiorite														
29-t14-2	170	0.1900	0.0028	14.10	0.28	0.5367	0.0098	0.20401	2740	19	2769	40	2762	18
29-t11-1	164	0.1919	0.0027	14.17	0.19	0.5346	0.0047	0.16435	2756	17	2760	19	2761	13
29-t6-2	167	0.1933	0.0030	14.28	0.24	0.5363	0.0060	0.39860	2765	12	2767	25	2769	16
29-t7-1	167	0.1946	0.0026	14.37	0.20	0.5396	0.0044	0.42561	2766	10	2781	18	2774	13
29-t14-1	161	0.1927	0.0045	14.04	0.32	0.5319	0.0045	0.35343	2778	19	2749	19	2751	20
29-t4-1	169	0.1968	0.0034	14.26	0.24	0.5282	0.0054	0.47012	2793	15	2730	23	2765	16
29-t10-2	188	0.1960	0.0028	14.76	0.23	0.5440	0.0049	0.46547	2798	13	2800	20	2805	15
29-t8-1	186	0.1957	0.0037	14.63	0.32	0.5428	0.0062	0.07681	2800	17	2795	25	2790	20
29-t3-1	159	0.1980	0.0031	14.93	0.24	0.5428	0.0057	0.52451	2815	13	2794	24	2809	16
29-t6-1	164	0.1988	0.0036	15.00	0.27	0.5448	0.0055	0.27615	2821	17	2803	23	2815	18
29-t9-1	155	0.1991	0.0034	14.98	0.32	0.5440	0.0081	0.38448	2829	20	2806	33	2813	19
29-t1-1*	253	0.2082	0.0047	16.38	0.47	0.5697	0.0063	0.20784	2894	18	2906	25	2898	25
29-t10-1*	500	0.2094	0.0052	14.65	0.64	0.5151	0.0100	0.63283	2906	13	2678	41	2792	31
29-t15-1*	918	no value	N/A	no value	N/A	no value	N/A	N/A	no value	N/A	no value	N/A	no value	N/A

Appendix F. (cont)

	Isotope ratios								Age (Ma)					
	^{204}Pb	$^{207*}Pb/^{206*}Pb$	2σ	$^{207*}Pb/^{235}U$	2σ	$^{206*}Pb/^{238}U$	2σ	Err. Corr.	$^{207*}Pb/^{206*}Pb$	2σ	$^{206*}Pb/^{238}U$	2σ	$^{207*}Pb/^{235}U$	2σ
Schade Lake gneissic complex														
71: K-feldspar-flooded granodiorite														
71Dt-15m	4.1	0.1996	0.0041	15.75	0.28	0.5732	0.0085	0.20969	2822	23	2920	35	2860	17
71Dt-9m	3.8	0.1996	0.0044	15.34	0.44	0.5530	0.0130	0.72102	2825	31	2834	53	2831	27
71Pt-13m	4.1	0.2025	0.0041	15.53	0.41	0.5543	0.0130	0.44633	2827	27	2842	52	2846	25
71Dt-16m	1.0	0.2014	0.0034	14.96	0.27	0.5480	0.0120	0.56682	2829	13	2816	48	2815	17
71Dt-1m	4.9	0.1999	0.0027	15.09	0.21	0.5512	0.0094	0.31803	2829	14	2830	40	2820	14
71Pt-22l	3.1	0.2010	0.0046	15.70	0.44	0.5683	0.0120	0.28789	2832	21	2901	47	2862	28
71Pt-18m	5.2	0.2027	0.0048	15.57	0.50	0.5553	0.0150	0.32564	2833	28	2846	65	2852	32
71Dt-8d	9.7	0.2005	0.0048	15.48	0.49	0.5560	0.0110	0.51531	2834	16	2847	44	2845	27
71Pt-20l	4.9	0.2020	0.0041	15.86	0.40	0.5668	0.0120	0.50419	2842	15	2894	45	2867	24
71Pt-5l	3.6	0.2039	0.0045	15.56	0.49	0.5588	0.0150	0.41733	2848	22	2861	62	2848	31
71Pt-14m	5.6	0.2038	0.0044	15.53	0.45	0.5562	0.0150	0.70298	2849	14	2850	62	2847	29
71Pt-21m	2.2	0.2028	0.0054	15.67	0.49	0.5570	0.0140	0.46135	2850	23	2853	60	2857	29
71Pt-1l	6.6	0.2036	0.0040	15.44	0.39	0.5564	0.0120	0.40258	2851	12	2851	49	2844	24
71Dt-14m	3.9	0.2019	0.0037	15.46	0.27	0.5560	0.0080	0.72333	2852	27	2848	31	2844	16
71Dt-7m	2.3	0.2048	0.0038	15.69	0.25	0.5581	0.0090	0.33642	2855	15	2858	37	2857	15
71Pt-10l	5.2	0.2041	0.0042	15.62	0.38	0.5568	0.0110	0.28038	2855	15	2853	46	2853	24
71Dt-18d	3.8	0.2041	0.0042	15.46	0.28	0.5491	0.0100	0.60562	2856	14	2821	41	2847	18
71Pt-8l	4.9	0.2052	0.0038	15.70	0.38	0.5598	0.0110	0.33263	2861	14	2866	47	2858	23
71Dt-4m	4.7	0.2037	0.0041	15.99	0.35	0.5611	0.0096	0.60165	2863	16	2870	39	2874	21
71Dt-10m	2.5	0.2040	0.0035	15.76	0.29	0.5601	0.0089	0.57582	2864	24	2866	36	2860	17
71Pt-24m	2.0	0.2053	0.0055	15.93	0.49	0.5632	0.0120	0.20588	2864	31	2879	48	2875	28
71Dt-3m	3.8	0.2059	0.0041	15.83	0.30	0.5595	0.0087	0.29412	2865	24	2864	36	2865	18
71Dt-6m	4.3	0.2051	0.0037	15.76	0.24	0.5596	0.0077	0.23117	2869	24	2864	32	2861	14
71Pt-4l	2.7	0.2051	0.0043	16.09	0.41	0.5686	0.0110	0.06394	2872	23	2902	47	2881	25
71Dt-20m	3.4	0.2078	0.0035	15.94	0.27	0.5646	0.0088	0.15341	2874	21	2886	36	2872	16
71Pt-11m	2.7	0.2063	0.0045	16.03	0.46	0.5620	0.0150	0.42171	2875	15	2879	59	2880	29
71Dt-2m	3.5	0.2060	0.0037	15.87	0.28	0.5620	0.0079	0.37243	2877	17	2874	32	2871	16
71Dt-11m	4.1	0.2086	0.0058	16.31	0.42	0.5710	0.0089	0.10613	2879	53	2911	36	2889	25
71Dt-5m	1.1	0.2069	0.0040	16.05	0.33	0.5646	0.0085	0.29407	2880	17	2885	37	2878	20
71Dt-10l	3.1	0.2079	0.0029	15.87	0.23	0.5641	0.0078	0.44346	2888	23	2883	32	2868	15

Appendix F. (cont)

	Isotope ratios								Age (Ma)					
	^{204}Pb	$^{207*}Pb/^{206*}Pb$	2σ	$^{207*}Pb/^{235}U$	2σ	$^{206*}Pb/^{238}U$	2σ	Err. Corr.	$^{207*}Pb/^{206*}Pb$	2σ	$^{206*}Pb/^{238}U$	2σ	$^{207*}Pb/^{235}U$	2σ
71Dt-19l	9.6	0.2067	0.0056	16.01	0.42	0.5611	0.0082	0.31524	2889	34	2871	34	2877	23
71Dt-17m	1.3	0.2098	0.0063	16.10	0.50	0.5630	0.0087	0.47743	2905	23	2879	36	2881	30
71Pt-23d	6.0	0.2112	0.0066	16.31	0.57	0.5674	0.0170	0.41224	2906	27	2896	70	2899	35
71Pt-10d	3.6	0.2167	0.0084	16.98	0.95	0.5740	0.0220	0.66934	2946	37	2920	92	2922	55
71Dt-12d*	3.6	0.2380	0.0120	20.20	0.91	0.6180	0.0630	0.26529	3030	86	3102	71	3095	39
Wharram Lake block														
55: Equigranular granodiorite														
55t-3m	0.4	0.1820	0.0047	12.69	0.41	0.5085	0.0130	0.58996	2652	31	2649	56	2653	31
55t-11m	6.3	0.1798	0.0043	13.13	0.38	0.5264	0.0120	0.51841	2654	27	2726	49	2689	28
55t-3d	2.7	0.1816	0.0079	12.84	0.62	0.5110	0.0160	0.17723	2661	44	2664	68	2659	44
55t-13m	2.5	0.1831	0.0038	13.15	0.32	0.5238	0.0110	0.13327	2675	16	2715	46	2690	23
55t-12d	1.3	0.1837	0.0058	12.86	0.46	0.5110	0.0150	0.47839	2678	27	2661	61	2667	34
55t-16l	2.7	0.1830	0.0038	13.33	0.35	0.5258	0.0110	0.43343	2682	17	2723	46	2702	25
55t-19m	4.5	0.1834	0.0040	13.51	0.41	0.5285	0.0120	0.67310	2682	21	2734	51	2717	28
55t-6m	3.3	0.1845	0.0049	13.43	0.42	0.5236	0.0110	0.18459	2687	35	2714	48	2708	30
55t-20l	1.9	0.1818	0.0037	13.02	0.34	0.5191	0.0110	0.62657	2692	32	2695	46	2679	24
55t-7d	4.6	0.1863	0.0045	13.32	0.47	0.5180	0.0140	0.41871	2700	34	2690	61	2699	36
55t-9m	4.2	0.1841	0.0050	13.37	0.42	0.5203	0.0140	0.49428	2701	23	2700	61	2703	31
55t-7m	0.6	0.1870	0.0049	13.73	0.45	0.5289	0.0150	0.39390	2712	32	2736	63	2729	33
55t-2-m	4.2	0.1880	0.0060	13.25	0.54	0.5147	0.0130	0.47377	2725	34	2676	52	2707	40
55t-4d	2.6	0.1851	0.0061	13.25	0.54	0.5240	0.0150	0.30767	2735	43	2715	63	2712	38
55t-15m	2.4	0.1939	0.0056	13.79	0.46	0.5283	0.0140	0.09761	2761	21	2733	62	2736	33

Appendix F. (cont)

	Isotope ratios								Age (Ma)					
	^{204}Pb	$^{207*}Pb/^{206*}Pb$	2σ	$^{207*}Pb/^{235}U$	2σ	$^{206*}Pb/^{238}U$	2σ	Err. Corr.	$^{207*}Pb/^{206*}Pb$	2σ	$^{206*}Pb/^{238}U$	2σ	$^{207*}Pb/^{235}U$	2σ
North Caribou batholith "pluton"														
46: Foliated granodiorite														
46t-7l	6.1	0.1866	0.0027	13.71	0.16	0.5348	0.0065	0.19165	2712	19	2762	27	2731	11
46t-20m	8.0	0.1894	0.0039	13.76	0.31	0.5290	0.0093	0.46281	2736	30	2738	39	2730	21
46t-2l	1.9	0.1905	0.0036	13.95	0.26	0.5349	0.0082	0.40147	2743	19	2761	34	2747	18
46t-18m	6.9	0.1939	0.0047	14.25	0.31	0.5372	0.0082	0.19150	2768	29	2771	35	2767	21
46t-1l	3.5	0.1968	0.0044	14.54	0.30	0.5415	0.0089	0.39383	2793	21	2789	37	2786	19
46t-17m	3.0	0.1965	0.0044	14.63	0.31	0.5422	0.0089	0.11083	2795	28	2796	37	2794	21
46t-15m	9.8	0.2027	0.0054	15.33	0.36	0.5494	0.0079	0.15005	2833	35	2822	33	2836	23
46t-19l	23.2	0.2065	0.0038	16.87	0.40	0.5981	0.0100	0.75135	2873	16	3022	41	2926	23
46t-11d	53.4	0.2083	0.0030	7.73	0.20	0.2726	0.0061	0.76532	2892	15	1554	31	2198	25
46t-5m	4.6	0.2100	0.0054	16.45	0.44	0.5672	0.0092	0.34525	2906	39	2895	38	2899	26
46t-1d*	6.9	0.2240	0.0076	17.81	0.56	0.5870	0.0120	0.05623	3029	35	2975	49	2976	30
46t-18d*	4.4	0.2291	0.0076	18.73	0.45	0.5820	0.0170	0.45859	3065	32	2953	70	3024	31
46t-8d*	10.3	0.2415	0.0063	13.56	0.51	0.4042	0.0110	0.53933	3138	29	2188	51	2724	36
46t-13d2*	3.9	0.2650	0.0200	23.40	1.50	0.6380	0.0180	0.25416	3288	66	3178	70	3232	56
66: High-strain tonalite														
66t-18l	2.7	0.1866	0.0040	13.84	0.35	0.5390	0.0110	0.31083	2704	13	2779	47	2738	24
66t-1m	0.8	0.1866	0.0037	14.01	0.36	0.5468	0.0110	0.51353	2713	17	2811	47	2751	24
66t-15m	0.0	0.1892	0.0055	13.81	0.46	0.5300	0.0160	0.42356	2716	23	2738	67	2737	34
66t-16l	4.0	0.1868	0.0050	13.45	0.43	0.5229	0.0130	0.12147	2716	31	2711	58	2710	32
66t-6l	3.2	0.1883	0.0042	13.62	0.42	0.5259	0.0130	0.64285	2738	18	2723	48	2724	29
66t-13l	4.4	0.1913	0.0049	14.34	0.43	0.5368	0.0120	0.25169	2770	28	2769	51	2770	27
66t-11m	1.9	0.1950	0.0063	14.34	0.54	0.5374	0.0160	0.03866	2781	35	2771	68	2772	38
66t-3m	4.9	0.2001	0.0062	14.70	0.55	0.5283	0.0150	0.24783	2825	31	2734	64	2796	38
66t-9m*	3.0	0.2020	0.0090	15.19	0.67	0.5520	0.0170	0.16560	2862	39	2832	71	2829	41
66t-4m*	1.4	0.2100	0.0110	16.50	0.97	0.5680	0.0220	0.32919	2909	68	2890	90	2890	55
66t-5l*	18.2	0.2197	0.0055	16.88	0.63	0.5599	0.0190	0.78793	2991	22	2865	72	2925	37
66t-8d*	1.4	0.2197	0.0085	18.24	0.65	0.5920	0.0180	0.12950	3007	37	3005	78	3007	36
66t-8l*	62.0	0.2800	0.0160	22.80	5.10	0.5910	0.0540	0.07185	3369	69	2992	190	3215	110

Appendix F. (cont)

	Isotope ratios								Age (Ma)					
	^{204}Pb	$^{207*}Pb/^{206*}Pb$	2σ	$^{207*}Pb/^{235}U$	2σ	$^{206*}Pb/^{238}U$	2σ	Err. Corr.	$^{207*}Pb/^{206*}Pb$	2σ	$^{206*}Pb/^{238}U$	2σ	$^{207*}Pb/^{235}U$	2σ
North Caribou batholith "core"														
51: K-feldspar augen gneiss														
51t-9d	3.2	0.1886	0.0041	13.91	0.28	0.5303	0.0090	0.41699	2730	27	2747	38	2744	19
51t-3m	2.9	0.1996	0.0047	14.51	0.26	0.5398	0.0081	0.12318	2790	37	2782	34	2787	17
51t-5m	7.8	0.1963	0.0048	14.43	0.39	0.5367	0.0088	0.24505	2796	32	2769	37	2783	26
51t-20m	3.7	0.1951	0.0041	14.38	0.25	0.5404	0.0082	0.23297	2798	18	2785	34	2776	16
51t-12m	3.5	0.1986	0.0055	14.73	0.36	0.5416	0.0110	0.05663	2815	36	2789	40	2793	24
51t-13l	4.2	0.1977	0.0047	14.95	0.32	0.5456	0.0088	0.24165	2815	24	2806	37	2809	21
51t-6m	2.8	0.1993	0.0053	14.87	0.30	0.5468	0.0094	0.11135	2819	36	2811	39	2808	20
51t-20l	6.4	0.2000	0.0047	14.82	0.29	0.5411	0.0077	0.24316	2820	29	2787	32	2804	20
51t-1l	5.3	0.1992	0.0048	14.92	0.36	0.5435	0.0093	0.10105	2824	27	2802	39	2805	23
51t-16m	7.6	0.2008	0.0053	14.82	0.39	0.5397	0.0095	0.36073	2833	39	2781	40	2799	25
51t-8l	3.1	0.2018	0.0060	14.71	0.43	0.5380	0.0095	0.37882	2834	41	2774	40	2792	28
51t-7l	5.2	0.2006	0.0048	14.73	0.39	0.5374	0.0088	0.27104	2843	27	2776	37	2806	25
51t-9l	1.4	0.2061	0.0044	14.96	0.35	0.5440	0.0096	0.58231	2850	23	2809	40	2817	22
51t-17m	1.2	0.2025	0.0053	15.00	0.39	0.5390	0.0084	0.12071	2859	33	2779	35	2816	25
51t-14l	2.8	0.2040	0.0054	15.13	0.34	0.5471	0.0090	0.25913	2861	23	2812	38	2821	22
51t-10d	5.8	0.2067	0.0051	15.83	0.42	0.5555	0.0100	0.44919	2866	25	2847	43	2867	26
51t-18l	9.6	0.2057	0.0053	15.08	0.39	0.5457	0.0080	0.26135	2876	16	2807	34	2826	25
51t-2l	5.3	0.2057	0.0057	15.18	0.39	0.5369	0.0076	0.06391	2881	33	2770	32	2822	25

Appendix F. (cont)

	Isotope ratios								Age (Ma)					
	^{204}Pb	$^{207*}Pb/^{206*}Pb$	2σ	$^{207*}Pb/^{235}U$	2σ	$^{206*}Pb/^{238}U$	2σ	Err. Corr.	$^{207*}Pb/^{206*}Pb$	2σ	$^{206*}Pb/^{238}U$	2σ	$^{207*}Pb/^{235}U$	2σ
61: Massive tonalite														
61t-3m	3.1	0.1886	0.0033	14.05	0.21	0.5358	0.0077	0.12374	2727	26	2766	32	2752	14
61t-11m	4.4	0.1910	0.0034	14.42	0.23	0.5465	0.0082	0.00648	2759	19	2814	34	2779	15
61t-7m	3.4	0.1929	0.0029	14.53	0.20	0.5419	0.0080	0.48407	2773	13	2791	33	2785	14
61t-9m	2.8	0.1939	0.0024	14.74	0.17	0.5491	0.0081	0.77365	2776	7	2821	34	2799	11
61t-1m	1.7	0.1956	0.0036	14.87	0.27	0.5533	0.0071	0.25613	2787	26	2838	30	2807	17
61t-5d	-0.7	0.1979	0.0065	14.41	0.42	0.5374	0.0098	0.09182	2801	26	2772	42	2779	28
61t-6l	22.1	0.1975	0.0034	14.60	0.25	0.5398	0.0075	0.61088	2809	26	2781	31	2790	16
61t-8m	0.7	0.2005	0.0033	15.19	0.24	0.5514	0.0081	0.14132	2815	18	2831	33	2827	14
61t-10m	2.3	0.2000	0.0033	15.39	0.20	0.5612	0.0110	0.33965	2821	15	2871	44	2839	13
61t-4d	0.9	0.2025	0.0054	15.24	0.52	0.5553	0.0098	0.27062	2843	31	2846	40	2837	25
61t-12d	3.4	0.2010	0.0078	14.49	0.69	0.5340	0.0110	0.34037	2850	42	2757	47	2778	41

Appendix F. (cont)

Libert Lake pluton

45: Melanocratic granite														
45t-4m	1.4	0.1839	0.0053	12.91	0.50	0.5166	0.0140	0.38855	2675	45	2684	56	2680	37
45t-11l	5.2	0.1827	0.0044	13.39	0.41	0.5335	0.0110	0.44825	2675	27	2756	45	2709	29
45t-6m	3.2	0.1820	0.0048	13.41	0.42	0.5393	0.0110	0.22025	2684	34	2780	48	2709	29
45t-16m	1.5	0.1836	0.0042	13.16	0.41	0.5193	0.0130	0.47653	2686	15	2696	57	2692	30
45t-14m	3.7	0.1846	0.0055	12.89	0.47	0.5142	0.0140	0.13305	2695	40	2674	59	2673	33
45t-1l	5.4	0.1867	0.0110	13.34	1.20	0.5198	0.0180	0.03178	2708	44	2697	73	2699	67
45t-9l*	17.3	0.1875	0.0190	14.90	4.00	0.5565	0.0520	0.53135	2725	36	2852	180	2806	120
45t-1d	2.7	0.1904	0.0063	13.70	0.56	0.5280	0.0170	0.00423	2735	42	2728	73	2722	41
45t-3d	1.9	0.1914	0.0061	13.09	0.46	0.5016	0.0170	0.30673	2740	44	2620	59	2689	35
45t-7d	4.6	0.1940	0.0058	13.98	0.53	0.5302	0.0160	0.28507	2745	41	2742	69	2745	40
45t-2m	5.1	0.1931	0.0054	14.26	0.45	0.5370	0.0120	0.12880	2758	43	2770	49	2763	30
45t-6l	10.0	0.1975	0.0059	14.78	0.51	0.5447	0.0120	0.50843	2798	45	2803	50	2801	34
45t-10m	1.9	0.1943	0.0077	14.12	0.63	0.5370	0.0160	0.30765	2807	60	2768	69	2765	42
45t-4d	3.5	0.2025	0.0069	14.31	0.58	0.5177	0.0140	0.21327	2843	41	2689	60	2774	42
45t-8m	4.3	0.2050	0.0077	15.17	0.58	0.5372	0.0150	0.04733	2867	44	2771	63	2820	37
45t-19d	7.6	0.2070	0.0097	15.51	0.71	0.5470	0.0170	0.02859	2899	50	2812	74	2843	45
45t-15l*	106.0	0.2306	0.0330	18.25	11.00	0.5750	0.1200	0.81426	3056	15	2930	380	3003	200
45t-3l*	63.5	0.2445	0.0120	21.16	1.90	0.6300	0.0230	0.35347	3147	34	3149	88	3144	64

Notes:

^{204}Pb (ppm)

All Pb values (except ^{204}Pb) are radiogenic Pb

^{204}Pb for 13 and 29 calculated with a different standard

*: Samples not used in age calculations

Appendix G. LA-ICP-MS results from trace elements of zircons from granitoids surrounding the NCGB

	P	Ti	2σ	La	Ce	Pr	Nd	Sm	Eu	Gd	Tb	Dy	Ho	Er	Tm	Yb	Lu	Hf	Pb	Th	U	Th/U
Southern batholith																						
01: Leucocratic granodiorite																						
01-24c	238	13.7	1.2	2	17	1	12	7	2	13	3	33	12	61	15	163	37	8188	43	55	119	0.46
01-21c	241	5.3	0.9	1	16	1	13	12	2	39	12	145	58	266	55	498	103	8400	155	129	194	0.67
01-19c	185	6.6	0.9	1	12	1	8	5	1	12	3	38	14	68	16	162	37	8520	145	55	158	0.34
01-10c*	19800	196.0	14.0	410	1150	243	1450	580	138	560	88	540	112	351	64	562	91	9860	243	335	486	0.62
01-25c	247	7.6	0.9	12	88	9	64	26	11	42	9	97	36	159	34	320	64	9274	460	186	796	0.23
13: Strongly foliated granodiorite																						
13z-1c	420	9.6	1.0	2	182	3	41	41	16	123	29	271	89	379	81	782	162	6770	177	1448	1133	1.27
13z-2c	234	7.8	0.8	25	186	10	67	29	13	74	17	156	50	209	43	407	85	7130	661	1746	1220	1.43
13z-4c	116	44.0	5.2	33	196	22	185	84	44	154	21	144	41	156	34	342	71	6800	644	640	1307	0.53
13z-5c	207	29.7	7.1	13	202	11	101	60	27	132	24	207	66	274	56	562	104	6800	694	770	523	1.35
13z-7c	253	11.0	2.2	5	78	4	45	36	12	90	21	196	66	285	62	607	126	6530	190	686	731	0.95
29: Moderately foliated granodiorite																						
29z-7r*	169	53.0	16.0	228	241	19	71	28	8	41	7	59	20	89	18	173	35	7450	966	52	121	0.42
29z-4r*	198	92.4	6.1	73	492	86	673	379	101	433	48	251	58	215	43	429	95	10290	321	118	772	0.14
29z-3r	60	12.8	1.1	11	81	15	109	60	24	76	9	59	18	79	18	193	45	10860	1080	43	554	0.08
29z-23r	71	26.5	2.0	18	142	23	192	118	33	135	17	96	26	105	23	238	56	9410	237	44	336	0.13
29z-21r*	212	123.0	20.0	58	373	68	544	337	92	347	36	169	37	131	26	248	53	10700	440	168	524	0.33
29z-17r	126	31.9	4.5	27	92	15	106	52	17	57	8	64	25	124	30	321	73	10710	265	101	865	0.11
29z-27r1	300	7.9	1.1	7	26	4	31	21	5	32	5	44	16	71	15	144	32	7710	113	63	70	0.88
29z-26c	381	31.8	3.1	40	263	44	342	191	59	240	27	173	49	196	41	373	79	8290	278	205	479	0.43
29z-24c	155	3.1	0.7	2	12	1	8	3	1	10	4	48	21	110	27	285	66	9910	418	54	401	0.13
29z-20c	91	7.2	1.1	5	56	7	62	32	8	39	7	62	23	117	29	314	73	12020	132	105	825	0.14
29z-13c	530	12.3	1.9	6	51	5	39	27	10	45	10	98	37	168	37	350	76	9740	223	173	333	0.52

Appendix G. (cont)

	P	Ti	2σ	La	Ce	Pr	Nd	Sm	Eu	Gd	Tb	Dy	Ho	Er	Tm	Yb	Lu	Hf	Pb	Th	U	Th/U
48: Weakly gneissic granite																						
48z-2c	515	57.4	6.0	88	500	81	440	203	30	247	51	376	102	378	76	694	124	18200	--	472	1940	0.25
48z-5r*	399	51.5	2.0	12	68	12	58	31	3	40	10	90	31	147	37	414	103	21980	--	101	896	0.11
48z-23c2*	177	59.0	10.0	12	85	10	54	20	5	44	13	143	55	283	69	735	141	27440	--	118	4060	0.03
48z-2c*	930	67.9	9.2	21	54	9	44	19	2	26	6	68	33	203	56	635	151	13410	1886	1890	3520	0.57
48z-5r*	671	211.0	25.0	53	332	57	286	148	16	196	40	266	61	201	35	297	56	11440	251	122	749	0.16
48z-23c2	229	10.6	1.8	7	49	6	36	20	3	38	9	88	30	130	28	266	55	9400	369	63	400	0.30
48z-10r*	3760	1260.0	160.0	696	3160	618	3150	1620	242	1800	271	1450	288	791	118	892	142	21730	--	218	727	0.30
48z-25r	1220	51.6	5.3	203	1270	254	1280	648	90	799	99	623	169	601	122	1118	198	27350	--	259	1370	0.19
48z-10r*	3590	462.0	45.0	677	3302	655	3394	1372	200	1454	178	875	164	427	60	475	80	12910	703	89	692	0.13
48z-25r*	720	347.0	28.0	270	1710	333	1980	890	109	960	124	640	130	328	54	483	90	13180	351	222	255	0.82
48z-5c	817	21.5	3.3	11	82	9	47	30	5	66	17	146	48	198	38	336	63	13900	--	123	292	0.43
48z-21c	474	15.0	2.0	3	33	4	23	19	4	46	12	130	44	198	42	388	82	14090	--	80	122	0.65
48z-25c	1710	46.1	6.0	400	2450	482	2560	1060	131	970	98	443	96	307	58	535	97	16850	--	340	860	0.40
48z-5c	355	35.1	3.1	19	106	17	85	42	4	61	13	102	30	129	31	368	83	12780	364	49	817	0.07
48z-21c	212	13.9	1.8	4	33	5	29	20	3	34	8	69	20	77	15	139	27	7980	37	29	41	0.68
48z-25c*	717	330.0	36.0	233	1390	278	1607	758	95	833	117	601	112	299	47	407	82	12810	327	114	198	0.58
Schade Lake gneissic complex																						
52: Gneissic tonalite																						
52z-1c	2400	8.2	1.4	29	55	9	44	16	4	23	5	47	18	87	20	193	44	9250	162	71	207	0.34
52z-2c*	1490	270.0	220.0	57	155	25	159	67	19	83	12	102	36	169	39	386	85	9280	465	274	628	0.43
52z-46c	520	33.0	13.0	37	125	20	159	79	23	105	14	88	26	106	24	229	49	10050	320	182	386	0.48
52z-44c	213	18.7	3.3	16	89	13	85	45	15	54	8	59	19	85	19	183	40	9160	261	171	339	0.51
52z-42c	1500	49.9	5.8	119	476	72	502	204	68	244	27	141	31	106	21	202	44	10420	277	254	507	0.51

Appendix G. (cont)

	P	Ti	2σ	La	Ce	Pr	Nd	Sm	Eu	Gd	Tb	Dy	Ho	Er	Tm	Yb	Lu	Hf	Pb	Th	U	Th/U
53: Heterogeneously deformed gneiss																						
53C-2r	890	7.0	9.1	5	33	4	17	8	3	17	5	69	23	105	17	127	21	12800	--	45	1880	0.02
53C-4c	559	9.6	1.2	13	51	3	14	7	1	45	16	187	69	316	69	681	123	16340	--	556	4381	0.13
53C-25c	461	12.5	2.2	15	64	7	41	23	12	54	15	161	52	197	38	332	54	24110	--	591	4690	0.13
53Fz -17r	830	11.0	4.9	3	29	5	29	23	2	27	9	97	41	220	53	527	108	23950	--	115	3661	0.03
53Fz -32r*	699	40.3	5.8	188	1310	263	1590	382	69	224	20	131	42	174	38	381	66	20890	--	1089	3220	0.35
53C-2r*	889	139.0	26.0	127	645	83	488	179	65	182	29	224	66	262	59	575	107	12810	1326	578	3290	0.17
53C-4c*	395	26.5	1.1	18	71	7	29	11	3	32	10	115	43	189	41	383	76	9710	1320	400	2176	0.18
53C-25c	326	6.2	0.8	0	6	0	2	4	1	23	8	98	33	131	24	202	37	14220	1871	370	2820	0.13
53Fz -17r	932	5.9	0.7	7	40	3	17	8	1	29	10	119	45	198	42	386	72	9960	1572	401	2220	0.18
53Fz -32r	380	10.9	1.4	27	219	32	217	74	12	74	11	94	28	114	24	229	47	8050	330	480	399	1.17
53Fz -1c	518	8.4	0.9	31	187	33	202	110	11	130	23	180	56	219	44	401	81	17800	--	252	855	0.30
53Fz -7r	256	6.0	1.8	13	63	6	33	16	5	26	6	56	14	41	8	78	16	20960	--	181	2903	0.06
53Fz -38c	960	13.8	1.7	8	70	3	26	29	7	97	25	246	81	319	63	579	104	12890	--	1408	2780	0.51
53Fz -1c	798	8.4	0.9	110	590	95	600	279	27	228	28	167	47	182	37	326	65	10360	414	202	719	0.29
53Fz -7r	1070	23.7	2.5	40	226	32	196	83	27	88	11	78	23	95	19	181	39	8970	317	346	442	0.81
53Fz -38c	226	10.9	2.0	40	193	25	127	14	9	13	3	37	15	67	15	147	28	12370	713	98	1101	0.10
53Fz -22c	735	41.4	3.8	78	444	61	352	164	20	185	31	236	70	300	62	576	115	17270	--	504	1055	0.49
53Fz -22c	372	28.9	2.8	109	470	74	442	164	24	140	18	105	26	108	23	220	41	12700	926	65	1774	0.04
53C-31c	570	22.8	2.9	122	622	91	572	245	78	258	35	260	74	282	54	480	91	15390	--	729	1389	0.53
53C-31c	1310	25.9	4.6	690	3720	570	3520	1330	141	970	88	396	79	224	38	312	58	8930	327	333	697	0.46

Appendix G. (cont)

	P	Ti	2σ	La	Ce	Pr	Nd	Sm	Eu	Gd	Tb	Dy	Ho	Er	Tm	Yb	Lu	Hf	Pb	Th	U	Th/U
71: K-feldspar-flooded granodiorite																						
71Pz-6c	1185	4.0	0.6	0	48	0	3	11	1	98	39	492	187	837	175	1593	301	21300	--	2690	9930	0.27
71Pz-11c*	863	440.0	140.0	40	122	9	43	24	5	86	30	359	128	571	115	1096	189	20920	--	907	3900	0.23
71Pz-24c*	1325	186.0	34.0	79	117	5	8	8	1	57	22	296	113	514	113	1079	195	25740	--	1455	7940	0.18
71Pz-6c*	184	504.0	36.0	168	629	96	583	224	60	315	42	269	75	272	51	436	81	10780	894	740	1988	0.37
71Pz-11c*	1400	260.0	110.0	98	199	15	42	13	3	68	26	320	121	515	105	935	167	14300	2978	618	5450	0.13
71Pz-24c	201	63.9	3.5	114	387	45	194	43	11	61	10	68	20	78	15	136	27	10020	275	101	399	0.25
71Dz-6c	162	58.3	4.0	127	560	88	448	84	24	83	11	92	32	139	30	290	58	16890	--	291	791	0.37
71Dz-8r	372	12.8	1.2	17	127	10	58	19	8	69	22	263	99	434	94	895	166	18090	--	1720	4580	0.38
71Dz-11c	399	38.1	4.5	188	730	92	537	117	50	107	14	144	51	230	51	479	99	15350	--	429	929	0.46
71Dz-25c	270	41.0	14.0	22	142	20	123	22	8	34	6	62	24	114	26	270	56	18560	--	300	1250	0.23
71Dz-28c	184	24.1	4.6	19	109	13	84	19	8	33	8	98	39	182	41	397	83	16600	--	239	743	0.32
71Pz-8r	414	31.4	3.7	70	255	38	237	81	18	100	15	121	34	135	28	251	49	16710	--	352	933	0.38
71Pz-17r	777	10.8	1.0	2	233	5	71	71	28	185	43	396	129	519	106	989	203	11340	--	972	532	1.80
71Dz-6c*	3600	105.0	14.0	216	920	147	850	151	37	145	18	145	48	200	43	395	73	9570	642	390	1490	0.27
71Dz-8r	890	31.7	2.6	73	326	44	300	61	22	63	10	93	33	143	30	285	58	8900	557	323	703	0.45
71Dz-11c	151	19.2	3.2	52	197	23	128	24	12	33	7	77	30	133	28	268	55	9420	572	284	744	0.38
71Dz-25c*	21800	127.0	25.0	139	526	87	499	115	34	111	15	125	44	183	39	363	71	9400	729	424	1148	0.36
71Dz-28c	316	55.6	5.9	50	247	35	218	44	24	51	9	88	33	155	33	312	63	9540	507	202	701	0.29
71Pz-8r	408	7.5	1.3	28	135	17	100	26	9	37	8	83	30	135	28	258	52	9000	455	311	604	0.52
71Pz-17r	359	7.9	0.7	4	60	1	7	11	3	58	19	205	71	299	57	491	92	8560	851	1011	1281	0.79
Skinner Lake block																						
41: Tonalite containing bleby pegmatite																						
41z-11r	216	2.4	0.4	4	34	4	24	15	2	24	5	53	20	99	24	247	52	19810	--	126	634	0.20
41z-35r	271	3.2	1.0	5	37	3	13	6	1	20	6	72	27	119	27	242	50	17080	--	150	521	0.28
41z-11r	19500	13.0	2.4	70	242	33	179	61	8	75	12	78	22	88	19	181	39	10800	180	62	235	0.28
41z-35r	131	1.9	0.4	0	3	0	0	1	0	4	2	23	10	53	13	134	32	9800	102	27	127	0.21
41z-20c	1360	7.2	0.8	6	33	4	23	20	5	52	12	110	35	141	27	246	47	15220	--	105	225	0.45
41z-27c	530	15.1	2.0	39	184	22	151	80	14	123	21	155	45	183	37	335	69	15940	--	207	490	0.43
41z-28c*	287	37.8	4.1	111	248	61	351	249	58	319	42	233	51	168	30	262	52	17920	--	216	483	0.45
41z-20c	250	3.4	0.5	4	17	2	15	14	3	33	7	56	17	66	12	107	22	8500	78	47	91	0.51
41z-27c	301	2.9	0.5	12	74	9	60	35	6	62	12	101	33	137	28	251	52	8090	179	102	218	0.47
41z-28c	161	11.5	2.2	20	52	11	59	37	8	56	10	72	21	87	17	151	32	9220	180	79	246	0.33

Appendix G. (cont)

	P	Ti	2σ	La	Ce	Pr	Nd	Sm	Eu	Gd	Tb	Dy	Ho	Er	Tm	Yb	Lu	Hf	Pb	Th	U	Th/U
43: K-feldspar augen gneiss																						
43z-6r*	176	530.0	190.0	48	167	29	168	92	9	111	17	96	26	105	23	216	47	10950	308	105	668	0.15
43z-10c*	196	80.0	32.0	25	218	14	88	40	6	59	10	70	20	84	17	157	33	10690	273	105	372	0.29
43z-15r	124	6.0	2.7	9	44	7	42	27	3	36	6	40	12	51	11	103	23	10360	218	70	348	0.20
43z-16r	141	18.2	3.1	13	70	11	67	46	6	76	12	74	23	88	18	175	38	11610	318	90	507	0.18
43z-22r	353	3.0	0.7	3	25	2	10	7	1	22	7	83	31	141	30	276	55	11410	545	261	735	0.37
43z-14r	207	45.4	6.2	138	380	64	364	235	30	308	42	202	41	124	22	189	38	11300	386	87	571	0.16
43z-22c	225	13.2	2.3	34	134	20	119	77	9	107	16	99	29	115	24	221	46	10810	477	103	717	0.14
43z-24r	249	5.6	1.0	16	65	9	54	28	3	39	7	61	22	97	22	212	45	12220	40	65	770	0.08
43z-8r	260	3.1	0.6	0	8	0	1	1	0	9	3	46	19	95	23	243	56	10980	349	103	446	0.24
43z-24c	214	7.8	1.0	22	43	8	42	23	3	38	7	54	17	69	14	134	29	8010	547	40	51	0.79
Wharram Lake block																						
55: Equigranular granodiorite																						
55z-3r1*	135	73.0	13.0	407	770	109	472	95	35	76	10	68	25	117	29	322	75	20250	--	77	725	0.11
55z-4r	54	3.7	1.2	10	50	4	25	6	3	6	2	20	10	59	17	229	61	22990	--	187	1453	0.13
55z-6r*	1710	45.0	5.8	221	532	70	305	71	8	61	13	161	71	398	117	1470	320	28300	--	158	3540	0.05
55z-10r	115	23.5	1.2	148	527	67	319	40	9	29	4	37	15	71	19	226	53	21130	--	206	1444	0.14
55z-15r	142	19.7	2.5	71	189	24	96	16	2	18	4	48	19	93	23	246	58	20060	--	187	1501	0.12
55z-25r	176	17.4	2.6	63	186	21	81	17	3	19	4	43	17	85	20	208	46	20370	--	79	751	0.10
55z-3r1*	51000	121.0	18.0	496	1000	135	601	106	33	86	9	61	19	84	20	209	48	12020	374	84	500	0.18
55z-4r	207	5.8	0.7	10	49	5	34	7	10	10	3	41	19	101	28	328	80	14370	894	125	1432	0.09
55z-6r*	318	96.0	10.0	299	867	121	598	135	13	94	9	66	22	104	26	297	63	11850	432	169	624	0.28
55z-10r	30000	34.5	2.9	175	581	82	458	97	10	80	9	56	16	66	15	149	36	10060	214	41	304	0.14
55z-15r	125	6.4	0.8	11	41	4	18	2	0	4	1	24	13	77	22	260	64	16150	726	26	991	0.03
55z-4c	190	78.1	6.0	42	49	6	18	3	1	9	3	37	15	74	18	184	40	18750	--	20	126	0.16
55z-8c	252	18.2	5.0	12	100	13	65	12	5	16	5	55	24	130	35	387	97	17800	--	98	560	0.17
55z-12c	390	6.0	0.7	10	76	7	31	5	2	26	9	122	51	238	53	507	113	16270	--	91	358	0.26
55z-21c2*	548	1936.0	86.0	18	130	19	152	58	16	74	16	174	64	286	59	551	113	14370	--	114	227	0.50
55z-4c*	2570	40.0	11.0	30	81	9	43	5	1	8	2	33	14	72	17	177	40	10990	285	37	397	0.10
55z-8c*	216	66.0	15.0	22	166	23	138	21	6	26	6	62	23	107	24	243	55	10010	277	112	357	0.34
55z-12c	207	6.4	0.7	6	47	5	26	6	2	24	7	85	32	141	29	272	58	8660	109	51	135	0.39
55z-21c2*	920	3800	1700	26	128	22	152	48	7	49	8	75	31	134	31	278	60	8300	149	64	140	0.43
55z-25r*	706	45.0	12.0	221	540	62	273	61	7	98	27	339	132	607	134	1270	236	12340	1159	439	2010	0.23

Appendix G. (cont)

	P	Ti	2σ	La	Ce	Pr	Nd	Sm	Eu	Gd	Tb	Dy	Ho	Er	Tm	Yb	Lu	Hf	Pb	Th	U	Th/U
North Caribou batholith "pluton"																						
46: Foliated granodiorite																						
46z-20c	18300	21.6	2.1	125	210	45	216	131	26	208	40	274	77	300	59	536	106	18180	--	450	1869	0.24
46z-22c	700	35.3	3.2	93	298	43	248	149	36	208	34	207	52	192	38	355	70	19110	--	119	916	0.13
46z-20c	81000	30.1	3.8	96	232	43	231	113	34	170	28	170	41	143	27	243	51	10520	416	120	526	0.23
46z-22c*	2080	197.0	18.0	28	66	11	60	32	7	50	9	68	20	86	19	179	38	10400	340	72	440	0.16
46z-1c*	627	183.0	25.0	139	291	56	285	196	43	334	58	362	90	318	59	525	105	12030	--	230	433	0.53
46z-16r	265	11.6	1.8	43	120	20	115	78	18	148	27	206	59	241	50	463	92	18740	--	315	1331	0.23
46z-1c*	222	43.4	8.4	37	85	15	80	59	13	115	21	146	40	153	29	269	54	8130	268	129	306	0.44
46z-16r	179	4.8	1.2	19	80	11	67	46	11	78	13	101	31	136	29	272	56	10530	450	112	577	0.20
46z-16c	1030	9.3	1.6	62	192	33	182	118	27	192	30	192	49	180	35	330	65	19500	--	200	1053	0.19
46z-16c*	7600	72.0	12.0	189	359	83	441	296	64	490	73	383	71	188	29	234	44	10690	375	125	526	0.23
49: Leucocratic granodiorite																						
49z-2r	140	7.3	1.9	20	117	22	132	90	16	139	23	132	31	105	21	193	41	10650	236	19	244	0.08
49z-14r	53	22.3	1.5	11	51	8	62	33	8	50	7	49	11	37	6	58	12	10430	83	12	138	0.09
49z-16r	123	15.1	1.1	3	17	2	14	8	5	24	7	85	31	137	29	271	54	10670	274	39	413	0.09
49z-26r	185	5.4	1.3	4	15	3	16	12	2	21	5	47	19	100	25	262	60	11700	389	20	569	0.04
49z-31r*	152	17.6	5.8	13	56	10	64	43	9	82	19	168	50	199	40	374	72	12400	375	22	450	0.06
49z-7c	149	39.6	4.6	17	93	11	80	56	12	99	18	114	25	77	14	119	25	10080	179	89	210	0.40
49z-11c*	335	273.0	41.0	132	550	103	690	394	57	490	63	308	51	137	23	196	39	9730	170	66	532	0.12
49z-12c	344	68.1	4.1	79	331	49	316	190	44	315	51	328	68	189	29	221	42	9800	322	158	376	0.43
49z-15c	231	20.2	5.3	14	94	11	71	38	8	69	14	106	30	117	24	231	50	9460	265	153	311	0.49
49z-30c	235	10.4	2.0	18	96	13	87	44	22	73	14	106	30	113	24	240	55	9330	351	136	386	0.35
66: High-strain tonalite																						
66z-2c*	1200	740000	180000	1780	5500	830	3800	1030	266	1080	168	950	231	690	111	890	167	15130	--	860	1340	0.66
66z-3r*	210	401.0	27.0	276	1541	253	1540	617	126	674	64	294	62	191	32	285	61	19290	--	307	1470	0.21
66z-6c	1246	42.2	2.6	37	248	12	79	55	21	228	65	707	244	988	213	2100	358	11150	--	6690	4740	1.41
66z-7c	840	17.3	2.1	82	456	66	379	100	14	83	12	111	43	201	46	461	95	16910	--	292	1074	0.27
66z-2c	832	47.1	7.7	8	92	5	37	21	7	83	26	320	123	548	117	1139	229	6200	1657	3350	2550	1.30
66z-3r	218	65.2	4.1	134	764	97	792	211	52	202	17	113	39	182	44	510	114	18120	1170	343	4000	0.09
66z-6c	756	22.3	1.9	13	93	8	54	22	6	61	18	220	89	414	94	960	198	6260	1341	2160	2050	1.06
66z-7c	298	31.0	15.0	74	385	56	362	90	13	71	9	70	23	106	24	239	49	9880	334	126	499	0.26

Appendix G. (cont)

	P	Ti	2σ	La	Ce	Pr	Nd	Sm	Eu	Gd	Tb	Dy	Ho	Er	Tm	Yb	Lu	Hf	Pb	Th	U	Th/U
North Caribou batholith "core"																						
51: K-feldspar augen gneiss																						
51z-8r	93	20.3	1.6	9	66	4	28	17	6	34	6	52	15	55	10	86	18	8150	76	91	88	1.04
51z-9r*	1170	543.0	31.0	84	357	63	377	153	42	141	19	105	23	73	13	113	21	9480	254	296	343	0.87
51z-14r*	328	50.7	8.4	41	312	35	222	103	27	140	27	185	53	170	31	230	41	7790	352	690	362	1.75
51z-17c	365	20.3	4.1	8	320	10	99	88	31	208	39	301	81	285	50	405	74	6810	349	940	331	2.80
51z-21c	217	15.4	2.4	22	68	9	56	36	9	79	17	145	44	166	32	277	54	6930	139	161	174	0.94
51z-6c	3700	15.2	2.1	54	299	38	211	70	14	84	15	121	40	166	36	334	67	10500	438	184	611	0.30
51z-19c	139	27.1	2.0	15	72	10	58	28	6	38	7	57	17	68	14	136	26	9590	114	49	151	0.33
51z-20r	750	3.6	0.6	56	132	20	108	47	10	66	12	100	28	101	21	180	35	9810	187	75	214	0.37
51z-3r	70	7.0	3.5	0	9	0	1	1	0	3	1	10	4	20	4	44	10	8920	22	10	28	0.38
61: Massive tonalite																						
61z-2c	208	21.0	2.6	2	24	2	19	15	4	31	7	60	19	78	17	164	35	14680	--	65	133	0.49
61z-22c	336	15.0	2.2	10	89	10	72	40	9	69	13	130	46	208	45	417	90	16110	--	244	595	0.41
61z-22r*	170	33.8	5.7	66	146	18	106	49	10	67	10	69	21	80	18	178	38	17040	--	116	343	0.34
61z-25c	415	28.5	3.4	22	137	18	106	52	12	81	16	149	53	241	53	505	107	17270	--	194	522	0.37
61z-26c	355	13.4	0.9	1	21	1	6	7	3	26	7	82	30	135	30	288	62	13450	--	78	151	0.52
61z-2c*	340	40.0	10.0	17	103	16	96	61	18	115	20	157	42	140	26	223	44	9060	126	75	178	0.42
61z-22c*	9900	65.0	11.0	62	187	26	140	52	10	68	11	79	24	97	19	182	40	8790	200	94	228	0.42
61z-22r*	1040	32.5	8.0	17	83	10	68	30	7	45	8	66	22	96	20	193	43	9224	184	102	257	0.39
61z-25c	126	18.1	1.5	28	146	20	123	46	10	53	7	47	14	60	13	138	33	11030	392	72	529	0.13
61z-26c	207	5.9	0.8	0	10	0	1	2	1	11	3	40	16	79	18	180	42	7441	73	37	92	0.40

Appendix G. (cont)

	P	Ti	2σ	La	Ce	Pr	Nd	Sm	Eu	Gd	Tb	Dy	Ho	Er	Tm	Yb	Lu	Hf	Pb	Th	U	Th/U
62/63: Gneissic tonalite																						
62-6r*	396	62.0	3.3	3	44	5	35	19	9	26	5	40	13	53	11	100	22	15550	--	25	39	0.66
62-11r*	1091	20.5	4.3	12	124	15	103	42	24	45	7	50	15	65	15	147	33	16480	--	53	125	0.42
62-12r*	336	10.6	1.7	7	68	10	70	24	12	25	4	35	12	54	11	106	23	15330	--	31	70	0.45
62-20r*	203	970.0	340.0	5	39	5	31	13	7	17	3	26	9	42	10	104	24	16840	--	24	83	0.30
63- 25c	218	13.9	1.9	12	68	11	69	32	13	41	6	36	10	40	9	90	21	17170	--	40	118	0.34
63- 26r	203	6.1	0.6	0	16	0	2	2	1	9	3	32	12	59	13	134	28	16620	--	20	42	0.47
62-6r*	552	109.7	8.7	16	129	19	121	51	26	56	9	61	17	62	12	120	25	9440	123	50	157	0.32
63- 7c	124	5.2	0.7	6	28	3	26	10	3	14	2	22	8	37	8	80	18	9170	37	20	44	0.46
63- 14c	102	5.1	0.5	5	60	2	11	4	1	7	1	15	6	28	7	72	17	9150	65	32	78	0.41
63- 25c	69	5.1	0.7	1	10	1	7	3	1	5	1	11	4	21	5	58	15	10320	91	14	122	0.12
63- 26r	93	2.5	0.6	0	8	0	1	1	0	3	1	11	4	21	5	48	11	9270	18	9	23	0.39
62-14c*	272	66.0	35.0	116	600	102	644	115	40	85	15	158	63	288	65	628	133	18110	--	464	1410	0.33
63- 7c	86	18.0	2.9	45	181	26	148	37	12	37	6	62	28	162	48	632	147	20320	--	317	2120	0.15
63- 9c	227	5.6	0.9	14	69	10	65	27	8	43	8	83	32	149	34	349	77	18050	--	160	476	0.34
63- 14c	257	12.9	1.3	31	234	8	39	16	6	38	9	85	30	131	29	290	63	12020	--	134	142	0.94
62-11r*	1200	59.3	4.2	44	365	54	359	128	71	121	16	105	26	94	20	191	39	9870	181	72	289	0.25
62-12r	418	15.9	2.2	59	196	29	216	59	26	53	6	38	12	48	10	89	19	9110	61	41	107	0.39
62-14c*	780	27.7	8.6	48	262	39	274	45	15	49	10	108	37	157	33	305	61	8900	434	267	561	0.47
62-20r*	347	493.0	43.0	15	94	16	106	35	17	34	5	42	15	66	15	142	29	10000	149	68	227	0.31
63- 9c	192	5.9	1.0	19	89	14	101	39	11	42	5	48	17	80	18	180	40	9370	209	95	258	0.41

Appendix G. (cont)

	P	Ti	2σ	La	Ce	Pr	Nd	Sm	Eu	Gd	Tb	Dy	Ho	Er	Tm	Yb	Lu	Hf	Pb	Th	U	Th/U
Libert Lake pluton																						
45: Melanocratic granite																						
45z-5r*	210	78.0	17.0	22	114	17	85	45	10	75	15	120	28	98	19	166	34	10410	363	108	630	0.17
45z-5c	230	10.9	1.2	4	40	3	17	10	2	24	6	61	21	89	18	163	33	10090	166	115	216	0.53
45z-1c	297	3.1	0.7	0	9	0	1	2	0	12	4	56	23	106	23	222	49	10230	116	64	158	0.40
45z-11c	402	4.6	0.8	3	31	2	12	10	2	37	11	118	42	175	35	307	60	9400	215	177	283	0.61
45z-2c	245	5.4	0.9	16	30	4	19	10	2	37	11	116	41	170	35	312	62	7760	110	112	141	0.78
Pegmatites																						
54: K-feldspar pegmatite																						
54z-15c*	2719	5.7	1.0	26	251	43	231	83	3	142	45	601	240	1161	275	2778	496	24930	--	1962	15730	0.12
54z-18c	1424	2.5	1.2	21	13	0	2	4	1	37	17	222	93	459	106	1130	199	20900	--	635	4320	0.15
54z-21c	1528	1.4	0.3	0	7	0	1	3	0	32	15	227	99	504	117	1136	239	25030	--	605	4848	0.12
54z-24c*	3270	11.0	3.2	6	39	3	15	13	1	98	45	654	274	1336	322	3270	581	25290	--	2084	16590	0.13
54z-26r	2540	2.8	0.7	0	8	0	1	4	0	50	27	380	168	857	205	2100	390	24840	--	930	10680	0.09
54z-15c*	1850	3.8	1.5	7	78	10	58	22	1	57	22	303	132	663	157	1588	301	14070	7890	676	6450	0.11
54z-18c	649	1.6	0.4	28	18	1	3	2	1	20	9	133	56	276	65	642	123	14510	1755	330	2500	0.13
54z-21c	855	2.1	0.4	2	6	1	5	2	0	19	9	132	57	284	66	651	131	13770	1739	350	2639	0.13
54z-24c	2120	3.1	0.5	18	47	4	11	6	0	53	25	363	156	773	178	1746	331	13560	4788	1178	8800	0.13
54z-26r	779	2.8	0.4	2	23	1	5	5	0	45	22	308	130	634	147	1475	266	15070	6723	736	7390	0.10
54z-28r	523	61.9	4.5	774	2410	185	627	189	8	168	29	257	91	415	97	965	183	29220	--	274	4030	0.07
54z-28r	876	82.0	13.0	193	790	76	300	60	3	89	29	361	147	711	168	1640	321	14750	2903	990	9680	0.10

Notes:
*: Samples not used in Ti thermometer calculations
Not all samples have Pb concentrations analyzed

Appendix H. EPMA results of major elements in amphiboles from granitoids surrounding the NCGB

		SiO_2	Al_2O_3	TiO_2	Cr_2O_3	MgO	NiO	ZnO	FeO	MnO	CaO	Na_2O	K_2O	Cl	F	Total	Plagioclase
01: Leucocratic tonalite																	
Carleton	01-1-1	44.68	8.93	0.74	0.00	10.03	--	--	18.58	0.44	11.95	1.24	1.05	--	--	97.65	Average
	01-1-2	44.93	9.08	0.86	0.01	9.79	--	--	18.92	0.41	11.95	1.34	1.06	--	--	98.35	Average
	01-1-3	44.93	9.10	0.85	0.01	9.80	--	--	18.61	0.41	11.94	1.30	1.09	--	--	98.03	Average
	01-1-4	44.60	8.89	0.76	0.02	9.94	--	--	18.60	0.38	12.00	1.28	1.04	--	--	97.51	Average
	01-1-5	44.01	9.02	0.87	0.02	9.82	--	--	18.51	0.40	11.95	1.25	1.08	--	--	96.93	Average
	01-1-6	44.35	9.17	0.79	0.02	9.87	--	--	18.73	0.39	11.97	1.15	1.07	--	--	97.50	Average
	01-1-7	43.78	9.13	0.82	0.03	9.82	--	--	18.76	0.37	11.91	1.19	1.05	--	--	96.85	Average
	01-1-8	43.88	9.13	0.80	0.01	9.77	--	--	18.67	0.34	12.00	1.23	1.12	--	--	96.95	Average
	01-1-9	44.29	8.97	0.60	0.02	10.09	--	--	18.75	0.37	11.99	1.13	1.04	--	--	97.24	Average
	01-1-10	43.92	9.07	0.72	0.02	10.07	--	--	18.39	0.41	11.91	1.17	1.03	--	--	96.70	Average
	01-2-1	44.91	9.06	1.03	0.03	9.66	--	--	18.93	0.38	11.79	1.30	1.02	0.020	0.162	98.28	Average
	01-2-2	44.19	9.42	0.95	0.00	9.56	--	--	19.22	0.40	11.80	1.21	1.12	0.002	0.198	98.09	Average
	01-2-3	43.97	9.12	1.14	0.00	9.62	--	--	19.30	0.42	11.83	1.31	1.14	--	--	97.85	Average
	01-2-4	44.08	9.11	1.01	0.00	9.52	--	--	19.16	0.45	11.84	1.35	1.15	--	--	97.67	Average
	01-2-5	43.82	9.08	1.04	0.00	9.58	--	--	19.13	0.35	11.91	1.39	1.18	--	--	97.48	Average
	01-2-6	44.27	9.33	0.92	0.00	9.65	--	--	19.34	0.38	11.75	1.38	1.13	--	--	98.14	Average
	01-2-7	44.23	9.09	1.09	0.00	9.65	--	--	19.24	0.42	11.72	1.37	1.18	--	--	97.98	Average
	01-2-8	44.88	9.25	0.92	0.01	9.46	--	--	19.10	0.41	11.72	1.27	1.11	--	--	98.14	Average
	01-2-9	43.64	9.31	1.15	0.00	9.49	--	--	19.19	0.43	11.57	1.38	1.20	--	--	97.35	Average
	01-2-10	44.81	8.90	0.79	0.01	9.78	--	--	19.01	0.39	11.83	1.18	1.01	--	--	97.70	Average
	01-2-11	44.42	9.04	1.02	0.00	9.54	--	--	19.22	0.44	11.76	1.30	1.12	--	--	97.85	Average
	01-2-12	44.11	9.08	1.10	0.00	9.61	--	--	19.22	0.41	11.79	1.22	1.11	--	--	97.66	Average
	01-3-1	43.96	8.83	0.92	0.00	10.00	--	--	18.09	0.37	11.42	1.39	1.06	0.003	0.165	96.20	Average
	01-3-2	44.46	8.84	0.85	0.01	9.78	--	--	17.75	0.40	11.44	1.31	1.00	0.006	0.139	96.00	Average
	01-3-3	43.41	9.05	0.94	0.00	9.91	--	--	18.08	0.43	11.50	1.29	1.02	--	--	95.63	Average
	01-3-4	43.70	9.09	0.93	0.01	9.66	--	--	18.18	0.38	11.50	1.31	1.07	--	--	95.82	Average
	01-3-5	44.21	9.04	0.82	0.00	9.90	--	--	17.96	0.35	11.60	1.25	1.00	--	--	96.12	Average
	01-3-6	44.03	8.93	0.86	0.01	9.81	--	--	17.73	0.43	11.66	1.28	0.98	--	--	95.72	Average
	01-3-7	44.04	8.94	0.86	0.01	9.84	--	--	17.95	0.36	11.63	1.27	0.99	--	--	95.89	Average
	01-3-8	44.15	9.03	0.91	0.01	9.74	--	--	17.77	0.38	11.54	1.33	1.03	--	--	95.88	Average
	01-4-1	44.24	9.37	1.18	0.03	9.80	--	--	19.04	0.47	11.89	1.30	1.07	--	--	98.38	Average
	01-4-2	44.22	9.29	1.05	0.03	9.76	--	--	18.71	0.36	11.91	1.29	1.04	--	--	97.66	Average
	01-4-3	44.80	9.26	1.12	0.05	10.00	--	--	18.41	0.36	12.17	1.30	1.05	--	--	98.51	Average
	01-4-4	44.60	9.11	0.91	0.01	9.96	--	--	18.49	0.37	12.04	1.19	0.98	--	--	97.66	Average
	01-4-5	44.13	9.31	1.17	0.07	9.62	--	--	18.55	0.40	11.91	1.26	1.11	--	--	97.55	Average
	01-4-6	44.23	9.45	1.21	0.09	9.76	--	--	18.84	0.41	11.85	1.24	1.04	--	--	98.12	Average

Appendix H. (cont)

		SiO_2	Al_2O_3	TiO_2	Cr_2O_3	MgO	NiO	ZnO	FeO	MnO	CaO	Na_2O	K_2O	Cl	F	Total	Plagioclase
Carleton	01-4-7	44.51	9.23	1.14	0.03	9.83	--	--	18.77	0.38	11.81	1.24	1.04	--	--	97.96	Average
	01-4-8	42.67	8.76	1.01	0.04	9.60	--	--	17.73	0.38	11.64	1.27	1.01	--	--	94.12	Average
	01-5-1	44.31	8.96	1.07	0.01	9.77	--	--	18.92	0.36	11.93	1.25	1.06	--	--	97.64	Average
	01-5-2	44.37	8.96	1.08	0.01	9.88	--	--	18.73	0.39	11.87	1.20	0.98	--	--	97.48	Average
	01-5-3	43.99	9.18	1.13	0.02	9.62	--	--	18.75	0.36	11.74	1.31	1.05	--	--	97.15	Average
	01-5-4	44.52	8.97	1.07	0.04	9.86	--	--	18.84	0.42	11.77	1.36	1.08	--	--	97.93	Average
	01-5-5	43.96	9.14	1.20	0.03	9.54	--	--	18.83	0.37	11.61	1.40	1.12	--	--	97.21	Average
	01-5-6	44.14	9.25	1.03	0.03	9.66	--	--	18.79	0.34	11.79	1.19	1.09	--	--	97.30	Average
	01-5-7	44.37	9.17	1.14	0.04	9.71	--	--	18.84	0.39	11.97	1.29	1.10	--	--	98.02	Average
	01-5-8	43.98	9.06	0.94	0.01	9.72	--	--	18.75	0.46	11.96	1.22	1.04	--	--	97.14	Average
	01-1-2	43.21	9.23	0.81	0.04	10.27	0.01	0.04	17.86	0.38	11.66	1.30	1.05	0.016	0.240	95.99	f01-1-4
	01-1-3	43.70	8.97	0.49	0.00	10.52	0.01	0.08	17.70	0.38	11.70	1.22	0.88	0.012	0.374	95.88	f01-1-4
	01-1-4	43.85	9.07	0.43	0.00	10.59	0.02	0.00	17.72	0.38	11.77	1.24	0.87	0.029	0.372	96.18	f01-1-4
	01-2-1	44.76	8.71	0.54	0.00	10.62	0.00	0.00	18.33	0.39	12.01	1.25	0.85	0.010	0.316	97.64	f01-2-4
	01-2-2	43.56	9.45	0.51	0.01	10.32	0.00	0.02	18.63	0.36	11.88	1.25	0.95	0.010	0.182	97.04	f01-2-6
	01-2-3	43.76	9.24	0.59	0.00	10.47	0.00	0.07	18.45	0.39	12.04	1.21	0.96	0.014	0.327	97.37	f01-2-5
	01-2-4	43.43	9.46	0.83	0.00	10.31	0.00	0.08	18.58	0.38	11.92	1.34	1.09	0.007	0.277	97.58	f01-2-2
	01-2-5	44.04	9.05	0.68	0.01	10.47	0.00	0.01	18.27	0.38	12.02	1.24	0.96	0.009	0.494	97.41	f01-2-3
	01-2-6	44.25	9.21	0.40	0.02	10.68	0.00	0.04	17.85	0.39	12.09	1.10	0.87	0.004	0.271	97.05	f01-2-1
	01-4-1	43.66	9.34	0.78	0.00	10.27	0.00	0.00	18.32	0.39	11.87	1.28	1.01	0.008	0.272	97.08	f01-4-2
	01-4-2	44.12	9.21	0.66	0.00	10.48	0.00	0.04	18.27	0.40	12.12	1.18	0.89	0.009	0.310	97.57	f01-4-1
	01-3-1	43.35	9.58	0.81	0.02	10.01	0.00	0.00	18.80	0.38	11.97	1.19	0.99	0.006	0.289	97.26	f01-3-5
	01-3-2	43.80	9.44	0.85	0.00	10.18	0.00	0.01	18.71	0.41	11.88	1.22	1.03	0.006	0.341	97.72	f01-3-4
	01-3-3	44.47	9.17	0.55	0.01	10.65	0.01	0.06	18.36	0.39	11.96	1.16	0.93	0.006	0.373	97.92	f01-3-3
	01-3-4	44.24	9.32	0.85	0.00	10.28	0.01	0.09	18.48	0.40	11.85	1.26	1.03	0.012	0.302	97.98	f01-3-2
	01-3-5	43.75	9.25	0.81	0.01	10.30	0.00	0.09	18.45	0.37	11.78	1.21	1.01	0.001	0.159	97.11	f01-3-1
	01-7-1	44.30	9.04	0.59	0.02	10.60	0.01	0.12	18.16	0.38	12.03	1.08	0.93	0.008	0.099	97.33	f01-7-4
	01-7-2	43.57	9.55	0.60	0.06	10.23	0.01	0.08	18.38	0.39	12.08	1.20	0.97	0.005	0.298	97.29	f01-7-3
	01-7-3	43.43	9.40	0.78	0.03	10.18	0.00	0.06	18.43	0.39	11.70	1.29	1.02	0.002	0.220	96.85	f01-7-2
	01-7-4	43.84	9.66	0.55	0.04	10.19	0.00	0.02	18.27	0.40	11.76	1.27	0.95	0.007	0.316	97.12	f01-7-5
	01-7-5	43.90	9.19	0.71	0.06	10.29	0.01	0.10	18.08	0.39	11.86	1.22	0.92	0.006	0.237	96.88	f01-7-1

Appendix H. (cont)

		SiO_2	Al_2O_3	TiO_2	Cr_2O_3	MgO	NiO	ZnO	FeO	MnO	CaO	Na_2O	K_2O	Cl	F	Total	Plagioclase
13/15: Strongly foliated granodiorite; cores																	
Carleton	13-1-2	43.44	9.64	0.49	0.04	9.46	--	--	17.98	0.37	11.39	1.21	0.92	0.017	0.044	94.99	Average
	13-1-10	42.51	10.66	0.48	0.01	8.81	--	--	19.01	0.43	11.49	1.26	1.06	--	--	95.72	Average
	13-1-18*	45.52	8.45	0.42	0.04	10.34	--	--	17.48	0.39	11.62	1.00	0.69	--	--	95.94	Average
	13-1-19	42.04	10.77	0.57	0.06	8.70	--	--	18.87	0.40	11.51	1.29	1.12	--	--	95.32	Average
	13-1-20	43.82	9.51	0.51	0.02	9.57	--	--	18.35	0.38	11.62	1.24	0.96	--	--	95.99	Average
	13-1-21	41.58	10.97	0.54	0.02	8.34	--	--	19.19	0.40	11.43	1.31	1.27	--	--	95.06	Average
	13-1-22	41.65	10.71	0.52	0.00	8.77	--	--	19.19	0.43	11.58	1.38	1.15	--	--	95.37	Average
	13-1-23	43.08	9.92	0.48	0.01	9.38	--	--	18.54	0.39	11.66	1.35	0.97	--	--	95.78	Average
	13-1-24	42.24	10.67	0.51	0.01	8.79	--	--	18.75	0.39	11.44	1.30	1.12	--	--	95.21	Average
	13-1-25	42.17	10.36	0.49	0.00	8.94	--	--	18.85	0.40	11.41	1.31	1.06	--	--	94.99	Average
	13-1-27*	44.71	8.37	0.46	0.01	10.33	--	--	17.48	0.40	11.62	1.12	0.73	--	--	95.25	Average
	13-1-31	41.78	10.96	0.53	0.00	8.58	--	--	19.10	0.38	11.63	1.28	1.16	--	--	95.41	Average
	13-1-32	42.56	10.61	0.47	0.01	8.78	--	--	18.80	0.39	11.58	1.25	1.06	--	--	95.52	Average
	13-2-3*	45.64	8.55	0.58	0.03	10.34	--	--	18.46	0.47	12.12	1.06	0.79	--	--	98.04	Average
	13-2-8	42.55	11.09	0.52	0.00	8.51	--	--	20.47	0.45	12.08	1.37	1.27	--	--	98.33	Average
	13-2-9	45.80	8.08	0.75	0.02	10.36	--	--	18.12	0.39	12.00	1.11	0.74	--	--	97.37	Average
	13-2-10	42.21	11.08	0.72	0.01	8.44	--	--	20.40	0.41	11.86	1.29	1.25	--	--	97.66	Average
	13-3-1	43.83	9.82	0.61	0.01	9.56	--	--	19.58	0.41	12.11	1.24	1.08	--	--	98.25	Average
	13-3-4	43.25	10.30	0.51	0.04	9.16	--	--	20.14	0.44	11.75	1.25	1.05	--	--	97.88	Average
	13-4-1	43.42	10.15	0.42	0.11	9.16	--	--	19.70	0.45	11.95	1.32	1.03	--	--	97.71	Average
	13-4-2	42.80	10.72	0.41	0.06	8.82	--	--	20.12	0.41	11.99	1.27	1.11	--	--	97.72	Average
	13-4-3	42.71	11.08	0.51	0.14	8.61	--	--	20.29	0.38	12.00	1.37	1.21	--	--	98.30	Average
	13-4-4	43.07	10.35	0.64	0.13	8.90	--	--	20.00	0.44	11.96	1.28	1.11	--	--	97.89	Average
	13-4-5	42.51	10.74	0.56	0.21	8.67	--	--	20.16	0.47	11.97	1.26	1.24	--	--	97.78	Average
	13-4-6	43.73	9.80	0.34	0.07	9.70	--	--	19.31	0.49	12.03	1.11	0.88	--	--	97.45	Average
	13-4-7	42.94	10.19	0.38	0.07	9.16	--	--	19.75	0.44	12.03	1.13	1.02	--	--	97.12	Average
	13-4-8	42.20	10.81	0.55	0.10	8.67	--	--	20.18	0.42	12.05	1.29	1.28	--	--	97.53	Average
	13-4-9	42.17	10.91	0.56	0.08	8.66	--	--	20.40	0.45	12.05	1.35	1.31	--	--	97.95	Average
	13-4-10	42.14	10.77	0.49	0.25	8.61	--	--	20.08	0.44	12.00	1.37	1.13	--	--	97.28	Average
	13-4-11	42.03	10.85	0.61	0.03	8.70	--	--	20.50	0.42	12.03	1.34	1.24	--	--	97.74	Average
	13-1-1	40.19	10.38	0.50	0.00	9.26	0.00	0.02	18.14	0.36	11.11	1.33	1.08	0.004	0.091	92.43	f13-1-3
	13-1-2	43.15	9.35	0.27	0.00	10.17	0.00	0.04	16.83	0.38	11.35	1.21	0.75	0.006	0.284	93.66	f13-1-1, f13-1-2
	13-2-1	43.65	9.77	0.35	0.01	9.93	0.00	0.00	19.17	0.45	11.84	1.18	0.82	0.011	0.030	97.19	f13-2-2
	13-2-2	43.43	9.87	1.11	0.00	9.81	0.01	0.00	19.17	0.43	12.27	1.25	0.88	0.010	0.061	98.26	f13-2-1
	13-3-1	43.20	10.33	0.37	0.00	9.65	0.01	0.02	19.71	0.43	11.84	1.29	0.94	0.013	0.016	97.80	f13-3-4, f13-3-5
	13-3-3	42.41	10.66	0.47	0.03	9.34	0.01	0.03	19.98	0.45	12.00	1.22	1.05	0.011	0.000	97.63	f13-3-2, f13-3-1
	13-3-4	44.46	9.21	0.32	0.00	10.63	0.01	0.07	18.64	0.43	11.96	1.14	0.76	0.007	0.137	97.72	f13-3-3

Appendix H. (cont)

		SiO_2	Al_2O_3	TiO_2	Cr_2O_3	MgO	NiO	ZnO	FeO	MnO	CaO	Na_2O	K_2O	Cl	F	Total	Plagioclase
	13-4-3	44.06	9.30	0.30	0.02	10.40	0.01	0.04	18.73	0.43	12.08	1.25	0.81	0.025	0.112	97.52	f13-4-1
	15-1-1	43.36	10.16	0.29	0.00	9.96	0.02	0.06	19.15	0.46	12.00	1.22	0.92	0.008	0.262	97.73	f15-1-2
	15-2-1	44.56	9.03	0.34	0.04	10.66	0.02	0.01	18.12	0.40	12.06	1.12	0.76	0.018	0.207	97.25	f15-2-1
	15-2-3	43.29	10.02	0.41	0.02	9.86	0.02	0.05	19.09	0.42	11.90	1.20	0.94	0.012	0.052	97.26	f15-2-3
	15-2-6*	45.60	8.50	0.31	0.00	11.16	0.01	0.01	17.62	0.39	11.97	1.04	0.64	0.006	0.144	97.33	f15-2-6
	15-2-7	44.25	9.33	0.34	0.00	10.62	0.02	0.05	18.44	0.41	11.94	1.12	0.80	0.017	0.269	97.49	f15-2-7
	15-3-2	43.26	10.35	0.44	0.02	9.75	0.02	0.01	19.31	0.42	11.88	1.15	0.93	0.012	0.024	97.58	f15-3-7
	15-3-3	44.03	9.48	0.32	0.01	10.42	0.00	0.02	18.48	0.41	12.10	1.14	0.83	0.010	0.000	97.24	f15-3-6
	15-3-4	42.96	10.28	0.49	0.04	9.82	0.02	0.03	19.20	0.42	12.06	1.16	0.96	0.009	0.081	97.48	f15-3-5
	15-3-5	45.12	8.98	0.31	0.00	10.66	0.01	0.00	18.16	0.40	12.12	1.14	0.75	0.010	0.062	97.70	f15-3-4, f15-3-3
	15-3-7*	45.37	8.46	0.29	0.00	11.05	0.01	0.05	17.72	0.43	12.02	1.13	0.69	0.004	0.297	97.40	f15-3-2, f15-3-1
rims																	
Carleton	13-1-1	46.09	7.61	0.92	0.01	10.95	-	-	16.47	0.40	11.56	0.92	0.60	0.007	0.068	95.59	Average
	13-1-17	45.77	7.66	0.85	0.01	10.76	-	-	16.81	0.37	11.73	1.03	0.70	--	--	95.69	Average
	13-1-26	46.23	7.47	0.75	0.01	10.95	-	-	16.47	0.37	11.67	0.97	0.66	--	--	95.56	Average
	13-1-28	45.50	7.94	0.87	0.01	10.66	-	-	17.01	0.40	11.67	1.01	0.73	--	--	95.79	Average
	13-1-29	45.89	7.66	0.79	0.01	10.79	-	-	16.89	0.35	11.64	0.96	0.70	--	--	95.67	Average
	13-1-30	45.70	7.94	0.67	0.03	10.60	-	-	17.01	0.44	11.51	1.02	0.70	--	--	95.62	Average
	13-2-1	46.43	7.56	0.97	0.02	10.73	-	-	17.39	0.41	12.04	0.99	0.72	0.008	0.066	97.34	Average
	13-2-2	46.18	7.56	1.01	0.02	10.95	-	-	17.50	0.41	12.01	0.99	0.75	0.000	0.066	97.45	Average
	13-2-5	46.36	7.90	0.54	0.02	10.88	-	-	17.71	0.45	12.11	1.00	0.69	--	--	97.65	Average
	13-2-6	45.65	7.55	1.07	0.03	10.85	-	-	17.74	0.43	12.18	1.04	0.69	--	--	97.23	Average
	13-2-7	46.97	7.72	1.09	0.01	10.79	-	-	17.91	0.44	11.96	0.97	0.70	--	--	98.56	Average
	13-3-2	46.55	7.89	0.75	0.01	10.67	-	-	18.02	0.47	12.14	1.03	0.73	--	--	98.28	Average
	13-3-3	46.35	7.91	0.88	0.04	10.73	-	-	18.26	0.45	12.11	1.02	0.68	--	--	98.43	Average
	13-4-2	46.71	7.46	0.25	0.00	11.97	0.00	0.06	17.05	0.39	12.08	0.98	0.54	0.004	0.106	97.56	f13-4-2, f13-4-3, f13-4-4
	15-2-2	46.17	7.90	0.27	0.00	11.60	0.00	0.00	17.15	0.43	12.19	0.96	0.58	0.019	0.164	97.36	f15-2-2
	15-3-1	46.75	7.65	0.25	0.00	11.85	0.00	0.03	17.00	0.43	12.19	0.96	0.54	0.002	0.048	97.69	f15-3-8
altered rims																	
	15-1-2	48.51	6.02	0.19	0.00	12.94	0.01	0.02	15.44	0.39	12.14	0.72	0.38	0.011	0.139	96.85	f15-1-1
	15-2-4	50.90	6.51	0.24	0.00	12.07	0.00	0.06	15.94	0.42	11.74	0.83	0.44	0.008	0.122	99.22	f15-2-4
	15-2-5	49.12	5.47	0.18	0.00	13.39	0.00	0.00	15.32	0.43	12.35	0.69	0.31	0.006	0.109	97.34	f15-2-5

Appendix H. (cont)

		SiO_2	Al_2O_3	TiO_2	Cr_2O_3	MgO	NiO	ZnO	FeO	MnO	CaO	Na_2O	K_2O	Cl	F	Total	Plagioclase
22: Mylonitic augen gneiss; cores																	
C	22-3-2	44.35	10.79	0.69	0.00	9.21	--	--	18.22	0.42	12.14	1.09	0.73	0.001	0.037	97.67	Average
	22-2-4	46.30	8.78	0.27	0.00	11.03	0.01	0.03	16.32	0.40	11.99	0.88	0.52	0.015	0.209	96.67	f22-2-4
	22-2-6	44.13	10.90	0.70	0.00	9.88	0.01	0.04	17.33	0.38	11.80	1.08	0.70	0.008	0.000	96.95	f22-2-2
	22-2-7	45.45	9.59	0.36	0.01	10.57	0.01	0.00	16.60	0.36	11.76	0.87	0.63	0.015	0.156	96.30	f22-2-1
	22-3-6	45.16	10.24	0.49	0.07	10.26	0.02	0.06	17.59	0.44	12.20	0.90	0.70	0.014	0.059	98.17	f22-3-7
	22-3-7	45.68	10.01	0.32	0.00	10.26	0.01	0.00	17.51	0.42	12.23	0.98	0.67	0.011	0.099	98.14	f22-3-8
rims																	
C	22-1-1	42.60	12.56	0.78	0.01	8.43	--	--	18.61	0.36	12.03	1.24	0.97	0.018	0.039	97.63	Average
C	22-2-1	42.78	11.99	0.77	0.01	8.50	--	--	18.54	0.38	12.09	1.21	0.90	0.019	0.084	97.27	Average
C	22-3-1	42.40	12.56	0.80	0.02	8.03	--	--	18.81	0.39	12.07	1.20	0.96	0.017	0.027	97.28	Average
	22-1-1	43.26	12.00	0.79	0.00	8.96	0.01	0.03	18.35	0.39	12.18	1.11	0.91	0.012	0.000	97.99	f22-1-6
	22-1-2	42.79	12.50	0.77	0.00	8.72	0.00	0.07	18.64	0.39	11.99	1.18	0.94	0.008	0.042	98.02	f22-1-5
	22-1-3	43.23	12.17	0.53	0.00	8.89	0.02	0.00	18.60	0.37	12.07	1.17	0.93	0.012	0.025	97.99	f22-1-4
	22-1-4	43.49	11.74	0.55	0.02	9.10	0.00	0.06	18.23	0.40	12.04	1.09	0.89	0.008	0.082	97.65	f22-1-7
	22-1-5	43.10	12.56	0.65	0.04	8.82	0.01	0.00	18.49	0.39	12.07	1.24	0.89	0.007	0.036	98.28	f22-1-3, f22-1-2
	22-1-6	42.89	12.53	0.74	0.02	8.68	0.00	0.00	18.64	0.41	12.00	1.18	0.98	0.009	0.027	98.10	f22-1-1
	22-2-1	42.77	11.77	0.64	0.00	9.06	0.00	0.02	17.39	0.39	11.89	1.14	0.88	0.018	0.056	96.01	f22-2-7
	22-2-2	42.70	12.26	0.51	0.00	8.85	0.01	0.00	18.05	0.38	11.94	1.19	0.92	0.013	0.139	96.89	f22-2-6
	22-2-3	42.47	12.41	0.68	0.00	8.60	0.01	0.00	17.99	0.36	11.94	1.21	0.93	0.012	0.000	96.61	f22-2-5
	22-2-5	42.29	12.40	0.62	0.00	8.85	0.00	0.00	18.20	0.41	12.03	1.12	0.95	0.008	0.066	96.90	f22-2-3
	22-3-1*	42.19	13.20	0.77	0.01	8.40	0.00	0.03	19.00	0.41	12.18	1.26	0.94	0.013	0.000	98.38	f22-3-1
	22-3-2	43.16	12.11	0.63	0.09	8.65	0.01	0.00	18.85	0.38	12.04	1.17	0.89	0.016	0.015	97.99	f22-3-2
	22-3-3	43.34	11.81	0.71	0.00	9.05	0.00	0.08	18.11	0.40	12.11	1.10	0.84	0.010	0.000	97.57	f22-3-3
	22-3-4	42.56	12.58	0.60	0.00	8.51	0.02	0.02	18.92	0.41	12.19	1.07	1.02	0.013	0.000	97.90	f22-3-4, f22-3-5
	22-3-5	42.68	12.48	0.70	0.02	8.54	0.00	0.00	18.83	0.40	12.08	1.20	0.92	0.010	0.000	97.85	f22-3-6
	22-3-8	42.80	12.36	0.52	0.06	8.50	0.02	0.07	18.78	0.40	12.03	1.16	0.91	0.018	0.000	97.62	f22-3-9

Appendix H. (cont)

		SiO_2	Al_2O_3	TiO_2	Cr_2O_3	MgO	NiO	ZnO	FeO	MnO	CaO	Na_2O	K_2O	Cl	F	Total	Plagioclase
29: Moderately foliated granodiorite; cores																	
Carleton	29-1-1	42.68	10.42	0.74	0.00	8.71	--	--	19.94	0.39	11.79	1.31	1.22	0.032	0.157	97.39	Average
	29-1-2*	42.64	10.01	1.68	0.00	8.63	--	--	19.68	0.38	12.30	1.25	1.19	--	--	97.77	Average
	29-1-3*	42.20	10.20	1.45	0.01	8.63	--	--	19.97	0.47	12.26	1.34	1.24	--	--	97.77	Average
	29-1-4	42.67	10.30	1.39	0.01	8.73	--	--	19.77	0.38	12.21	1.30	1.21	--	--	97.97	Average
	29-1-5	42.39	10.43	1.49	0.00	8.68	--	--	20.13	0.39	12.23	1.35	1.22	--	--	98.31	Average
	29-1-6	41.81	10.63	0.77	0.00	8.44	--	--	20.10	0.42	11.75	1.41	1.32	--	--	96.65	Average
	29-1-7	42.10	10.49	0.77	0.01	8.38	--	--	20.07	0.43	11.72	1.39	1.29	--	--	96.64	Average
	29-1-8	42.37	10.28	1.40	0.01	8.72	--	--	19.89	0.43	12.01	1.34	1.19	--	--	97.63	Average
	29-1-9*	42.13	10.45	1.38	0.01	8.70	--	--	20.11	0.38	12.29	1.37	1.26	--	--	98.10	Average
	29-1-11	41.86	10.46	0.76	0.01	8.58	--	--	20.01	0.42	11.60	1.34	1.27	--	--	96.31	Average
	29-1-12	42.17	10.43	0.76	0.00	8.70	--	--	19.82	0.44	11.68	1.40	1.27	--	--	96.68	Average
	29-1-13	42.34	10.14	0.66	0.01	8.90	--	--	19.58	0.44	11.78	1.26	1.19	--	--	96.31	Average
	29-2-1	42.61	10.37	0.81	0.04	8.80	--	--	20.07	0.34	11.72	1.36	1.27	0.022	0.195	97.60	Average
	29-2-2	42.30	10.58	0.79	0.02	8.48	--	--	20.25	0.42	11.84	1.35	1.28	0.022	0.111	97.45	Average
	29-2-4	42.16	10.68	1.06	0.06	8.59	--	--	20.02	0.40	12.05	1.34	1.25	--	--	97.62	Average
	29-2-8	42.10	10.79	1.47	0.02	8.40	--	--	20.31	0.42	12.00	1.47	1.33	--	--	98.33	Average
	29-2-9*	41.75	10.78	1.46	0.03	8.37	--	--	20.14	0.44	12.42	1.38	1.30	--	--	98.06	Average
	29-2-10	42.42	10.28	1.18	0.04	8.79	--	--	19.59	0.39	12.17	1.41	1.28	--	--	97.56	Average
	29-3-1	42.03	10.48	0.92	0.01	8.48	--	--	20.13	0.40	11.66	1.36	1.29	0.008	0.172	96.93	Average
	29-3-2	42.10	10.51	0.84	0.01	8.56	--	--	19.89	0.39	11.89	1.35	1.26	0.025	0.174	97.00	Average
	29-3-3	41.79	10.83	0.91	0.02	8.31	--	--	20.29	0.40	11.86	1.47	1.27	--	--	97.15	Average
	29-3-4	41.86	10.75	0.90	0.03	8.42	--	--	19.95	0.36	11.73	1.47	1.25	--	--	96.72	Average
	29-3-5	42.09	10.79	0.91	0.01	8.28	--	--	20.33	0.44	11.75	1.54	1.32	--	--	97.46	Average
	29-3-6	41.29	10.97	0.90	0.02	8.18	--	--	20.37	0.45	11.60	1.47	1.34	--	--	96.60	Average
	29-3-7	42.42	10.53	0.76	0.01	8.65	--	--	19.92	0.37	11.68	1.51	1.29	--	--	97.15	Average
	29-3-8	42.23	10.46	0.76	0.02	8.73	--	--	19.97	0.43	11.74	1.43	1.23	--	--	97.00	Average
	29-3-9	41.78	10.79	0.85	0.03	8.56	--	--	20.19	0.37	11.67	1.43	1.30	--	--	96.96	Average
	29-3-10	42.38	10.48	0.86	0.01	8.59	--	--	20.05	0.43	11.85	1.33	1.26	--	--	97.24	Average
	29-3-11	42.23	10.65	0.85	0.02	8.46	--	--	20.14	0.36	11.64	1.46	1.29	--	--	97.10	Average
	29-3-12	42.12	10.45	1.30	0.01	8.54	--	--	20.16	0.43	11.84	1.50	1.23	--	--	97.58	Average
	29-3-13	42.70	10.22	0.89	0.02	8.87	--	--	19.72	0.43	12.21	1.29	1.19	--	--	97.52	Average
	29-2-2	42.52	10.18	0.69	0.02	9.51	0.01	0.02	19.47	0.40	11.81	1.26	1.18	0.014	0.281	97.23	f29-3-2, f29-3-3
	29-3-3	43.77	10.44	0.57	0.00	9.21	0.01	0.02	18.42	0.38	11.18	1.82	1.01	0.018	0.251	96.98	f29-3-4
	29-4-1	42.36	10.44	0.44	0.11	9.76	0.02	0.00	19.08	0.38	11.88	1.21	1.11	0.016	0.192	96.93	f29-4-3

Appendix H. (cont)

		SiO_2	Al_2O_3	TiO_2	Cr_2O_3	MgO	NiO	ZnO	FeO	MnO	CaO	Na_2O	K_2O	Cl	F	Total	Plagioclase
rims																	
Carleton	29-1-1	43.60	9.06	0.56	0.01	9.53	--	--	18.80	0.38	11.78	1.24	1.02	--	--	95.98	Average
	29-1-10	42.71	9.78	0.73	0.02	8.97	--	--	19.49	0.37	11.74	1.27	1.14	--	--	96.22	Average
	29-1-14	43.09	9.91	1.10	0.01	9.01	--	--	19.45	0.43	12.10	1.27	1.09	--	--	97.47	Average
	29-2-3	43.68	9.32	1.22	0.04	9.38	--	--	19.05	0.42	12.14	1.32	1.03	--	--	97.60	Average
	29-2-5	43.58	9.52	0.59	0.06	9.38	--	--	19.02	0.40	11.76	1.30	1.07	--	--	96.69	Average
	29-2-6	43.83	9.51	0.60	0.01	9.42	--	--	19.18	0.42	11.88	1.19	1.06	--	--	97.10	Average
	29-2-7	43.83	9.33	1.38	0.01	9.52	--	--	19.31	0.41	12.29	1.39	1.08	--	--	98.54	Average
	29-2-11	43.33	9.96	1.07	0.01	9.35	--	--	19.17	0.43	12.20	1.30	1.10	--	--	97.93	Average
	29-1-1	44.10	8.82	0.54	0.00	10.50	0.00	0.00	18.87	0.40	11.83	1.30	0.94	0.026	0.112	97.39	f29-1-1
	29-2-1	44.05	9.42	0.45	0.00	10.33	0.02	0.05	18.66	0.39	11.74	1.23	0.97	0.008	0.270	97.46	f29-3-2, f29-3-3
	29-3-1	43.58	9.48	0.49	0.00	10.22	0.00	0.03	18.83	0.42	11.99	1.28	0.98	0.011	0.257	97.45	f29-3-2
	29-3-2	44.04	9.26	0.52	0.00	10.38	0.02	0.03	18.67	0.39	11.94	1.22	0.98	0.011	0.213	97.57	f29-3-3
	29-3-4	43.28	9.87	0.27	0.00	10.25	0.00	0.00	18.84	0.39	11.93	1.26	0.97	0.014	0.426	97.32	f29-3-6
	29-3-5	43.69	9.54	0.45	0.00	10.19	0.02	0.05	18.84	0.41	11.79	1.41	0.99	0.010	0.471	97.67	f29-3-5
	29-3-6	43.36	9.48	0.49	0.01	10.27	0.02	0.04	18.24	0.39	11.98	1.22	1.01	0.012	0.301	96.69	f29-3-1
	29-4-2	43.26	9.76	0.45	0.03	10.18	0.00	0.00	18.92	0.41	11.85	1.23	1.03	0.013	0.346	97.33	f29-4-2
	29-4-3	43.12	9.97	0.44	0.01	9.95	0.02	0.08	19.07	0.39	12.01	1.22	1.05	0.010	0.268	97.50	f29-4-1
	29-5-1	43.59	9.45	0.38	0.00	10.31	0.02	0.00	18.56	0.39	12.03	1.15	0.97	0.016	0.315	97.03	f29-5-3
	29-5-2	44.20	9.40	0.32	0.01	10.39	0.01	0.07	18.61	0.37	11.88	1.27	0.91	0.016	0.364	97.66	f29-5-2
	29-5-3	44.05	9.04	0.55	0.00	10.34	0.00	0.08	18.49	0.37	11.74	1.33	0.98	0.008	0.201	97.08	f29-5-1

Appendix H. (cont)

		SiO_2	Al_2O_3	TiO_2	Cr_2O_3	MgO	NiO	ZnO	FeO	MnO	CaO	Na_2O	K_2O	Cl	F	Total	Plagioclase
36: Strongly foliated tonalite																	
Carleton	36-1-1	41.79	11.30	0.60	0.01	7.34	--	--	21.38	0.51	11.57	1.36	1.43	0.016	0.187	97.50	Average
	36-1-2	41.52	11.24	0.60	0.04	7.37	--	--	21.38	0.45	11.56	1.34	1.41	0.007	0.093	97.01	Average
	36-2-1	41.97	10.66	0.59	0.02	7.94	--	--	20.77	0.52	11.57	1.39	1.26	0.029	0.153	96.88	Average
	36-2-2	42.42	10.58	0.60	0.00	8.01	--	--	21.05	0.49	11.60	1.38	1.31	0.018	0.076	97.54	Average
	36-1-1	39.90	12.35	0.37	0.00	6.80	0.00	0.03	22.94	0.50	11.55	1.39	1.34	0.041	0.207	97.32	f36-1-1
	36-1-2	41.29	11.41	0.67	0.00	8.26	0.01	0.03	21.54	0.47	11.69	1.31	1.33	0.009	0.166	98.12	f36-1-12
	36-1-3	41.15	11.73	0.56	0.00	7.92	0.00	0.06	21.73	0.46	11.68	1.29	1.31	0.010	0.382	98.10	f36-1-13
	36-1-4	41.02	11.77	0.58	0.00	7.80	0.00	0.04	21.72	0.47	11.69	1.30	1.35	0.010	0.164	97.83	f36-1-14
	36-1-5	41.20	11.59	0.58	0.04	8.01	0.01	0.08	21.63	0.50	11.82	1.27	1.33	0.003	0.168	98.13	f36-1-15
	36-1-6	40.98	11.79	0.49	0.00	7.77	0.01	0.04	21.66	0.48	11.73	1.29	1.34	0.007	0.204	97.70	f36-1-16
	36-1-7	40.92	11.88	0.58	0.02	7.72	0.00	0.00	21.60	0.44	11.64	1.27	1.35	0.008	0.276	97.60	f36-1-17
	36-1-8	41.39	11.54	0.60	0.03	8.01	0.00	0.04	21.36	0.47	11.71	1.24	1.37	0.012	0.247	97.90	f36-1-18
	36-1-9	41.24	11.57	0.59	0.00	7.86	0.01	0.00	21.62	0.49	11.71	1.32	1.29	0.015	0.118	97.75	f36-1-19
	36-1-10	41.18	11.83	0.57	0.01	7.72	0.00	0.04	21.85	0.46	11.73	1.28	1.36	0.017	0.092	98.09	f36-1-2
	36-1-11	41.27	11.92	0.50	0.01	7.84	0.01	0.02	21.39	0.52	11.71	1.20	1.28	0.016	0.232	97.82	f36-1-3, f36-1-4
	36-1-12	41.26	11.62	0.55	0.01	7.74	0.00	0.00	21.73	0.45	11.82	1.28	1.26	0.024	0.146	97.81	f36-1-5
	36-1-13	41.12	11.69	0.61	0.00	8.04	0.02	0.02	21.47	0.44	11.64	1.28	1.35	0.000	0.259	97.82	f36-1-6
	36-1-14	41.37	11.68	0.58	0.00	7.96	0.00	0.00	21.59	0.48	11.77	1.35	1.30	0.025	0.346	98.30	f36-1-7, f36-1-8
	36-1-15	41.10	11.85	0.47	0.00	7.57	0.00	0.08	22.01	0.50	11.78	1.30	1.36	0.011	0.308	98.20	f36-1-9
	36-1-16	41.15	11.80	0.50	0.00	7.84	0.01	0.03	21.46	0.47	11.77	1.26	1.34	0.010	0.309	97.81	f36-1-10
	36-1-17	41.15	11.61	0.65	0.03	8.11	0.02	0.05	21.28	0.45	11.65	1.34	1.38	0.013	0.266	97.88	f36-1-11
	36-3-1	40.92	11.44	0.63	0.02	7.67	0.00	0.01	21.64	0.47	11.73	1.34	1.35	0.018	0.179	97.33	f36-3-1
	36-3-2	40.95	11.97	0.40	0.00	7.54	0.00	0.04	21.81	0.51	11.73	1.33	1.31	0.006	0.196	97.69	f36-3-9
	36-3-3	41.30	11.63	0.52	0.00	7.70	0.00	0.04	21.77	0.48	11.80	1.22	1.28	0.021	0.320	97.93	f36-3-10
	36-3-4	40.79	11.84	0.48	0.00	7.42	0.00	0.00	22.06	0.50	11.75	1.34	1.35	0.017	0.375	97.76	f36-3-11
	36-3-5	41.11	11.64	0.62	0.04	7.98	0.01	0.01	20.97	0.46	11.75	1.35	1.29	0.009	0.076	97.26	f36-3-12
	36-3-6	41.24	11.85	0.51	0.00	7.73	0.00	0.13	21.54	0.49	11.64	1.28	1.32	0.015	0.276	97.89	f36-3-13
	36-3-7	40.97	11.77	0.60	0.00	7.77	0.00	0.05	21.54	0.52	11.68	1.37	1.28	0.014	0.419	97.80	f36-3-14
	36-3-8	40.90	11.76	0.56	0.00	7.87	0.02	0.02	21.45	0.48	11.70	1.30	1.30	0.005	0.359	97.57	f36-3-15
	36-3-9	41.14	11.67	0.68	0.00	7.86	0.00	0.02	21.64	0.46	11.73	1.33	1.39	0.019	0.272	98.08	f36-3-16
	36-3-10	41.16	11.87	0.49	0.00	7.77	0.02	0.01	21.76	0.47	11.76	1.20	1.26	0.007	0.160	97.86	f36-3-2
	36-3-11	40.98	11.80	0.67	0.00	7.93	0.00	0.00	21.51	0.46	11.73	1.34	1.38	0.012	0.183	97.91	f36-3-3
	36-3-12	41.21	11.94	0.52	0.01	7.98	0.00	0.06	21.54	0.46	11.72	1.31	1.33	0.007	0.067	98.11	f36-3-4
	36-3-13	40.95	11.52	0.63	0.00	7.87	0.02	0.07	21.74	0.44	11.66	1.38	1.43	0.014	0.204	97.84	f36-3-5
	36-3-14	41.36	11.37	0.53	0.00	7.60	0.00	0.00	21.50	0.47	11.56	1.31	1.28	0.019	0.126	97.07	f36-3-6
	36-3-15	40.91	11.59	0.62	0.03	7.86	0.01	0.00	21.29	0.43	11.80	1.26	1.32	0.006	0.180	97.22	f36-3-7
	36-3-16	41.10	11.56	0.58	0.00	7.79	0.00	0.07	21.55	0.48	11.72	1.29	1.33	0.014	0.172	97.59	f36-3-8

Appendix H. (cont)

		SiO_2	Al_2O_3	TiO_2	Cr_2O_3	MgO	NiO	ZnO	FeO	MnO	CaO	Na_2O	K_2O	Cl	F	Total	Plagioclase
40: Tonalite containing blebby pegmatite																	
C	40-1-1	49.05	6.59	0.72	0.05	13.59	--	--	13.47	0.33	12.35	0.95	0.63	0.008	0.057	97.79	Average
	40-1-2	49.64	6.70	0.71	0.06	13.83	--	--	13.08	0.29	12.27	0.95	0.61	0.017	0.109	98.27	Average
	40-1-1	47.75	6.85	0.90	0.07	14.18	0.02	0.02	13.43	0.29	12.38	0.99	0.66	0.081	0.174	97.70	f40-1-1
	40-1-2	48.49	6.37	0.74	0.07	14.26	0.01	0.00	13.60	0.29	12.51	0.80	0.56	0.035	0.137	97.81	f40-1-2
	40-1-3	48.01	6.68	0.79	0.10	14.27	0.02	0.00	13.22	0.27	12.42	0.90	0.58	0.017	0.232	97.40	f40-1-3
	40-1-4	48.38	6.49	0.75	0.02	14.50	0.01	0.00	12.82	0.31	12.35	0.90	0.61	0.019	0.215	97.28	f40-1-4
	40-1-5	48.27	6.58	0.74	0.11	14.39	0.03	0.00	12.65	0.28	12.49	0.74	0.56	0.015	0.104	96.90	f40-1-5
	40-2-1	48.22	6.69	0.77	0.02	14.37	0.02	0.03	13.28	0.31	12.27	0.93	0.61	0.011	0.250	97.66	f40-2-6, f40-3-4
	40-2-2	49.35	5.78	0.65	0.00	14.66	0.03	0.00	12.97	0.29	12.32	0.77	0.49	0.016	0.334	97.52	f40-2-6
	40-2-3	48.31	6.49	0.74	0.09	14.48	0.02	0.00	13.17	0.32	12.24	0.95	0.60	0.018	0.049	97.45	f40-2-6, f40-3-3
	40-2-4	49.04	6.00	0.65	0.00	14.67	0.01	0.03	12.86	0.30	12.39	0.75	0.51	0.001	0.174	97.32	f40-2-6, f40-3-1
	40-2-5	47.63	6.85	0.73	0.07	13.91	0.02	0.04	13.60	0.28	12.29	0.89	0.61	0.010	0.096	96.98	f40-2-6, f40-3-2
	40-2-6	47.91	6.86	0.79	0.11	14.23	0.01	0.03	13.56	0.30	12.24	0.86	0.61	0.013	0.102	97.55	f40-2-6

Appendix H. (cont)

		SiO_2	Al_2O_3	TiO_2	Cr_2O_3	MgO	NiO	ZnO	FeO	MnO	CaO	Na_2O	K_2O	Cl	F	Total	Plagioclase
52: Gneissic tonalite																	
Carleton	52-1-1	42.18	11.37	1.06	0.00	7.62	--	--	20.85	0.38	11.58	1.32	0.79	0.023	0.042	97.21	Average
	52-1-2	42.20	11.62	0.91	0.00	7.55	--	--	20.55	0.31	11.59	1.36	0.84	0.015	0.020	96.97	Average
	52-1-3	41.70	11.32	1.07	0.03	7.78	--	--	20.65	0.37	11.61	1.43	0.80	--	--	96.75	Average
	52-1-4	42.18	11.31	1.03	0.04	7.72	--	--	20.50	0.42	11.54	1.44	0.82	--	--	97.00	Average
	52-1-5	42.35	11.57	0.96	0.03	7.65	--	--	20.80	0.34	11.69	1.30	0.82	--	--	97.51	Average
	52-1-6	41.55	11.71	0.90	0.00	7.40	--	--	21.01	0.36	11.65	1.29	0.87	--	--	96.74	Average
	52-1-7	42.64	11.44	1.03	0.04	7.71	--	--	20.51	0.39	11.56	1.30	0.77	--	--	97.38	Average
	52-1-8	41.57	11.66	1.07	0.03	7.54	--	--	20.71	0.33	11.65	1.36	0.83	--	--	96.75	Average
	52-1-9	42.26	11.72	1.00	0.04	7.52	--	--	20.60	0.39	11.46	1.35	0.84	--	--	97.18	Average
	52-1-10	41.59	11.73	0.89	0.04	7.61	--	--	20.39	0.44	11.35	1.53	0.81	--	--	96.38	Average
	52-1-11	41.72	11.53	0.70	0.02	7.48	--	--	20.84	0.32	11.51	1.18	0.83	--	--	96.13	Average
	52-1-12	41.95	11.47	0.98	0.02	7.58	--	--	20.69	0.31	11.50	1.27	0.84	--	--	96.61	Average
	52-1-13	42.52	11.58	1.00	0.02	7.62	--	--	20.78	0.35	11.64	1.34	0.84	--	--	97.68	Average
	52-1-14	42.82	11.34	0.90	0.03	7.74	--	--	20.42	0.35	11.58	1.44	0.75	--	--	97.35	Average
	52-1-15	42.55	11.54	0.89	0.02	7.63	--	--	20.41	0.40	11.49	1.39	0.83	--	--	97.16	Average
	52-1-16	42.33	11.88	0.71	0.04	7.41	--	--	20.67	0.33	11.68	1.23	0.84	--	--	97.13	Average
	52-1-17	41.94	12.00	0.65	0.04	7.21	--	--	21.03	0.32	11.56	1.26	0.83	--	--	96.84	Average
	52-1-18	41.85	11.67	0.82	0.03	7.51	--	--	20.87	0.32	11.75	1.33	0.89	--	--	97.04	Average
	52-1-19	42.66	11.50	0.95	0.02	7.70	--	--	20.48	0.41	11.48	1.45	0.82	--	--	97.47	Average
	52-2-1	41.89	11.70	0.95	0.03	7.35	--	--	20.72	0.31	11.39	1.35	0.83	0.037	0.044	96.60	Average
	52-2-2	42.38	11.65	0.95	0.01	7.45	--	--	20.98	0.35	11.44	1.41	0.83	0.018	0.040	97.51	Average
	52-2-3	42.03	11.96	1.47	0.03	7.26	--	--	21.07	0.36	12.32	1.36	0.89	--	--	98.74	Average
	52-2-4	42.14	11.72	1.87	0.03	7.41	--	--	21.16	0.39	12.07	1.39	0.85	--	--	99.01	Average
	52-2-5	42.06	11.78	0.78	0.02	7.43	--	--	20.94	0.37	11.64	1.37	0.87	--	--	97.27	Average
	52-2-6	41.54	12.58	0.27	0.01	6.92	--	--	21.60	0.36	11.76	1.30	0.71	--	--	97.06	Average
	52-2-7	42.57	11.54	0.80	0.04	7.52	--	--	20.78	0.38	11.77	1.16	0.81	--	--	97.36	Average
	52-2-8	42.07	11.62	0.90	0.03	7.33	--	--	21.04	0.36	11.55	1.35	0.84	--	--	97.08	Average
	52-2-9	41.69	11.88	0.76	0.04	7.29	--	--	20.84	0.38	11.49	1.24	0.86	--	--	96.47	Average
	52-2-10	42.26	11.77	0.93	0.02	7.25	--	--	21.03	0.37	11.41	1.46	0.84	--	--	97.34	Average
	52-2-11	42.27	11.60	0.87	0.03	7.47	--	--	20.76	0.30	11.79	1.29	0.88	--	--	97.26	Average
	52-2-12	41.91	11.78	0.88	0.04	7.42	--	--	20.90	0.32	11.54	1.34	0.82	--	--	96.93	Average
	52-2-13	41.72	11.62	0.92	0.03	7.44	--	--	20.78	0.38	11.57	1.31	0.86	--	--	96.62	Average
	52-2-14	42.07	11.75	0.74	0.05	7.27	--	--	21.01	0.36	11.38	1.44	0.87	--	--	96.94	Average
	52-3-1	42.26	11.64	0.95	0.00	7.43	--	--	20.84	0.31	11.61	1.28	0.88	0.025	0.034	97.26	Average
	52-3-2	42.83	11.33	0.88	0.01	7.63	--	--	21.08	0.35	11.51	1.36	0.83	0.029	0.047	97.87	Average
	52-3-3	42.02	11.61	0.72	0.03	7.37	--	--	20.83	0.36	11.67	1.27	0.85	--	--	96.73	Average
	52-3-4	42.27	11.85	0.74	0.01	7.31	--	--	21.19	0.33	11.54	1.16	0.84	--	--	97.24	Average

Appendix H. (cont)

		SiO_2	Al_2O_3	TiO_2	Cr_2O_3	MgO	NiO	ZnO	FeO	MnO	CaO	Na_2O	K_2O	Cl	F	Total	Plagioclase
Carleton	52-3-5	41.72	11.75	0.85	0.03	7.38	--	--	21.03	0.36	11.66	1.39	0.85	--	--	97.02	Average
	52-3-6	41.81	11.71	0.78	0.02	7.38	--	--	20.81	0.38	11.40	1.48	0.82	--	--	96.60	Average
	52-3-7	42.06	11.56	0.88	0.05	7.27	--	--	20.93	0.36	11.38	1.32	0.83	--	--	96.64	Average
	52-3-8	42.05	11.64	0.85	0.04	7.39	--	--	20.99	0.37	11.65	1.18	0.82	--	--	96.99	Average
	52-3-9	42.15	11.66	2.24	0.04	7.42	--	--	20.90	0.35	11.59	1.29	0.87	--	--	98.50	Average
	52-3-10	42.05	11.61	0.85	0.03	7.33	--	--	20.88	0.39	11.60	1.25	0.84	--	--	96.82	Average
	52-3-11	42.03	11.77	0.73	0.04	7.44	--	--	20.78	0.38	11.53	1.23	0.86	--	--	96.78	Average
	52-3-12	42.03	11.54	0.70	0.03	7.27	--	--	21.00	0.31	11.68	1.18	0.86	--	--	96.60	Average
	52-1-1	41.36	12.43	0.91	0.04	7.81	0.02	0.00	21.16	0.34	11.72	1.39	0.89	0.041	0.065	98.12	f52-1-1
	52-1-2	41.35	12.23	0.91	0.00	7.91	0.02	0.03	20.82	0.31	11.80	1.29	0.89	0.038	0.103	97.65	f52-1-2
	52-1-3	41.29	12.50	0.60	0.00	7.44	0.01	0.00	21.50	0.30	11.89	1.19	0.90	0.046	0.000	97.65	f52-1-3
	52-1-4	41.54	12.17	0.89	0.00	7.75	0.01	0.00	21.13	0.34	11.79	1.34	0.83	0.037	0.086	97.87	f52-1-4
	52-1-5*	39.11	13.48	1.12	0.00	8.93	0.02	0.05	21.34	0.27	6.80	0.78	4.27	0.049	0.192	96.32	f52-1-5
	52-1-6	41.74	11.94	0.80	0.00	8.01	0.01	0.00	21.05	0.33	11.92	1.21	0.81	0.043	0.016	97.86	f52-1-6
	52-2-1	41.93	11.97	0.77	0.02	7.93	0.00	0.00	21.03	0.31	11.89	1.29	0.86	0.046	0.074	98.09	f52-2-1
	52-2-2	40.43	13.03	0.48	0.01	6.85	0.00	0.10	22.22	0.33	11.79	1.23	0.92	0.043	0.000	97.43	f52-2-2
	52-2-3	41.73	11.97	0.88	0.00	7.93	0.02	0.00	21.04	0.32	11.69	1.30	0.82	0.035	0.000	97.74	f52-2-3
	52-2-4	42.65	12.23	1.27	0.00	8.06	0.01	0.02	18.79	0.26	12.22	0.96	0.71	0.038	0.000	97.21	f52-2-4
	52-3-1	40.90	12.85	0.64	0.00	7.38	0.00	0.01	21.50	0.30	11.84	1.26	0.93	0.048	0.028	97.66	f52-3-1
	52-3-2	41.95	11.85	0.86	0.00	7.96	0.02	0.06	21.18	0.35	11.69	1.27	0.84	0.032	0.000	98.06	f52-3-2
	52-3-3	41.38	12.11	0.91	0.00	7.60	0.02	0.02	21.18	0.32	11.71	1.37	0.89	0.100	0.105	97.64	f52-3-3
	52-3-4	41.86	12.07	0.79	0.00	7.94	0.02	0.00	20.76	0.34	11.76	1.41	0.84	0.039	0.023	97.84	f52-3-4
	52-3-5	41.84	11.63	0.80	0.00	7.80	0.01	0.00	20.90	0.33	11.72	1.40	0.77	0.031	0.116	97.28	f52-3-5
	52-3-6	41.88	11.87	0.74	0.02	7.89	0.01	0.01	21.09	0.31	11.73	1.22	0.82	0.039	0.000	97.60	f52-3-6, f52-3-7
	52-3-8	42.00	11.70	0.81	0.00	7.94	0.00	0.03	21.15	0.35	11.80	1.26	0.81	0.046	0.137	97.97	f52-3-8
	52-3-9	41.25	12.21	0.68	0.05	7.33	0.01	0.01	21.75	0.32	11.71	1.25	0.87	0.068	0.000	97.48	f52-3-9

Appendix H. (cont)

	SiO_2	Al_2O_3	TiO_2	Cr_2O_3	MgO	NiO	ZnO	FeO	MnO	CaO	Na_2O	K_2O	Cl	F	Total	Plagioclase
61: Massive tonalite; cores																
61-1-1	41.21	12.03	0.63	0.00	8.26	0.01	0.07	20.67	0.45	11.80	1.27	1.25	0.014	0.190	97.78	f61-1-2
61-1-2	41.26	12.04	0.51	0.00	8.37	0.03	0.05	20.43	0.46	11.93	1.13	1.25	0.023	0.109	97.53	f61-1-3, f61-1-5
61-1-3	41.09	11.96	0.53	0.01	8.14	0.00	0.01	20.72	0.42	11.96	1.21	1.18	0.017	0.070	97.29	f61-1-4, f61-1-6
61-1-6	41.45	11.98	0.60	0.00	8.54	0.00	0.00	20.20	0.44	11.89	1.16	1.24	0.016	0.022	97.54	f61-1-1
61-2-1	40.85	12.44	0.51	0.00	8.06	0.02	0.06	20.50	0.43	11.81	1.23	1.25	0.022	0.028	97.20	f61-2-2
61-2-2	41.26	12.65	0.42	0.08	7.71	0.01	0.02	20.69	0.47	11.50	1.24	1.17	0.027	0.338	97.45	f61-2-5
61-2-4	40.72	12.20	0.61	0.00	8.12	0.01	0.09	20.33	0.43	11.74	1.18	1.18	0.021	0.008	96.63	f61-2-3
61-3-1	41.25	12.39	0.56	0.00	8.50	0.00	0.00	19.93	0.45	11.94	1.26	1.22	0.015	0.231	97.65	f61-3-1
61-3-2	41.18	12.48	0.34	0.00	8.01	0.00	0.02	20.96	0.46	11.82	1.28	1.18	0.022	0.085	97.79	f61-3-2
61-5-5	40.52	12.85	0.61	0.00	7.94	0.01	0.01	20.55	0.49	12.00	1.25	1.26	0.044	0.245	97.66	f61-5-4
rims																
61-2-3	41.45	11.50	0.79	0.02	8.46	0.01	0.00	20.08	0.46	11.86	1.16	1.25	0.013	0.025	97.05	f61-2-6
61-2-5	41.63	11.45	0.95	0.00	8.56	0.00	0.06	20.25	0.42	11.77	1.27	1.27	0.014	0.224	97.76	f61-2-4
61-2-6	41.60	11.60	0.68	0.00	7.99	0.00	0.09	20.86	0.45	11.75	1.18	1.22	0.012	0.075	97.46	f61-2-1
61-2-7	41.54	11.66	0.61	0.05	8.03	0.01	0.00	20.75	0.45	11.85	1.15	1.18	0.013	0.104	97.34	f61-2-1
61-4-1	41.67	11.32	0.92	0.00	8.86	0.00	0.00	19.70	0.46	11.75	1.25	1.25	0.021	0.118	97.26	f61-4-5
61-4-2	41.52	11.54	0.78	0.03	8.88	0.01	0.00	19.91	0.46	11.83	1.17	1.24	0.021	0.092	97.43	f61-4-3
61-4-3	41.75	11.81	0.50	0.02	8.77	0.00	0.02	19.77	0.48	11.92	1.19	1.17	0.017	0.103	97.46	f61-4-3
61-4-4	42.01	11.50	0.54	0.03	9.06	0.01	0.04	19.48	0.50	11.91	1.26	1.19	0.020	0.209	97.67	f61-4-2
61-4-5	41.80	11.52	0.72	0.00	8.91	0.02	0.03	19.66	0.44	11.89	1.08	1.20	0.021	0.041	97.30	f61-4-1
61-5-1	42.14	11.24	0.77	0.03	8.94	0.02	0.04	19.76	0.44	11.88	1.22	1.19	0.020	0.297	97.85	f61-5-1
61-5-2	41.83	11.25	0.90	0.00	8.82	0.01	0.06	19.66	0.50	11.80	1.15	1.21	0.018	0.160	97.29	f61-5-2
61-5-3	42.13	11.23	0.81	0.00	9.01	0.01	0.00	19.70	0.47	11.81	1.25	1.22	0.007	0.237	97.78	f61-5-1
61-5-4	41.77	11.76	0.53	0.00	8.62	0.00	0.09	20.39	0.52	11.94	1.13	1.12	0.030	0.058	97.91	f61-5-5
61-5-6	42.05	11.59	0.65	0.00	9.08	0.00	0.04	19.68	0.49	11.80	1.23	1.16	0.012	0.153	97.86	f61-5-3

Appendix H. (cont)

	SiO_2	Al_2O_3	TiO_2	Cr_2O_3	MgO	NiO	ZnO	FeO	MnO	CaO	Na_2O	K_2O	Cl	F	Total	Plagioclase
62: Gneissic tonalite; cores																
62-2-4	43.98	11.17	0.54	0.01	11.28	0.01	0.00	15.84	0.39	11.87	1.23	0.42	0.041	0.106	96.82	f62-2-6
62-2-5	43.77	11.49	0.49	0.00	11.12	0.00	0.08	16.10	0.39	11.95	1.18	0.42	0.046	0.242	97.17	f62-2-1
62-4-4	43.38	11.68	0.65	0.00	10.88	0.01	0.01	16.92	0.43	11.50	1.38	0.48	0.044	0.058	97.37	f62-4-1
62-5-1	43.23	12.20	0.43	0.01	10.80	0.00	0.09	16.62	0.34	11.76	1.35	0.45	0.043	0.344	97.52	f62-5-2
62-5-2	43.86	11.20	0.78	0.00	11.47	0.01	0.06	16.14	0.41	11.58	1.37	0.46	0.042	0.435	97.63	f62-5-3
62-5-5	43.35	11.85	0.70	0.00	10.83	0.01	0.03	16.86	0.38	11.52	1.37	0.47	0.049	0.257	97.54	f62-5-4
rims																
62-1-1	45.27	10.41	0.62	0.02	12.07	0.00	0.03	15.31	0.38	11.96	1.18	0.36	0.036	0.242	97.76	f62-1-6
62-1-2	45.43	10.35	0.59	0.00	12.07	0.00	0.10	15.41	0.41	11.80	1.11	0.35	0.034	0.158	97.74	f62-1-5
62-1-3	45.31	10.17	0.80	0.00	12.63	0.01	0.06	15.09	0.57	11.10	1.49	0.35	0.034	0.066	97.63	f62-1-4
62-1-4	44.84	10.58	0.56	0.00	11.70	0.00	0.00	15.59	0.40	11.86	1.12	0.40	0.036	0.133	97.16	f62-1-2
62-1-5	44.49	10.74	0.69	0.00	11.55	0.03	0.00	15.77	0.46	11.50	1.29	0.40	0.037	0.270	97.12	f62-1-3
62-1-6	45.00	10.14	0.65	0.01	12.30	0.00	0.05	15.17	0.47	11.67	1.16	0.39	0.032	0.390	97.27	f62-1-1
62-2-1	45.28	10.51	0.52	0.00	11.92	0.01	0.08	15.09	0.43	11.85	1.16	0.37	0.033	0.367	97.45	f62-2-2
62-2-2	45.68	9.94	0.45	0.03	12.41	0.01	0.06	14.80	0.42	11.83	1.12	0.32	0.029	0.000	97.09	f62-2-3
62-2-3	44.90	10.32	0.56	0.00	12.06	0.01	0.03	15.38	0.49	11.56	1.23	0.39	0.034	0.099	97.02	f62-2-4
62-2-6	44.86	10.24	0.63	0.00	12.09	0.00	0.00	15.26	0.47	11.70	1.19	0.37	0.042	0.258	96.99	f62-2-5
62-3-1	45.23	10.25	0.64	0.01	12.04	0.01	0.03	15.27	0.41	11.74	1.19	0.38	0.030	0.252	97.37	f62-3-2
62-3-2	44.83	10.36	0.64	0.00	11.93	0.01	0.02	15.36	0.39	11.61	1.13	0.39	0.036	0.129	96.78	f62-3-3
62-3-3	45.36	10.27	0.58	0.00	12.35	0.02	0.02	14.80	0.35	11.84	1.09	0.36	0.033	0.435	97.30	f62-3-4
62-3-4	44.82	10.90	0.41	0.00	11.76	0.00	0.01	15.28	0.37	11.99	1.14	0.36	0.035	0.209	97.19	f62-3-1
62-3-5	45.78	10.00	0.54	0.00	12.32	0.00	0.04	14.70	0.39	11.90	1.13	0.33	0.033	0.128	97.21	f62-3-5
62-4-1	45.21	10.33	0.49	0.00	11.82	0.00	0.00	15.64	0.37	11.97	1.15	0.38	0.034	0.203	97.50	f62-4-3
62-4-2	44.92	10.39	0.50	0.06	11.64	0.00	0.06	15.71	0.38	11.92	1.10	0.36	0.034	0.179	97.15	f62-4-2
62-4-3	44.81	10.31	0.65	0.00	11.86	0.00	0.00	15.49	0.39	11.83	1.15	0.39	0.033	0.440	97.16	f62-4-3
62-5-3	44.55	10.60	0.55	0.03	11.63	0.02	0.04	15.92	0.37	11.71	1.22	0.40	0.037	0.318	97.24	f62-5-1
62-5-4	45.40	9.93	0.66	0.00	12.14	0.00	0.00	15.56	0.38	11.63	1.22	0.37	0.023	0.237	97.44	f62-5-7
62-5-6	44.91	10.67	0.52	0.00	11.69	0.00	0.01	15.90	0.40	11.79	1.29	0.39	0.038	0.104	97.66	f62-5-9
62-5-7*	41.47	14.49	0.24	0.01	9.21	0.02	0.00	17.61	0.29	11.94	1.34	0.51	0.064	0.220	97.31	f62-5-8
62-5-8	44.88	10.62	0.75	0.00	11.89	0.01	0.00	15.87	0.40	11.60	1.31	0.40	0.042	0.246	97.90	f62-5-6
62-5-9	44.60	10.84	0.63	0.00	11.79	0.00	0.02	15.64	0.31	11.92	1.19	0.38	0.034	0.337	97.55	f62-5-5

Appendix H. (cont)

	SiO_2	Al_2O_3	TiO_2	Cr_2O_3	MgO	NiO	ZnO	FeO	MnO	CaO	Na_2O	K_2O	Cl	F	Total	Plagioclase
64/65: Weakly gneissic tonalite; cores																
64-3-3	43.22	12.45	0.42	0.00	9.53	0.00	0.00	17.89	0.22	11.74	1.26	0.42	0.054	0.070	97.24	f64-3-1
64-3-4	42.66	12.83	0.52	0.00	9.27	0.01	0.00	18.09	0.21	11.68	1.23	0.45	0.061	0.144	97.09	f64-3-3
64-3-5	43.41	12.08	0.51	0.00	9.84	0.00	0.09	17.56	0.21	11.70	1.23	0.42	0.046	0.125	97.15	f64-3-2
64-5-3	42.61	12.69	0.60	0.00	8.91	0.01	0.02	18.85	0.29	11.66	1.38	0.46	0.130	0.126	97.65	f64-5-3
64-7-4	42.53	12.81	0.59	0.00	9.25	0.00	0.04	18.43	0.27	11.61	1.39	0.50	0.056	0.000	97.45	f64-7-5
64-7-5	43.13	12.31	0.69	0.00	9.66	0.01	0.00	17.96	0.22	11.55	1.28	0.45	0.054	0.070	97.34	f64-7-7
64-7-6	43.51	12.12	0.54	0.00	9.93	0.02	0.05	18.20	0.28	11.42	1.31	0.44	0.058	0.104	97.92	f64-6-7
65-3-3	43.56	12.22	0.06	0.06	9.40	0.01	0.00	18.48	0.46	11.45	1.19	0.50	0.026	0.000	97.40	f65-3-4
65-4-4	42.92	12.65	0.15	0.00	9.00	0.00	0.03	18.89	0.35	11.85	1.02	0.45	0.021	0.027	97.35	f65-4-3
65-5-5	43.84	11.95	0.10	0.00	9.53	0.00	0.07	17.92	0.35	11.92	0.89	0.40	0.011	0.008	96.98	f65-5-2, f65-5-1
rims																
64-1-1	44.24	11.09	0.72	0.01	10.36	0.03	0.00	17.47	0.25	11.39	1.25	0.40	0.047	0.252	97.40	f64-1-5
64-1-2	44.57	11.06	0.59	0.00	10.38	0.02	0.09	17.56	0.27	11.44	1.25	0.38	0.041	0.131	97.68	f64-1-4, f64-1-3
64-1-3	43.58	12.01	0.58	0.00	9.93	0.01	0.03	17.64	0.25	11.58	1.21	0.45	0.051	0.170	97.42	f64-1-2
64-1-4	44.58	10.71	0.62	0.04	10.54	0.00	0.07	17.13	0.27	11.37	1.16	0.37	0.048	0.084	96.95	f64-1-1
64-2-1	43.69	11.18	0.76	0.00	10.09	0.02	0.09	17.67	0.31	11.35	1.28	0.38	0.043	0.054	96.87	f64-2-2
64-2-2	44.25	11.44	0.49	0.00	10.41	0.01	0.13	17.28	0.29	11.55	1.19	0.38	0.052	0.000	97.46	f64-2-6
64-2-3	44.44	11.20	0.56	0.00	10.35	0.01	0.05	17.38	0.27	11.69	1.20	0.38	0.048	0.104	97.62	f64-2-5
64-2-4	44.36	11.20	0.70	0.00	10.40	0.00	0.12	17.10	0.30	11.37	1.19	0.39	0.042	0.000	97.15	f64-2-4
64-2-5	44.05	10.94	0.70	0.02	10.43	0.00	0.02	17.36	0.25	11.49	1.18	0.39	0.048	0.015	96.88	f64-2-3
64-2-6	44.47	10.82	0.59	0.00	10.39	0.00	0.00	17.49	0.29	11.45	1.29	0.39	0.050	0.000	97.22	f64-2-1
64-3-1	44.32	10.87	0.68	0.02	10.16	0.01	0.00	17.70	0.23	11.64	1.14	0.36	0.091	0.000	97.19	f64-3-5
64-3-2*	44.43	13.01	0.50	0.00	8.66	0.02	0.08	18.24	0.20	11.37	1.55	0.37	0.053	0.098	98.53	f64-3-4
64-3-6	44.46	10.90	0.76	0.00	10.59	0.01	0.10	17.30	0.26	11.60	1.13	0.35	0.042	0.000	97.49	f64-3-1
64-4-1	44.24	10.92	0.73	0.00	10.42	0.01	0.00	17.76	0.34	11.22	1.32	0.36	0.047	0.114	97.41	f64-4-4, f64-4-5
64-4-2	44.40	11.03	0.63	0.00	10.19	0.00	0.02	17.59	0.24	11.55	1.12	0.41	0.049	0.000	97.22	f64-4-3
64-4-3	44.28	11.15	0.65	0.00	10.29	0.01	0.05	17.95	0.31	11.26	1.33	0.42	0.045	0.027	97.74	f64-4-2
64-4-4	44.19	11.11	0.66	0.00	10.36	0.00	0.04	17.69	0.31	11.61	1.17	0.40	0.056	0.095	97.64	f64-4-1
64-5-1*	40.62	15.83	0.09	0.00	7.14	0.01	0.00	20.38	0.26	11.62	1.35	0.46	0.122	0.101	97.92	f64-5-7
64-5-2	44.37	10.91	0.68	0.00	10.02	0.00	0.00	17.96	0.33	11.62	1.19	0.36	0.048	0.098	97.54	f64-5-2
64-5-4	43.56	11.81	0.63	0.00	9.72	0.02	0.01	18.08	0.29	11.64	1.14	0.41	0.058	0.000	97.35	f64-5-4
64-5-5	43.98	11.10	0.59	0.00	10.04	0.00	0.03	18.24	0.34	11.49	1.17	0.41	0.046	0.000	97.43	f64-5-5
64-5-6	43.44	11.38	0.80	0.00	9.64	0.03	0.05	18.33	0.35	11.27	1.23	0.42	0.059	0.103	97.06	f64-5-6
64-5-7	44.20	11.21	0.60	0.00	10.11	0.01	0.06	18.13	0.32	11.54	1.18	0.38	0.053	0.131	97.84	f64-5-1
64-6-1	44.31	11.46	0.51	0.00	10.27	0.02	0.04	17.39	0.19	11.86	1.15	0.38	0.052	0.000	97.61	f64-6-5
64-6-2	44.39	10.99	0.53	0.00	10.29	0.01	0.00	17.44	0.24	11.60	1.23	0.37	0.038	0.081	97.14	f64-6-3
64-6-3	44.61	10.96	0.73	0.00	10.48	0.01	0.02	17.28	0.24	11.68	1.17	0.38	0.043	0.000	97.61	f64-6-4

Appendix H. (cont)

	SiO_2	Al_2O_3	TiO_2	Cr_2O_3	MgO	NiO	ZnO	FeO	MnO	CaO	Na_2O	K_2O	Cl	F	Total	Plagioclase
64-6-4	43.61	11.60	0.76	0.01	9.99	0.01	0.06	18.06	0.27	11.19	1.37	0.45	0.060	0.000	97.43	f64-6-2
64-6-5	44.17	11.22	0.69	0.00	10.25	0.00	0.01	17.68	0.27	11.37	1.33	0.40	0.053	0.104	97.48	f64-6-1, f64-6-6
64-7-1	44.45	11.05	0.95	0.00	10.66	0.00	0.00	17.27	0.30	11.05	1.43	0.41	0.045	0.115	97.67	f64-6-9
64-7-2	44.06	11.31	0.82	0.00	10.34	0.00	0.04	17.50	0.23	11.72	1.15	0.43	0.051	0.047	97.66	f64-7-4, f64-6-8
64-7-3	43.95	11.24	0.65	0.00	10.35	0.00	0.07	17.32	0.23	11.69	1.12	0.40	0.047	0.159	97.15	f64-7-6
65-1-1	44.40	10.96	0.30	0.02	10.14	0.00	0.01	18.10	0.47	11.49	1.12	0.40	0.023	0.000	97.41	f65-1-4
65-1-2	44.83	10.62	0.20	0.00	10.56	0.01	0.00	17.44	0.40	11.82	0.88	0.35	0.014	0.031	97.12	f65-1-3
65-1-3	45.12	10.74	0.15	0.00	10.22	0.00	0.07	17.97	0.46	11.53	1.09	0.35	0.029	0.120	97.79	f65-1-3
65-1-4	44.97	10.68	0.24	0.00	10.24	0.01	0.07	17.86	0.43	11.89	0.97	0.38	0.027	0.000	97.74	f65-1-2
65-1-5	44.48	10.68	0.32	0.00	10.24	0.00	0.05	18.20	0.46	11.59	1.05	0.40	0.043	0.132	97.57	f65-1-1
65-2-1	44.36	10.83	0.21	0.00	10.12	0.00	0.08	18.00	0.39	11.57	1.04	0.39	0.024	0.138	97.07	f65-2-6
65-2-2	44.99	10.75	0.20	0.04	10.49	0.01	0.05	17.56	0.32	11.81	0.86	0.39	0.017	0.000	97.48	f65-2-4, f65-2-6
65-2-3	44.32	10.99	0.21	0.00	10.52	0.01	0.10	17.76	0.34	11.90	0.93	0.39	0.023	0.138	97.57	f65-2-6
65-2-4	44.73	10.64	0.22	0.00	10.51	0.00	0.03	17.76	0.42	11.45	1.00	0.36	0.017	0.115	97.22	f65-2-5
65-2-5	44.40	10.81	0.27	0.00	10.40	0.01	0.00	17.41	0.33	11.86	0.91	0.36	0.023	0.000	96.77	f65-2-3
65-2-6	43.90	11.69	0.24	0.01	9.72	0.01	0.03	18.15	0.33	11.89	0.95	0.47	0.025	0.000	97.40	f65-2-2, f65-2-1
65-3-1*	42.72	13.12	0.09	0.00	8.82	0.00	0.03	18.85	0.39	11.94	0.96	0.50	0.038	0.076	97.47	f65-3-2
65-3-2	44.97	10.70	0.13	0.00	10.50	0.01	0.10	17.50	0.42	11.92	0.85	0.37	0.019	0.000	97.48	f65-3-3
65-3-4	44.22	11.51	0.06	0.02	9.95	0.01	0.04	17.89	0.45	11.84	0.92	0.40	0.028	0.003	97.33	f65-3-5
65-3-5*	41.28	14.54	0.07	0.00	7.92	0.00	0.02	19.10	0.41	11.85	1.12	0.58	0.030	0.000	96.90	f65-3-1
65-4-1	43.96	11.84	0.20	0.00	9.75	0.00	0.00	18.47	0.36	11.74	0.97	0.42	0.013	0.000	97.72	f65-4-5
65-4-2	45.09	10.38	0.20	0.01	10.59	0.00	0.00	17.89	0.43	11.51	1.06	0.33	0.012	0.000	97.51	f65-4-6
65-4-3*	41.13	14.63	0.04	0.00	8.09	0.00	0.11	19.41	0.36	11.84	1.24	0.68	0.023	0.000	97.54	f65-4-4
65-4-5	44.39	10.99	0.28	0.00	10.03	0.00	0.08	18.10	0.35	11.99	0.88	0.40	0.017	0.000	97.53	f65-4-2
65-4-6	44.27	11.02	0.31	0.00	9.75	0.00	0.06	18.19	0.33	11.84	0.89	0.39	0.017	0.000	97.06	f65-4-1
65-5-1	43.86	11.35	0.24	0.00	9.89	0.01	0.02	18.29	0.51	11.18	1.21	0.43	0.024	0.000	97.01	f65-5-6
65-5-2	44.47	10.92	0.15	0.02	10.21	0.00	0.07	17.90	0.49	11.49	1.07	0.35	0.014	0.181	97.25	f65-5-5
65-5-3	43.93	11.35	0.37	0.00	9.91	0.00	0.06	18.44	0.45	11.25	1.24	0.44	0.024	0.000	97.46	f65-5-4
65-5-4*	42.02	13.38	0.11	0.00	8.43	0.01	0.01	18.91	0.41	11.59	1.24	0.56	0.016	0.000	96.67	f65-5-3

Appendix H. (cont)

	SiO_2	Al_2O_3	TiO_2	Cr_2O_3	MgO	NiO	ZnO	FeO	MnO	CaO	Na_2O	K_2O	Cl	F	Total	Plagioclase
66: High-strain tonalite																
66-1-1	43.42	10.65	0.76	0.00	10.11	0.04	0.05	16.99	0.30	12.17	0.97	1.04	0.069	0.011	16.30	f66-1-4
66-1-2	43.61	10.71	0.70	0.02	10.09	0.01	0.02	17.86	0.34	12.14	1.16	1.08	0.057	0.079	16.43	f66-1-5
66-1-3	43.61	10.52	0.77	0.07	10.27	0.03	0.00	17.86	0.29	12.10	1.15	1.15	0.066	0.028	16.40	f66-1-6
66-1-4	43.44	10.46	0.81	0.04	10.07	0.01	0.03	17.57	0.32	12.09	1.11	1.12	0.057	0.172	97.21	f66-1-3
66-1-5	43.63	10.68	0.84	0.01	10.10	0.01	0.03	17.84	0.32	12.18	1.14	1.15	0.060	0.093	98.01	f66-1-3
66-1-6	43.03	10.48	1.13	0.04	10.20	0.02	0.01	17.69	0.30	12.07	1.22	1.20	0.065	0.190	97.56	f66-1-2
66-1-7	43.97	10.36	0.93	0.02	10.51	0.02	0.05	17.47	0.30	12.16	1.16	1.14	0.061	0.404	98.35	f66-1-1
66-2-1	43.50	10.32	0.93	0.02	10.13	0.03	0.01	17.61	0.32	12.19	1.14	1.14	0.056	0.116	97.44	f66-2-6
66-2-2	43.34	10.54	0.74	0.04	10.18	0.01	0.00	17.78	0.33	12.09	1.15	1.15	0.055	0.030	97.41	f66-2-7
66-2-3	44.01	10.30	0.57	0.00	10.28	0.02	0.04	17.75	0.29	12.11	0.99	1.01	0.055	0.122	97.48	f66-2-5
66-2-4	43.64	10.40	0.55	0.06	10.26	0.02	0.14	17.67	0.32	12.20	1.03	1.02	0.070	0.083	97.42	f66-2-4
66-2-5	43.62	10.56	0.61	0.06	10.15	0.02	0.14	17.93	0.30	12.17	1.08	1.06	0.062	0.081	97.79	f66-2-3
66-2-6	44.14	10.23	0.74	0.00	10.35	0.01	0.00	17.62	0.30	12.11	0.96	0.99	0.059	0.230	97.61	f66-2-5
66-2-7	43.56	10.64	0.86	0.05	10.11	0.00	0.00	17.83	0.30	12.00	1.17	1.17	0.075	0.088	97.78	f66-2-8
66-2-8	43.53	10.66	0.81	0.03	9.99	0.00	0.06	17.72	0.31	12.12	1.17	1.12	0.068	0.000	97.56	f66-2-1
66-2-9	43.88	10.39	0.77	0.05	10.19	0.01	0.06	17.68	0.29	12.20	1.00	1.08	0.063	0.180	97.75	f66-2-2
66-3-1	43.46	10.67	0.77	0.00	10.01	0.02	0.04	17.67	0.33	12.15	1.15	1.13	0.066	0.178	97.57	f66-3-7
66-3-2	43.29	10.61	0.85	0.00	10.09	0.01	0.00	18.03	0.31	12.14	1.17	1.21	0.070	0.300	97.93	f66-3-7
66-3-3	43.93	10.55	0.66	0.00	9.90	0.03	0.02	18.09	0.30	12.14	1.05	1.16	0.067	0.031	97.90	f66-3-5, f66-3-8
66-3-4	43.36	10.71	0.79	0.04	10.14	0.02	0.00	17.68	0.31	12.11	1.13	1.16	0.062	0.139	97.56	f66-3-6
66-3-5	43.45	10.41	1.02	0.02	10.19	0.02	0.09	17.63	0.31	12.07	1.08	1.21	0.062	0.000	97.54	f66-3-4, f66-3-2
66-3-6	43.79	10.48	0.84	0.00	10.16	0.03	0.04	17.91	0.33	12.08	1.09	1.10	0.061	0.208	98.01	f66-3-3
66-3-7	43.75	10.69	0.76	0.02	10.21	0.04	0.01	17.52	0.32	11.88	1.08	1.26	0.063	0.195	97.71	f66-3-1
66-4-1	44.29	10.26	0.59	0.03	10.38	0.01	0.02	17.66	0.32	12.06	1.03	1.02	0.062	0.094	97.75	f66-4-7
66-4-2	44.00	10.46	0.69	0.02	10.41	0.02	0.00	17.40	0.31	12.24	1.00	1.08	0.067	0.054	97.70	f66-4-6
66-4-3	44.04	10.52	0.76	0.00	10.17	0.03	0.06	17.67	0.33	12.20	1.09	1.09	0.063	0.000	97.99	f66-4-5
66-4-4	43.10	10.72	0.89	0.04	10.01	0.01	0.01	17.68	0.31	12.11	1.17	1.22	0.065	0.173	97.43	f66-4-4
66-4-5	43.66	10.51	0.95	0.02	10.05	0.00	0.00	17.58	0.32	12.03	1.16	1.15	0.062	0.167	97.58	f66-4-3
66-4-6	43.36	10.56	0.92	0.06	10.05	0.01	0.01	17.76	0.31	12.24	1.07	1.16	0.064	0.030	97.57	f66-4-2
66-4-7	44.05	10.37	0.88	0.01	10.25	0.04	0.00	17.76	0.31	12.18	0.97	1.07	0.056	0.160	98.02	f66-4-1
66-5-1	43.89	10.49	0.65	0.04	10.24	0.02	0.05	17.71	0.32	12.20	1.05	1.05	0.066	0.041	97.78	f66-5-4
66-5-2	43.55	10.80	0.65	0.00	9.87	0.01	0.05	18.11	0.29	12.19	1.06	1.17	0.072	0.162	97.89	f66-5-3, f66-5-2
66-5-3*	44.95	9.52	0.53	0.03	10.81	0.00	0.00	17.36	0.30	12.22	1.07	0.91	0.047	0.111	97.80	f66-5-1
66-6-1	43.98	10.33	0.94	0.00	10.07	0.01	0.00	17.94	0.31	12.02	1.05	1.19	0.072	0.095	97.96	f66-6-2
66-6-2	43.93	10.57	0.95	0.00	10.17	0.02	0.00	17.82	0.33	12.09	1.16	1.17	0.066	0.247	98.40	f66-6-1

Appendix H. (cont)

	SiO_2	Al_2O_3	TiO_2	Cr_2O_3	MgO	NiO	ZnO	FeO	MnO	CaO	Na_2O	K_2O	Cl	F	Total	Plagioclase
68/69: Heterogeneously deformed tonalite																
68-1-1	41.87	11.97	0.81	0.00	7.87	0.02	0.00	20.88	0.42	11.61	1.34	0.88	0.031	0.048	97.72	f68-1-2
68-1-2	42.62	11.49	0.78	0.02	8.49	0.02	0.03	20.11	0.43	11.66	1.22	0.82	0.023	0.000	97.70	f68-1-1
68-2-1	42.34	11.51	0.73	0.01	8.35	0.01	0.07	20.13	0.43	11.82	1.24	0.84	0.028	0.000	97.50	f68-2-2
68-2-2	41.86	12.17	0.68	0.00	7.49	0.01	0.06	20.86	0.37	11.73	1.17	0.87	0.024	0.003	97.28	f68-2-1
68-3-1	41.36	12.31	0.79	0.00	7.75	0.03	0.00	20.86	0.39	11.76	1.29	0.95	0.032	0.000	97.49	f68-3-1, f68-3-4
68-3-2	41.97	12.07	0.68	0.00	7.76	0.01	0.00	20.88	0.42	11.75	1.28	0.86	0.025	0.000	97.68	f68-3-1, f68-3-3, f68-3-6
68-3-3	42.53	11.98	0.64	0.00	7.97	0.01	0.05	20.82	0.40	11.79	1.23	0.89	0.027	0.076	98.37	f68-3-2, f68-3-5
68-4-1	41.69	12.09	0.81	0.04	7.86	0.00	0.00	20.62	0.41	11.71	1.28	0.92	0.030	0.234	97.57	f68-4-4, f68-4-6
68-4-2	41.78	11.95	0.71	0.00	8.05	0.01	0.03	20.75	0.38	11.82	1.28	0.87	0.027	0.000	97.65	f68-4-5, f68-4-7
68-4-4	41.94	11.97	0.58	0.00	8.12	0.02	0.00	20.40	0.42	11.70	1.30	0.84	0.022	0.030	97.31	f68-4-3, f68-4-2
68-4-5	41.65	12.30	0.90	0.00	7.91	0.00	0.01	20.45	0.40	11.69	1.33	0.92	0.028	0.000	97.58	f68-4-1
69-1-1	42.86	11.88	0.80	0.00	8.62	0.02	0.04	19.64	0.42	11.71	1.46	0.72	0.012	0.014	98.18	f69-1-5
69-1-2	42.83	11.58	0.80	0.01	8.71	0.00	0.02	19.56	0.41	11.75	1.31	0.66	0.010	0.114	97.72	f69-1-4
69-1-3	42.54	11.56	0.70	0.00	8.55	0.00	0.06	19.68	0.36	11.84	1.24	0.78	0.020	0.000	97.32	f69-1-3
69-1-4	42.04	12.26	0.82	0.00	8.35	0.02	0.09	20.12	0.38	11.76	1.24	0.83	0.022	0.016	97.94	f69-1-2
69-1-5	42.85	11.41	0.71	0.00	8.83	0.02	0.03	19.58	0.40	11.82	1.27	0.73	0.020	0.000	97.67	f69-1-1
69-2-1	42.38	12.12	0.91	0.00	8.39	0.01	0.03	19.96	0.41	11.69	1.37	0.76	0.015	0.207	98.15	f69-2-3
69-2-2	42.73	12.01	0.90	0.00	8.66	0.01	0.01	19.48	0.32	11.70	1.29	0.81	0.019	0.000	97.93	f69-2-2
69-2-3	43.69	11.77	0.62	0.01	8.77	0.01	0.06	19.28	0.36	11.21	1.30	0.77	0.012	0.105	97.92	f69-2-1
69-3-1	42.93	11.50	0.76	0.00	8.92	0.01	0.04	19.82	0.43	11.77	1.35	0.73	0.010	0.105	98.32	f69-3-4
69-3-2	41.77	12.32	0.80	0.00	7.93	0.02	0.04	20.37	0.36	11.79	1.27	0.87	0.023	0.000	97.55	f69-3-4, f69-3-5
69-3-3	42.34	12.34	0.67	0.00	8.03	0.02	0.00	20.34	0.37	11.81	1.35	0.73	0.013	0.129	98.07	f69-3-3
69-3-4	42.77	11.59	0.77	0.00	8.44	0.00	0.06	19.98	0.40	11.80	1.31	0.75	0.028	0.169	97.98	f69-3-2
69-3-5	43.11	11.37	0.74	0.00	8.91	0.01	0.00	19.83	0.35	11.89	1.24	0.77	0.016	0.000	98.23	f69-3-1
69-4-1	42.88	11.25	0.65	0.01	8.63	0.00	0.10	19.92	0.37	11.83	1.20	0.78	0.019	0.000	97.62	f69-4-2
69-4-2	42.45	11.92	0.77	0.02	8.31	0.02	0.07	20.18	0.36	11.77	1.22	0.80	0.016	0.163	97.98	f69-4-1
69-5-1	42.77	11.52	0.68	0.00	8.35	0.00	0.05	20.11	0.37	11.74	1.14	0.77	0.011	0.115	97.58	f69-5-3
69-5-2	42.53	11.59	0.81	0.03	8.46	0.01	0.04	20.00	0.31	11.87	1.18	0.82	0.015	0.000	97.65	f69-5-2
69-5-3	42.36	11.71	0.80	0.02	8.33	0.01	0.01	20.10	0.35	11.83	1.19	0.78	0.018	0.060	97.54	f69-5-1

Notes:
*: Samples not included in T-P calculations

Appendix I. EPMA results for feldspars from granitoids of the NCGB

Plagioclase

	SiO_2	TiO_2	Al_2O_3	FeO	MnO	MgO	CaO	Na_2O	K_2O	BaO	Total
01: Leucocratic tonalite											
f01-1-3	62.111	0.012	22.991	0.150	0.000	0.006	4.540	9.375	0.119	0.023	99.327
f01-1-4	62.735	0.012	22.521	0.124	0.000	0.024	3.796	9.738	0.146	0.042	99.138
f01-2-1	62.562	0.007	23.557	0.113	0.004	0.004	4.712	9.262	0.149	0.000	100.370
f01-2-2	62.476	0.000	23.522	0.128	0.007	0.000	4.734	9.220	0.152	0.017	100.256
f01-2-3	62.798	0.009	23.525	0.112	0.000	0.001	4.470	9.294	0.088	0.000	100.297
f01-2-4	62.925	0.006	23.461	0.133	0.000	0.001	4.584	9.264	0.139	0.008	100.521
f01-2-5	62.673	0.013	23.340	0.089	0.000	0.000	4.720	9.115	0.129	0.002	100.081
f01-2-6	62.579	0.001	23.667	0.150	0.000	0.010	4.700	9.341	0.168	0.000	100.616
f01-4-1	62.717	0.002	23.359	0.120	0.000	0.000	4.498	9.394	0.114	0.000	100.204
f01-4-2	62.350	0.000	23.500	0.111	0.000	0.015	4.613	9.225	0.171	0.039	100.024
f01-3-1	62.976	0.003	23.185	0.220	0.004	0.034	4.024	9.291	0.248	0.012	99.997
f01-3-2	62.695	0.003	23.308	0.209	0.000	0.000	4.817	9.057	0.110	0.000	100.199
f01-3-3	63.086	0.000	23.019	0.104	0.000	0.000	4.531	9.161	0.101	0.000	100.002
f01-3-4	62.930	0.000	23.308	0.060	0.000	0.012	4.481	9.338	0.144	0.000	100.273
f01-3-5	62.635	0.000	23.392	0.098	0.000	0.003	4.477	9.365	0.132	0.000	100.102
f01-7-1	62.137	0.001	23.293	0.123	0.000	0.005	4.590	9.051	0.136	0.015	99.351
f01-7-2	63.629	0.025	22.214	0.219	0.006	0.004	3.408	10.019	0.074	0.008	99.606
f01-7-3	62.239	0.009	23.309	0.083	0.000	0.008	4.643	9.275	0.082	0.000	99.648
f01-7-4	63.141	0.007	23.192	0.134	0.000	0.016	4.352	9.357	0.105	0.010	100.314
f01-7-5	65.495	0.017	21.113	0.186	0.003	0.000	1.876	10.824	0.102	0.013	99.629

Appendix I. (cont)

	SiO_2	TiO_2	Al_2O_3	FeO	MnO	MgO	CaO	Na_2O	K_2O	BaO	Total
13/15: Strongly foliated granodiorite											
f13-1-1	60.594	0.011	23.540	0.092	0.002	0.006	5.041	8.960	0.104	0.027	98.377
f13-1-2	61.102	0.002	23.242	0.072	0.000	0.000	4.777	9.228	0.066	0.000	98.489
f13-1-3	59.255	0.000	22.752	0.074	0.004	0.000	4.814	8.998	0.137	0.015	96.049
f13-4-1	62.288	0.000	23.727	0.194	0.000	0.005	4.995	9.226	0.107	0.010	100.552
f13-4-2	65.713	0.000	21.783	0.277	0.003	0.004	3.396	9.910	0.072	0.000	101.158
f13-4-3	63.726	0.019	22.751	0.198	0.004	0.005	3.828	9.917	0.097	0.002	100.547
f13-4-4	65.388	0.000	22.078	0.069	0.004	0.000	2.868	10.378	0.102	0.013	100.900
f13-3-1	62.813	0.004	23.727	0.178	0.000	0.000	4.799	9.241	0.058	0.009	100.829
f13-3-2	63.788	0.000	22.933	0.253	0.011	0.000	3.681	9.938	0.119	0.017	100.740
f13-3-3	62.157	0.004	24.228	0.292	0.011	0.003	5.569	8.791	0.092	0.025	101.172
f13-3-4	63.425	0.010	23.267	0.195	0.005	0.002	4.285	9.574	0.105	0.016	100.884
f13-3-5	62.056	0.004	24.106	0.181	0.000	0.000	5.177	8.922	0.086	0.014	100.546
f13-2-1	62.841	0.000	23.611	0.094	0.002	0.000	4.772	9.177	0.118	0.001	100.616
f13-2-2	61.739	0.014	24.221	0.102	0.022	0.000	5.472	8.808	0.116	0.004	100.498
f15-1-1	62.116	0.000	23.842	0.050	0.008	0.009	4.970	9.177	0.130	0.030	100.332
f15-1-2	61.578	0.009	24.280	0.204	0.012	0.003	5.460	8.885	0.084	0.000	100.515
f15-2-1	61.945	0.000	23.966	0.114	0.003	0.000	5.197	8.811	0.096	0.009	100.141
f15-2-2	62.131	0.004	23.894	0.117	0.007	0.010	4.942	9.001	0.088	0.017	100.211
f15-2-3	62.456	0.001	23.747	0.132	0.000	0.004	4.985	9.047	0.080	0.000	100.452
f15-2-4	62.622	0.018	23.485	0.181	0.009	0.000	4.756	9.160	0.106	0.012	100.349
f15-2-5	61.496	0.007	24.380	0.165	0.006	0.015	5.642	8.650	0.106	0.000	100.467
f15-2-6	63.281	0.000	23.011	0.281	0.014	0.027	4.311	9.415	0.128	0.000	100.468
f15-2-7	62.613	0.015	23.673	0.169	0.005	0.000	4.981	9.174	0.089	0.012	100.731
f15-3-1	62.594	0.018	23.402	0.194	0.000	0.026	4.566	9.431	0.134	0.000	100.365
f15-3-2	62.680	0.000	23.576	0.187	0.009	0.001	4.859	9.079	0.148	0.000	100.539
f15-3-3	65.264	0.000	20.762	0.539	0.019	0.025	2.239	10.854	0.130	0.000	99.832
f15-3-4	63.121	0.000	23.374	0.141	0.002	0.000	4.768	9.245	0.078	0.023	100.752
f15-3-5	62.086	0.052	23.984	0.211	0.007	0.002	5.304	8.980	0.098	0.000	100.724
f15-3-6	61.244	0.016	24.240	0.148	0.022	0.000	5.586	8.835	0.096	0.006	100.193
f15-3-7	62.430	0.001	23.681	0.173	0.004	0.000	4.729	9.209	0.155	0.049	100.431
f15-3-8	64.680	0.000	22.276	0.116	0.000	0.000	3.084	10.232	0.061	0.001	100.450

Appendix I. (cont)

	SiO_2	TiO_2	Al_2O_3	FeO	MnO	MgO	CaO	Na_2O	K_2O	BaO	Total
22: Mylonitic augen gneiss											
f22-1-1	58.593	0.000	26.496	0.066	0.004	0.001	8.370	6.899	0.096	0.007	100.532
f22-1-2	58.528	0.007	26.528	0.104	0.012	0.000	8.325	7.010	0.057	0.019	100.590
f22-1-3	58.594	0.011	26.339	0.129	0.000	0.000	7.951	7.249	0.071	0.019	100.363
f22-1-4	58.954	0.000	26.441	0.124	0.005	0.005	8.285	7.058	0.066	0.024	100.962
f22-1-5	58.644	0.000	26.270	0.138	0.012	0.000	8.256	7.023	0.084	0.010	100.437
f22-1-6	58.941	0.000	26.416	0.119	0.000	0.000	8.295	7.079	0.077	0.000	100.927
f22-1-7	58.452	0.005	26.420	0.114	0.002	0.000	8.176	6.978	0.081	0.000	100.228
f22-2-1	57.925	0.013	26.159	0.106	0.016	0.013	8.175	6.999	0.065	0.023	99.494
f22-2-2	58.224	0.018	26.335	0.095	0.000	0.000	8.193	7.014	0.123	0.022	100.024
f22-2-3	58.324	0.000	26.389	0.076	0.000	0.007	8.030	7.040	0.118	0.000	99.984
f22-2-4	59.310	0.005	25.977	0.061	0.000	0.007	7.651	7.438	0.100	0.009	100.558
f22-2-5	58.798	0.020	26.349	0.118	0.007	0.002	8.055	7.115	0.105	0.003	100.572
f22-2-6	58.670	0.000	26.199	0.062	0.000	0.001	8.008	7.135	0.053	0.003	100.131
f22-2-7	58.651	0.019	26.163	0.095	0.000	0.000	7.910	7.066	0.080	0.010	99.994
f22-3-1	58.644	0.000	26.585	0.153	0.000	0.000	8.398	7.030	0.081	0.009	100.900
f22-3-2	59.031	0.008	26.453	0.140	0.000	0.000	8.115	7.152	0.080	0.026	101.005
f22-3-3	58.737	0.005	26.406	0.091	0.000	0.001	8.207	7.048	0.079	0.040	100.614
f22-3-4	58.764	0.002	25.700	0.545	0.009	0.044	7.144	7.164	0.234	0.000	99.606
f22-3-5	58.256	0.000	26.533	0.116	0.006	0.000	8.314	7.051	0.096	0.016	100.388
f22-3-6	58.718	0.008	26.586	0.127	0.004	0.004	8.323	6.996	0.081	0.004	100.851
f22-3-7	58.135	0.002	26.365	0.102	0.000	0.000	8.285	6.840	0.106	0.037	99.872
f22-3-8	59.243	0.000	26.383	0.086	0.000	0.001	8.043	7.141	0.049	0.026	100.972
f22-3-9	58.655	0.008	26.486	0.135	0.000	0.000	8.295	6.976	0.076	0.019	100.650
29: Moderately foliated granodiorite											
f29-1-1	63.058	0.003	22.889	0.158	0.000	0.000	4.073	9.487	0.177	0.021	99.866
f29-3-1	63.237	0.004	23.215	0.061	0.000	0.006	4.007	9.683	0.137	0.025	100.375
f29-3-2	64.647	0.005	22.245	0.153	0.008	0.007	3.249	9.943	0.121	0.026	100.404
f29-3-3	63.711	0.000	22.763	0.187	0.000	0.004	4.010	9.663	0.107	0.054	100.499
f29-3-4	65.264	0.016	22.146	0.217	0.000	0.006	2.933	10.305	0.082	0.000	100.969
f29-3-5	67.065	0.000	20.914	0.174	0.000	0.011	1.245	11.591	0.079	0.007	101.086
f29-3-6	67.142	0.018	20.715	0.262	0.003	0.000	1.033	11.427	0.079	0.006	100.685
f29-4-1	63.171	0.016	22.900	0.108	0.003	0.001	4.010	9.473	0.091	0.005	99.778
f29-4-2	64.767	0.014	22.168	0.054	0.000	0.000	3.050	9.974	0.064	0.016	100.107
f29-4-3	63.623	0.029	22.945	0.121	0.013	0.000	3.932	9.642	0.142	0.044	100.491
f29-5-1	64.043	0.002	22.685	0.063	0.006	0.000	3.641	10.022	0.071	0.000	100.533
f29-5-2	63.637	0.001	23.041	0.188	0.002	0.000	4.049	9.549	0.133	0.003	100.603
f29-5-3	63.055	0.000	23.079	0.082	0.009	0.001	4.077	9.555	0.109	0.032	99.999

Appendix I. (cont)

	SiO_2	TiO_2	Al_2O_3	FeO	MnO	MgO	CaO	Na_2O	K_2O	BaO	Total
36: Strongly foliated tonalite											
f36-1-1	61.289	0.000	24.258	0.130	0.000	0.009	5.696	8.497	0.098	0.020	99.997
f36-1-2	61.791	0.013	24.078	0.173	0.010	0.000	5.407	8.797	0.134	0.012	100.415
f36-1-3	61.499	0.013	24.398	0.215	0.003	0.001	5.587	8.725	0.108	0.000	100.549
f36-1-4	61.521	0.011	24.265	0.145	0.000	0.000	5.626	8.756	0.148	0.000	100.472
f36-1-5	61.438	0.008	24.398	0.189	0.007	0.000	5.699	8.659	0.137	0.022	100.557
f36-1-6	61.696	0.008	24.237	0.162	0.007	0.000	5.515	8.719	0.141	0.029	100.514
f36-1-7	62.169	0.000	24.030	0.295	0.000	0.000	5.337	8.812	0.148	0.013	100.804
f36-1-8	61.129	0.000	24.400	0.141	0.000	0.000	5.807	8.535	0.142	0.011	100.165
f36-1-9	61.298	0.014	24.239	0.219	0.011	0.000	5.673	8.601	0.090	0.025	100.170
f36-1-10	61.263	0.000	24.326	0.170	0.020	0.008	5.655	8.656	0.090	0.000	100.188
f36-1-11	60.952	0.000	24.666	0.177	0.018	0.003	5.957	8.741	0.150	0.000	100.664
f36-1-12	61.258	0.000	24.345	0.187	0.000	0.001	5.796	8.653	0.138	0.021	100.399
f36-1-13	61.267	0.003	24.326	0.242	0.005	0.000	5.666	8.795	0.116	0.042	100.462
f36-1-14	61.801	0.012	23.940	0.352	0.003	0.021	5.307	8.991	0.127	0.021	100.575
f36-1-15	61.280	0.006	24.378	0.137	0.000	0.003	5.690	8.755	0.085	0.009	100.343
f36-1-16	61.334	0.008	24.210	0.206	0.004	0.000	5.649	8.578	0.142	0.051	100.182
f36-1-17	61.459	0.000	24.245	0.156	0.000	0.000	5.665	8.550	0.120	0.000	100.195
f36-1-18	62.306	0.011	23.754	0.136	0.000	0.000	5.192	9.080	0.117	0.000	100.596
f36-1-19	61.624	0.000	24.193	0.119	0.000	0.007	5.555	8.683	0.124	0.019	100.324
f36-3-1	62.118	0.000	23.936	0.128	0.008	0.007	5.199	8.979	0.141	0.052	100.568
f36-3-2	61.428	0.000	24.344	0.200	0.000	0.000	5.668	8.749	0.145	0.026	100.560
f36-3-3	61.063	0.023	23.940	0.243	0.001	0.060	5.586	8.608	0.190	0.005	99.719
f36-3-4	61.668	0.000	23.927	0.154	0.005	0.003	5.380	8.681	0.135	0.005	99.958
f36-3-5	61.550	0.005	24.022	0.143	0.000	0.017	5.443	8.687	0.137	0.000	100.004
f36-3-6	61.595	0.011	24.075	0.122	0.000	0.001	5.674	8.656	0.135	0.001	100.270
f36-3-7	61.242	0.017	24.329	0.182	0.018	0.004	5.597	8.736	0.150	0.034	100.309
f36-3-8	61.104	0.000	24.544	0.197	0.000	0.001	5.638	8.720	0.133	0.000	100.337
f36-3-9	61.069	0.000	24.220	0.270	0.000	0.017	5.701	8.544	0.155	0.026	100.002
f36-3-10	61.265	0.009	24.544	0.189	0.000	0.000	5.816	8.574	0.116	0.012	100.525
f36-3-11	61.227	0.010	24.293	0.121	0.000	0.005	5.656	8.440	0.138	0.011	99.901
f36-3-12	61.482	0.012	24.242	0.167	0.005	0.000	5.585	8.774	0.129	0.000	100.396
f36-3-13	61.139	0.016	24.479	0.148	0.000	0.000	5.804	8.642	0.141	0.000	100.369
f36-3-14	61.246	0.007	24.330	0.175	0.000	0.002	5.803	8.719	0.148	0.032	100.462
f36-3-15	60.928	0.000	24.379	0.178	0.023	0.000	5.796	8.558	0.133	0.000	99.995
f36-3-16	61.066	0.008	24.180	0.123	0.000	0.000	5.901	8.410	0.147	0.037	99.872
40: Tonalite containing blebby pegmatite											
f40-1-1	61.983	0.004	23.803	0.086	0.000	0.000	4.294	9.009	0.410	0.024	99.613
f40-1-2	62.448	0.000	23.354	0.272	0.006	0.128	4.316	9.198	0.192	0.000	99.914
f40-1-3	61.144	0.000	23.487	0.856	0.018	0.298	2.927	8.807	1.196	0.037	98.770
f40-1-4	61.340	0.000	24.102	0.071	0.001	0.000	5.113	8.799	0.146	0.000	99.572
f40-1-5	61.915	0.000	23.651	0.098	0.007	0.046	5.330	8.860	0.110	0.032	100.049
f40-2-6	62.150	0.010	23.798	0.164	0.000	0.052	3.773	8.762	0.839	0.032	99.580
f40-3-1	61.449	0.000	24.051	0.073	0.003	0.000	5.554	8.729	0.116	0.040	100.015
f40-3-2	62.006	0.005	23.837	0.094	0.000	0.017	5.064	8.937	0.299	0.026	100.285
f40-3-3	61.978	0.009	23.757	0.045	0.001	0.012	5.115	8.938	0.075	0.016	99.946
f40-3-4	61.836	0.000	24.059	0.069	0.013	0.000	5.277	8.884	0.095	0.000	100.233

Appendix I. (cont)

	SiO_2	TiO_2	Al_2O_3	FeO	MnO	MgO	CaO	Na_2O	K_2O	BaO	Total
52: Gneissic tonalite											
f52-1-1	60.406	0.000	25.063	0.167	0.000	0.004	6.558	8.249	0.097	0.003	100.547
f52-1-2	60.079	0.000	24.905	0.141	0.013	0.000	6.679	8.093	0.092	0.019	100.021
f52-1-3	59.980	0.014	25.179	0.162	0.006	0.000	6.722	8.167	0.077	0.005	100.312
f52-1-4	60.092	0.000	24.929	0.093	0.000	0.000	6.594	8.122	0.081	0.017	99.928
f52-1-5	60.275	0.013	25.039	0.105	0.000	0.008	6.564	8.188	0.041	0.000	100.233
f52-1-6	60.122	0.000	25.079	0.107	0.000	0.000	6.627	8.162	0.048	0.002	100.147
f52-2-1	60.319	0.000	25.243	0.050	0.000	0.008	6.537	8.366	0.060	0.017	100.600
f52-2-2	59.822	0.021	25.251	0.173	0.000	0.000	6.691	8.145	0.056	0.032	100.191
f52-2-3	60.191	0.000	25.157	0.192	0.014	0.001	6.567	8.325	0.064	0.000	100.511
f52-2-4	60.391	0.000	24.891	0.180	0.006	0.000	6.529	8.042	0.091	0.027	100.157
f52-3-1	59.977	0.003	25.064	0.129	0.013	0.001	6.749	7.900	0.157	0.003	99.996
f52-3-2	60.354	0.008	24.865	0.093	0.003	0.000	6.464	8.262	0.067	0.010	100.126
f52-3-3	60.393	0.016	24.885	0.110	0.000	0.211	6.275	8.089	0.094	0.000	100.073
f52-3-4	60.044	0.012	25.030	0.118	0.010	0.000	6.621	8.097	0.054	0.015	100.001
f52-3-5	60.144	0.012	25.096	0.103	0.000	0.011	6.511	8.159	0.061	0.000	100.097
f52-3-6	60.123	0.002	25.034	0.152	0.000	0.004	6.761	7.987	0.127	0.029	100.219
f52-3-7	60.194	0.000	25.046	0.126	0.009	0.000	6.594	8.175	0.093	0.012	100.249
f52-3-8	60.188	0.000	24.975	0.081	0.000	0.000	6.610	8.230	0.076	0.029	100.189
f52-3-9	60.263	0.001	25.125	0.051	0.007	0.000	6.383	8.300	0.071	0.028	100.229
61: Massive tonalite											
f61-5-1	61.153	0.023	25.062	0.169	0.000	0.005	5.569	8.827	0.145	0.010	100.963
f61-5-2	61.364	0.013	24.846	0.137	0.024	0.000	5.522	8.812	0.130	0.000	100.848
f61-5-3	61.302	0.000	24.952	0.051	0.002	0.004	5.505	8.884	0.060	0.027	100.787
f61-5-4	60.809	0.000	25.120	0.224	0.000	0.000	5.669	8.687	0.078	0.000	100.587
f61-5-5	61.513	0.000	24.986	0.203	0.014	0.000	5.556	8.808	0.170	0.030	101.280
f61-3-1	61.281	0.105	24.991	0.091	0.003	0.011	5.548	8.835	0.091	0.001	100.957
f61-3-2	61.015	0.016	25.274	0.125	0.000	0.004	5.788	8.699	0.154	0.021	101.096
f61-2-1	61.350	0.000	25.219	0.225	0.000	0.009	5.902	8.591	0.113	0.011	101.420
f61-2-2	61.305	0.019	24.843	0.151	0.011	0.000	5.494	8.761	0.113	0.007	100.704
f61-2-3	61.283	0.000	24.860	0.192	0.015	0.003	5.608	8.754	0.140	0.000	100.855
f61-2-4	60.589	0.000	25.261	0.192	0.001	0.004	5.959	8.513	0.138	0.007	100.664
f61-2-5	61.098	0.005	25.166	0.127	0.000	0.006	5.770	8.666	0.117	0.000	100.955
f61-2-6	61.244	0.009	24.998	0.087	0.002	0.000	5.538	8.740	0.119	0.043	100.780
f61-4-1	60.680	0.017	24.730	0.554	0.019	0.154	4.339	8.312	1.096	0.007	99.908
f61-4-2	61.012	0.000	25.031	0.161	0.000	0.000	5.740	8.573	0.161	0.000	100.678
f61-4-3	61.185	0.008	25.017	0.134	0.000	0.002	5.694	8.683	0.082	0.056	100.861
f61-4-5	61.587	0.000	24.792	0.124	0.025	0.007	5.459	8.802	0.097	0.045	100.938
f61-1-1	60.859	0.024	24.886	0.171	0.006	0.000	5.489	8.806	0.120	0.020	100.381
f61-1-2	61.253	0.020	24.779	0.184	0.000	0.000	5.481	8.730	0.166	0.021	100.634
f61-1-3	61.113	0.014	24.992	0.200	0.011	0.000	5.612	8.676	0.104	0.000	100.722
f61-1-4	61.704	0.000	25.153	0.272	0.006	0.000	5.633	8.777	0.095	0.018	101.658
f61-1-5	61.445	0.000	24.672	0.272	0.020	0.015	5.373	8.802	0.146	0.000	100.745
f61-1-6	61.388	0.015	24.709	0.165	0.006	0.000	5.411	8.900	0.109	0.015	100.718

Appendix I. (cont)

	SiO_2	TiO_2	Al_2O_3	FeO	MnO	MgO	CaO	Na_2O	K_2O	BaO	Total
62: Gneissic tonalite											
f62-1-1	60.863	0.000	25.198	0.171	0.007	0.000	6.157	8.432	0.066	0.008	100.902
f62-1-2	60.559	0.024	25.497	0.126	0.017	0.000	6.048	8.644	0.065	0.009	100.989
f62-1-3	60.752	0.000	25.377	0.112	0.006	0.000	5.962	8.700	0.067	0.034	101.010
f62-1-4	60.969	0.000	25.249	0.155	0.003	0.004	5.576	8.620	0.069	0.020	100.665
f62-1-5	60.606	0.011	25.461	0.127	0.003	0.009	5.906	8.718	0.065	0.013	100.919
f62-1-6	60.421	0.015	25.348	0.137	0.000	0.001	6.018	8.688	0.055	0.022	100.705
f62-2-1	60.729	0.001	25.051	0.234	0.008	0.000	5.881	8.509	0.087	0.018	100.518
f62-2-2	60.750	0.000	25.323	0.111	0.017	0.012	6.028	8.421	0.062	0.000	100.724
f62-2-3	60.952	0.009	25.197	0.149	0.000	0.007	5.982	8.555	0.055	0.055	100.961
f62-2-4	60.971	0.021	25.263	0.193	0.003	0.004	5.838	8.606	0.071	0.046	101.016
f62-2-5	60.940	0.014	25.097	0.163	0.002	0.000	5.596	8.814	0.048	0.003	100.677
f62-2-6	60.628	0.002	25.386	0.091	0.007	0.006	5.954	8.601	0.053	0.010	100.738
f62-3-1	60.478	0.000	25.246	0.141	0.000	0.007	6.026	8.503	0.072	0.040	100.513
f62-3-2	60.684	0.000	25.461	0.231	0.000	0.000	6.239	8.401	0.058	0.007	101.081
f62-3-3	60.336	0.009	25.480	0.157	0.009	0.008	6.042	8.409	0.054	0.032	100.536
f62-3-4	60.024	0.005	25.612	0.236	0.005	0.013	6.217	8.368	0.055	0.018	100.553
f62-3-5	60.421	0.000	25.536	0.219	0.000	0.008	6.014	8.600	0.078	0.009	100.885
f62-4-1	60.612	0.011	25.329	0.183	0.009	0.000	5.995	8.436	0.060	0.036	100.671
f62-4-2	60.777	0.000	25.548	0.162	0.012	0.011	6.023	8.582	0.051	0.018	101.184
f62-4-3	60.962	0.000	25.228	0.160	0.000	0.000	5.837	8.530	0.072	0.041	100.830
f62-5-1	61.167	0.023	25.026	0.319	0.000	0.010	5.636	8.804	0.073	0.039	101.097
f62-5-2	60.537	0.000	25.348	0.108	0.013	0.006	6.014	8.407	0.053	0.015	100.501
f62-5-3	60.271	0.023	25.373	0.175	0.000	0.002	6.123	8.368	0.062	0.018	100.415
f62-5-4	60.262	0.000	25.740	0.120	0.005	0.003	6.400	8.259	0.061	0.038	100.888
f62-5-5	60.344	0.001	25.308	0.086	0.008	0.005	6.058	8.528	0.062	0.042	100.442
f62-5-6	60.449	0.004	25.436	0.110	0.000	0.000	5.977	8.527	0.066	0.056	100.625
f62-5-7	60.267	0.016	25.270	0.093	0.000	0.008	6.061	8.548	0.067	0.039	100.369
f62-5-8	60.474	0.009	25.440	0.054	0.003	0.008	5.992	8.428	0.036	0.026	100.470
f62-5-9	60.529	0.010	25.624	0.145	0.000	0.000	6.224	8.405	0.064	0.015	101.016

Appendix I. (cont)

	SiO_2	TiO_2	Al_2O_3	FeO	MnO	MgO	CaO	Na_2O	K_2O	BaO	Total
64/65: Weakly gneissic tonalite											
f64-1-1	60.466	0.001	25.139	0.101	0.010	0.010	6.048	8.474	0.063	0.026	100.338
f64-1-2	61.122	0.010	25.188	0.070	0.000	0.000	5.880	8.648	0.045	0.020	100.983
f64-1-3	60.433	0.014	25.331	0.115	0.000	0.000	6.099	8.431	0.075	0.000	100.498
f64-1-4	60.843	0.018	25.317	0.195	0.000	0.000	5.992	8.755	0.055	0.027	101.202
f64-1-5	60.611	0.019	25.287	0.111	0.000	0.011	5.986	8.561	0.050	0.009	100.645
f64-2-1	60.998	0.006	25.147	0.099	0.000	0.005	5.882	8.593	0.051	0.009	100.790
f64-2-2	60.525	0.001	25.416	0.118	0.000	0.001	6.097	8.545	0.051	0.035	100.789
f64-2-3	60.293	0.010	25.369	0.060	0.000	0.000	5.952	8.664	0.064	0.003	100.415
f64-2-4	60.970	0.000	25.283	0.085	0.005	0.000	6.021	8.514	0.048	0.031	100.957
f64-2-5	60.777	0.000	25.355	0.128	0.000	0.000	5.866	8.663	0.076	0.030	100.895
f64-2-6	60.621	0.010	25.485	0.108	0.006	0.009	6.016	8.525	0.052	0.015	100.847
f64-3-1	60.831	0.000	25.305	0.145	0.009	0.004	5.963	8.515	0.072	0.010	100.854
f64-3-2	60.877	0.020	25.299	0.099	0.001	0.015	5.871	8.709	0.042	0.023	100.956
f64-3-3	60.594	0.021	25.406	0.156	0.017	0.000	5.974	8.721	0.071	0.011	100.971
f64-3-4	60.443	0.015	25.118	0.158	0.008	0.002	5.989	8.541	0.050	0.043	100.367
f64-3-5	60.220	0.007	25.544	0.197	0.000	0.000	6.043	8.387	0.053	0.020	100.471
f64-4-1	60.592	0.020	25.382	0.207	0.004	0.000	5.946	8.504	0.058	0.027	100.740
f64-4-2	60.807	0.004	25.250	0.160	0.012	0.004	5.920	8.412	0.055	0.049	100.673
f64-4-3	60.683	0.006	25.376	0.107	0.000	0.003	6.037	8.635	0.052	0.015	100.914
f64-4-4	60.612	0.000	25.366	0.091	0.000	0.000	5.990	8.588	0.059	0.035	100.741
f64-4-5	60.688	0.027	25.012	0.175	0.006	0.000	5.833	8.456	0.331	0.026	100.554
f64-5-1	60.971	0.001	25.117	0.142	0.000	0.000	5.878	8.620	0.056	0.055	100.840
f64-5-2	60.530	0.014	25.425	0.086	0.006	0.000	6.116	8.553	0.059	0.067	100.856
f64-5-3	60.545	0.013	25.288	0.130	0.000	0.016	6.031	8.569	0.068	0.000	100.660
f64-5-4	60.710	0.009	25.261	0.109	0.017	0.006	5.969	8.694	0.050	0.040	100.865
f64-5-5	60.411	0.003	25.636	0.100	0.000	0.000	6.079	8.556	0.060	0.034	100.879
f64-5-6	60.644	0.007	25.363	0.243	0.003	0.000	5.845	8.734	0.083	0.000	100.922
f64-5-7	60.401	0.001	25.381	0.156	0.008	0.000	6.090	8.541	0.053	0.042	100.673
f64-6-1	60.977	0.012	24.939	0.140	0.000	0.010	5.638	8.794	0.065	0.014	100.589
f64-6-2	60.317	0.004	25.638	0.109	0.018	0.000	6.129	8.507	0.072	0.037	100.831
f64-6-3	60.780	0.000	25.309	0.164	0.000	0.006	5.917	8.560	0.046	0.027	100.809
f64-6-4	60.898	0.012	25.218	0.119	0.001	0.005	5.951	8.531	0.060	0.022	100.817
f64-6-5	61.083	0.000	25.186	0.248	0.011	0.000	5.952	8.513	0.059	0.016	101.068
f64-6-6	60.440	0.001	25.327	0.068	0.017	0.007	5.863	8.634	0.050	0.036	100.443
f64-6-7	59.140	0.000	26.259	0.111	0.000	0.000	7.032	7.931	0.059	0.032	100.564
f64-6-8	60.380	0.020	25.433	0.143	0.006	0.004	5.977	8.560	0.050	0.000	100.573
f64-6-9	60.550	0.011	25.329	0.151	0.007	0.004	5.983	8.642	0.032	0.006	100.715
f64-7-4	60.514	0.000	25.226	0.128	0.000	0.000	5.996	8.596	0.058	0.007	100.525
f64-7-5	60.621	0.001	25.520	0.131	0.009	0.000	6.024	8.567	0.051	0.019	100.943
f64-7-6	60.682	0.002	25.294	0.123	0.026	0.001	5.952	8.651	0.048	0.022	100.801
f64-7-7	60.567	0.007	25.326	0.207	0.016	0.007	6.081	8.431	0.057	0.016	100.715
f65-1-1	60.580	0.005	25.188	0.090	0.000	0.004	6.166	8.431	0.094	0.037	100.595
f65-1-2	60.504	0.013	25.128	0.085	0.000	0.002	6.116	8.469	0.097	0.042	100.456
f65-1-3	60.811	0.000	25.267	0.142	0.006	0.000	5.961	8.828	0.089	0.025	101.129
f65-1-4	60.584	0.005	25.212	0.139	0.000	0.005	6.033	8.737	0.096	0.022	100.833
f65-2-1	60.595	0.007	25.457	0.066	0.000	0.000	6.101	8.658	0.068	0.038	100.990
f65-2-2	60.624	0.012	25.315	0.116	0.000	0.000	6.114	8.512	0.104	0.035	100.832
f65-2-3	60.476	0.001	25.340	0.117	0.000	0.003	6.203	8.533	0.047	0.010	100.730
f65-2-4	60.563	0.011	25.111	0.150	0.000	0.006	6.012	8.556	0.068	0.032	100.509
f65-2-5	60.714	0.021	25.264	0.144	0.000	0.019	6.046	8.682	0.095	0.013	100.998
f65-2-6	60.252	0.000	25.307	0.142	0.007	0.003	6.256	8.483	0.061	0.000	100.511
f65-3-1	60.233	0.004	25.256	0.084	0.007	0.002	6.121	8.598	0.111	0.008	100.424

Appendix I. (cont)

	SiO_2	TiO_2	Al_2O_3	FeO	MnO	MgO	CaO	Na_2O	K_2O	BaO	Total
f65-3-2	60.759	0.019	25.134	0.234	0.011	0.000	6.163	8.531	0.096	0.053	101.000
f65-3-3	60.666	0.000	25.144	0.109	0.011	0.001	6.118	8.571	0.064	0.039	100.723
f65-3-4	60.750	0.003	25.140	0.086	0.000	0.007	5.974	8.508	0.138	0.029	100.635
f65-3-5	60.813	0.004	25.077	0.104	0.013	0.000	6.012	8.667	0.118	0.007	100.815
f65-4-1	60.443	0.007	25.341	0.111	0.000	0.000	6.156	8.576	0.075	0.022	100.731
f65-4-2	60.781	0.000	25.454	0.159	0.000	0.000	6.099	8.679	0.075	0.049	101.296
f65-4-3	60.659	0.000	25.248	0.130	0.019	0.000	5.979	8.709	0.059	0.007	100.810
f65-4-4	60.358	0.006	25.109	0.161	0.009	0.000	6.101	8.748	0.081	0.009	100.582
f65-4-5	60.671	0.000	25.123	0.235	0.000	0.000	6.161	8.598	0.079	0.015	100.882
f65-4-6	60.887	0.001	25.134	0.174	0.008	0.004	6.175	8.536	0.080	0.046	101.045
f65-5-1	61.074	0.000	24.935	0.048	0.000	0.003	6.043	8.546	0.081	0.034	100.764
f65-5-2	61.268	0.000	24.846	0.142	0.012	0.000	5.862	8.610	0.104	0.051	100.895
f65-5-3	60.825	0.003	25.007	0.107	0.000	0.000	6.041	8.567	0.108	0.007	100.665
f65-5-4	60.662	0.030	25.092	0.133	0.001	0.000	5.998	8.634	0.114	0.033	100.697
f65-5-5	60.361	0.000	25.202	0.173	0.000	0.000	6.061	8.634	0.102	0.035	100.568
f65-5-6	60.599	0.000	25.067	0.120	0.000	0.011	6.015	8.655	0.100	0.042	100.609
66: High-strain tonalite											
f66-1-1	61.411	0.025	24.972	0.161	0.001	0.004	6.305	8.286	0.073	0.001	101.239
f66-1-2	60.615	0.015	25.320	0.147	0.001	0.000	6.786	7.932	0.096	0.003	100.915
f66-1-3	61.134	0.003	24.823	0.148	0.000	0.011	6.381	8.126	0.163	0.002	100.791
f66-1-4	61.087	0.016	24.743	0.150	0.013	0.003	6.339	8.274	0.102	0.033	100.760
f66-1-5	60.730	0.000	24.847	0.123	0.000	0.000	6.475	8.198	0.134	0.000	100.507
f66-1-6	61.771	0.014	24.206	0.165	0.000	0.011	5.683	8.627	0.083	0.056	100.616
f66-2-1	60.893	0.011	25.208	0.159	0.000	0.000	6.491	8.158	0.090	0.036	101.046
f66-2-2	61.207	0.002	24.960	0.110	0.005	0.000	6.317	8.229	0.083	0.000	100.913
f66-2-3	61.359	0.000	25.020	0.175	0.004	0.000	6.366	8.317	0.128	0.011	101.380
f66-2-4	61.722	0.008	24.914	0.250	0.020	0.000	6.227	8.320	0.117	0.004	101.582
f66-2-5	61.087	0.000	24.993	0.171	0.000	0.000	6.393	8.315	0.099	0.022	101.080
f66-2-6	61.472	0.000	24.747	0.121	0.000	0.000	6.382	8.303	0.084	0.000	101.109
f66-2-7	61.813	0.011	24.564	0.157	0.007	0.000	5.995	8.449	0.082	0.054	101.132
f66-2-8	61.379	0.001	24.871	0.179	0.000	0.002	6.318	8.194	0.107	0.005	101.056
f66-3-1	61.453	0.031	24.862	0.136	0.003	0.007	6.236	8.278	0.087	0.017	101.110
f66-3-2	61.454	0.000	24.824	0.200	0.023	0.005	6.274	8.303	0.146	0.024	101.253
f66-3-3	61.196	0.012	24.837	0.116	0.006	0.004	6.377	8.137	0.097	0.000	100.782
f66-3-4	60.354	0.014	25.470	0.173	0.015	0.008	7.157	7.743	0.129	0.022	101.085
f66-3-5	60.926	0.003	25.025	0.117	0.001	0.000	6.329	8.202	0.120	0.003	100.726
f66-3-6	61.367	0.007	24.881	0.173	0.003	0.086	6.200	7.974	0.287	0.025	101.003
f66-3-7	60.862	0.003	24.939	0.141	0.002	0.000	6.354	8.219	0.111	0.020	100.651
f66-3-8	61.167	0.000	24.819	0.185	0.015	0.000	6.324	8.045	0.088	0.000	100.643
f66-4-1	61.372	0.000	24.837	0.120	0.000	0.004	6.313	8.192	0.112	0.000	100.950
f66-4-2	60.954	0.003	25.038	0.118	0.012	0.013	6.524	8.189	0.101	0.000	100.952
f66-4-3	61.407	0.012	24.724	0.106	0.002	0.000	6.056	8.333	0.191	0.000	100.831
f66-4-4	60.874	0.001	24.948	0.082	0.000	0.010	6.418	8.118	0.118	0.000	100.569
f66-4-5	60.737	0.012	24.954	0.152	0.010	0.001	6.329	8.204	0.078	0.038	100.515
f66-4-6	60.903	0.004	25.023	0.221	0.009	0.004	6.508	8.146	0.102	0.000	100.920
f66-4-7	61.251	0.005	24.739	0.140	0.009	0.000	6.341	8.116	0.145	0.002	100.748
f66-5-1	61.002	0.004	24.896	0.099	0.000	0.000	6.383	8.187	0.086	0.000	100.657
f66-5-2	61.166	0.003	24.943	0.139	0.004	0.004	6.365	8.111	0.352	0.079	101.166
f66-5-3	61.092	0.000	24.959	0.187	0.011	0.000	6.314	8.198	0.099	0.000	100.860
f66-5-4	60.976	0.000	24.889	0.149	0.000	0.005	6.436	8.091	0.082	0.001	100.629
f66-6-1	61.102	0.004	24.748	0.076	0.006	0.006	6.284	8.236	0.151	0.000	100.613
f66-6-2	61.200	0.001	24.958	0.102	0.004	0.000	6.344	8.216	0.096	0.029	100.950

Appendix I. (cont)

	SiO_2	TiO_2	Al_2O_3	FeO	MnO	MgO	CaO	Na_2O	K_2O	BaO	Total
68/69: Heterogeneously deformed tonalite											
f68-1-1	61.253	0.017	24.726	0.184	0.001	0.002	6.228	8.239	0.092	0.016	100.758
f68-1-2	61.777	0.000	24.221	0.135	0.000	0.000	5.916	8.230	0.084	0.010	100.373
f68-2-1	61.438	0.005	24.090	0.440	0.013	0.096	4.697	8.024	1.706	0.026	100.535
f68-2-2	59.659	0.184	24.213	1.297	0.024	0.629	5.504	8.066	0.409	0.020	100.005
f68-3-1	62.081	0.016	24.166	0.178	0.000	0.008	5.684	8.465	0.097	0.020	100.715
f68-3-2	62.046	0.009	24.379	0.150	0.008	0.007	6.171	7.976	0.102	0.018	100.866
f68-3-3	61.577	0.000	24.613	0.121	0.005	0.004	6.040	8.370	0.101	0.024	100.855
f68-3-4	61.223	0.000	24.803	0.109	0.005	0.000	6.189	8.236	0.096	0.000	100.661
f68-3-5	61.286	0.000	24.517	0.086	0.009	0.011	5.971	8.205	0.051	0.015	100.151
f68-3-6	61.615	0.002	24.554	0.081	0.000	0.000	5.999	8.316	0.060	0.022	100.649
f68-4-1	61.679	0.000	23.936	0.125	0.000	0.000	5.380	8.397	0.190	0.009	99.716
f68-4-2	61.471	0.028	24.495	0.277	0.000	0.000	6.026	8.311	0.134	0.032	100.774
f68-4-3	61.413	0.009	24.604	0.103	0.001	0.000	6.003	8.361	0.121	0.022	100.637
f68-4-4	61.475	0.000	24.600	0.211	0.000	0.000	6.062	8.298	0.078	0.022	100.746
f68-4-5	61.334	0.006	24.443	0.187	0.000	0.000	6.060	8.256	0.070	0.027	100.383
f68-4-6	63.544	0.012	23.156	0.153	0.005	0.001	4.569	9.109	0.061	0.000	100.610
f68-4-7	61.830	0.000	24.189	0.137	0.000	0.000	5.921	8.435	0.053	0.025	100.590
f69-1-1	65.912	0.007	21.623	0.174	0.020	0.000	2.277	10.855	0.061	0.048	100.977
f69-1-2	61.632	0.000	24.432	0.134	0.015	0.032	5.578	8.354	0.206	0.041	100.424
f69-1-3	61.649	0.000	24.279	0.218	0.009	0.066	4.436	8.379	1.014	0.021	100.071
f69-1-4	61.988	0.011	24.183	0.089	0.000	0.000	5.844	8.352	0.081	0.000	100.548
f69-1-5	62.003	0.000	24.206	0.116	0.000	0.003	5.853	8.463	0.136	0.065	100.845
f69-2-1	61.431	0.005	24.270	0.219	0.002	0.053	5.598	8.434	0.266	0.017	100.295
f69-2-2	61.584	0.005	24.427	0.131	0.000	0.000	5.881	8.395	0.078	0.021	100.522
f69-2-3	62.681	0.000	23.470	0.217	0.086	0.080	4.734	8.605	0.489	0.044	100.406
f69-3-1	60.515	0.000	24.348	0.357	0.005	0.808	5.707	8.013	0.357	0.009	100.119
f69-3-2	61.719	0.012	24.205	0.133	0.000	0.027	5.620	8.160	0.647	0.022	100.545
f69-3-3	62.458	0.000	24.115	0.130	0.000	0.000	5.763	8.452	0.052	0.007	100.977
f69-3-4	61.432	0.000	24.743	0.174	0.016	0.000	5.984	8.416	0.086	0.021	100.872
f69-3-5	61.937	0.012	24.595	0.155	0.015	0.000	5.893	8.590	0.098	0.000	101.295
f69-4-1	62.782	0.045	23.428	0.417	0.010	0.146	4.600	9.213	0.212	0.030	100.883
f69-4-2	62.144	0.000	24.050	0.156	0.000	0.004	5.364	8.780	0.067	0.021	100.586
f69-5-1	61.650	0.015	24.515	0.057	0.012	0.000	5.866	8.492	0.090	0.000	100.697
f69-5-2	62.486	0.005	24.086	0.172	0.000	0.000	5.479	8.536	0.107	0.016	100.887
f69-5-3	62.018	0.008	24.220	0.141	0.012	0.029	5.466	7.825	1.320	0.026	101.065

Appendix I. (cont)

K-feldspar

	SiO_2	TiO_2	Al_2O_3	FeO	MnO	MgO	CaO	Na_2O	K_2O	BaO	Total
01: Leucocratic tonalite											
f1-1-2	63.904	0.037	18.395	0.073	0.000	0.004	0.000	0.578	15.506	1.014	99.511
29: Moderately deformed granodiorite											
f29-2-1	64.560	0.030	18.589	0.129	0.000	0.011	0.000	0.369	15.852	1.025	100.565
f29-2-2	64.499	0.047	18.667	0.143	0.000	0.001	0.000	0.339	16.009	0.911	100.616
40: Tonalite containing blebby pegmatite											
f40-2-1	64.317	0.000	18.833	0.136	0.008	0.000	0.002	0.632	15.905	0.496	100.329
f40-2-2	64.579	0.009	18.674	0.068	0.000	0.000	0.000	0.648	15.743	0.585	100.306
f40-2-3	64.899	0.000	18.462	0.162	0.000	0.000	0.000	0.515	15.948	0.556	100.542
f40-2-4	64.399	0.013	18.723	0.092	0.003	0.000	0.000	0.653	15.749	0.641	100.273
f40-2-5	65.064	0.024	18.607	0.097	0.000	0.011	0.000	0.668	15.679	0.644	100.794
61: Massive tonalite											
f61-4-4	63.607	0.025	19.610	0.218	0.000	0.001	0.011	0.488	15.452	1.725	101.137